The circadian regulation of eclosion in *Drosophila melanogaster*

Die zeitliche Steuerung des Adultschlupfes in *Drosophila melanogaster*

Doctoral thesis for a doctoral degree

at the Graduate School of Life Sciences,

Julius-Maximilians-Universität Würzburg,

Section Integrative Biology

Submitted by

Franziska Ruf

from Heilbronn

Würzburg, 2016

The present work was accomplished at the Department of Neurobiology and Genetics at the University of Würzburg.

Submitted on: 24.06.2016

Members of the *Promotionskomitee*:

Chairperson: Prof. Dr. Jörg Schultz

Primary Supervisor: Prof. Dr. Christian Wegener

Supervisor (Second): Prof. Dr. Wolfgang Rössler

Supervisor (Third): Prof. Dr. Sakiko Shiga

Date of Public Defence: ……

Date of Receipt of Certificates: ……

Table of contents

Summary

Eclosion is the emergence of an adult insect from the pupal case at the end of development. In the fruit fly *Drosophila melanogaster*, eclosion is a circadian clock-gated event and is regulated by various peptides. When studied on the population level, eclosion reveals a clear rhythmicity with a peak at the beginning of the light-phase that persists also under constant conditions. It is a long standing hypothesis that eclosion gating to the morning hours with more humid conditions is an adaption to reduce water loss and increase the survival. Eclosion behavior, including the motor pattern required for the fly to hatch out of the puparium, is orchestrated by a well-characterized cascade of peptides. The main components are ecdysis-triggering hormone (ETH), eclosion hormone (EH) and crustacean cardioactive peptide (CCAP). The molt is initiated by a peak level and pupal ecdysis by a subsequent decline of the ecdysteroid ecdysone. Ecdysteroids are produced by the prothoracic gland (PG), an endocrine tissue that contains a peripheral clock and degenerates shortly after eclosion. Production and release of ecdysteroids are regulated by the prothoracicotropic hormone (PTTH).

Although many aspects of the circadian clock and the peptidergic control of the eclosion behavior are known, it still remains unclear how both systems are interconnected. The aim of this dissertation research was to dissect this connection and evaluate the importance of different Zeitgebers on eclosion rhythmicity under natural conditions.

Potential interactions between the central clock and the peptides regulating ecdysis motor behavior were evaluated by analyzing the influence of CCAP on eclosion rhythmicity. Ablation and silencing of CCAP neurons, as well as CCAP null-mutation did not affect eclosion rhythmicity under either light or temperature entrainment nor under natural conditions.

To dissect the connection between the central and the peripheral clock, PTTH neurons were ablated. Monitoring eclosion under light and temperature entrainment revealed that eclosion became arrhythmic under constant conditions. However, qPCR expression analysis revealed no evidence for cycling of *Ptth* mRNA in pharate flies. To test for a connection with pigment-dispersing factor (PDF)-expressing neurons, the PDF receptor (PDFR) and short neuropeptide F receptor (sNPFR) were knocked down in the PTTH neurons. Knockdown of sNPFR, but not PDFR, resulted in arrhythmic eclosion under constant darkness conditions. PCR analysis of the PTTH receptor, Torso, revealed its expression in the PG and the gonads, but not in the brain or eyes, of pharate flies. Knockdown of *torso* in the PG lead to arrhythmicity under constant

conditions, which provides strong evidence for the specific effect of PTTH on the PG. These results suggest connections from the PDF positive lateral neurons to the PTTH neurons via sNPF signaling, and to the PG via PTTH and Torso. This interaction presumably couples the period of the peripheral clock in the PG to that of the central clock in the brain.

To identify a starting signal for eclosion and possible further candidates in the regulation of eclosion behavior, chemically defined peptidergic and aminergic neurons were optogenetically activated in pharate pupae via ChR2-XXL. This screen approach revealed two candidates for the regulation of eclosion behavior: Dromyosuppressin (DMS) and myo-inhibitory peptides (MIP). However, ablation of DMS neurons did not affect eclosion rhythmicity or success and the exact function of MIP must be evaluated in future studies.

To assess the importance of the clock and of possible Zeitgebers in nature, eclosion of the wildtype *Canton S* and the clock mutant per^{01} and the PDF signaling mutants pdf^{01} and han^{5304} was monitored under natural conditions. For this purpose, the Würzburg eclosion monitor (WEclMon) was developed, which is a new open monitoring system that allows direct exposure of pupae to the environment. A general decline of rhythmicity under natural conditions compared to laboratory conditions was observed in all tested strains. While the wildtype and the pdf^{01} and han^{5304} mutants stayed weakly rhythmic, the per^{01} mutant flies eclosed mostly arrhythmic. PDF and its receptor (PDFR encoded by *han*) are required for the synchronization of the clock network and functional loss can obviously be compensated by a persisting synchronization to external Zeitgebers. The loss of the central clock protein PER, however, lead to a non-functional clock and revealed the absolute importance of the clock for eclosion rhythmicity. To quantitatively analyze the effect of the clock and abiotic factors on eclosion rhythmicity, a statistical model was developed in cooperation with Oliver Mitesser and Thomas Hovestadt. The modelling results confirmed the clock as the most important factor for eclosion rhythmicity. Moreover, temperature was found to have the strongest effect on the actual shape of the daily emergence pattern, while light has only minor effects. Relative humidity could be excluded as Zeitgeber for eclosion and therefore was not further analyzed.

Taken together, the present dissertation identified the so far unknown connection between the central and peripheral clock regulating eclosion. Furthermore, a new method for the analysis of eclosion rhythms under natural conditions was established and the necessity of a functional clock for rhythmic eclosion even in the presence of multiple Zeitgebers was shown.

Zusammenfassung

Der Schlupf adulter Fliegen aus dem Puparium wird in der Taufliege *Drosophila melanogaster* zum einen von der inneren Uhr und zum anderen von Peptiden gesteuert. Beobachtet man den Schlupf auf der Populationsebene, lässt sich erkennen, dass die meisten Fliegen zu Beginn der Lichtphase schlüpfen. Diese Rhythmizität im Schlupfverhalten von Fliegenpopulationen hält auch unter konstanten Bedingungen an. Seit langer Zeit wird angenommen, dass der Schlupf am Morgen eine Anpassung an feuchte Bedingungen ist, wodurch der Wasserverlust verringert und die Überlebenswahrscheinlichkeit erhöht werden könnte. Das stereotype motorische Schlupfverhalten, mit dem sich die Fliege aus der Puppenhülle befreit, wird durch das gut untersuchte Zusammenspiel zahlreicher Peptide gesteuert. Die wichtigsten Peptide sind hierbei das ecdysis-triggering hormone (ETH), das Schlupfhormon (EH) und das crustacean cardioactive peptide (CCAP). Wie bei jedem Schlupf wird die Häutung durch eine stark erhöhte Produktion des Ecdysteroids Ecdyson ausgelöst. Der anschließende Abfall der Ecdyson-Titer löst dann den Adultschlupf aus. Ecdysteroide werden in der Prothorakaldrüse (PD) gebildet, die eine periphere Uhr besitzt und kurz nach dem Adultschlupf zurückgebildet wird. Das prothorakotrope Hormon (PTTH) reguliert sowohl die Produktion als auch die Freisetzung der Ecdysteroide aus der PD.

Obwohl bereits viel über den Aufbau und die Funktionsweise der inneren Uhr und der Kontrolle des Adultschlupfes durch Peptide bekannt ist, weiß man bisher nicht, wie beide Systeme miteinander interagieren. Das Hauptziel der vorliegenden Arbeit war es, einerseits diese Verbindung zu untersuchen und andererseits die Gewichtung verschiedener Zeitgeber für den Adultschlupf unter natürlichen Bedingungen zu bewerten.

Um eine mögliche Verbindung zwischen der zentralen Uhr und den Peptiden, die das motorische Verhalten während des Schlupfes steuern, zu untersuchen, wurde der Einfluss von CCAP auf die Schlupfrhythmik betrachtet. Hierzu wurden die CCAP-exprimierenden Neurone genetisch ablatiert oder elektrisch stillgelegt, sowie zusätzlich eine CCAP-defiziente Mutante getestet. Weder unter künstlichen Licht- oder Temperaturzyklen, noch unter natürlichen Bedingungen wurden Effekte auf den Schlupfrhythmus bei veränderter CCAP Verfügbarkeit beobachtet.

Die Verbindung zwischen der zentralen und der peripheren Uhr der PD wurde untersucht, indem die PTTH-exprimierenden Neurone in Fliegen ablatiert wurden. Dies führte sowohl

unter konstanten Licht- als auch Temperaturbedingungen zu arrhythmischem Schlupf der Populationen. Die Analyse der Expression von *Ptth* mRNA mittels qPCR lieferte keine Hinweise auf eine zyklische Regulation des *Ptth* Transkripts in pharaten Tieren. Um eine Verbindung zu pigment-dispersing factor (PDF)-exprimierenden Uhrneuronen nachzuweisen, wurden die Rezeptoren von PDF (PDFR) und dem short Neuropeptide F (sNPFR) in den PTTH- Neuronen herunterreguliert. Nur der Verlust von sNPFR führte unter konstanten Bedingungen zu arrhythmischem Schlupf. RT-PCR-Analyse der mRNA Expression des Rezeptors von PTTH, Torso, ergab, dass *torso* mRNA in pharaten Fliegen nur in der PD und in den Gonaden exprimiert wird, nicht jedoch im Gehirn. Das Herrunterregulieren der *torso* mRNA in der PD führte unter konstanten Bedingungen zu arrhythmischem Schlupf und lieferte deutliche Hinweise zur spezifischen Funktion von PTTH in der PD. Diese Ergebnisse zeigen eine sNPF-vermittelte Verbindung zwischen den PDF-positiven lateralen Neuronen und den PTTH-Neuronen, welche über PTTH und Torso weiter bis in die PD reicht. Durch diese Verbindung wird vermutlich die Periode der peripheren Uhr in der PD an die Periode der zentralen Uhr im Gehirn angepasst.

Um ein Startsignal für den Adultschlupf und weitere mögliche Kandidaten, die eine Rolle in der Steuerung des Schlupfes spielen, zu identifizieren, wurden chemisch definierte kleine Gruppen peptiderger und aminerger Neurone optogenetisch durch das Kanalrhodopsin ChR2-XXL aktiviert. In dieser Testreihe wurden Dromyosuppressin (DMS) und myoinhibitorisches Peptid (MIP) als mögliche Kandidaten ermittelt. Eine Ablation der DMS-Neurone hatte jedoch keine Auswirkungen auf Schlupfrhythmik und -erfolg. Die genaue Funktion von MIP sollte in zukünftigen Experimenten untersucht werden.

Um die Gewichtung der Uhr und möglicher Zeitgeber für das natürliche Verhalten zu bestimmen, wurde der Schlupf des Wildtyps *Canton S,* der Uhrmutante per^{01} sowie der PDF-Signalwegsmutanten pdf^{01} und han^{5304} (*han* codiert für den PDFR) unter natürlichen Bedingungen beobachtet. Hierfür wurde ein neues und offenes Aufzeichnungssystem entwickelt: der Würzburger Schlupfmonitor (WEclMon), der einen direkten Kontakt der Puppen mit den sie umgebenden abiotischen Bedingungen ermöglicht.

Im Vergleich zu Laborbedingungen war die Rhythmizität des Schlupfes unter natürlichen Bedingungen in allen getesteten Fliegenlinien weniger ausgeprägt. Während der Wildtyp sowie die pdf^{01} und han^{5304} Mutanten weiterhin schwach rhythmisch schlüpften, schlüpfte die per^{01} Mutante hauptsächlich arrhythmisch. Das Zusammenspiel zwischen PDF und seinem

Rezeptor synchronisiert das Uhrnetzwerk, und der Verlust dieser Interaktion kann durch tägliches neues Ausrichten an den Zeitgebern ausgeglichen werden. Der Verlust des Uhrproteins PER unterbindet jedoch die komplette Funktionsfähigkeit der Uhr. Dadurch wird die Notwendigkeit der Uhr für einen rhythmischen Schlupf unterstrichen. Um den Einfluss der Uhr und abiotischer Faktoren auf den Schlupfrhythmus zu untersuchen, wurde im Rahmen einer Kooperation mit Oliver Mitesser und Thomas Hovestadt ein statistisches Modell entwickelt. Die Ergebnisse der Modellierung unterstützen die Hypothese, dass die Uhr der wichtigste Faktor für einen rhythmischen Schlupf auch unter Zeitgeber-Bedingungen ist. Die Umgebungstemperatur übt hingegen den stärksten Einfluss auf die Form des täglichen Schlupfmusters aus, während Licht hier nur einen schwachen Einfluss hat. Es konnte gezeigt werden, dass sich relative Luftfeuchtigkeit nicht als Zeitgeber für den Schlupf eignet, weshalb sie in weiteren Untersuchungen nicht berücksichtigt wurde.

Zusammenfassend lässt sich sagen, dass mit der vorliegenden Arbeit die Verbindung zwischen der zentralen und peripheren Uhr in der Steuerung des Schlupfes identifiziert werden konnten, die bisher nicht bekannt war. Außerdem wurde eine neue Methode der Untersuchung des Adultschlupfes unter natürlichen Bedingungen etabliert und die Notwendigkeit einer intakten Uhr für einen rhythmischen Adultschlupf selbst in Anwesenheit mehrerer Zeitgeber konnte herausgestellt werden.

Introduction

1. The clock – an endogenous timekeeping system

The rotation of the earth around its own axis and around the sun leads to periodic changes in the environment that can occur daily, monthly or annually. To adapt physiological and biochemical processes as well as their behavior to these changes, all known organisms, from bacteria to mammals, evolved endogenous timekeeping systems, so called endogenous clocks. These clocks allow the anticipation of periodic changes in the environment and are therefore thought to increase the fitness of the individual. Rhythms can be found at different levels of organization, ranging from cells over tissues to individuals and even populations (Saunders, 2002; Zordan *et al*., 2009). Endogenous clocks that oscillate with rhythms of approximately 24 hours are called circadian (from the Latin *circa* = around and *dianus* = daily) and represent the majority of clocks.

Among the first reports on rhythmic behaviors are studies of the French scientist De Mairan on the daily leaf movements of *Mimosa pudica* from 1729. Around 200 years later, one of the first experimental studies on rhythmic animal behavior was on the eclosion of fly (Pegomyia hyoscyami) and moth (*Ephestia kühniella*) populations in the morning (Bremer, 1926) and an underlying endogenous timekeeping system was later described for the fruit fly *Drosophila melanogaster* (Bünning, 1935; Kalmus, 1935; Kalmus, 1938; Kalmus, 1940). Early works on the properties of biological clocks by Pittendrigh, Zimmerman, Bruce and others in the 1950-1960ies lead to the following defining characteristics (reviewed in Saunders, 2002):

1) clocks are able to entrain to so called Zeitgebers, which means they synchronize their period to environmental variables
2) clocks display rhythms that persist also under constant conditions in the absence of cues from the environment; they are then free-running
3) the free-running period is close to the period of the environment to which the rhythm is entrained
4) clocks are temperature-compensated; while most biochemical and physiological processes increase their rate with increasing temperatures, the period of the clock is not affected by temperature changes.

While the most prominent Zeitgebers are daily changes in light and temperature, also humidity, social contacts, food availability, tidal changes and other environmental influences can entrain the clock. Besides the central clock, which is located in the brain, many body tissues have peripheral clocks that oscillate autonomously but are coupled with the central clock in animals (Figure 1).

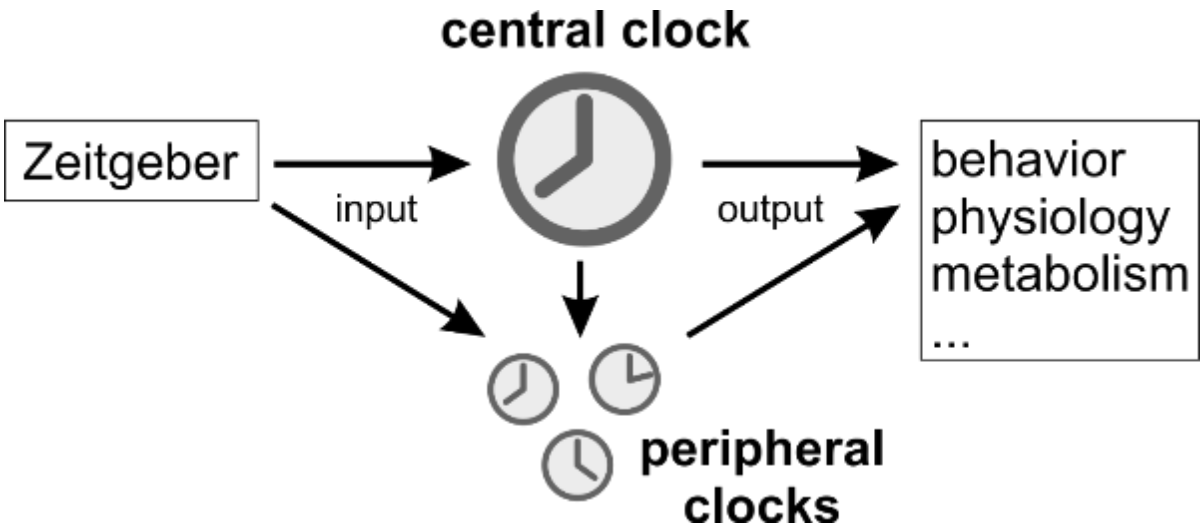

Figure 1: Schematic model of the clock system
The central clock receives input from Zeitgebers like light, temperature or food availability, and thereby entrains its period to the period of the Zeitgeber. Peripheral clocks also receive input from Zeitgebers, but may also be coupled to the central clock. Alone or together with peripheral clocks, the central clock generates different outputs, for example on the physiological or behavioral level.

2. The circadian clock of *Drosophila melanogaster*

Drosophila melanogaster is one of the most used model organisms for research on circadian clocks. Early chronobiologists like Bünning and Pittendrigh studied *Drosophila melanogaster* and *D. pseudoobscura* to characterize the general properties of clocks (reviewed in Saunders, 2002). The first clock gene, *period*, was discovered in *Drosophila* (Konopka and Benzer, 1971). Many fly behaviors have been shown to be under circadian regulation, for example locomotor activity (Roberts, 1956), eclosion (Bremer, 1926; Pittendrigh, 1954), oviposition (Allemand, 1976a; Allemand, 1976b), sensitivity to olfactory (Krishnan *et al.*, 1999) and gustatory stimulation (Chatterjee *et al*., 2010), courtship behavior (Hardeland, 1972; Fujii *et al.*, 2007) and learning and memory (Lyons and Roman, 2009).

2.1 The molecular clock

The molecular clock of *Drosophila melanogaster* consists of two interlocked transcriptional feedback loops that comprise the basic generator of the circadian clock (Figure 2). At the center of these feedback loops are the clock proteins CLOCK (CLK) and CYCLE (CYC) that form heterodimers and act as transcriptional activators (Hogenesch *et al.*, 1998). They induce expression of target genes by binding to target sequences, so called E boxes, located in the promotor regions (Allada *et al.*, 1998; Darlington *et al.*, 1998; Rutila *et al.*, 1998). In the first feedback loop, CLK-CYC activates the transcription of the clock genes *period* (*per*) and *timeless* (*tim*). PER and TIM proteins accumulate in the cytoplasm and enter the nucleus as heterodimers (Curtin *et al.*, 1995; Gekakis *et al.*, 1995; Saez and Young, 1996; Zeng *et al.*, 1996; Kloss *et al.*, 1998; Price *et al.*, 1998). In the nucleus, the complex inhibits the transcription of their own genes through an interaction of PER with CLK, which disables the CLK-CYC heterodimer from binding to the E boxes (Darlington *et al.*, 1998). The mRNA levels of *per* and *tim* peak at the end of the light phase (Hardin *et al.*, 1990; Sehgal *et al.*, 1995) and their proteins accumulate in the nucleus only during the dark phase (Hardin *et al.*, 1990). This is due to the action of the blue-light receptor protein Cryptochrome (CRY) which is activated by light (Emery *et al.*, 1998; Stanewsky *et al.*, 1998). Activated CRY binds to TIM and leads to its proteasome-mediated degradation (Ceriani *et al.*, 1999; Naidoo *et al.*, 1999; Busza *et al.*, 2004). Without TIM, PER is phosphorylated by the kinase Double-Time (DBT), which leads to PER degradation (Kloss *et al.*, 1998; Price *et al.*, 1998; Kloss *et al.*, 2001). The process of light-mediated degradation of TIM and PER synchronizes the circadian clock with the environment. The kinase Shaggy (SGG) stabilizes CRY through binding and saves TIM from degradation by an unknown mechanism (Martinek *et al.*, 2001; Stoleru *et al.*, 2007). In the first feedback loop, PER and TIM can accumulate in the nucleus and inhibit CLK-CYC only during the night, while during the day, CLK-CYC can promote *per* and *tim* transcription and restart the transcriptional loop.

In a second feedback loop, CLK-CYC induces the transcription of the clock genes *vrille* (*vri*) (Blau and Young, 1999) and *Par domain protein 1* (*Pdp1*) (McDonald and Rosbash, 2001; Ueda *et al.*, 2002) by binding to their E-boxes. The proteins then bind to V/P boxes in the promotor region of *clk* (Cyran *et al.*, 2003; Glossop *et al.*, 2003) and regulate its transcription: while VRI is acting as a repressor for *clk* expression (Glossop *et al.*, 2003), PDP1 is acting as an activator (Cyran *et al.*, 2003). With *clockwork orange* (*cwo*) another CLK-CYC activated clock gene was

discovered, which acts as a transcriptional repressor of CLK target genes by binding to their E boxes (Figure 3) (Kadener *et al.*, 2007; Lim *et al.*, 2007; Matsumoto *et al.*, 2007).

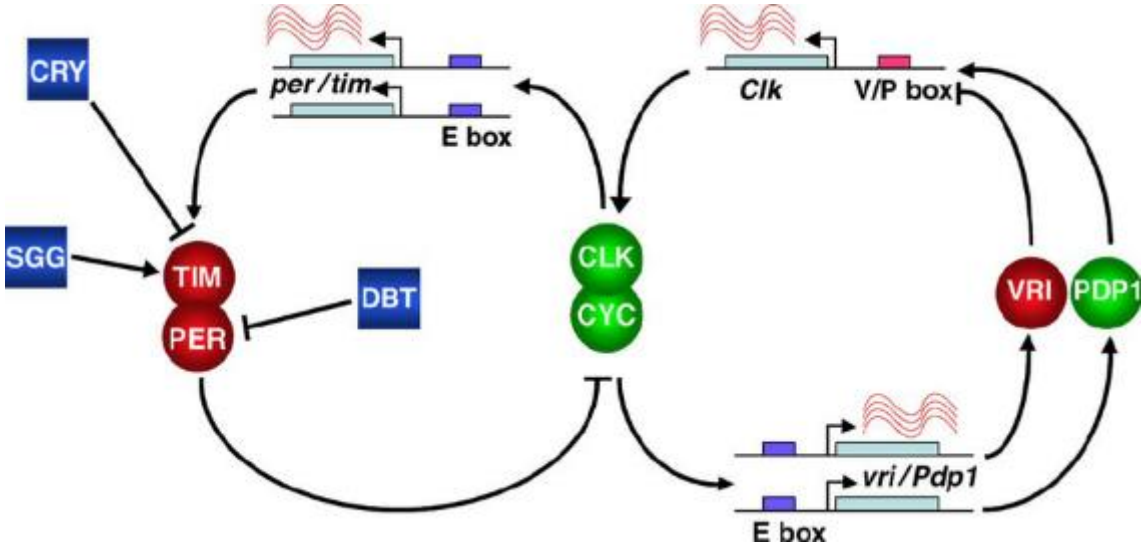

Figure 2: The molecular mechanism of the clock
The transcription factors CLOCK (CLK) and CYCLE (CYC) activate the transcription of the target genes *period* (*per*), *timeless* (*tim*), *vrille* (*vri*) and *Par domain protein 1* (*Pdp1*) by binding to E boxes in their promotor regions. The proteins regulate their own transcription and the expression of other clock genes by either inhibiting CLK-CYC (first feedback loop with PER and TIM) or by regulating *clk* transcription (second feedback loop with VRI and PDP1). Cryptochrome (CRY) mediates the light-induced degradation of TIM and is modulated by Shaggy (SGG). Double-Time (DBT) leads to PER degradation if it is not stabilized by TIM. Activators are colored in green, repressors in red. For details see text. From Collins and Blau (2007)

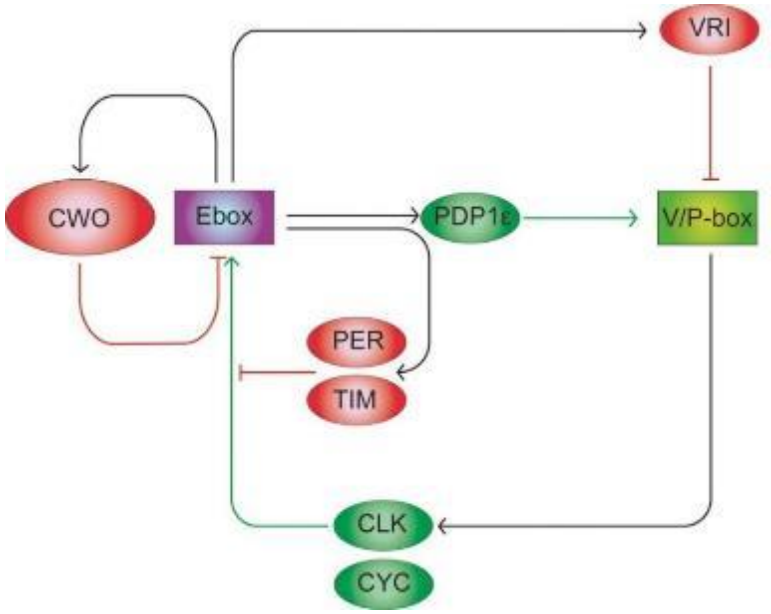

Figure 3: The function of *clockwork orange* (*cwo*)
CWO binds to the E boxes of clock genes and represses their transcription. Activators are colored in green, repressors in red. From Matsumoto *et al.* (2007)

2.2 The clock network

In the brain of *Drosophila melanogaster*, about 150 neurons express clock genes – they are therefore called clock cells and comprise the circadian clock or central pacemaker. According to their anatomical location, the clock cells can be divided into two main neuron clusters: the dorsal neurons (DN) and the lateral neurons (LN). These clusters can be further subdivided into 3 DN clusters and 4 LN clusters. Each brain hemisphere contains 16 DN1s, 2 DN2s and 40 DN3s, as well as 5 small ventral lateral neurons (sLNv), 4 large ventral lateral neurons (lLNv), 6 dorsal lateral neurons (LNd) and 3 lateral posterior neurons (LPN) (see Figure 4). Of the 5 sLNvs, only 4 express the neuropeptide pigment-dispersing factor (PDF), as do the lLNvs, while the 5th sLNv does not (Helfrich-Förster, 1995; Helfrich-Förster, 2007; Peschel and Helfrich-Förster, 2011).

While all clock cells interact to produce normal rhythms of behavior, the LNs seem to be the most important pacemakers as they were shown to be both necessary and sufficient for normal locomotor activity rhythmicity (Ewer *et al.*, 1992; Renn *et al.*, 1999). For eclosion rhythmicity, the LNs are necessary, but not sufficient (Myers *et al.*, 2003).

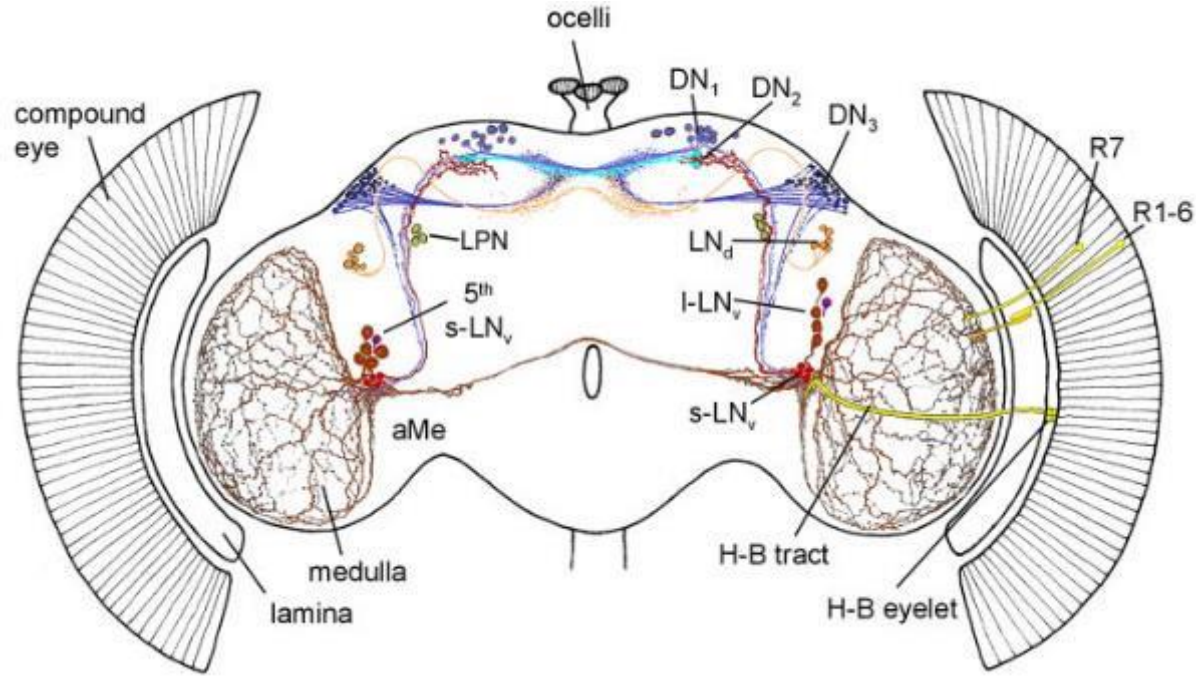

Figure 4: The clock neurons in the adult brain of *Drosophila melanogaster*
The clock neurons can be divided into dorsal (DN) and lateral (LN) neuron clusters. These clusters can be further subdivided into DN1, DN2 and DN3 as well as small ventral lateral neurons (sLNv), large ventral lateral neurons (lLNv), dorsal lateral neurons (LNd) and lateral posterior neurons (LPN). From Helfrich-Förster (2007)

Other tissues outside of the brain were shown to express clock genes that oscillate autonomously (Plautz *et al.*, 1997). As opposed to the central clock in the brain, they are called peripheral clocks and can be found in many tissues, for example in the antennae (Plautz *et al.*, 1997), the Malpighian tubules (Giebultowicz and Hege, 1997), the fat body (Xu *et al.*, 2008) and the prothoracic gland (PG) (Emery *et al.*, 1997). They can be independent of the central clock or coupled to it, but can all be directly entrained by light (reviewed in Ito and Tomioka, 2016).

2.3 Entrainment pathways of the circadian clock

2.3.1 Light entrainment

Drosophila has one internal and three external photoreceptive systems: the blue light receptor Cryptochrome (CRY) as internal photoreceptor and the compound eyes, the ocelli and the Hofbauer-Buchner-eyelets (HB-eyelets) as external photoreceptive structures (Figure 4) (Rieger *et al.*, 2003). The compound eye consist of about 800 ommatidia, each containing 8 photoreceptor cells, called R1 to R8. Each photoreceptor cell expresses one type of rhodopsin (Rh), the visual pigments of the eye. The outer photoreceptor cells R1 to R6 express Rh1, while the inner photoreceptor cells R7 and R8 express RH3 and Rh5 (in the pale type) or Rh4 and Rh6 (in the yellow type), respectively (reviewed in Montell, 2012). The HB-eyelet consists of 4 neurons between the retina and the lamina of the compound eyes (Hofbauer and Buchner, 1989). It develops from the Bolwigs organ, which depicts the photoreceptors in larvae. The HB-eyelet expresses Rh6 and its projections innervate the LNvs (Helfrich-Förster *et al.*, 2002). The ocelli are three simple eyes on the adult head (Goodman, 1970; Hu *et al.*, 1978) that express Rh2 (Pollock and Benzer, 1988). While all three structures were shown to contribute to locomotor rhythmicity under light entrainment, the compound eyes are the main organs to adapt the phase of activity and mediate the masking effect of light (Rieger *et al.*, 2003). Action spectra for eclosion rhythmicity showed a peak of sensitivity between 420 nm and 480 nm, while wavelengths longer than 540 nm could not shift eclosion any more (Frank and Zimmerman, 1969).

CRY is sensitive to light in the UV-A/blue range (Van Vickle-Chavez and Van Gelder, 2007) and is expressed in all five sLNvs, the four lLNvs, in three of the LNds and 8 DN1s, as well as non-clock cells in the adult brain (Benito *et al.*, 2008; Yoshii *et al.*, 2008). The function of CRY in resetting the clock under light entrainment is described in Chapter 2.1. Flies mutant for *cry* can entrain normally to light cycles, but need longer to re-entrain after phase shifts (Emery *et*

al., 1998; Stanewsky *et al.*, 1998) and stay rhythmic under constant light (Emery *et al.*, 2000a; Dolezelova *et al.*, 2007a). Overexpression of CRY in clock cells increases their photosensitivity (Emery *et al.*, 2000b). For eclosion, contradictory results for *cry* mutants have been reported: while Myers *et al.* (2003) reported arrhythmic eclosion (Myers *et al.*, 2003), Mealey-Ferrara *et al.* (2003) and Dolezelova *et al.* (2007a) found eclosion to stay rhythmic (Mealey-Ferrara *et al.*, 2003; Dolezelova *et al.*, 2007b), even under constant light (Dolezelova *et al.*, 2007a). In *cry* mutants, the circadian oscillators in peripheral tissues are largely arrhythmic (Krishnan *et al.*, 2001; Levine *et al.*, 2002) and PER and TIM oscillations in the PG exhibit smaller phase-responses (Morioka *et al.*, 2012).

2.3.2 Temperature entrainment

Temperature is a strong Zeitgeber for *Drosophila*, and an amplitude of 2-3°C is enough to synchronize locomotor activity behavior (Wheeler *et al.*, 1993) and eclosion (Zimmerman *et al.*, 1968b). Temperature cycles can entrain behavior together with light (Yoshii *et al.*, 2009) or under constant darkness (Stanewsky *et al.*, 1998; Yoshii *et al.*, 2002; Yoshii *et al.*, 2005) and even under constant light, that otherwise renders behavior arrhythmic (Yoshii *et al.*, 2002; Glaser and Stanewsky, 2005; Yoshii *et al.*, 2005). This entrainment is clock-dependent, as *per* mutants can merely react to temperature changes, but not entrain any more (Wheeler *et al.*, 1993).

Many tissues and organs express *per* and *tim* (reviewed in Hall, 1995), and their oscillations can be entrained to temperature, implying that temperature entrainment is a cell-autonomous mechanism (Glaser and Stanewsky, 2005). The existence of a cell-autonomous thermoreceptor, comparable to CRY for light detection, was hypothesized (Glaser and Stanewsky, 2005). However, Sehadova *et al.* (2009) reported that isolated brains are able to synchronize to light cycles, but not to temperature cycles. The clock neurons are therefore dependent on input from other neurons or tissues (Sehadova *et al.*, 2009).

Two mutant fly strains have been identified that are not able to entrain to temperature cycles: *norpA* and *nocte* (Glaser and Stanewsky, 2005). *NorpA* encodes for phospholipase C, which plays a role in the thermosensitive splicing of *per* as an adaption to seasonal changes (Collins *et al.*, 2004; Majercak *et al.*, 2004) and is also involved in the phototransduction cascade of the photoreceptors reviewed in Hardie (2001). *Nocte* seems to have a specific function in the entrainment to temperature cycles as flies mutant for *nocte* are still able to entrain to light cycles and their clocks are temperature compensated (Glaser and Stanewsky, 2005).

Knockdown of *nocte* in peripheral tissues impairs their temperature synchronization and leads to arrhythmic behavior (Sehadova *et al.*, 2009). The chordotonal organs (ch organs) were identified to play a role in temperature entrainment, although they possess no functional clock (Sehadova *et al.*, 2009). *Nocte* mutants show strongly deformed ch organs which may cause the observed impairments in temperature entrainment. Further candidates for the entrainment to thermocycles are the DN2 and LPN clock neurons that showed stronger *per* oscillations under temperature cycles than under light cycles (Yoshii *et al.*, 2005; Busza *et al.*, 2007; Miyasako *et al.*, 2007; Picot *et al.*, 2009).

2.4 The clock-related roles of pigment-dispersing factor (PDF)

The neuropeptide pigment-dispersing factor (PDF) was first isolated and characterized in *Drosophila* in 1998 (Park and Hall, 1998) and soon identified as the main output factor of the clock cells in the brain (Renn *et al*., 1999; Helfrich-Förster *et al.*, 2000). Flies mutant for *pdf* or with ablated PDF neurons show arrhythmic locomotor activity (Renn *et al*., 1999) as well as eclosion (Myers *et al.*, 2003) under DD. The same is true when the molecular clock is disrupted in these neurons (Blanchardon *et al.*, 2001) or when PDF is overexpressed (Helfrich-Förster *et al*., 2000). PDF is expressed in the four lLNvs and in four of the five sLNvs (Helfrich-Förster, 1995), as well as in the tritocerebral PDF neurons that arise in the mid-pupal stage and degrade after eclosion (Helfrich-Förster, 1997). Besides PDF, the sLNvs also express the small Neuropeptide F (sNPF) (Johard *et al*., 2009). The receptor of PDF, PDFR or Han, was discovered in 2005 (Hyun *et al.*, 2005; Lear *et al.*, 2005; Mertens *et al.*, 2005) and was shown to be expressed in CRY positive clock neurons and other cells outside the clock network (Hyun *et al.*, 2005; Im and Taghert, 2010; Im *et al*., 2011). Like *pdf* mutants, flies mutant for *han* become arrhythmic under DD (Hyun *et al*., 2005; Lear *et al*., 2005; Mertens *et al*., 2005).

3. Eclosion in *Drosophila melanogaster*

Like all arthropods, *Drosophila melanogaster* has to shed its rigid exoskeleton to be able to grow. This process is called molting. *Drosophila* has three larval stages (L1 to L3), called instars. Each developmental transition from one instar to the next is accompanied by an ecdysis. At the end of the third instar, the larvae start to wander out of the food and pupariate. As a holometabolous insect, *Drosophila* undergoes a complete metamorphosis, and the last ecdysis including the emergence of the adult fly is called eclosion. This critical behavior is

regulated by the interplay of the circadian clock, hormones and peptides that all act together to generate a precisely timed eclosion motor pattern (reviewed in Ewer, 2007).

Although eclosion happens only once in the lifetime of a fly, a clear rhythm in the eclosion of mixed-age populations of flies can be observed. Eclosion profiles show the number of flies that eclosed within a certain timeframe over several days. As the number of eclosed flies changes from day to day and between experiments, the number of flies that eclosed per hour is usually normalized to the total number of flies that eclosed per day, which allows for a comparison of different days during one experiment and between experiments. The percentage of eclosed flies per hour is depicted as a bar. The light or temperature regime, under which the experiment was conducted, is shown in colored rectangles above the eclosion profile.

When pupae are raised under light:dark cycles (LD), most flies eclose during the light phase, and only few during the dark phase. The onset of light is accompanied by a lights-on peak in eclosion, which is a masking effect of the light: a startle response induced directly by the Zeitgeber, but not regulated by the circadian clock (Figure 5).

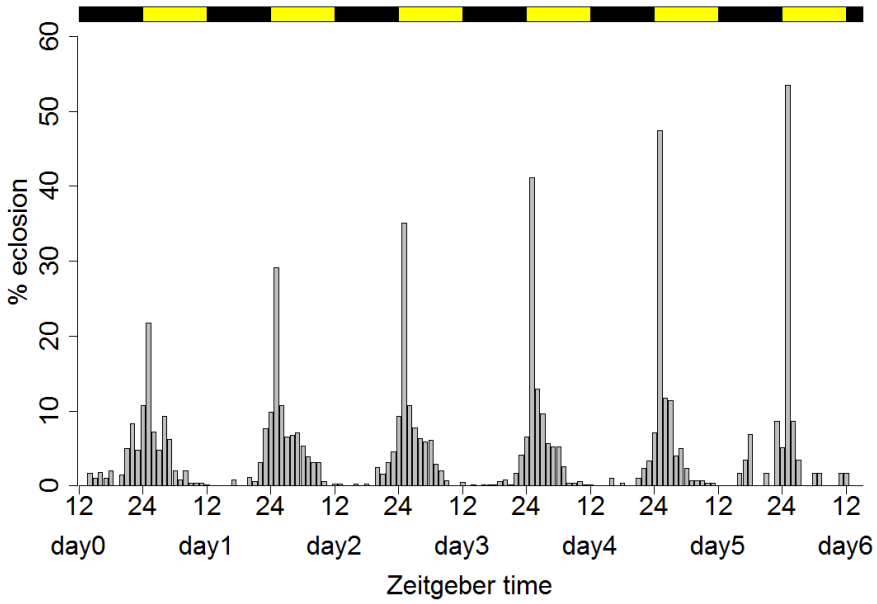

Figure 5: Eclosion rhythm under light:dark conditions (LD)
Eclosion profiles of the control strain w^{1118} under LD conditions. Each bar represents the percentage of eclosed flies per hour normalized to the number of eclosed flies per day. The black and yellow rectangles on top represent the light regime (yellow: light phase; black: dark phase).

As eclosion is a circadian behavior, eclosion rhythms persist also under constant darkness conditions (DD). There are no distinct lights-on peaks any more, and the eclosion events are more broadly distributed. The beginning of the free-run after around two days results in even broader distributed eclosion events. As the free-running period is usually slightly longer than 24 hours, the peaks are shifted a bit later each day. Under constant conditions, the time is no longer defined by the Zeitgeber, and is therefore called circadian time (Figure 6).

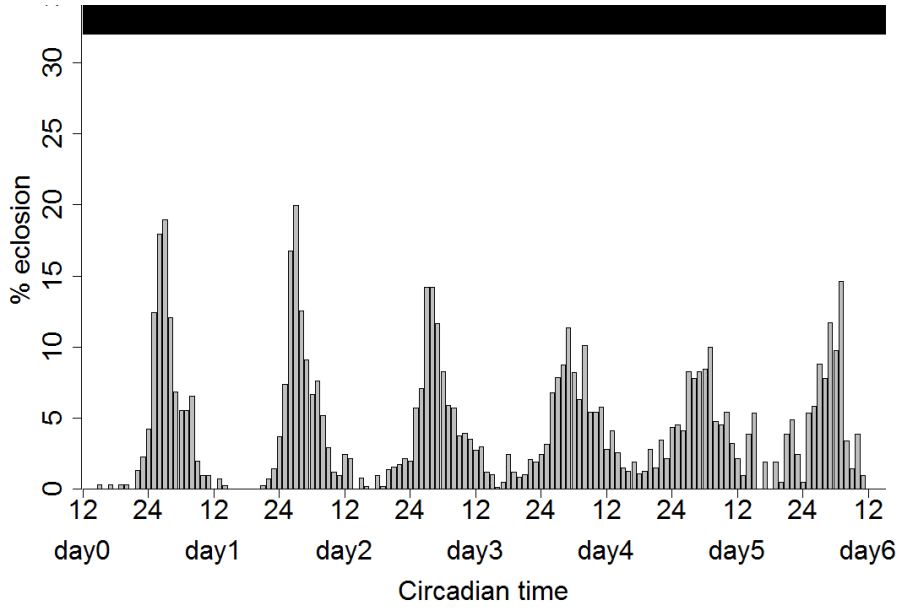

Figure 6: Eclosion rhythm under constant darkness conditions (DD)
Eclosion profiles of the control strain w^{1118} under DD conditions. Each bar represents the percentage of eclosed flies per hour normalized to the number of eclosed flies per day. The black rectangles on top represent the light regime (black: dark phase).

The characterizing features of eclosion rhythms are the amplitude, the period and the gate. The amplitude describes the height of the eclosion peak, i.e. how many flies eclosed during one hour. The period is the time between two eclosion peaks. Under LD conditions it will be synchronized to the given Zeitgeber, while under DD conditions it represents the endogenous free-run period. The gate is the number of hours per day in which eclosion occurs (Figure 7). The gate is the “allowed zone” for eclosion, which is determined by the circadian clock (Pittendrigh, 1954). Flies can eclose only during this gate, and if they reach the pharate state too late at one day after the gate has closed, they have to wait until the gate opens again the next day to eclose (Pittendrigh and Skopik, 1970). Through gating, eclosion is limited to a specific time of the day.

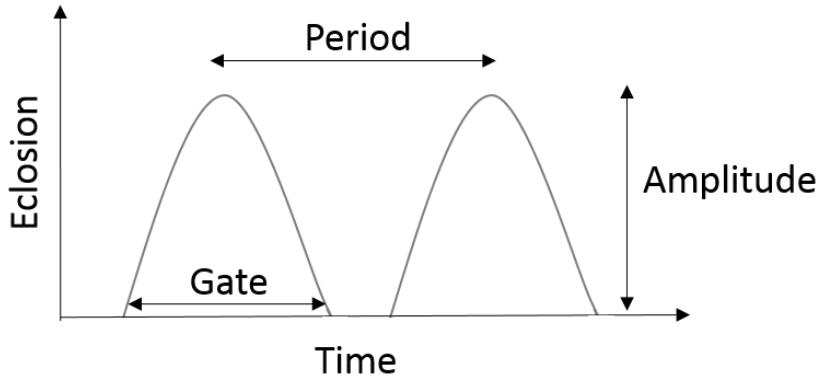

Figure 7: General features of eclosion rhythms
The general features that describe an eclosion profile are the amplitude, that represents the number or percentage of flies that eclosed during one hour; the period, that is defined as the time between two consecutive eclosion peaks; and the gate, which gives the timeframe in which eclosion happens during one day.

3.1 Hormonal regulation of eclosion

The ring gland (RG) of larvae depicts the most important endocrine organ for the regulation of development. It consists of three parts, the prothoracic gland (PG), the corpora allata (CA) and the corpora cardiaca (CC) and is located behind the brain in close association with the aorta (Figure 8). The two main antagonists regulating developmental transitions are Juvenile Hormone (JH), which is produced in the CA, and ecdysone (20E), which is produced in the PG. The production of 20E is induced by the prothoracicotropic hormone (PTTH) via its receptor Torso (for details see Chapter III). Each molt or developmental transition is preceded by a pulse of 20E. As long as JH titers are high, metamorphosis is repressed and the molt ends in the next larval stage. Decreasing JH titers allow 20E to induce the wandering behavior, pupariation, pupal metamorphosis and finally eclosion of the adult fly (reviewed in Di Cara and King-Jones, 2013) (Figure 9). The titers of JH are bound to checkpoints during the development: the threshold size between second and third instar, as well as the minimal viable weight and the critical weight during the last larval stage. These checkpoints ensure the larvae to survive the metamorphosis into a fertile adult. When the checkpoint for critical weight is passed, JH titers decrease and metamorphosis is induced. In contrast, shortweight provokes molting which results in another larval stage (reviewed in Mirth and Shingleton, 2012). The PG was identified as the size-assessing tissue for these checkpoints, as changing the size of the PG influenced the size of the adult fly (Mirth *et al.*, 2005). The PG was reported to be mostly degenerated shortly before eclosion (Dai and Gilbert, 1991), but newer studies indicate that it degenerates only after eclosion (Mareike Selcho, personal communication).

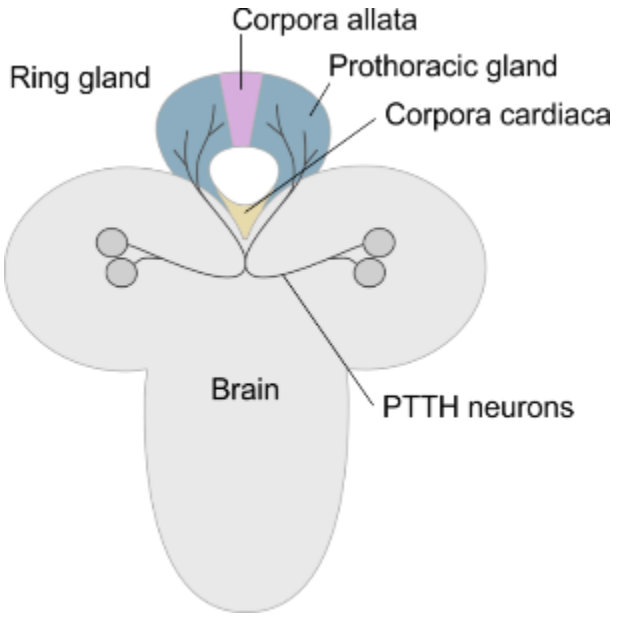

Figure 8: The ring gland (RG) of *Drosophila melanogaster*
The RG is located behind the larval brain and consists of the prothoracic gland (PG; blue-green), the corpora allata (CA; purple) and the corpora cardiaca (CC; yellow). The endings of the prothoracicotropic hormone (PTTH) neurons (grey) terminate on the PG portion of the RG.

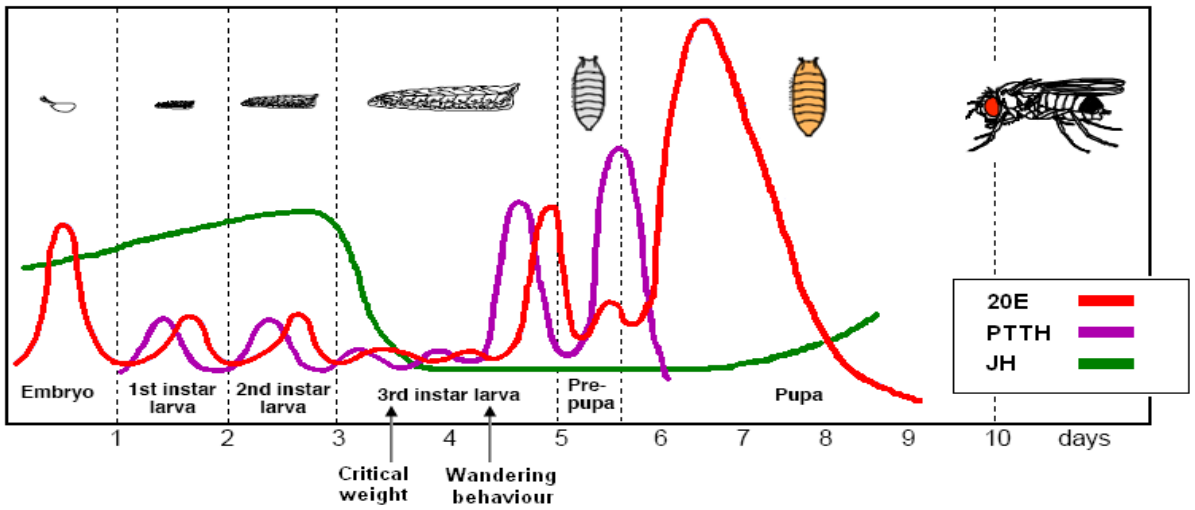

Figure 9: Levels of hormones regulating eclosion during development
Each developmental transition is preceeded by a pulse of ecdysone (20E; red line). As production and secretion of ecdysone is induced by the prothoracicotropic hormone (PTTH; purple line), PTTH peaks can be detected before 20E pulses. As long as titers of the Juvenile Hormone (JH; green line) are elevated, the 20E pulses induce transition to another larval stage. When the critical weight is reached, JH titers decrease and 20E induces wandering behavior, pupariation and eclosion. From Lange *et al.* (2010)

3.2 Circadian regulation of eclosion

The most important clock cells for rhythmic eclosion are the PDF-expressing LNs: overexpression of PDF or disturbance of the molecular clockwork in the LNs as well as their ablation results in arrhythmic eclosion under constant conditions (Helfrich-Förster *et al.*, 2000; Blanchardon *et al.*, 2001; Myers *et al.*, 2003). Observation of *per* and *tim* cycling revealed a functional clock in the PG at the time of eclosion (Emery *et al.*, 1997; Myers *et al.*, 2003) and disruption of this clock leads to arrhythmic eclosion as well (Myers *et al.*, 2003). Therefore, both the central clock in the brain and the peripheral clock in the PG are required to maintain eclosion rhythmicity. Morioka *et al.* (2012) reported that *per* cycling is enhanced by signals from the CNS and that light input to the PG is mediated through the CNS (Morioka *et al.*, 2012). The interconnection of both clocks is unknown, but anatomical studies suggest that the sLNvs innervate the PG indirectly via the PTTH neurons whose endings terminate on the PG (Siegmund and Korge, 2001). It was shown in *Manduca sexta*, *Bombyx mori* and *Rhodnius prolixus* that PTTH is released only during a clock-regulated gate and that the cycling in PTTH release coincides with a cycling of 20E levels (Truman, 1972; Truman and Riddiford, 1974; Ampleford and Steel, 1985; Satake *et al.*, 1998). Whether PTTH and 20E are rhythmically released in *Drosophila* is unknown. The titers of 20E are very low at the end of pupal development (Handler, 1982) (Figure 9), and so far it was not possible to detect 20E synthesis (Dai and Gilbert, 1991) or rhythmic release of 20E (Handler, 1982) on the day prior to eclosion. Another factor influencing eclosion rhythmicity is the RNA-binding protein LARK (Jackson, 1993; McNeil *et al.*, 1998). LARK is expressed pan-neuronally and affects eclosion rhythmicity when overexpressed or knocked down in EH, CCAP or PDF neurons and *tim* expressing cells (Schroeder *et al.*, 2003; Sundram *et al.*, 2012). Neither cell morphology nor clock protein cycling are affected, but PDF neurons show decreased PDF immunoreactivity in *lark* mutants. Therefore, a function in the output of clock cells is suggested (Schroeder *et al.*, 2003). Knockdown of *lark* in the PG also leads to arrhythmic eclosion (Sundram *et al.*, 2012).

3.3 Peptidergic regulation of eclosion in *Drosophila melanogaster*

Each ecdysis is a sequence of specific motor patterns, divided into pre-ecdysis, ecdysis and post-ecdysis behaviors. Eclosion is orchestrated by a signaling cascade of peptides that ensures the right succession of each of these behaviors. The main regulators are ecdysis-triggering hormone (ETH), which is secreted by peripheral epitracheal cells, also called Inka

cells, eclosion hormone (EH) from the Vm neurons in the brain and crustacean cardioactive peptide (CCAP) from CCAP neurons in the brain and thoracic ganglion. ETH and EH form a positive feedback loop, where each peptide induces the release of the other until all stores are depleted (Ewer *et al.*, 1997). Eclosion starts with a release of ETH from the Inka cells (Figure 10 ①) (Zitnan *et al.*, 1996; Ewer *et al.*, 1997) which induces via its receptor the release of EH from the Vm neurons (Figure 10 ②) (Ewer *et al.*, 1997; Kim *et al.*, 2006b). EH then leads to the rapid secretion of ETH from the Inka cells via its receptor (Chang *et al.*, 2009) and an increase of cGMP levels (Figure 10 ③) (Clark *et al.*, 2004). Studies in *eh* null-mutants showed that ETH is secreted normally even without the EH cells and that the first release of ETH was not accompanied by an increase of cGMP levels, suggesting that the initial release of ETH is independent of EH (Clark *et al.*, 2004). In *Manduca sexta*, Corazonin (Crz) was shown to trigger this first release of ETH from Inka cells (Kim *et al.*, 2004) while no comparable starting signal is known in *Drosophila*.

Mainly ETH activates further target neurons via its receptor (Kim *et al.*, 2006a) and thereby promotes together with EH pre-ecdysis (Figure 10 ④) and ecdysis behavior (Figure 10 ⑤). Among the main targets of ETH and EH are the CCAP neurons (McNabb *et al.*, 1997a; Kim *et al.*, 2006b). CCAP inhibits pre-ecdysis behavior and further promotes ecdysis behavior (Figure 10 ⑥) (Gammie and Truman, 1997). CCAP neurons express additionally to CCAP also myoinhibitory peptide (MIP) and bursicon (Kim *et al.*, 2006a; Vömel and Wegener, 2007). While MIP acts together with CCAP to promote ecdysis behavior, bursicon is necessary for post-ecdysis behaviors like sclerotonization, pigmentation and wing inflation (Figure 10 ⑦) (Dewey *et al.*, 2004; Luo *et al.*, 2005; Peabody *et al.*, 2008; Lahr *et al.*, 2012; Kim *et al.*, 2015; Krüger *et al.*, 2015).

Ecdysis must start only at the end of the molt when the old cuticle can be shed and the new cuticle is already synthesized (Ewer, 2007). A main regulator of this timing is 20E, as the increase of 20E levels induces the production of ETH (Zitnan *et al.*, 1999) via an Ecdysone-response element (Park *et al.*, 1999), raises the sensitivity of the CNS to ETH (Zitnan *et al.*, 1999) and regulates the secretory competence of the Inka cells (Kingan and Adams, 2000; Cho *et al.*, 2013). The system is now “armed” and injection of ETH (Zitnan *et al.*, 1996) or EH (Truman *et al.*, 1983) at this stage can induce premature eclosion. But Inka cells become sensitive to EH only after the drop of 20E levels, preventing the positive feedback loop from starting too early (Ewer *et al.*, 1997; Zitnan *et al.*, 1999).

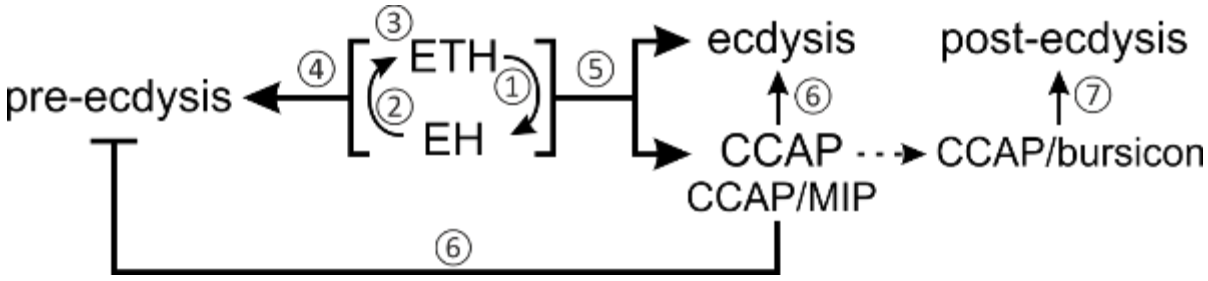

Figure 10: The peptide signaling cascade regulating eclosion behavior
Eclosion starts with an initial release of the ecdysis-triggering hormone (ETH) from the epitracheal Inka cells ① which induces release of the eclosion hormone (EH) from the Vm neurons with somata in the brain ②. EH and ETH form a positive feedback loop and EH promotes complete depletion of ETH ③. EH and ETH activate target neurons and thereby promote pre-ecdysis ④ and ecdysis behavior ⑤. Among their main targets are crustacean cardioactive peptide (CCAP) neurons that also express the peptides myoinhibitory peptide (MIP) and bursicon. CCAP and MIP inhibit pre-ecdysis behavior and further promote ecdysis behavior ⑥. Bursicon is necessary for post-ecdysis behaviors like hardening and pigmentation of the cuticle and wing inflation ⑦. After Ewer (2005).

4. Aim of the present dissertation research

The general aim of this dissertation research is to dissect the connection between the central clock and the peptides regulating eclosion behavior on different organization levels.

The first part focuses on the impact of Zeitgebers and PDF signaling on natural eclosion rhythmicity. To this end, a new eclosion monitoring system was developed to allow the study of eclosion behavior under natural conditions. For the analysis of the complex interactions between clock and environment, a statistical model was established in a collaborative effort within the collaborative research center (CRC) 1047 “Insect timing”.

The second part of the present work focuses on the interaction of the central clock and the peripheral clock in the PG (Emery *et al.*, 1997), as both systems were shown to be necessary for rhythmic eclosion (Myers *et al.*, 2003). The PTTH signaling cascade seemed to be a good candidate pathway for this connection, as PTTH neurons terminate on the PG (Siegmund and Korge, 2001) and their dendrites are in close proximity of arborizations from PDF neurons (McBrayer *et al.*, 2007; Selcho *et al.*, unpublished-a). Indeed, first results from our group implied their role in eclosion rhythmicity (Chen, 2012). Ablation and silencing experiments were conducted under light and temperature entrainment, and possible cycling of *Ptth* mRNA levels was analyzed by means of qPCR. To dissect the connection between the PDF and PTTH neurons, the receptors of the two peptides expressed in PDF neurons, PDF (Helfrich-Förster, 1995) and sNPF (Johard *et al.*, 2009), were knocked down in PTTH neurons. The receptor of

PTTH, Torso, was knocked down pan-neuronally and in the PG and its expression pattern was analyzed by PCR.

The third part of this dissertation research focuses on the connection between the central clock and the peptide cascade regulating eclosion behavior. CCAP is a main promotor of ecdysis behavior (Gammie and Truman, 1997; McNabb *et al.*, 1997a) and the synaptic endings of CCAP-expressing neurons overlap with clock neurons and the PDFTri neurons (Park *et al*., 2003) for which a potential role in the circadian timing of eclosion is hypothesized (Helfrich-Förster, 1997). Ablation of CCAP neurons was shown to impair eclosion rhythmicity (Park *et al.*, 2003) and in a first set these experiments were repeated. During this thesis, a null-mutation for *ccap* was published which showed that CCAP does not affect eclosion rhythmicity (Lahr *et al.*, 2012). This mutant was tested in the present work under light and temperature entrainment as well as under natural conditions for possible consequences on eclosion rhythmicity.

The fourth part of this thesis was designated to identify peptidergic starting signals for eclosion behavior, comparable to the role of Corazonin in *Manduca* (Kim *et al.*, 2004). An optogenetic screen was established in which specific peptidergic neurons were activated to reveal their potential to trigger eclosion.

Materials and Methods

1. Eclosion assays

All flies were raised on standard *Drosophila* food medium (0.8% agar, 2.2% sugarbeet syrup, 8.0% malt extract, 1.8% yeast, 1.0% soy flour, 8.0% corn flour and 0.3% hydroxybenzoic acid). For each eclosion experiment, at least 3 culture vials with a volume of 165 ml (K-TK; Retzstadt, Germany) were prepared with a minimum of 50 flies each. Flies were transferred to new culture vials every 2 to 3 days and were entrained either under LD (see 1.1) or WC conditions (see 1.2). For each experiment, pupae with an age span of one week were used. For experiments under natural conditions, at least 6 culture vials with a volume of 165 ml (K-TK; Retzstadt, Germany) were prepared and flies were transferred to new culture vials twice a week. New adult flies were added regularly to compensate loss of old flies.

1.1 Würzburg Eclosion Monitor (WEclMon)

The eclosion monitors were custom-made by the Biocenter workshop (Johann Kaderschabeck) and the department's electronician Konrad Öchsner. First, eclosion plates were made out of acrylic glass plates with 1,000 2 mm high platforms and a built-in metal frame to reduce static current. Illumination came from below by lighting plates consisting of LED Stripes in red (12V SMD 3528 Red 60 LED/m; λ=635 nm), white (12V SMD 3528 Cool White 60 Led/m; max. emission at λ=450 nm) or infrared (YB-G3528IR60F08N12, IR850, 12V; λ=850 nm) fixed around an acrylic glass plate by a metal frame. For the activation of channelrhodopsin, blue LEDs (LXHL-LB5C 470 nm) were additionally built into the monitors.

As recording cameras, either a Logitech HD - C920 (Logitech, Romanel-sur-Morges, Switzerland) or the board camera Delock 95955 (Tragant Handels- und Beteiligungs GmbH, Berlin, Germany) were used. Camera filters to eliminate normal day light were either 625/30 ET bandpass filters (AHF analysentechnik AG, Tübingen, Germany) for the red LED light with a wavelength of λ=635 nm, or unexposed yet developed photographic film for infrared light. For intervalled image recording the freely available software Yawcam (http://www.yawcam.com) was used. Image and data analysis was performed in FiJi (Schindelin *et al*, 2012) using the "Eclosion bar" macro developed by Martin Fraunholz, Department of Microbiology, University of Würzburg, described in Chapter I.

1.2 Eclosion assays under light entrainment

Flies were raised under a light regime of 12 hours light and 12 hours darkness, with 20°C and 65% relative humidity. 12 to 17 days old pupae were collected and transferred into the monitoring systems. Eclosion was monitored using either the Trikinetics (TriKinetics, Massachusetts, USA) or the WEclMon monitoring systems (for description see Chapter I and Ruf *et al*, in preparation).

For experiments using the TriKinetics monitoring system, pupae attached to the walls of the culture vial were rinsed with water and carefully removed with a spatula. The collected pupae were washed in water to remove rests of the food medium and then separated on filter paper (Whatman® Blotting Papers). After drying, pupae were fixed on plastic eclosion plates using a thinly spread out cellulose-based glue (Auro Tapetenkleister Nr. 389; 1:30). At the end of the light phase, the eclosion plates were mounted on top of glass funnels within the monitors (day 0) and eclosion was monitored for one week at 20°C, either under 12 hours light and 12 hours darkness (LD) or under constant darkness (DD). In the TriKinetics monitoring system, freshly eclosed flies are shaken from the eclosion plate by a tapping solenoid that pushes down the plate and the funnel once every minute. The freshly eclosed flies with folded wings fall through the funnel into beakers filled with water and detergent. While falling through the funnel, the flies interrupt an infrared beam, which is automatically counted by the DAMSystem Collection Software (DAMSystem303) and read out as a text file by the recording computer.

For experiments using the WEclMon monitoring systems, pupae were individually taken out of the culture vial and glued onto a platform on the eclosion plates by a drop of cellulose-based glue (Auro Tapetenkleister Nr. 389; 1:30). At the end of the light phase of day 0, the eclosion plates were mounted in the eclosion monitors and eclosion was monitored for one week at 20°C, either under 12 hours light and 12 hours darkness (LD) or under constant darkness (DD). Infrared light (λ=850 nm) was given throughout the experiment.

1.3 Eclosion assays under temperature entrainment

Flies were raised under constant red light (λ=635 nm) and 65% relative humidity in climate chambers (Plant Growth Chamber, DR-36NL, Percival Scientific, Inc., Perry, USA) and entrained to a temperature regime of 12 hours at 25°C and 12 hours at 16°C. The temperature increase and decrease was ramped by 1°C every 10 minutes. Eclosion was monitored using the WEclMon monitoring systems. After 13 to 18 days, the pupae were individually mounted

on eclosion plates and placed in the monitors. Eclosion was monitored for one week either under 12:12 hours 25°C:16°C (WC) or under a constant temperature of 20°C (CC) as well as 65% relative humidity and constant red light (λ=635 nm) in the same incubators.

1.4 Eclosion assays after optogenetic activation via channelrhodopsin

Flies were raised under constant red light (λ=635 nm) and 65% relative humidity in climate chambers (Plant Growth Chamber, DR-36NL, Percival Scientific, Inc., Perry, USA) and entrained to a temperature regime of 12 hours at 25°C and 12 hours at 16°C. The temperature increase and decrease was ramped by 1°C every 10 minutes. Eclosion was monitored using the WEclMon monitoring systems. After 14 to 19 days, the pupae were individually mounted on eclosion plates and placed in the monitors. Eclosion was monitored for one week under 12:12 hours 25°C:16°C at 65% relative humidity and constant red light (λ=635 nm) in the same incubators. At day one of the experiment, blue light of 586 µW/cm2 (λ=470 nm) was given for one hour at the indicated time point.

1.5 Eclosion assays under natural condition

The experiments under natural conditions were conducted from July to October 2014 in an enclosure at the bee station of the University of Würzburg (Figure S 5). The enclosure was shaded from direct sunlight by bushes and a dark tarpaulin. The walls were lined with insect mesh to allow air circulation and to reduce effects on the relative humidity. The mesh also kept off other insects and birds and, most of all, kept the eclosed flies inside the enclosure where they were caught with sticking paper and vinegar traps. During their whole development, flies were raised in culture vials in the enclosure and prepared for eclosion monitoring once pharate pupae had appeared. Eclosion was monitored using the WEclMon monitoring systems. At the day of preparation, the vials were taken into the lab and pupae were individually transferred onto the platforms of the eclosion plates. On the same day, the ready eclosion plates were then transferred back into the enclosure and mounted in the open WEclMon. Eclosion was monitored for one week under constant red light (λ=850 nm) without further manipulating the pupae. In parallel, temperature, light intensity and relative humidity were measured directly in the eclosion monitors using a datalogger (MSR 145S, MSR Electronics GmbH Seuzach, Switzerland).

1.6 Analysis of rhythmicity

Rhythmicity and period length of the eclosion profiles were analyzed using MATLAB (MathWorks, Inc., Natick, USA) and the appropriate Matlab toolbox (Levine *et al*., 2002). Statistical analysis with one-way ANOVA followed by Tukey post-hoc test and independent-samples t-test were performed with IBM® SPSS® Statistics software (version 20).Graphical output

Graphs of eclosion profiles were compiled in R (version 3.2.0; The R Project for Statistical Computing).

2. Molecular analysis

2.1 Analysis of *torso* expression via Reverse Transcription Polymerase-Chain-Reaction (RT-PCR)

Isolation of total RNA

For total RNA extraction, the Quick-RNA™ MicroPrep Kit from Zymo Research (Irvine, USA) was used and all steps were performed according to the manufacturer´s instruction.

Pharate and adult *Canton S* flies not older than 3 days were dissected in HL3.1 medium (Yanfei Feng, 2004). Central brains, optic lobes and retinae of 15 flies of each group were transferred into 300 µl RNA lysis buffer on ice. Additionally, the gonads of 10 adult males and females, as well as the complete abdomen of 10 male and female pharate flies, were collected in 300 µl RNA lysis buffer on ice. As positive control, brains with ring glands from *Canton S* L3 wanderer larvae were collected and treated the same way. The tissues were mechanically homogenized by means of a plastic pestle. Following washing and centrifugation steps as described in the manufacturer´s manual, total RNA was eluted in 8 µl water.

Reverse Transcription (RT)

For cDNA synthesis, the QuantiTect® Reverse Transcription Kit from Qiagen (Venlo, Netherlands) was used and all steps were performed according to the protocol provided by the manufacturer.

Genomic DNA remnants were removed by adding 1 µl of gDNA wipeout buffer to 6 µl of the eluted RNA. Following incubation at 42°C for 2 minutes, the samples were placed for 2 minutes at 4°C to suppress the reaction. 3 µl mastermix composed of 2 µl RT Buffer, 0.5 µl RT Primer

Mix and 0.5 µl Reverse Transcriptase were added to the RNA and the samples were placed into a thermocycler (MJ Mini, Bio-Rad; Hercules, USA) to perform the following temperature steps: 30 minutes at 42°C, 3 minutes at 95°C and 2 minutes at 4°C. Finally, 40 µl water were added and the cDNA samples were frozen and stored at -20°C.

PCR

To validate the expression of *torso* mRNA in the isolated fly tissues, the reverse-transcribed cDNA was used in a PCR assay. Primers were designed by means of the Primer-BLAST function of NCBI (http://www.ncbi.nlm.nih.gov/tools/primer-blast/) and synthesized by Sigma-Aldrich (Munich, Germany). As a positive control, expression of *α-tubulin* was measured in the same samples. The primer sequences are provided in Table 1. Composition of the PCR reaction mix is presented in Table 2, the PCR temperature program in Table 3. PCRs were performed with a MJ Mini thermocycler (Bio-Rad, Hercules, USA). As negative control, the cDNA was substituted by pure water. The PCR products were separated by agarose gel electrophoresis on a 1% gel (Roti®garose, Agarose Standard; Carl Roth, Karlsruhe, Germany) with the GeneRuler® 100 bp Plus DNA ladder from Fermentas (now ThermoFischer Scientific; Waltham, USA) in a Mini-Sub® Cell GT system from Bio-Rad (Hercules, USA) and documented using the E-Box version 15.05 (Vilber Lourmat; Eberhardzell, Germany) and evaluated with E-Capt version 15.06.

Table 1: Primers used for the analysis of *torso* expression

Target	Primer name	Primer sequence (5'-3')	Product size
torso	torso 7 forward	TCATCGAGAGGGCAACATGG'	667 bp
	torso 7 reverse	CACAGTGGACAGCATCGAGT	
α-tubulin	tubulin forward	TCTGCGATTCGATGGTGCCCTTAAC	198 bp
	tubulin reverse	GGATCGCACTTGACCATCTGGTTGGC	

Table 2: PCR reaction

JumpStart™ REDTaq® ReadyMix™ Reaction Mix (Sigma-Aldrich; Missouri, USA)	12.5 µl
forward primer 10 µM	1 µl
reverse primer 10 µM	1 µl
cDNA template	5 µl
H_2O	5.5 µl
total reaction volume	25 µl

Table 3: PCR program

95°C	5 minutes	
95°C	30 seconds	35 cycles
63°C	30 seconds	
72°C	1 minute	
72°C	5 minute	
4°C	hold	

2.2 Analysis of the temporal expression of *Ptth* mRNA via quantitative Real-time Polymerase-Chain-Reaction (qPCR)

mRNA extraction

For mRNA extraction, the Quick-RNA™ MicroPrep Kit from Zymo Research (Irvine, USA) was used and all steps were performed according to the manufacturer´s protocol.

Canton S flies were reared under a light regime of 12 hours light and 12 hours darkness at a constant temperature of 20°C and 65% relative humidity in big culture vials. Half of the vials were transferred into DD conditions at the end of the light phase after 11 days.

After 17 days, sample collection started. Heads of 20 pharate flies per light regime were collected every 4 hours (ZT 0, ZT 4, ZT 8, ZT 12, ZT 16, ZT 20) in 300 µl RNA lysis buffer and immediately frozen in liquid nitrogen. For the time points at night or under DD, flies were

prepared under red light of λ=635 nm. For each time point, two samples were collected on 5 consecutive days. The tissues were manually homogenized with a plastic pestle. Following the washing and centrifugation steps described in the manufacturer´s protocol, mRNA was eluted in 8 µl water and the mRNA samples were frozen and stored at -80°C.

Reverse Transcription (RT)

For cDNA synthesis the QuantiTect® Reverse Transcription Kit from Qiagen (Venlo, Netherlands) was used and all steps were performed according to the manufacturer´s protocol.

To make sure that every sample contains the same amount of cDNA, the amount of mRNA in each sample was measured by a NanoDrop™ 2000c spectral photometer from ThermoFischer Scientific (Waltham, USA). For each reaction, 1 µg mRNA, diluted in pure water, was used and reverse-transcribed into cDNA. 1 µl gDNA wipeout buffer was added according to the volume of diluted RNA and incubated for 2 minutes at 42°C until the reaction was suppressed by placing the samples for 2 minutes at 4°C. 3 µl mastermix composed of 2µl RT buffer, 0.5µl RT primer mix and 0.5µl reverse transcriptase were added to the mRNA and the samples were placed into a MJ Mini Personal Thermal Cycler from Bio-Rad (Hercules, USA) to perform the following temperature steps: 30 minutes at 42°C, 3 minutes at 95°C and 2 minutes at 4°C. Finally, 40 µl water were added and the cDNA samples were frozen and stored at -20°C.

qPCR

For quantification of *Ptth* mRNA expression, qPCR was performed with the previously obtained cDNA. Specific primers were designed using the Primer-BLAST function of NCBI (http://www.ncbi.nlm.nih.gov/tools/primer-blast/) and synthesized by Sigma-Aldrich (Missouri, USA). *α-tubulin* and *RpL32* were chosen as reference genes for later normalization (Ponton *et al*., 2011). Primer efficiency was tested by a dilution series (1:10^3 to 1:10^6) utilizing the PCR product from a standard PCR for each primer tested. The sequences for the primers used are shown in Table 4. The optimal annealing temperature of 60.5°C for all three primers was determined through a gradient PCR with temperatures ranging from 59°C to 67°C. The ideal cDNA concentration of 100 ng per sample was identified by testing different concentrations between 10 ng and 100 ng. 5 biological replicates were measured in three technical replicates. Additionally, non-template control reactions, for which cDNA was

substituted by water, served as negative controls. qPCR reactions were mixed in Eppendorf® twin.tec PCR 96 well plates and sealed with adhesive Eppendorf® Masterclear real-time PCR film and the qPCR was performed in an Eppendorf Mastercycler (Hamburg, Germany) using the SensiMix™ SYBR® No-ROX Kit from Bioline (London, UK). The qPCR reaction components are shown in Table 5, the qPCR program in
Table 6.

Table 4: Primers for qPCR

Target	Primer name	Primer sequence (5'-3')	Product size	Tm
Ptth	ptth 7 forward	AAAGGTAATCCGAGAGGCGG	136 bp	59.54°C
	ptth 7 reverse	ATAATGGAAATGGGCAACCACG		59.57°C
α-tubulin	tubulin 2 forward	TTTACGTTTGTCAAGCCTCATAG	149 bp	57.14°C
	tubulin 2 reverse	AGATACATTCACGCATATTGAGTTT		57.21°C
RpL32	rpl32 2 forward	ATGCATTAGTGGGACACCTTCTT	130 bp	59.99°C
	rpl32 2 reverse	GCCATTTGTGCGACAGCTTAG		60.47°C

Table 5: qPCR reaction

SensiMix SYBR® No-ROX (Bioline)	10 µl
forward Primer 10 µM	0.8 µl
reverse Primer 10 µM	0.8 µl
cDNA template (for a concentration of 20 ng/µl)	5 µl
H_2O	3.4 µl
total reaction volume	20 µl

Table 6: qPCR program

95°C	2 minutes	
95°C	5 seconds	35 cycles
60.5°C	10 seconds	
72°C	15 seconds	
melting curve		
4°C	hold	

qPCR data analysis

The SYBR-Green fluorescence signal was monitored in real time as amplification curves. A threshold for the fluorescence signal was automatically set by the Eppendorf® Mastercycler ep realplex software version 2.2 (Eppendorf®; Hamburg, Germany) with consideration of the noise band calculation. The number of PCR cycles until the signal surpassed the threshold was determined for each sample (cycle threshold, C_T). The mean C_T value of the technical triplicates was calculated. If values differed from the other C_T values by > 0.5 C_T, they were considered as outlier and excluded from data analysis. As the difference between the reference genes was rather large, calculations were performed separately for each reference gene. For each sample, the ΔC_T value was calculated by subtracting the C_T value of the target gene (*Ptth*) from one of the reference genes. The $2^{-\Delta\Delta CT}$ value was calculated by subtracting the median of the ΔC_T values for each reference gene and light regime from the ΔC_T values ($\Delta\Delta C_T$) and building the negative quadratic term of the $\Delta\Delta C_T$. The mean of the $2^{-\Delta\Delta CT}$ values for each tested time point was plotted with standard deviations. For statistical analysis, a one-way ANOVA was performed between the $2^{-\Delta\Delta CT}$ values for each time point and reference gene for LD and DD conditions. Statistics were performed with IBM® SPSS® Statistics software (Version 20).

3. Fly strains

For targeted expression of transgenes with high spatial control, the GAL4-UAS system was employed (Brand and Perrimon, 1993). This binary system consists of the yeast GAL4 transcriptional activator and its target sequence UAS (Upstream Activation Sequence). Two lines of transgenic flies are created: one comprising the GAL4 cloned downstream of a particular enhancer sequence, and a second including the UAS upstream of an effector gene. By combination of these transgenic flies, effector genes are expressed with a high spatial control in the F1 generation (Brand and Perrimon, 1993). One of the numerous extensions of the GAL-UAS system that was used in this thesis is the selective blocking of the GAL4 via the GAL80 repressor (Suster *et al.*, 2004). The fly strains used in this thesis are summarized in Table 7.

Table 7: Fly strains used in this thesis

Fly strain	Reference
akh-GAL4	Lee and Park (2004), kind gift of Jae Park
w; ap/cyo-GAL4	Bloomington Drosophila Stock Center #3041
AstA-GAL4	Hergarden *et al.* (2012), kind gift of David Anderson
Canton S	Stern and Schaeffer (1943), stock collection
capa-GAL4	Bloomington Drosophila Stock Center #51969
	Bloomington Drosophila Stock Center #51970
CCAP ^{exc7}	Lahr *et al.* (2012), kind gift of John Ewer
ccap-GAL4	Lahr *et al.* (2012), kind gift of John Ewer
w; UAS ChR2-XXL	Dawydow *et al.* (2014), kind gift of Robert Kittel
dh31-GAL4	Bloomington Drosophila Stock Center #51988
	Bloomington Drosophila Stock Center #51989
dh44-GAL4	Bloomington Drosophila Stock Center #39347

	Vienna Drosophila Resource Center VT039046
UAS *dicer2* (II)	Vienna Drosophila Resource Cente #24666
UAS *dicer2 (*III)	Vienna Drosophila Resource Cente #24667
dms-GAL4 8	Sellami *et al.* (2012), kind gift of Jan Veenstra
yw;+;UAS *dORKΔ-C1*	Nitabach *et al.* (2002), Bloomington Drosophila Stock Center #6586
yw;+;UAS d*ORKΔ-NC1*	Nitabach *et al.* (2002), Bloomington Drosophila Stock Center #6587
Eh-Gal4	McNabb *et al.* (1997a), kind gift of John Ewer
elav-GAL4; UAS *dicer*	Bloomington Drosophila Stock Center #25750
w; eth-Gal4	Park *et al.* (2002) , kind gift of Michael Adams
w; UAS *grim*;+	Wing *et al.* (1998), Bloomington Drosophila Stock Center #9923
w^{+}; han^{5304}	Hyun *et al.* (2005), stock collection
hug-GAL4	Bader *et al.* (2007), kind gift of Michael Pankratz
Mai 316-Gal4	Siegmund and Korge (2001), kind gift of Thomas Siegmund
mip-GAL4	*mip*-Gal4-4M (III), stock collection
npf-GAL4	Bloomington Drosophila Stock Center #25683
*nSyb*GAL80	Harris *et al.* (2015)
*nSyb*GAL80; *mip*-GAL4	crossed for this thesis
pdf-GAL4	Renn *et al.* (1999), kind gift of Paul Taghert
w^{+}; pdf^{01}	Renn *et al.* (1999), kind gift of Paul Taghert
UAS *pdfr* RNAi	Vienna Drosophila Resource Center #42724

w^{+}; *per*^{01}	Konopka and Benzer (1971), stock collection
w;+;*phm*-Gal4,UAS-*gfp*/TM6B	Mirth *et al.* (2005), kind gift of Naoki Yamanaka
ptth-Gal4	McBrayer *et al.* (2007), kind gift of Naoki Yamanaka
snpf-GAL4	Bloomington Drosophila Stock Center #202196
w;; UAS *snpfr* RNAi	Bloomington Drosophila Stock Center #27507
tdc-GAL4	Cole *et al.* (2005)
th-GAL4	Friggi-Grelin *et al.* (2003)
trh-GAL4	Sitaraman *et al.* (2012)
w^{1118}	stock collection

Chapter I. Development of a new eclosion monitoring system (WEclMon)

1. Introduction

Eclosion, the emergence of the adult fly from the puparium, is a circadian behavior under regulation of peptides in *Drosophila*. It was among the first rhythmic animal behaviors discovered (Bremer, 1926; Bünning, 1935; Kalmus, 1935; Kalmus, 1938; Kalmus, 1940). Later on, chronobiologists like Pittendrigh, Bruce or Zimmermann used eclosion in *Drosophila* as model behavior to study the properties of circadian clocks (Pittendrigh, 1954; Pittendrigh and Bruce, 1959b; Skopik and Pittendrigh, 1967; Zimmerman *et al.*, 1968a) and eclosion assays were also used to identify the first clock gene *period* (Konopka and Benzer, 1971). Eclosion is an ideal behavioral model to study the coherencies of the internal clock and peptidergic regulatory system as it is not influenced by the motivational state of the animal, or by hunger, aggression, social contacts or reproductive state. As eclosion happens only once in the lifetime of the fly, rhythmicity can only be observed when monitoring in a bigger population of flies of mixed-age.

Over time, different methods have been established to monitor eclosion rhythms. The simplest way is to empty the culture vials in defined intervals and count the number of eclosed flies per hand. Early systems developed were the so-called bang-boxes, where the pupae were glued to metal plates that where mechanically lifted and let fallen down, so that freshly eclosed flies were forced to fall through a funnel into water-filled containers (Engelmann, 2003). These containers were automatically exchanged by a turning device. The U.S. company *TriKinetics Inc.* further developed and refined this system into the commercially available *Drosophila Eclosion Monitor* (http://www.trikinetics.com/). Here, the pupae are glued onto plastic discs which are placed upside-down (pupae facing downwards) on top of a funnel. A small weight periodically “hammers” onto the plastic disc and by that shakes down freshly eclosed flies in fixed time intervals, which fall through a funnel and are automatically counted by crossing an infrared-beam. Although very easy to handle, this system has some disadvantages. For example, the funnels are often blocked, so that experiments cannot be used for analysis. Also it is unclear whether the constant tapping of the pupae has an influence on the eclosion rhythm of the flies. As the TriKinetics monitors are closed systems, they are

not suited to monitor eclosion rhythms under natural conditions, since temperature, humidity and air cannot be freely exchanged.

Therefore a novel open monitoring system was developed that would allow the pupae to come in direct contact with light, temperature and humidity and exclude other experimental influence.

2. Results

2.1 WEclMon

The Würzburg Eclosion Monitor (WEclMon) is a camera-based, open system. This system provides the advantages that pupae can come in direct contact with abiotic environmental factors, like light, temperature and relative humidity. Moreover, no mechanical manipulations are needed as in the Trikinetics Monitors. The WEclMon consists of three parts: a digital camera (Figure 11, a), an eclosion plate (Figure 11, b) and one or two light plates (Figure 11, c, c').

The camera (Figure 11, a) is positioned centrally above the eclosion plate. Essentially any camera can be used, according to the requirements of the experiment. A simple webcam (Logitech C910) was chosen whose resolution was sufficient to reliably and simultaneously monitor eclosion events of a high number of pupae. To take images in certain time intervals, the freely available software Yawcam (http://www.yawcam.com/) was used.

The eclosion plate (Figure 11, b) is an acrylic glass plate with 1,000 2 mm high platforms. Platforms instead of notches were chosen, as otherwise flies often were unable to leave their puparium due to space restrictions. On each platform, one single pupa is placed and fixed with cellulose-based glue, which allows to monitor the eclosion events of 1,000 flies in one experiment.

Illumination comes from the light plates (Figure 11, c, c'), which are positioned below the eclosion plate. Each light plate consists of a LED stripe of a defined wavelength fixed around an acrylic glass plate and a metallic frame to reduce the static current. To be able to monitor eclosion during the night or during the dark phase, respectively, constant red light of a long wavelength is given constantly. In the beginning, a wavelength of λ=635 nm was chosen that flies should not be able to perceive (Salcedo *et al*, 1999) and should not influence their eclosion behavior (Frank and Zimmerman, 1969; Helfrich-Förster, 2002). First results however showed a strong influence on eclosion rhythms after LD entrainment (Figure S 1, Figure S 2). In a new set of monitors, the use of infrared light with a wavelength of λ=850 nm was therefore established. Changes in light intensity, for example at sunrise or sunset or the switch on and off of light, impede the data analysis and give false positive results. Therefore, optic filters optimized for the applied illumination wavelength were added to reduce these

differences in illumination. These were either bandpass filters for the wavelength λ=635 nm or unexposed, yet developed photographic film for infrared light.

All parts of the monitor are assembled on a wooden base and can be covered by a metallic light-tight case, so that each monitor is an independent unit and many can be used in parallel for different experiments.

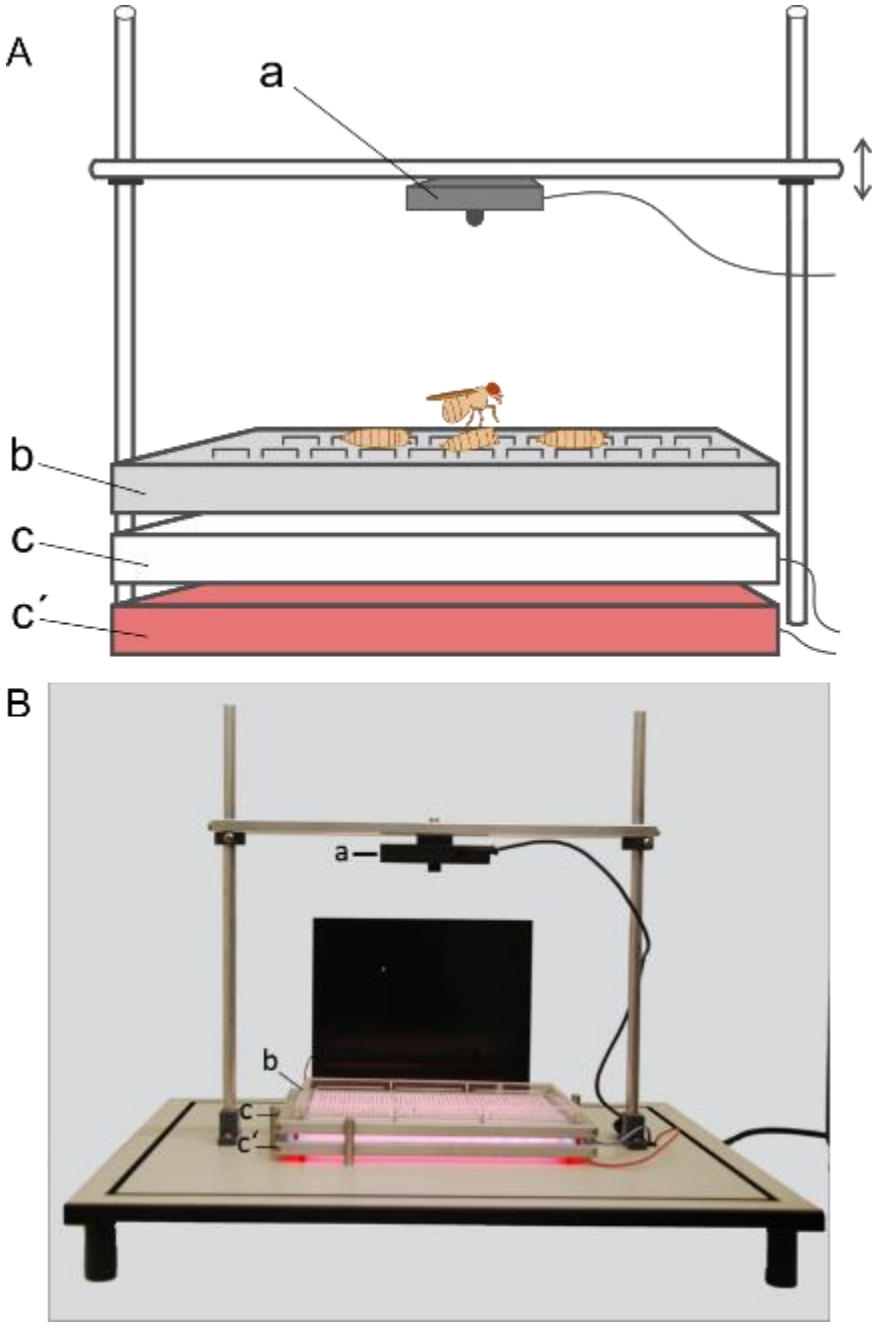

Figure 11: The Würzburg Eclosion Monitor (WEclMon)
Schematic drawing (A) and picture (B) of the Würzburg Eclosion Monitor (WEclMon). It consists of a simple camera (a) centered above the eclosion plate, on which the pupa are glued (b). Illumination comes from the light plates (c, c') below. One light plate gives white light for entrainment (c), the other gives constant red light (λ=635 nm/ λ=850; c') as illumination for the camera.

2.2 FiJi macro

For analysis of the recorded images and eclosion detection, a macro for ImageJ/FiJi was developed by Martin Fraunholz, Microbiology, University of Würzburg. It is based on the fact that after eclosion, the fly leaves behind an empty puparium, which is more light-permeable ("brighter") than a puparium with a pharate fly inside (and thus "darker"). An eclosion event can therefore be identified by a change of intensity values of the illumination coming from below.

The recorded images in the png format were opened as image stack in FiJi, converted to 8-bit grey scale and the contrast was enhanced (saturated=10). To minimize effects of different light conditions, the background was subtracted from each image using the rolling ball algorithm (diameter: 4, light background). Each pupae was identified by setting of the intensity threshold and subsequent particle analysis (size range 10 pixels to infinity) after conversion into binary images. Square regions of interest (ROI) with a side-length of 15 pixels were defined around the center of each particle and added to the ROI manager. Each ROI had to be aligned and false-positive ROIs had to be removed manually. The MultiMeasure function could then monitor the intensity of each ROI over the time course of the recorded images. The macro then analyzed the resulting changes in intensity values between two consecutive time points in each ROI. If a defined threshold of intensity changes between two images was crossed, this was registered as an eclosion event and the according ROI was highlighted. Two strategies were applied to prevent false-positive results: first, a ROI in which an eclosion event had been registered could not be registered again. Second, it was manually checked that each highlighted ROI actually fitted to an empty puparium on the eclosion plate.

2.3 Comparison of eclosion profiles recoreded in the WEclMon system and the TriKinetics system

To test whether the WEclMon system is able to reliably record eclosion rhythmicity, eclosion profiles of two wildtype strains, *Canton S* and *Lindelbach*, were recorded with the WEclMon and the commercially available TriKinetics system and the results were compared (Figure 12 - Figure 15).

For *Canton S,* no difference in the eclosion profiles between the two monitor systems could be observed, neither under LD conditions (Figure 12) nor under constant conditions (Figure 13). There was also no significant difference between the rhythmicity indices under either condition (Figure 12 C, Figure 13 C) or the period lengths under constant conditions (Figure S 3).

For the second wildtype, *Lindelbach*, there were no differences between the eclosion profiles recorded in the two monitoring system und either condition (Figure 14, Figure 15). No significant difference could be observed between the rhythmicity indices under LD conditions (Figure 14 C), while under DD conditions the rhythmicity index in the WEclMon is decreased compared to the results from the Trikineitcs (Figure 15 C). There was no significant difference between the period lengths however (Figure S 3).

2.4 The wildtypes *Canton S* and *Lindelbach* under temperature entrainment

To test if the WEclMon system is suitable for the monitoring of eclosion under temperature entrainment, flies were entrained to cycles of 12 hours at 25°C and 12 hours at 16°C, with constant relative humidity of 65% and under constant red light of λ=635 nm.

The wildtypes *Canton S* and *Lindelbach* showed normal eclosion rhythms under WC conditions (Figure 16). Although no statistical significance could be observed, *Lindelbach* showed a trend to be less rhythmic than *Canton S* (Figure 16 C). This can also be seen in the eclosion profiles, as the peaks were not as high and the eclosion gate was broader in *Lindelbach* (Figure 16 B) compared to *Canton S* (Figure 16 A). In both wildtypes, the eclosion peaks occurred in the cold phase, before the beginning of the temperature increase (Figure 16 A, B). Under constant conditions, *Canton S* became distinctly less rhythmic and *Lindelbach* became arrhythmic (Figure 17). There is no significant difference between the period lengths of both wildtypes observable (Figure S 4)

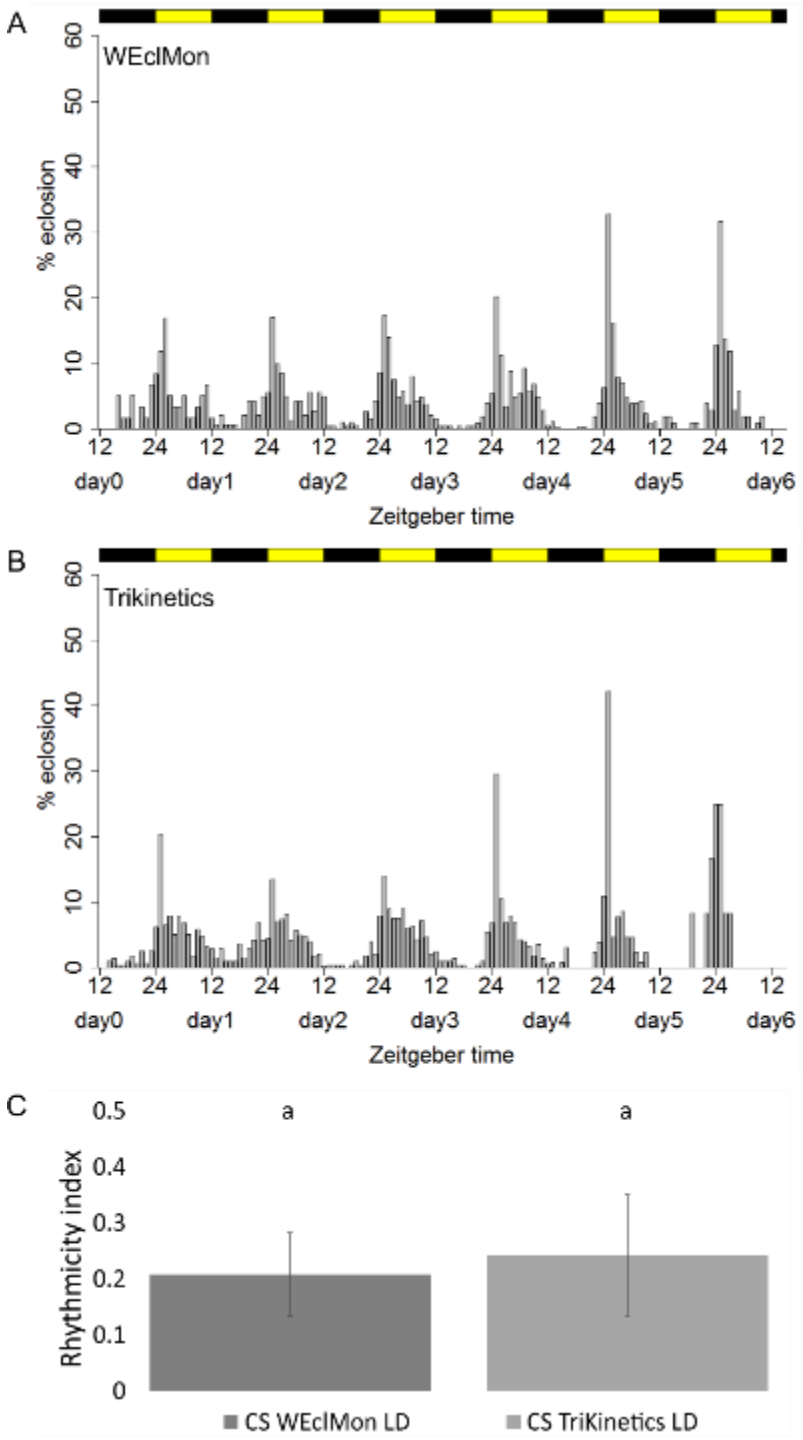

Figure 12: Comparison between eclosion profiles of the wildtype *Canton S* recorded with the WEclMon and the TriKinetics system under LD conditions

Eclosion profiles of the wildtype *Canton S* recorded with the WEclMon (A) and the TriKinetics (B) system under LD conditions. Each bar represents the percentage of eclosed flies per hour normalized to the number of eclosed flies per day. The black and yellow rectangles represent the light regime. (C) shows the means of the rhythmicity indices (±SD). Different letters above columns indicate significant difference ($p<0.05$). Experiments in the WEclMon were performed under constant infrared light. (N=6, 4; n=942, 1346)

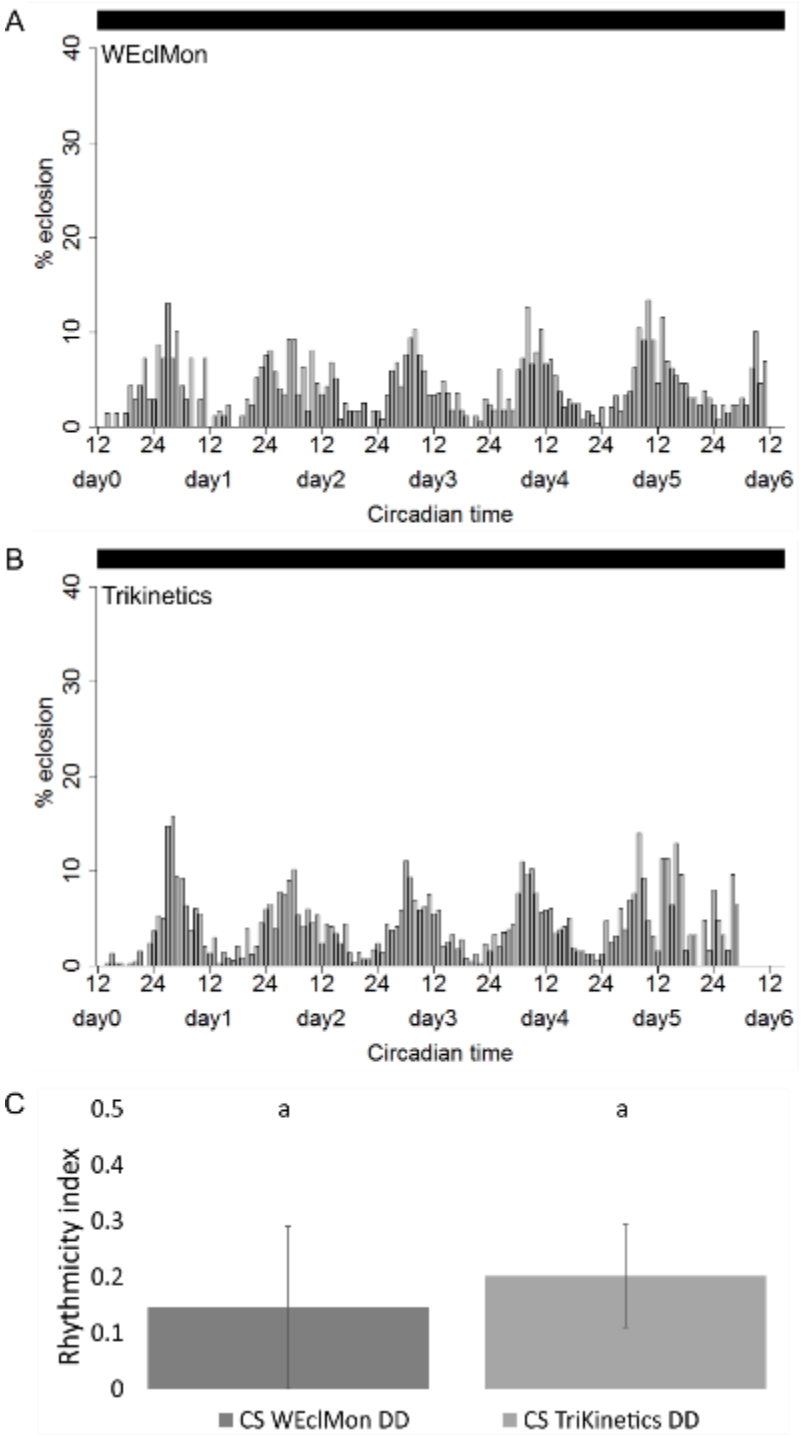

Figure 13: Comparison between eclosion profiles of the wildtype *Canton S* recorded with the WEclMon and the TriKinetics system under DD conditions

Eclosion profiles of the wildtype *Canton S* recorded with the WEclMon (A) and the TriKinetics (B) system under DD conditions. Each bar represents the percentage of eclosed flies per hour normalized to the number of eclosed flies per day. The black rectangles represent the light regime. (C) shows the means of the rhythmicity indices (±SD). Different letters above columns indicate significant difference ($p<0.05$). Experiments in the WEclMon were performed under constant infrared light. (N=5, 4; n=891, 1768)

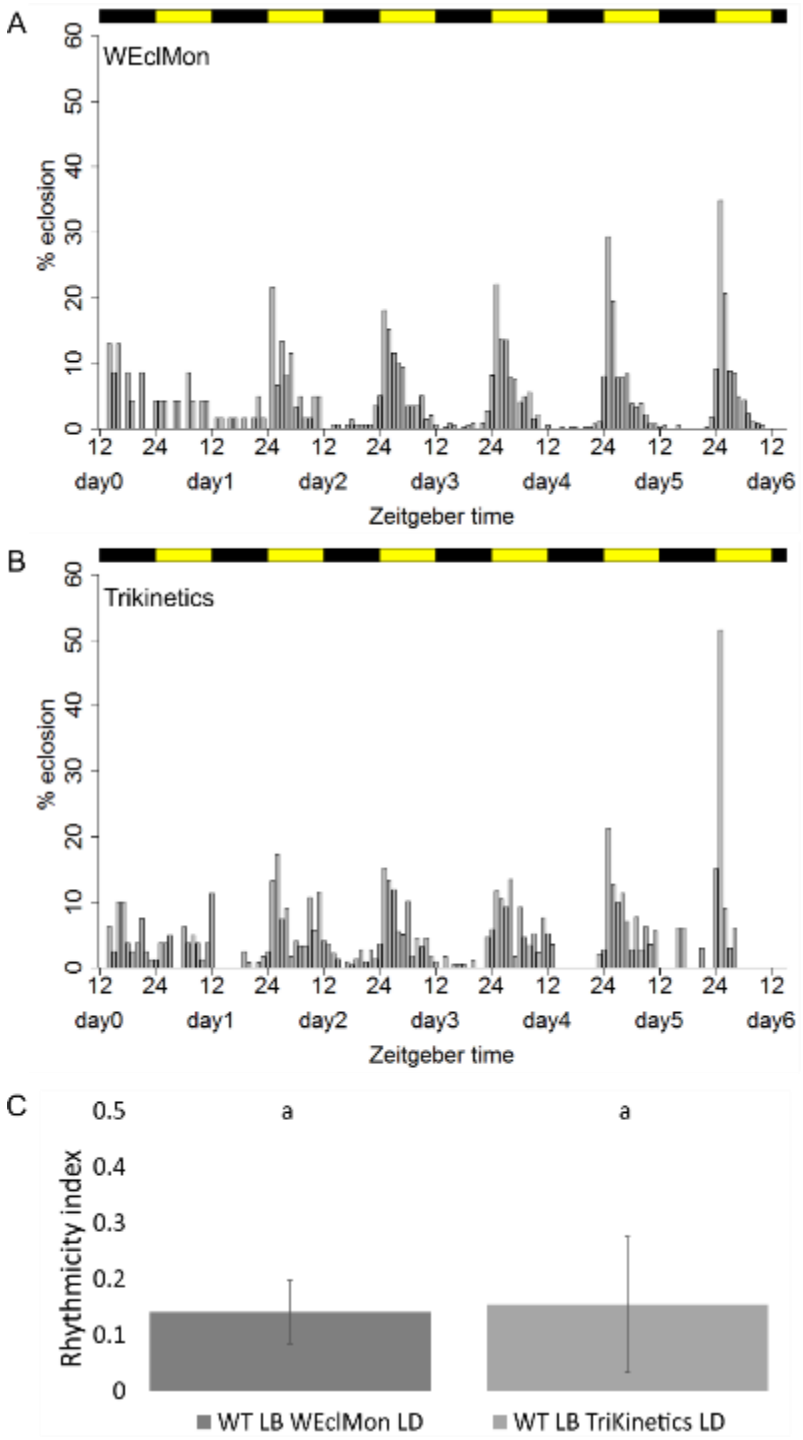

Figure 14: Comparison between eclosion profiles of the wildtype *Lindelbach* recorded with the WEclMon and the TriKinetics system under LD conditions

Eclosion profiles of the wildtype *Lindelbach* recorded with the WEclMon (A) and the TriKinetics (B) system under LD conditions. Each bar represents the percentage of eclosed flies per hour normalized to the number of eclosed flies per day. The black and yellow rectangles represent the light regime. (C) shows the means of the rhythmicity indices (±SD). Different letters above columns indicate significant difference ($p<0.05$). Experiments in the WEclMon were performed under constant infrared light. (N=6, 4; n=1233, 762)

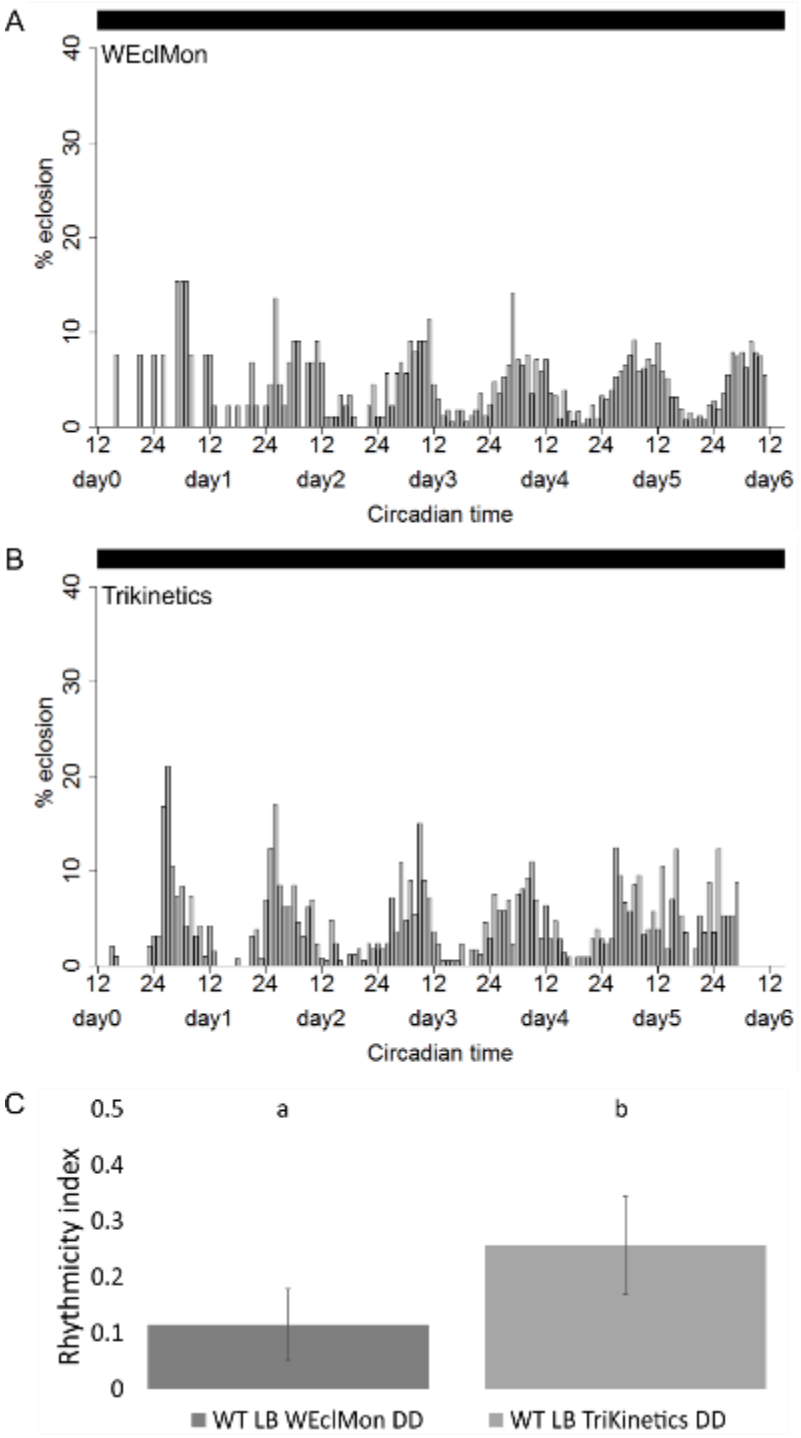

Figure 15: Comparison between eclosion profiles of the wildtype *Lindelbach* recorded with the WEclMon and the TriKinetics system under DD conditions

Eclosion profiles of the wildtype *Lindelbach* recorded with the WEclMon (A) and the TriKinetics (B) system under DD conditions. Each bar represents the percentage of eclosed flies per hour normalized to the number of eclosed flies per day. The black rectangles represent the light regime. (C) shows the means of the rhythmicity indices (±SD). Different letters above columns indicate significant difference ($p<0.05$). Experiments in the WEclMon were performed under constant infrared light. (N=5, 3; n=872, 828)

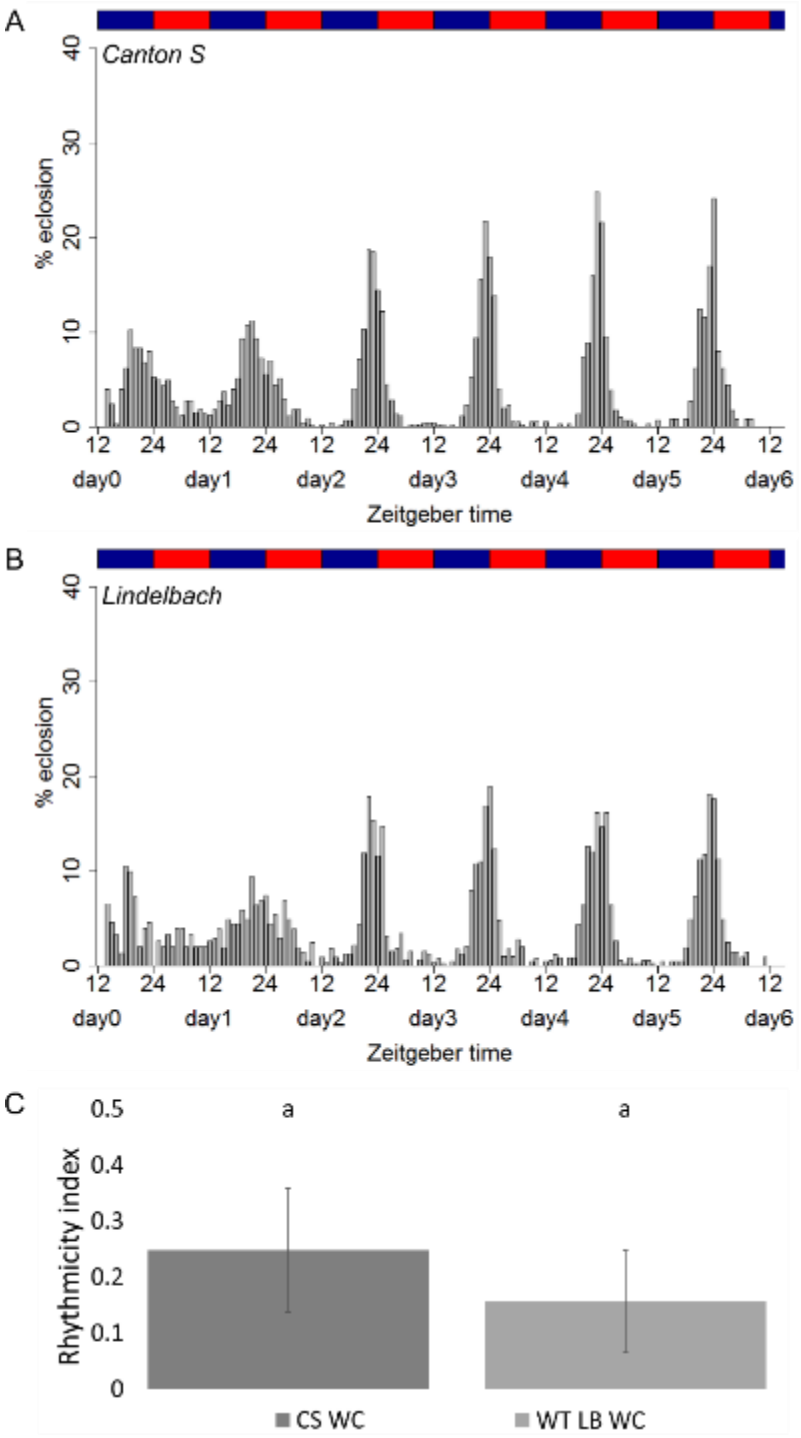

Figure 16: Eclosion rhythms of the wildtypes *Canton S* and *Lindelbach* under WC conditions

Eclosion profiles for populations of the wildtypes *Canton S* (A) and *Lindelbach* (B) under WC (25°C:16°C) conditions. Each bar represents the percentage of eclosed flies per hour normalized to the number of eclosed flies per day. The blue and red rectangles represent the temperature regime. (C) shows the means of the rhythmicity indices (±SD). Different letters above columns indicate significant difference ($p<0.05$). Experiments were performed under constant red light. (N=12, 6; n=1948, 1684)

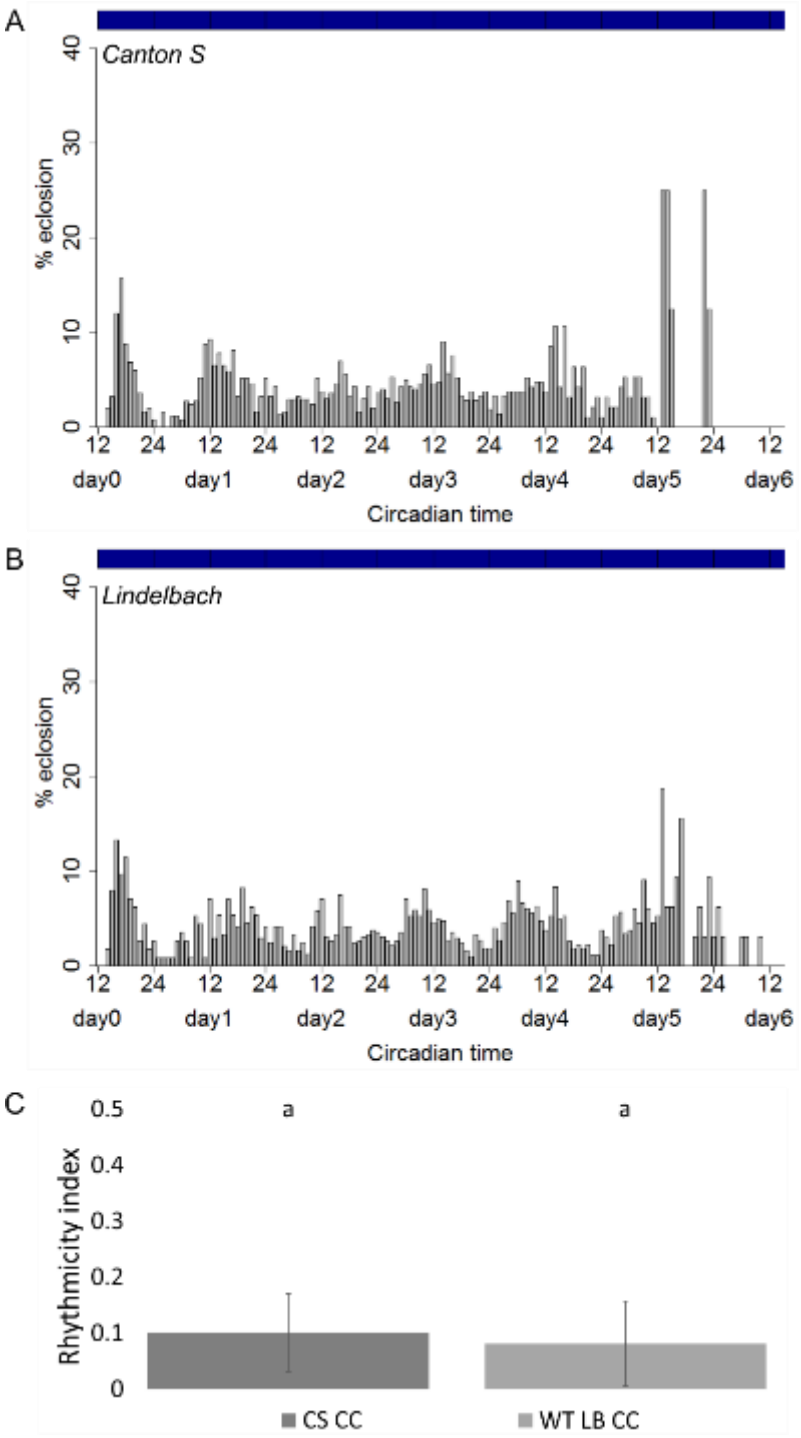

Figure 17: Eclosion rhythms of the wildtypes *Canton S* and *Lindelbach* under CC conditions

Eclosion profiles for populations of the wildtypes *Canton S* (A) and *Lindelbach* (B) under CC (20°C) conditions. Each bar represents the percentage of eclosed flies per hour normalized to the number of eclosed flies per day. The blue rectangles represent the temperature regime. (C) shows the means of the rhythmicity indices (±SD). Different letters above columns indicate significant difference ($p<0.05$). Experiments were performed under constant red light. (N=8, 6; n=1234, 1583)

3. Discussion

The results show that the WEclMon is a reliable new system for monitoring eclosion rhythms. For the two tested wildtypes, *Canton S* and *Lindelbach*, no difference was observable between the eclosion rhythms under LD conditions between the WEclMon and the TriKinetics monitoring system. Under DD conditions, the *Lindelbach* strain eclosed less rhythmic in the WEclMon than in the Trikinetics monitors, whereas there were no significant differences for *Canton S* observable. With the WEclMon, there is no undesirable impact on the flies' eclosion by mechanical tapping as used in the Trikinetics system. Once the pupae are put inside the monitor, they are not manipulated anymore, excluding any distortion of the resulting rhythms. Moreover, as it is an open system, the pupae are immediately and directly exposed to all changes in their direct environment. The monitor is made of commercially available components and presents a low-cost alternative to commonly available systems. It can be easily adapted for other applications, for example observation of other *Drosophila* behaviors like pupariation or the monitoring of behaviors and rhythms in other model organisms. As the system is camera-based, there is no data loss due to funnels blocked by stucked flies. By comparing the empty pupariums on the plate to the outcome from the image analysis after the experiment, it is possible to achieve data with virtually no false positive results.

Tests also showed that the WEclMon system is suitable for eclosion monitoring under temperature entrainment. Both wildtypes were able to entrain to temperature cycles of 25°C:16°C. Under a constant temperature of 20°C, however, both wildtypes became severely less rhythmic. While *Canton S* still showed weakly rhythmic behavior, eclosion in *Lindelbach* became arrhythmic. Other strains tested under the same conditions performed better and showed higher rhythmicity indices (compare Figure 51and Figure 71). Why especially *Lindelbach* shows arrhythmic behavior under constant temperature conditions remains unclear. A possible explanation could be that the *Lindelbach* strain is not as susceptible for temperature cycles and therefore cannot entrain to them as well as others. All strains tested showed reduced rhythmicity under constant temperature after temperature entrainment, while the flies had no problems in adapting their behavior to temperature cycles. The eclosion peaks always lie in the cold phase before the temperature increase, excluding a mere masking effect. This leads to the conclusion that temperature is not as strong a Zeitgeber as light is, at least for eclosion.

Chapter II. Eclosion rhythms under natural conditions

1. Introduction

Drosophila melanogaster was introduced for laboratory use at the beginning of the 20th century with studies on the effects of inbreeding and crossbreeding on the female fertility and viability (Castle *et al.*, 1906) and on the role of chromosomes in heredity (Morgan, 1910; Morgan, 1911). Since then, *Drosophila* served as a model organism in numerous studies concerning processes of evolution, cell and developmental biology and neurobiology and was used in the Nobel Prize winning works from Thomas Hunt Morgan, Herman J Muller, Edward B. Norris, Christiane Nüsslein-Vollhard and Eric F Wischaus as well as Jules Hoffman. Still, little is known about its natural biology and ecology.

Drosophila melanogaster was first described by the German entomologist Johann Meigen in 1830. It has originated in the tropical Africa south of the Sahara (Lachaise *et al*., 1988) and colonized Europe and Asia about 15,000 years ago. It was brought to America and Australia some hundred years ago by humans, mainly in the course of the slave trade (David and Capy, 1988). *D. melanogaster* and *D. simulans* are the only members of the genus *Drosophila* that can be found on every continent and most islands worldwide and have adapted to both tropical and temperate climates (David and Capy, 1988; Markow and O'Grady, 2005b; Markow, 2015). *D. melanogaster* is associated with decaying fruit, vegetables and other plant matter (Markow, 2015) and "lives where it eats" (Reaume and Sokolowski, 2006). Courting, mating, oviposition and the development all happen on and within the food source (Reaume and Sokolowski, 2006). The pupae can be found in close vicinity to fruits: on or underneath the cuticle, directly under the fruit or in surrounding soil. The distribution of pupae depends on the humidity of fruit and soil and whether the larvae are of the "rover" or "sitter" genotype (Reaume and Sokolowski, 2006; Beltramí *et al.*, 2009). While it is still unclear whether *D. melanogaster* die in cold winters and recolonize locations again in warmer months in Europe, it was shown that they can enter a diapause state regulated by photoperiod and temperature (Saunders *et al*., 1989), and that they overwinter as diapausing adults in Northern America (Schmidt *et al.*, 2005). As cosmopolitan species, *D. melanogaster* adapted to many different climates, ranging from tropical regions with rather stable conditions to temperate regions with seasonal changes of climate conditions. This adaption lead to latitudinal clines of different

traits, for example of morphological and behavioral traits (David and Capy, 1988): *Drosophila* in the wild have, as compared to those kept in the lab, a different body size (smaller: James *et al.* (1997), bigger: Chown and Gaston (2010)), are associated with more microbes (Chandler *et al*., 2011) and show a different courtship and mating behavior (Markow, 2015). Also, the clock shows multiple adaptations to different climatic conditions. On the anatomical level, it was shown that *Drosophila* species that are more common in the north do not express CRY in the lLNvs and only reduced levels of PDF in the sLNvs, as compared to more southern species (Hermann *et al.*, 2013). The clock protein PER carries a region of threonine-glycine repeats (Thr-Gly) of different length, influencing the rhythmicity behavior (Yu *et al*., 1987a). The longer $(Thr\text{-}Gly)_{20}$ alleles are dominant in populations in northern Europe (Costa *et al*., 1992). Flies carrying these alleles show a reduced period slightly shorter than 24 hours and are insensitive to temperature changes (Sawyer *et al.*, 1997). The shorter $(Thr\text{-}Gly)_{17}$ alleles are found mainly in southern Europe (Costa *et al.*, 1992) and flies with this variant have a 24 hours period at high temperatures that shortens under reduced temperatures (Sawyer *et al.*, 1997). Furthermore, splicing of *per* is influenced by temperature. Under low temperatures, the splicing of an intron that advances the phases of *per* mRNA and protein levels is enhanced, which leads to a more diurnal behavior of the flies (Majercak *et al.*, 1999). Under high temperatures, however, expression of alternative splice variants results in a prolonged midday siesta, thus flies avoid high midday temperatures (Low *et al.*, 2008). Under natural conditions, the *per* mRNA cycles only in summer, while *tim* mRNA shows cycling throughout the year (Montelli *et al*., 2015). It could also be shown that the expression of PER protein changes throughout the seasons whereas levels of TIM protein stay more constant (Menegazzi *et al.*, 2013). It is therefore hypothesized that it is mainly PER that couples behavioral to seasonal changes (Rivas *et al*., 2015) although it was shown that *per* is not involved in the photoperiodic measurement regulating diapause (Saunders *et al*., 1989; Saunders, 1990). Also, the second clock gene *tim* shows a polymorphism specific for geographic regions. In fly populations of southern Europe, the *ls-tim* allel dominates and encodes for a long and a short TIM protein, while in populations of northern Europe, the *s-tim* allel dominates, which leads to an expression of only the short TIM (Rosato *et al.*, 1997; Sandrelli *et al*., 2007; Tauber *et al*., 2007). Flies carrying the *ls-tim* have a reduced photosensitivity (Sandrelli *et al*., 2007) and females show higher levels of diapause under long days (Tauber *et al.*, 2007). Therefore, the *ls-tim* would rather be expected to be found in the north, where flies would be less sensitive to

constant light during midsummer or the loss of light in winters, than in the south (Kyriacou *et al*., 2008). This discrepancy can possibly be explained by the fact that the *ls-tim* mutation arose only 8,000 years ago in southern Italy and has yet not spread so far (Tauber *et al.*, 2007).

Although it was shown in *D. littoralis* that there is an adaptive latitudinal cline in the eclosion rhythm (Lankinen, 1986), most experiments under laboratory conditions reflect the rather stable conditions at lower latitudes and ignore the more fluctuative conditions at higher latitudes. Yet the daily behavior of an animal is influenced by the circadian pacemaker and by responses to immediate environmental changes. Observations made on animals kept in the laboratory therefore often differ dramatically from results obtained under natural or semi-natural conditions. This could be shown for hamsters (Gattermann *et al*., 2008) and mice (Daan *et al.*, 2011), that became diurnal under natural conditions while they are nocturnal in the laboratory, as well as for the locomotor activity (Vanin *et al*., 2012) and the eclosion behavior (De *et al*., 2012) of *D. melanogaster*. Vanin *et al.* (2012) could show that clock mutant flies were not arrhythmic any more under seminatural conditions, but instead showed high levels of rhythmicity. The group also reports that under high temperatures, the typical midday siesta was replaced by an additional activity peak that was previously observed in the per^{s} mutant and therefore seems to be under clock control. Moreover, the flies were no longer crepuscular but became diurnal under seminatural conditions (Vanin *et al.*, 2012). De *et al.* (2012) also found that the robustness of eclosion was increased under semi-natural conditions, as compared to laboratory conditions and even otherwise arrhythmic clock mutants eclosed rhythmically (De *et al.*, 2012).

All behaviors are influenced by multiple factors, for example interaction with other individuals or with predators, the hunger state or the drive for sexual reproduction. Eclosion however is free of motivational states and inter-individual interactions, thereby allowing a clearer study of the underlying factors. It is therefore an ideal model to study the influence of the clock and abiotic factors on the rhythmicity of behavior. To this end, the wildtype strain *Canton S* and the clock mutant per^{01} as well as the clock output mutants pdf^{01} and han^{5304} were reared and their eclosion behavior was monitored under natural conditions using the newly developed WEclMon system (see Chapter I). Statistical modelling was applied to assess the importance of the clock and the generally accepted Zeitgebers light and temperature, as well as of the potential Zeitgeber relative humidity. Furthermore, the new local wildtype strain *Hubland* was established.

2. Results

The experiments under natural conditions were conducted from July to October 2014 in an enclosure at the bee station of the University of Würzburg (Figure S 5). Eclosion was monitored using the newly developed WEclMon system (see Chapter I).

Four different genotypes were tested: the wildtype *Canton S*, the clock mutant per^{01} as well as the PDF-signaling mutants pdf^{01} and han^{5304}.

The per^{01} mutant carries a point mutation in the *per* gene (Yu *et al.*, 1987b) which leads to a non-functional protein (Stanewsky *et al.*, 1997). As per^{01} mutant flies have no intact clock, they eclose arrhythmically under constant conditions (Konopka and Benzer, 1971). Therefore, they were chosen to study the impact of the clock on the eclosion rhythmicity under natural conditions.

The pdf^{01} mutant carries a nonsense mutation in the *pdf* gene which converts the Tyr at residue 21 into a stop codon (Renn *et al.*, 1999). PDF is the main output factor of the central clock and a synchronizing signal within the clock network (reviewed in Helfrich-Förster, 2007; Shafer and Yao, 2014). Pdf^{01} mutant flies were shown to eclose arrhythmically under constant conditions (Myers *et al.*, 2003). Han is the PDF receptor and expressed in CRY positive clock neurons and other cells outside the clock network (Hyun *et al.*, 2005; Im and Taghert, 2010; Im *et al.*, 2011). The han^{5304} mutant carries a deletion of the transmembrane domain at the C-terminus of the expressed Han protein (Hyun *et al.*, 2005). Han^{5304} mutant flies eclose less rhythmic under constant conditions (Figure S 12 B, C; Figure S 13 B, C). Both mutants were chosen to study the role of PDF and the importance of synchronization between clock cells for eclosion under natural conditions.

The number of eclosed flies and the rhythmicity index for each strain per experiment is summarized in Table 8 and Table 9.

Table 8: Summary of the number of eclosed flies per experiment under natural conditions

	17.07.-24.07. 2014	24.07.-31.07. 2014	31.07.-07.08. 2014	07.08.-14.08. 2014	21.08.-28.08. 2014	28.08.-04.09. 2014	04.09.-11.09. 2014	11.09.-18.09. 2014	25.09.-02.10. 2014
Canton S	488	292	537	736	366	664	1036	764	582
per^{01}			576	210	222	258	298	358	316
pdf^{01}	178		323	234	132	271	299	354	
han^{5304}	280	171	241	256	135	246	330		291
$CCAP^{exc7}$			362	263	235	289	351		
$CCAP^{+}$			317	158	199	322	343		

Table 9: Summary of the rhythmicity indices per experiment under natural conditions (RI<0.1 arrhythmic; 0.1≤RI≤0.3 weakly rhythmic; RI>0.3 rhythmic)

	17.07.-24.07. 2014	24.07.-31.07. 2014	31.07.-07.08. 2014	07.08.-14.08. 2014	21.08.-28.08. 2014	28.08.-04.09. 2014	04.09.-11.09. 2014	11.09.-18.09. 2014	25.09.-02.10. 2014
Canton S	0.04	0.21	0.28	0.1	0.25	0.17	0.07	0.27	0.1
per^{01}			0	0	0.21	0.07	0.04	0.09	0.01
pdf^{01}	0.04		0.14	0.34	0.12	-	0:03	0.2	
han^{5304}	0.06	0.21	0.23	0.03	0.22	-	0.06		0.35
$CCAP^{exc7}$			0.33	-	0.3	0.06	0.19		
$CCAP^{+}$			0.1	-	0.2	0	0.05		

2.1 Humidity entrainment

To assess whether humidity can potentially act as a Zeitgeber for eclosion, *Canton S* flies were entrained to humidity cycles of 12 hours 70% and 12 hours 30% relative humidity under constant red light (λ=635 nm) at 20°C. Under these conditions, flies eclosed completely arrhythmically and showed no preference to either the wet or the dry phase (Figure 18 A). This was also shown in the mean of the rhythmicity index that shows a value of 0 and signifies arrhythmicity. The wildtype flies were therefore not able to use humidity as a Zeitgeber.

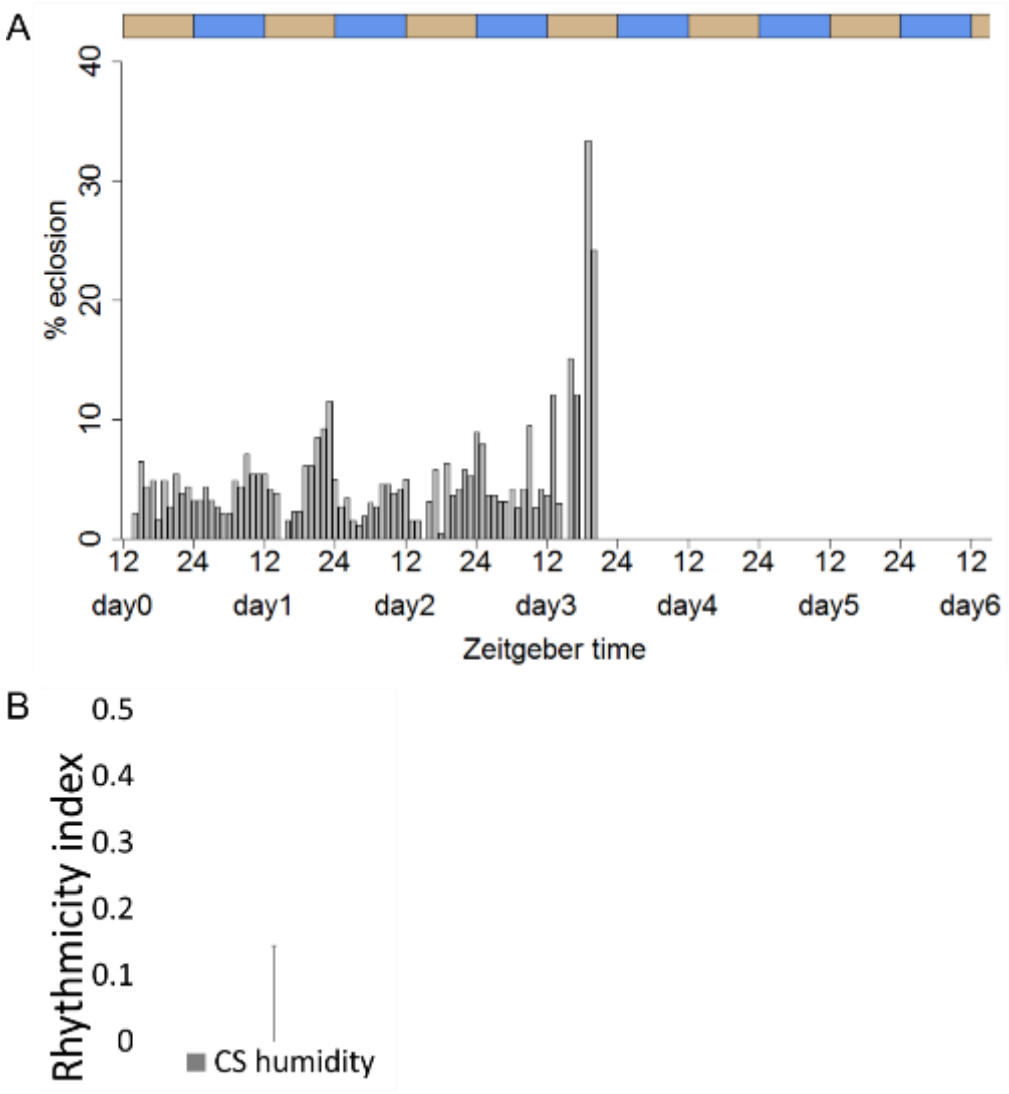

Figure 18: Eclosion rhythms of the wildtypes *Canton S* under humidity entrainment
Eclosion profiles for populations of the wildtype *Canton S* under humidity cycles with 12 hours 70% and 12 hours 30% of relative humidity (A). Experiments were performed under constant red light and constant temperature of 20°C. Each bar represents the percentage of eclosed flies per hour normalized to the number of eclosed flies per day. The beige and blue rectangles represent the humidity regime. (B) shows the mean of the rhythmicity indices (±SD). (N=4; n=664)

2.2 Statistical modelling

As the influence of clock and abiotic factors on the daily eclosion pattern and their interactions are quite complex, statistical modelling was applied to analyze these effects in cooperation with Dr. Oliver Mitesser and Prof. Dr. Thomas Hovestadt, Zoology III, University of Würzburg (CRC 1047, Project C6). A logistic regression model describing the daily eclosion pattern was developed based on the eclosion data collected under natural conditions. In a first step, several variables were included into the model, like a linear and a quadratic component for the hour of the day, temperature, light intensity, genotype, week of eclosion and day of eclosion, as well as the interactions of these variables. Because temperature and relative humidity are negatively correlated, the effect of only one of the two factors could be dissected. As relative humidity does not function as a Zeitgeber to entrain eclosion (Chapter 1.1), it was not further taken into account for the statistical modelling. To identify potential variables that influence the daily eclosion patterns, backward simplification after Crawley (Crawley, 2007) was applied. For this method, one factor after the other is removed from a complex model and the effect on the significance is tested by an ANOVA comparison of the models. If a variable is important for the observed effects, its elimination will result in a significant difference compared to the other model. If a factor is negligible, no significant difference will emerge and the next variable can be removed. In the end, the most parsimonious model comprising only the most important and necessary variables will be considered as the model which best describes the observations.

The results for each genotype will be discussed in the respective sections. All computations and the graphical output were performed by Dr. Oliver Mitesser.

2.3 Eclosion profiles of *Canton S* under natural conditions

The rhythmicity index for each experiment under natural conditions was calculated (Figure 19 C) and compared to results under laboratory LD and WC conditions (Figure 19 A, B). The eclosion profiles of *Canton S* under LD (Figure S 6) and WC (Figure S 7) conditions can be found in the appendix. The flies eclosed rhythmically in 78% of the experiments under natural conditions compared to 75% and 92% of the experiments under LD and WC conditions, respectively. While under laboratory conditions the flies showed a strong rhythmicity, they eclosed only weakly rhythmic under natural conditions. The experiments with arrhythmic eclosion were nearly the same under natural and LD conditions with 25% and 22%, respectively, while under WC conditions the flies eclosed arrhythmically in only 8% of the experiments (Figure 19 A). Mean rhythmicity was not significantly different between the three tested conditions (Figure 19 B).

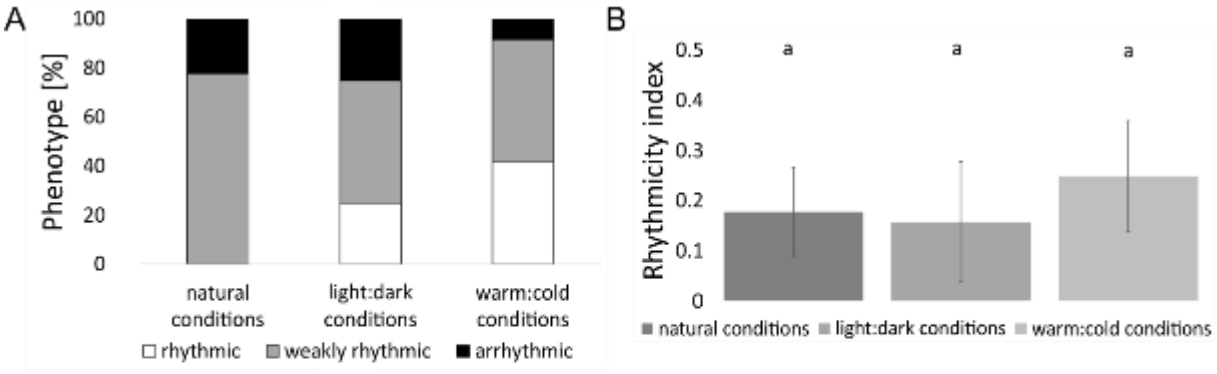

C

	17.07.- 24.07.2014	24.07.- 31.07.2014	31.07.- 07.08.2014	07.08.- 14.08.2014	21.08.- 28.08.2014	28.08.- 04.09.2014	04.09.- 11.09.2014	11.09.- 18.09.2014	25.09.- 02.10.2014
Canton S	0.04	0.21	0.28	0.1	0.25	0.17	0.07	0.27	0.1

Figure 19: Rhythmicity of the wildtype *Canton S* under different entrainment conditions
In A, the percentage of experiments with rhythmic (white), weakly rhythmic (gray) and arrhythmic (black) eclosion behavior under natural conditions, LD conditions and WC conditions is shown. The means of the rhythmicity indices (±SD) are presented in B. Different letters above columns indicate significant difference ($p<0.05$). The rhythmicity indices *for Canton S* in each experiment are listed in C ($RI>0.3$: rhythmic, $0.1<RI<0.3$: weakly rhythmic, $RI<0.1$: arrhythmic). (N=5465, 2223, 1948; n=9, 4, 12)

While gate breadth and amplitude of the eclosion peaks were changing in the eclosion profiles between the experiments, a gate was always clearly recognizable. The flies showed a clear lights-on peak although there was also some eclosion during the night in each experiment (Figure 20 - Figure 24).

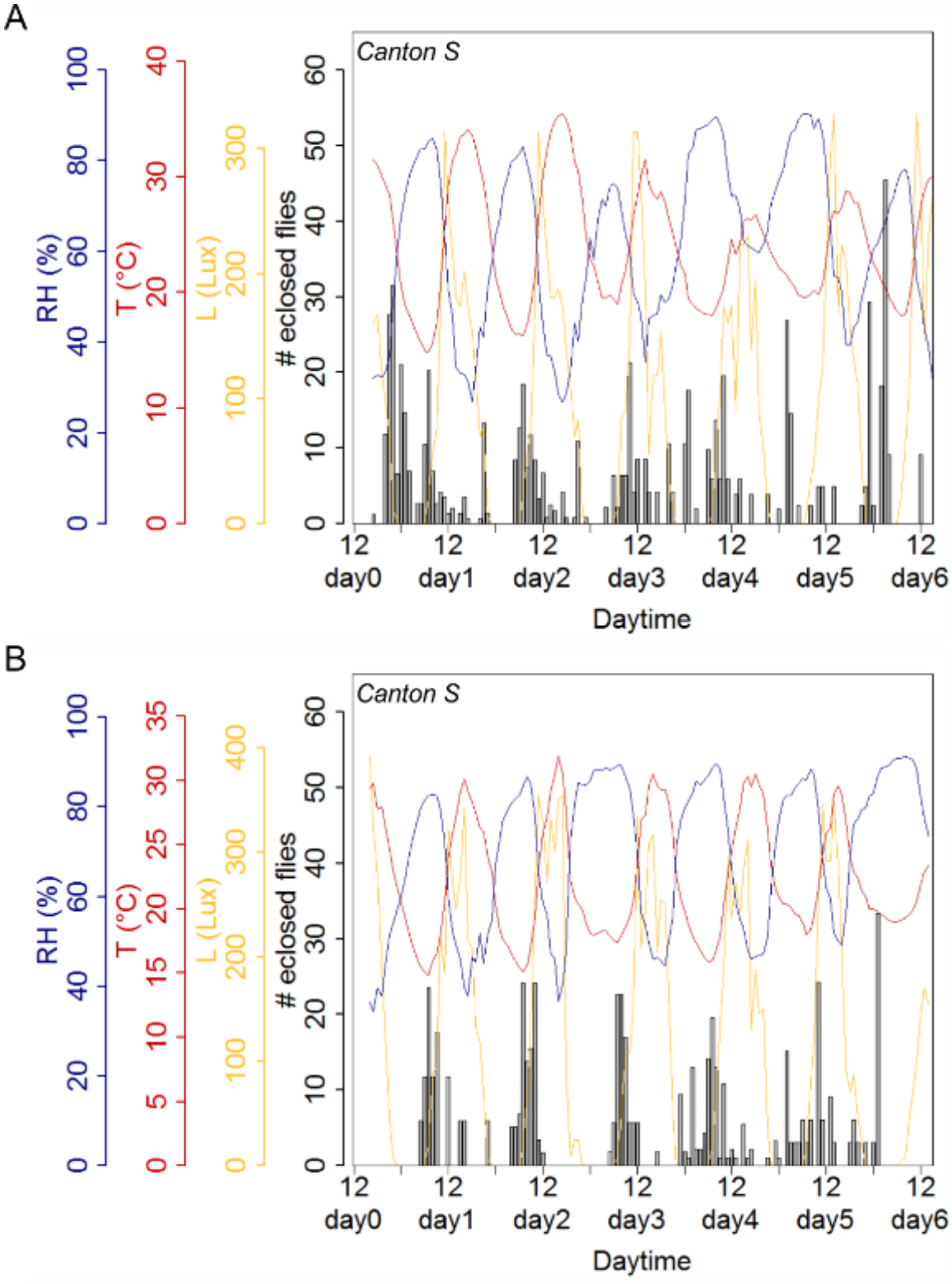

Figure 20: Eclosion rhythms of *Canton S* under natural conditions from 17.07.-31.07.2014
Eclosion profiles for populations of *Canton S* under natural conditions from 17.07.-24.07.2014 (A) and from 24.07.-31.07.2014 (B). Each bar represents the percentage of eclosed flies per hour normalized to the number of eclosed flies per day. Superimposed curves represent abiotic environmental factors measured once every hour: light intensity (yellow), temperature (red) and relative humidity (blue). Experiments were performed under constant red light. (N=1, 1; n=488, 292)

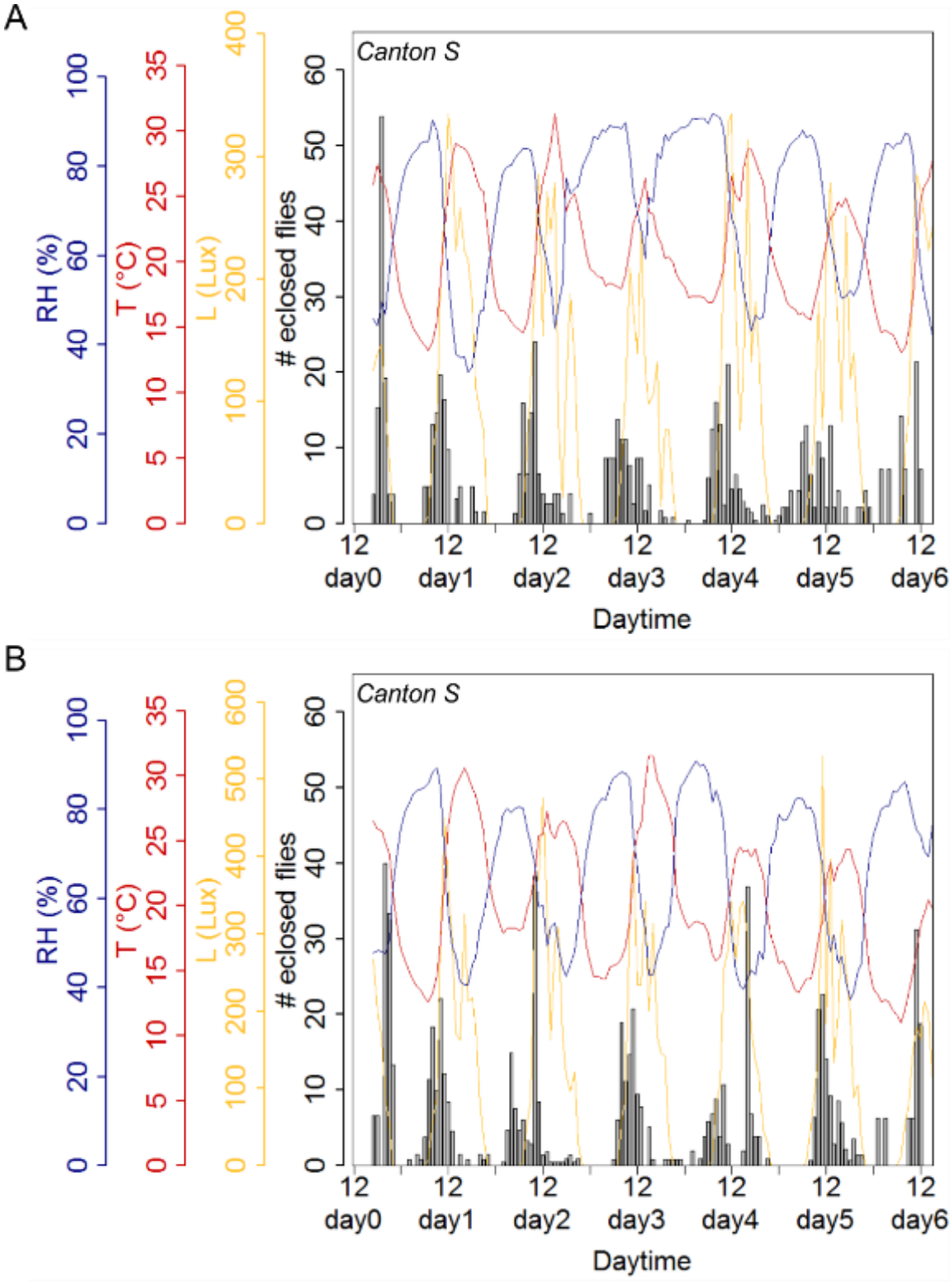

Figure 21: Eclosion rhythms of *Canton S* under natural conditions from 31.07.-14.08.2014
Eclosion profiles for populations of *Canton S* under natural conditions from 31.07.-07.08.2014 (A) and from 07.08.-14.08.2014 (B). Each bar represents the percentage of eclosed flies per hour normalized to the number of eclosed flies per day. Superimposed curves represent abiotic environmental factors measured once every hour: light intensity (yellow), temperature (red) and relative humidity (blue). Experiments were performed under constant red light. (N=1, 1; n=537, 736)

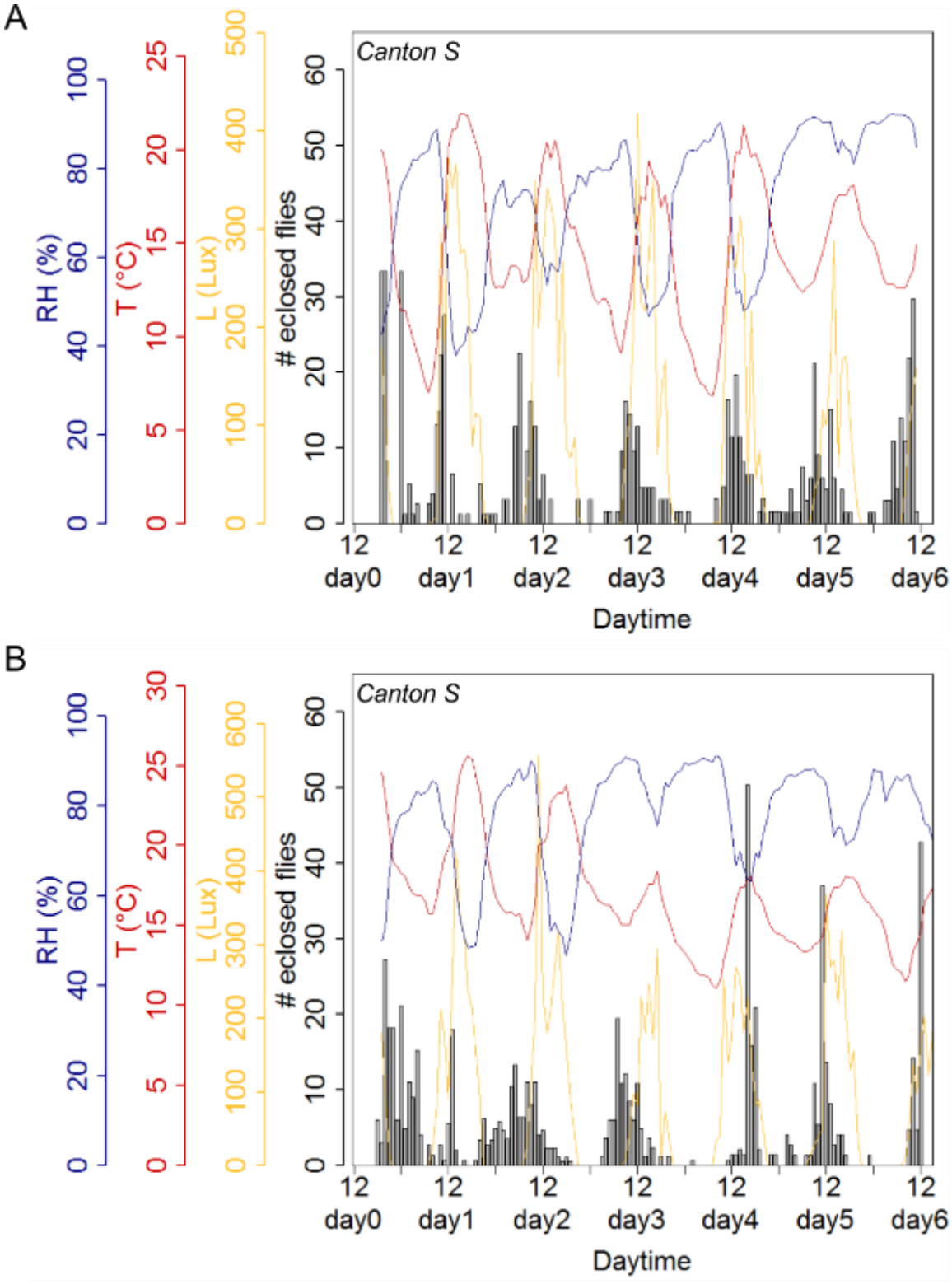

Figure 22: Eclosion rhythms of *Canton S* under natural conditions from 21.08.-04.09.2014
Eclosion profiles for populations of *Canton S* under natural conditions from 21.08.-28.08.2014 (A) and from 28.08.-04.09.2014 (B). Each bar represents the percentage of eclosed flies per hour normalized to the number of eclosed flies per day. Superimposed curves represent abiotic environmental factors measured once every hour: light intensity (yellow), temperature (red) and relative humidity (blue). Experiments were performed under constant red light. (N=1, 1; n=366, 664)

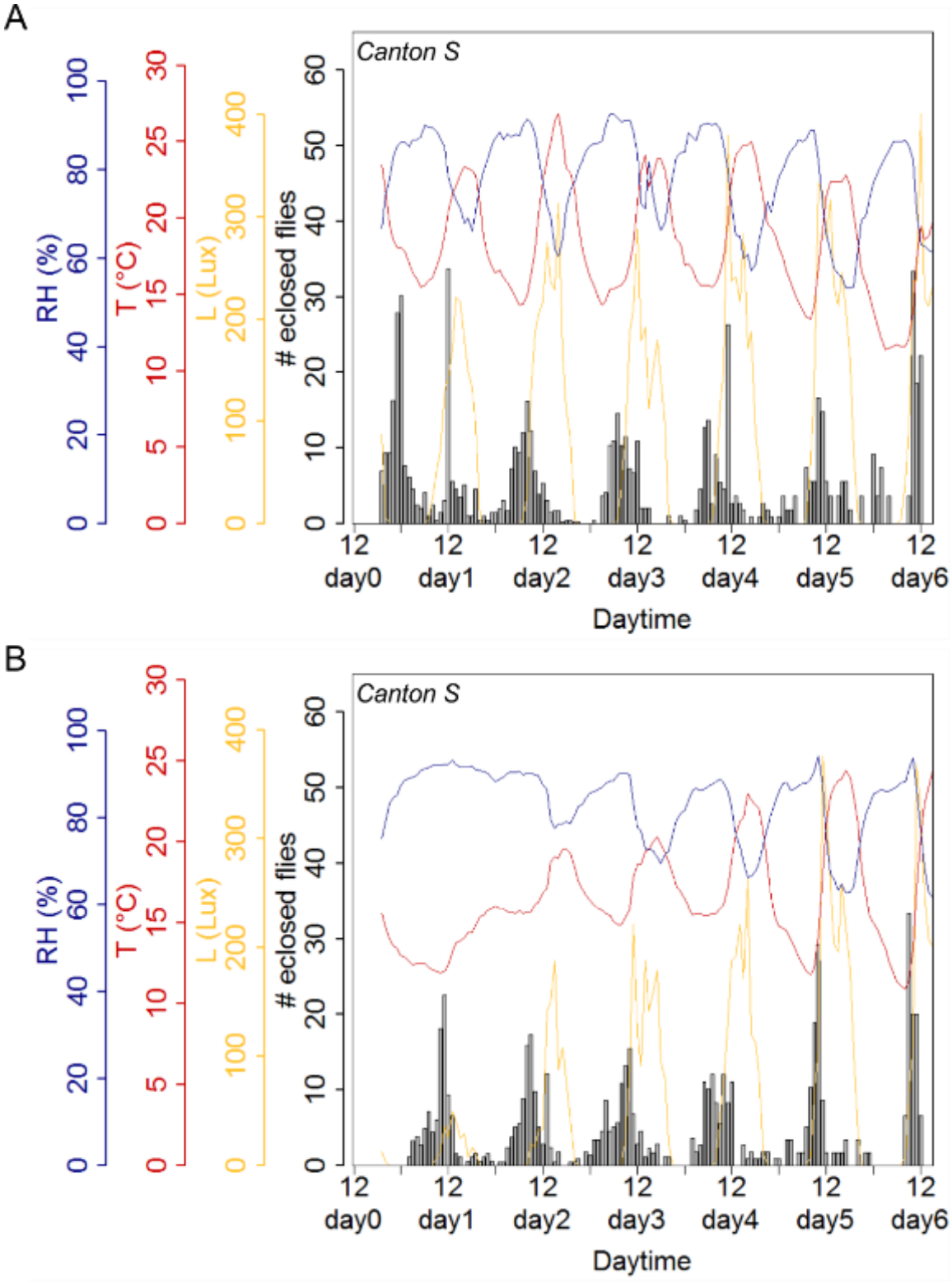

Figure 23: Eclosion rhythms of *Canton S* under natural conditions from 04.09.-18.09.2014
Eclosion profiles for populations of *Canton S* under natural conditions from 04.09.-11.09.2014 (A) and from 11.09.-18.09.2014 (B). Each bar represents the percentage of eclosed flies per hour normalized to the number of eclosed flies per day. Superimposed curves represent abiotic environmental factors measured once every hour: light intensity (yellow), temperature (red) and relative humidity (blue). Experiments were performed under constant red light. (N=1, 1; n=1036, 764)

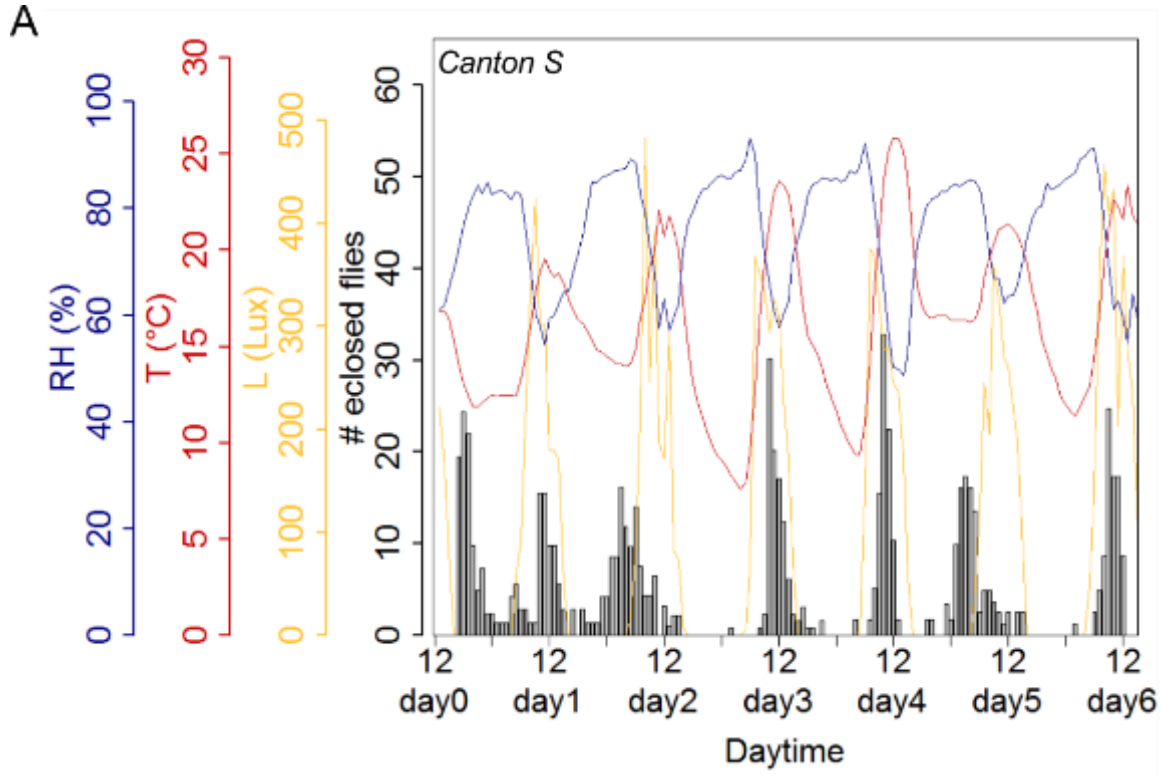

Figure 24: Eclosion rhythms of *Canton S* under natural conditions from 25.09.-02.10.2014
Eclosion profiles for populations of *Canton S* under natural conditions from 25.09.-02.10.2014. Each bar represents the percentage of eclosed flies per hour normalized to the number of eclosed flies per day. Superimposed curves represent abiotic environmental factors measured once every hour: light intensity (yellow), temperature (red) and relative humidity (blue). Experiments were performed under constant red light. (N=1; n=582)

2.4 Eclosion profiles of the *per*^{01} mutant under natural conditions

The rhythmicity index for each experiment under natural conditions was calculated (Figure 25 C) and compared to results under laboratory LD and WC conditions (Figure 25 A, B). The eclosion profiles of the *per*^{01} mutant under LD (Figure S 8) and WC (Figure S 9) conditions can be found in the appendix. While under LD conditions the *per*^{01} mutant flies showed weakly rhythmic behavior in all conducted experiments, they only did so in 66% of the experiments under WC conditions and in only one of the experiments (15%) under natural conditions. In all the other experiments under natural conditions, they eclosed arrhythmically (85%) (Figure 25 A). The means of the rhythmicity indices however showed no significant differences between the experimental conditions, although the *per*^{01} mutant flies showed a trend to reduced rhythmicity under natural conditions (Figure 25 B).

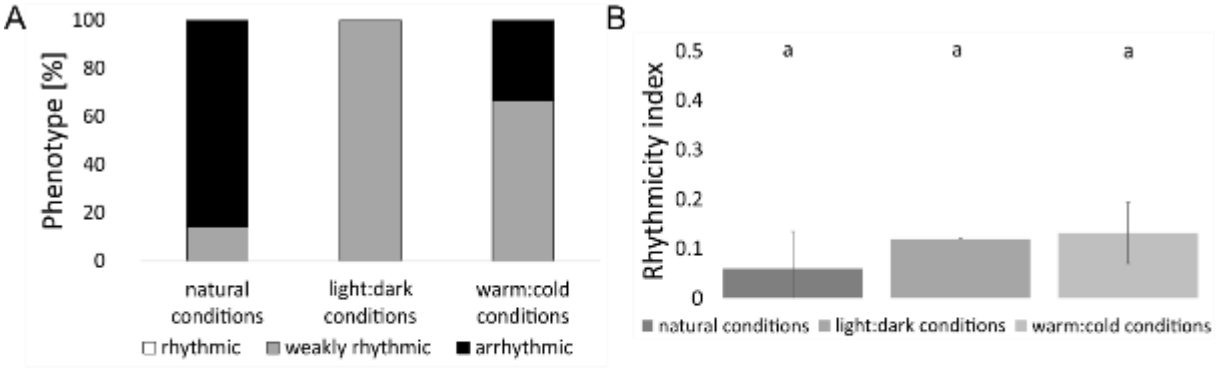

C

	31.07.-07.08.2014	07.08.-14.08.2014	21.08.-28.08.2014	28.08.-04.09.2014	04.09.-11.09.2014	11.09.-18.09.2014	25.09.-02.10.2014
per^{01}	0	0	0.21	0.07	0.04	0.09	0.01

Figure 25: Rhythmicity of the *per*^{01} mutant under different entrainment conditions
In A, the percentage of experiments with rhythmic (white), weakly rhythmic (gray) and arrhythmic (black) eclosion behavior under natural conditions, LD conditions and WC conditions is shown. The means of the rhythmicity indices (±SD) are presented in B. Different letters above columns indicate significant difference ($p<0.05$). The rhythmicity indices for *per*^{01} in each experiment are listed in C (RI>0.3: rhythmic, 0.1<RI<0.3: weakly rhythmic, RI<0.1: arrhythmic). (N=7, 2, 6; n= 2238, 1148, 1195)

The eclosion profiles of the *per*^{01} mutant showed eclosion throughout the day, with an increased amount of eclosion during the night, reduced eclosion peaks and no recognizable gate compared to the wildtype *Canton S*. Their lights-on peaks were strongly reduced or completely missing (Figure 26 -Figure 29). The only exception is the experiment from the 21st

to the 28th of August, where the eclosion profiles of the mutant and the wildtype were quite similar (Figure 27 B) and which represents the only experiment in which the flies exhibited weakly rhythmic eclosion (Figure 25 C).

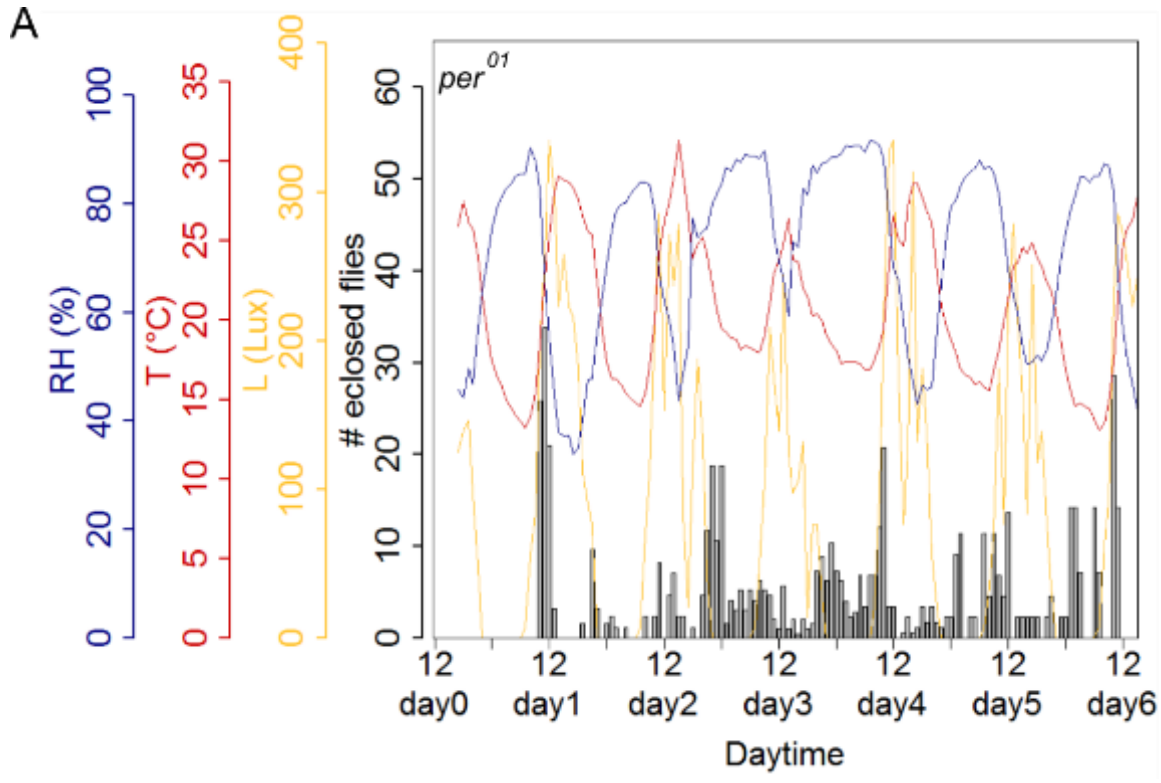

Figure 26: Eclosion rhythms of the *per*^{01} mutant under natural conditions from 31.07.-07.08.2014

Eclosion profiles for populations of the *per*^{01} mutant under natural conditions. Each bar represents the percentage of eclosed flies per hour normalized to the number of eclosed flies per day. Superimposed curves represent abiotic environmental factors measured once every hour: light intensity (yellow), temperature (red) and relative humidity (blue). Experiments were performed under constant red light. (N=1; n=576)

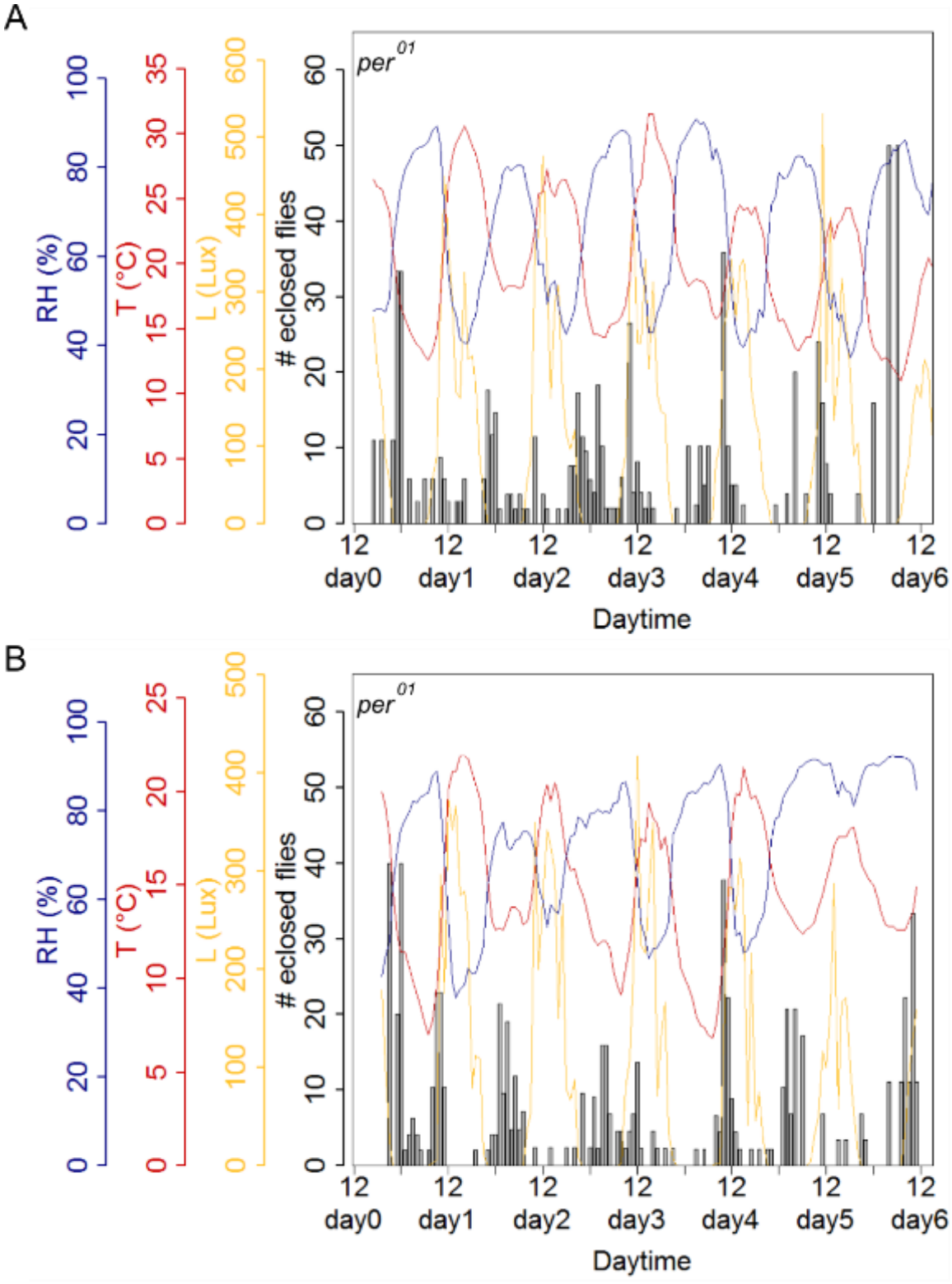

Figure 27: Eclosion rhythms of the *per*^{01} mutant under natural conditions from 07.08.-28.08.2014

Eclosion profiles for populations of the *per*^{01} mutant under natural conditions from 07.08.-14.08.2014 (A) and from 21.08.-28.08.2014 (B). Each bar represents the percentage of eclosed flies per hour normalized to the number of eclosed flies per day. Superimposed curves represent abiotic environmental factors measured once every hour: light intensity (yellow), temperature (red) and relative humidity (blue). Experiments were performed under constant red light. (N=1, 1; n: A=210, B=222)

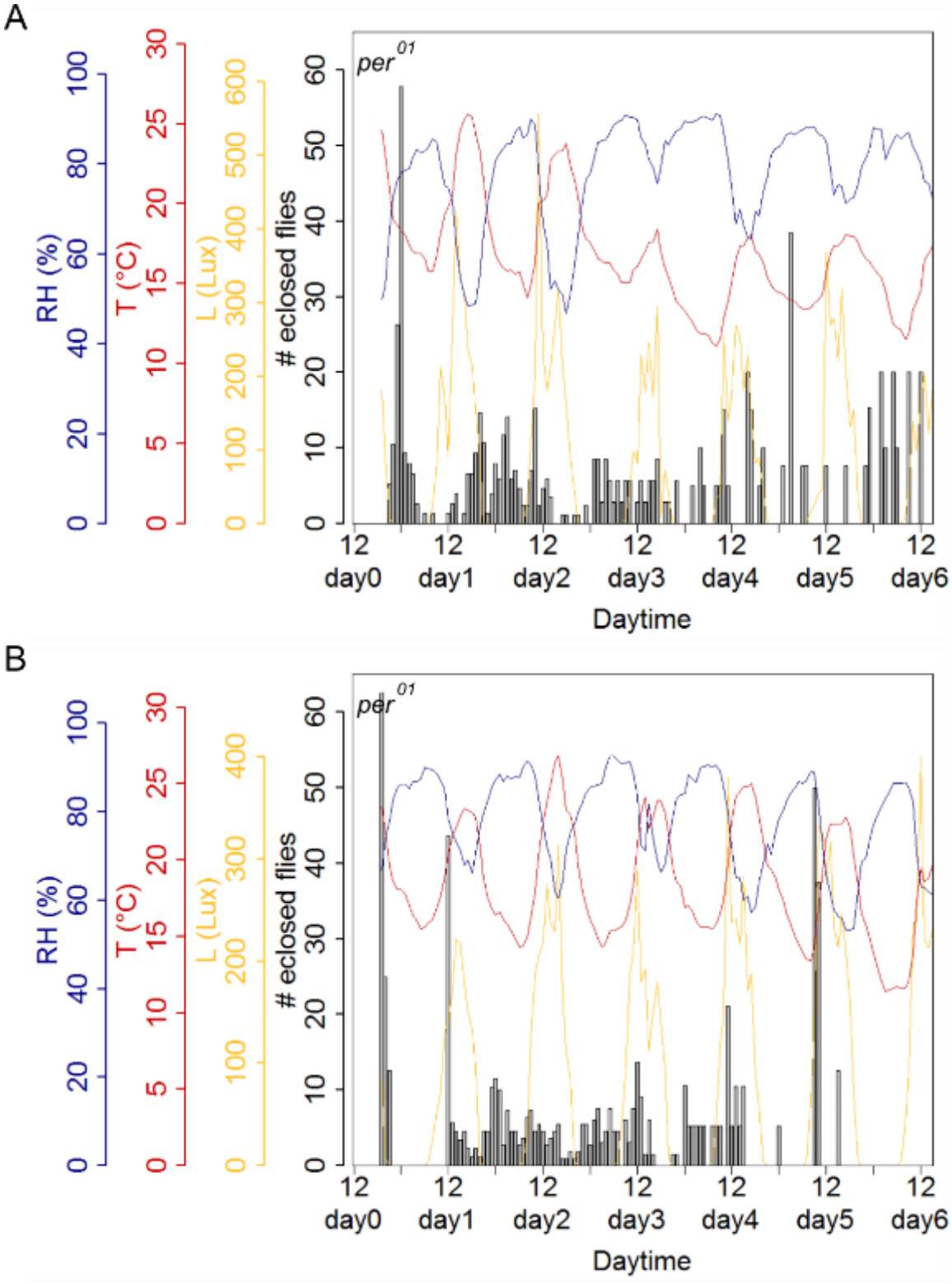

Figure 28: Eclosion rhythms of the *per*^{01} mutant under natural conditions from 28.08.-11.09.2014

Eclosion profiles for populations of the *per*^{01} mutant under natural conditions from 28.08.-04.09.2014 (A) and from 04.09.-11.09.2014 (B). Each bar represents the percentage of eclosed flies per hour normalized to the number of eclosed flies per day. Superimposed curves represent abiotic environmental factors measured once every hour: light intensity (yellow), temperature (red) and relative humidity (blue). Experiments were performed under constant red light. (N=1, 1; n: A=258, B=298)

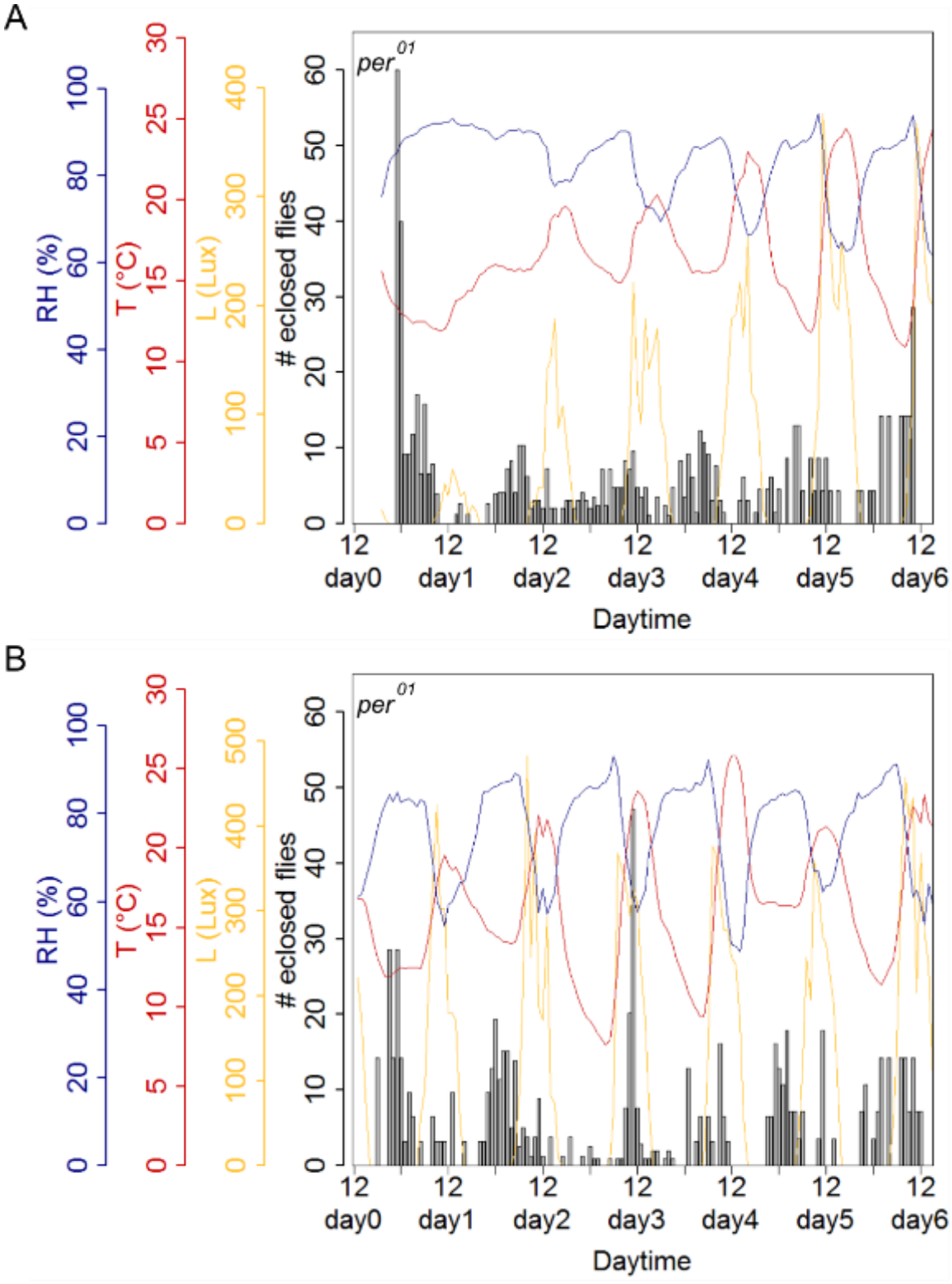

Figure 29: Eclosion rhythms of the *per*^{01} mutant under natural conditions from 11.09.-02.10.2014

Eclosion profiles for populations of the *per*^{01} mutant under natural conditions from 11.09.-18.09.2014 (A) and from 25.09.-02.10.2014 (B). Each bar represents the percentage of eclosed flies per hour normalized to the number of eclosed flies per day. Superimposed curves represent abiotic environmental factors measured once every hour: light intensity (yellow), temperature (red) and relative humidity (blue). Experiments were performed under constant red light. (N=1, 1; n: A=358, B=316)

2.5 Eclosion profiles of the *pdf*^{01} mutant under natural conditions

The rhythmicity index for each experiment under natural conditions was summarized (Figure 30 C) and compared to results under laboratory LD and WC conditions (Figure 30 A, B). The eclosion profiles of the *pdf*^{01} mutant under LD (Figure S 10) and WC (Figure S 11) conditions can be found in the appendix. While under LD conditions the flies eclosed rhythmically in all experiments (100%), the amount of rhythmic experiments wass slightly decreased under WC conditions (84%) and even more under natural conditions (67%). While the percentage of experiments with weakly rhythmic eclosion was about the same in all conditions (LD: 50%, WC: 42%, natural conditions: 50%), the *pdf*^{01} mutant flies eclosed arrhythmically in more experiments under natural conditions (33%) than under laboratory conditions (0% under LD and 16% under WC) (Figure 30 A). The means of the rhythmicity indices revealed a significantly decreased rhythmicity of the *pdf*^{01} mutants under natural conditions compared to LD conditions. There was however no significant difference observable compared to WC conditions or between the laboratory conditions (Figure 30 B).

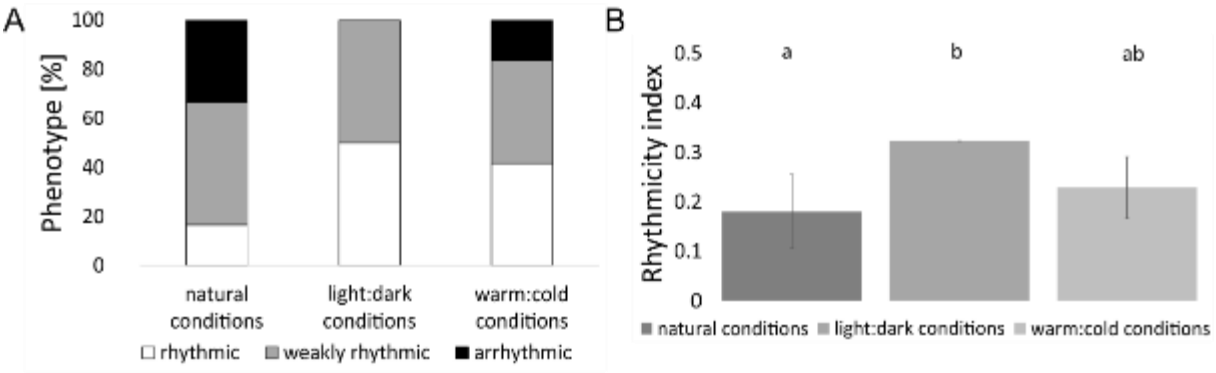

C

	17.07.-24.07.2014	31.07.-07.08.2014	07.08.-14.08.2014	21.08.-28.08.2014	28.08.-04.09.2014	04.09.-11.09.2014	11.09.-18.09.2014
pdf^{01}	0.04	0.14	0.34	0.12	-	0.03	0.2

Figure 30: Rhythmicity of the *pdf*^{01} mutant under different entrainment conditions
In A, the percentage of experiments with rhythmic (white), weakly rhythmic (gray) and arrhythmic (black) eclosion behavior under natural conditions, LD conditions and WC conditions is shown. The means of the rhythmicity indices (±SD) are presented in B. Different letters above columns indicate significant difference ($p<0.05$). The rhythmicity indices for *pdf*^{01} in each experiment are listed in C ($RI>0.3$: rhythmic, $0.1<RI<0.3$: weakly rhythmic, $RI<0.1$: arrhythmic). (N=7, 4, 12; n= 1791, 1672, 969)

The eclosion profiles of the *pdf*^{01} mutant showed very narrow eclosion gates with distinct eclosion peaks, clear lights-on peaks and only some eclosion during the night (Figure 31 - Figure 34). With that, they showed a high similarity to the eclosion profiles of the wildtype *Cantons S* (Figure 20 - Figure 24), but not to that of the clock mutant *per*^{01} (Figure 26 - Figure 29).

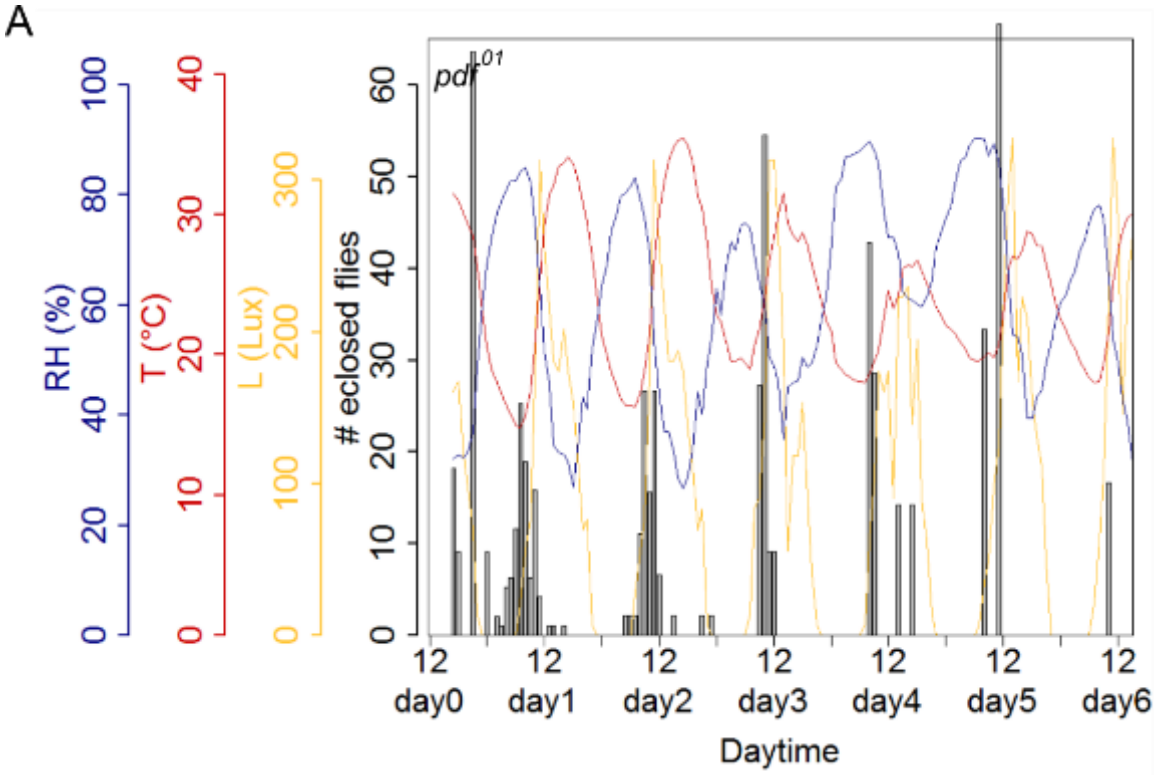

Figure 31: Eclosion rhythms of the *pdf*^{01} mutant under natural conditions from 17.07.-24.07.2014

Eclosion profiles for populations of the *pdf*^{01} mutant under natural conditions. Each bar represents the percentage of eclosed flies per hour normalized to the number of eclosed flies per day. Superimposed curves represent abiotic environmental factors measured once every hour: light intensity (yellow), temperature (red) and relative humidity (blue). Experiments were performed under constant red light. (N=1; n=178)

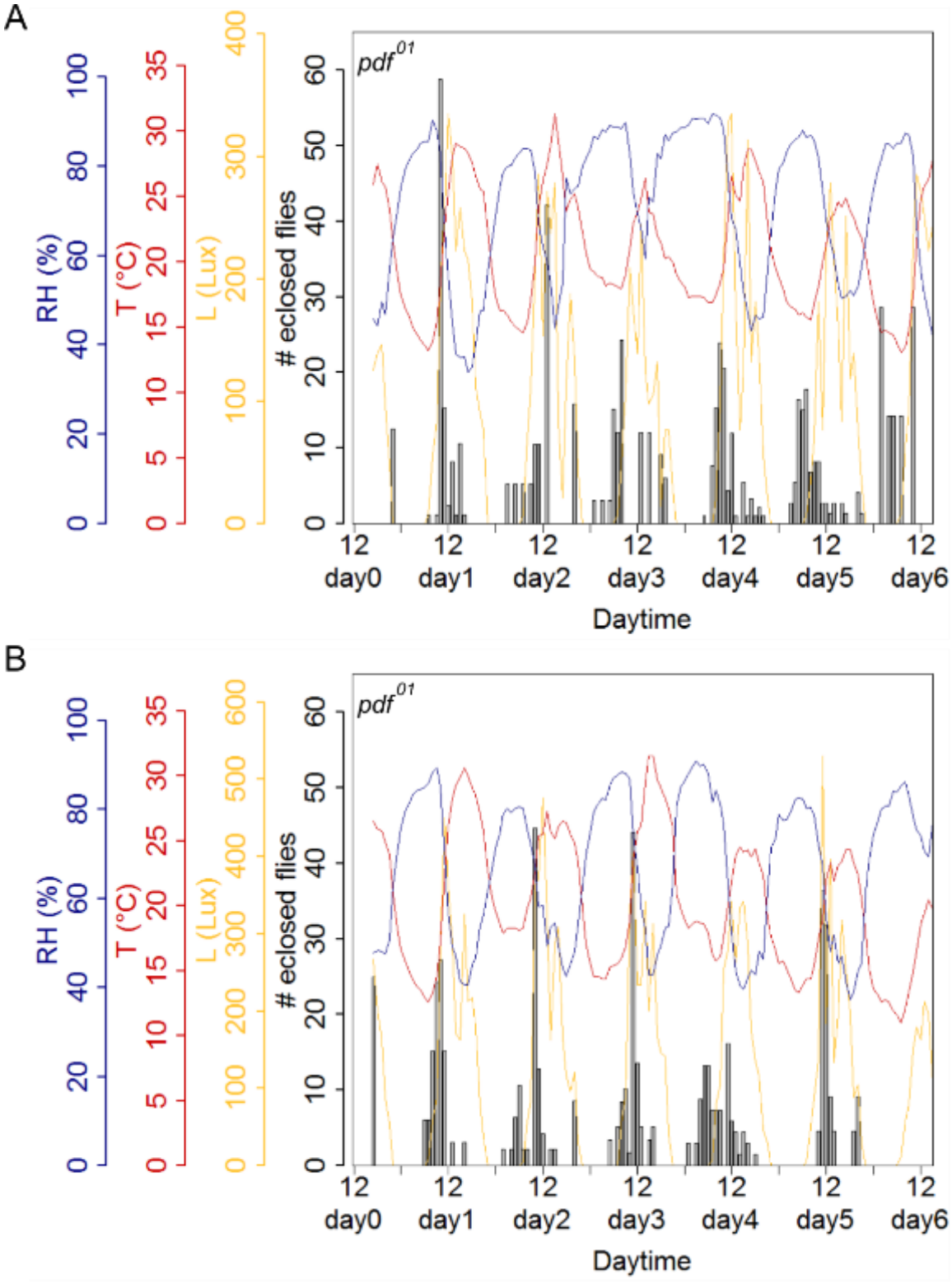

Figure 32: Eclosion rhythms of the *pdf*^{01} mutant under natural conditions from 31.07.-14.08.2014

Eclosion profiles for populations of the *pdf*^{01} mutant under natural conditions from 31.07.-07.08.2014 (A) and from 07.08.-14.08.2014 (B). Each bar represents the percentage of eclosed flies per hour normalized to the number of eclosed flies per day. Superimposed curves represent abiotic environmental factors measured once every hour: light intensity (yellow), temperature (red) and relative humidity (blue). Experiments were performed under constant red light. (N=1, 1; n: A=323, B=234)

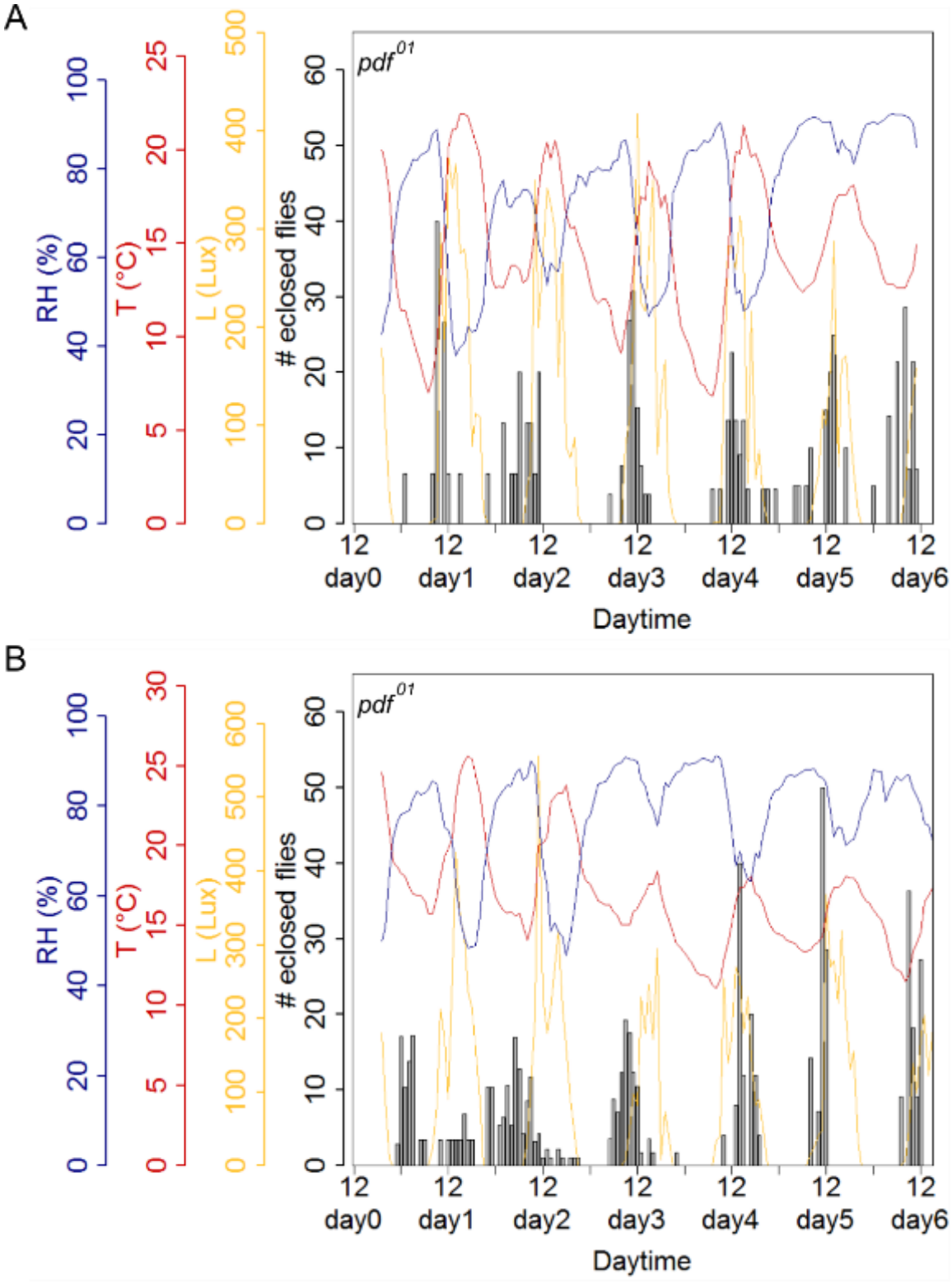

Figure 33: Eclosion rhythms of the *pdf*^{01} mutant under natural conditions from 21.08.-04.09.2014

Eclosion profiles for populations of the *pdf*^{01} mutant under natural conditions from 21.08.-28.08.2014 (A) and from 28.08.-04.09.2014 (B). Each bar represents the percentage of eclosed flies per hour normalized to the number of eclosed flies per day. Superimposed curves represent abiotic environmental factors measured once every hour: light intensity (yellow), temperature (red) and relative humidity (blue). Experiments were performed under constant red light. (N=1, 1; n: A=132, B=271)

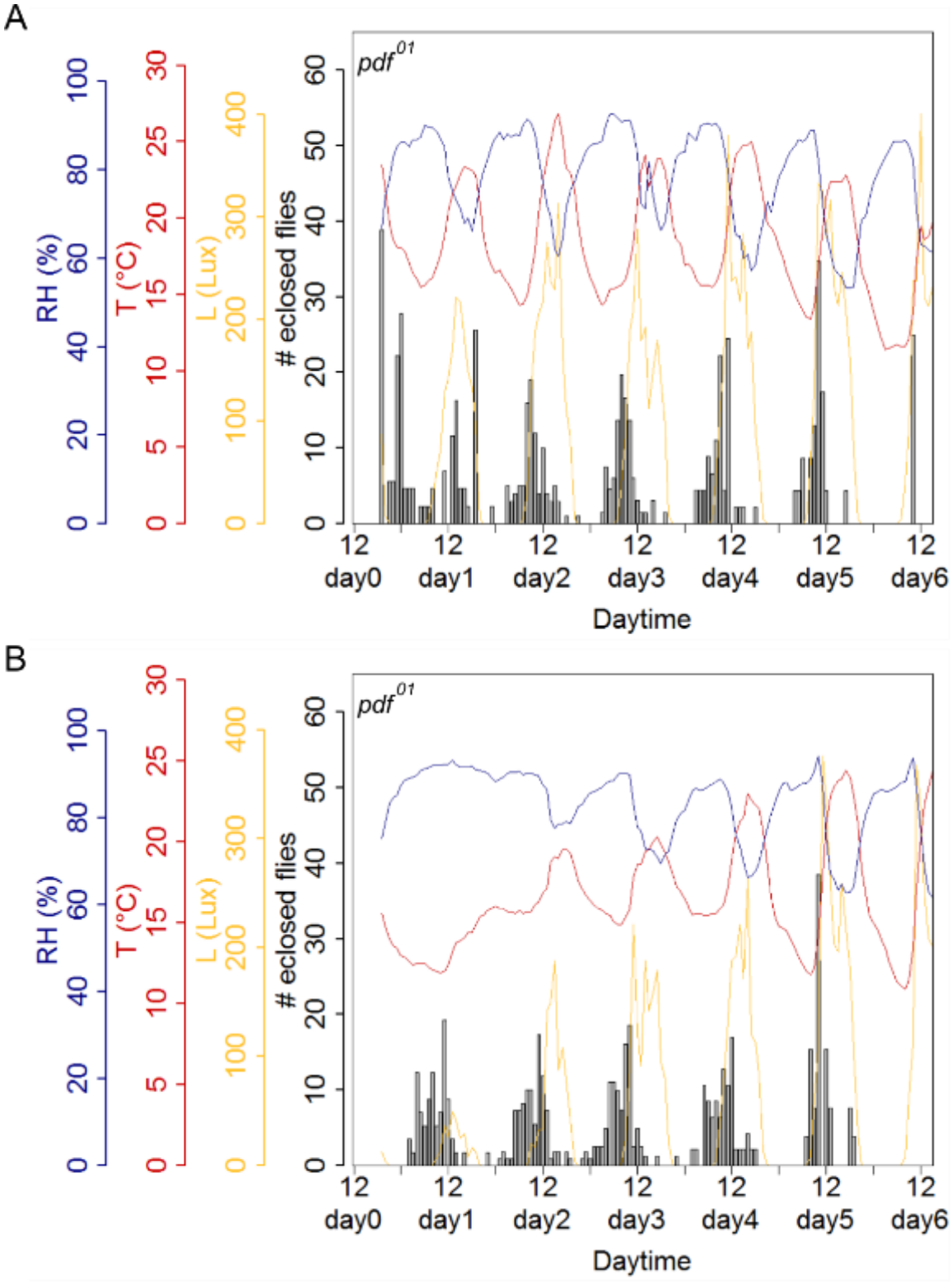

Figure 34: Eclosion rhythms of the *pdf*^{01} mutant under natural conditions from 04.09.-18.09.2014

Eclosion profiles for populations of the *pdf*^{01} mutant under natural conditions from 04.09.-11.09.2014 (A) and from 11.09.-18.09.2014 (B). Each bar represents the percentage of eclosed flies per hour normalized to the number of eclosed flies per day. Superimposed curves represent abiotic environmental factors measured once every hour: light intensity (yellow), temperature (red) and relative humidity (blue). Experiments were performed under constant red light. (N=1, 1; n: A=299, B=354)

2.6 Eclosion profiles of the *han*^{5304} mutant under natural conditions

The rhythmicity index for each experiment under natural conditions was calculated (Figure 35 C) and compared to results under laboratory LD and WC conditions (Figure 35 A, B). The eclosion profiles of the *han*^{5304} mutant under LD (Figure S 12) and WC (Figure S 13) conditions can be found in the appendix. While *han*^{5304} mutant flies eclosed rhythmically in all experiments under LD and WC conditions (100% each), the amount of rhythmic experiments decreased under natural conditions (57%). At the same time, the number of arrhythmic experiments increased (43%) compared to both laboratory conditions (0% each) (Figure 35 A). The means of the rhythmicity indices revealed a significantly decreased rhythmicity of the *han*^{5304} mutants under natural conditions compared to under LD conditions, but no significant difference compared to WC conditions or between the laboratory conditions (Figure 35 B).

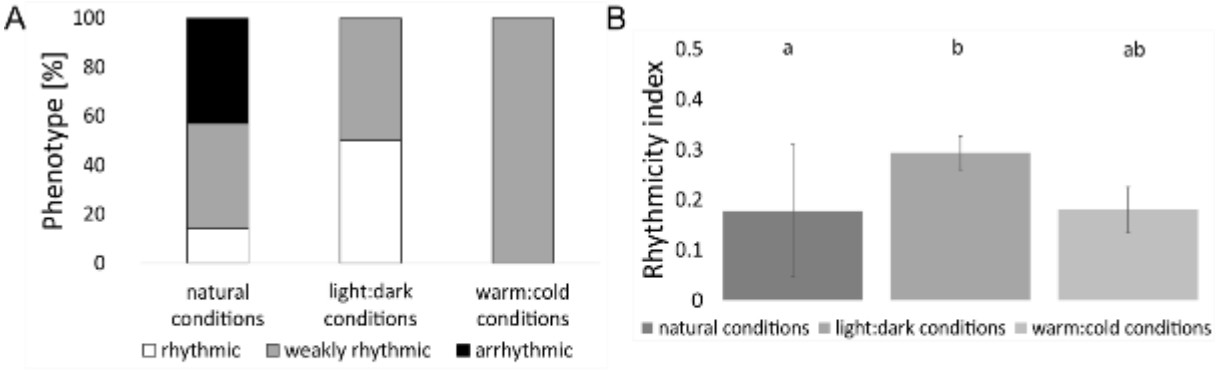

C

	17.07.-24.07.2014	24.07.-31.07.2014	31.07.-07.08.2014	07.08.-14.08.2014	21.08.-28.08.2014	28.08.-04.09.2014	04.09.-11.09.2014	25.09.-02.10.2014
han ^{5304}	0.06	0.21	0.23	0.03	0.22		0.06	0.35

Figure 35: Rhythmicity of the *han*^{5304} mutant under different entrainment conditions
In A, the percentage of experiments with rhythmic (white), weakly rhythmic (gray) and arrhythmic (black) eclosion behavior under natural conditions, LD conditions and WC conditions is shown. The means of the rhythmicity indices (±SD) are presented in B. Different letters above columns indicate significant difference ($p<0.05$). The rhythmicity indices for *han*^{5304} in each experiment are listed in C (RI>0.3: rhythmic, 0.1<RI<0.3: weakly rhythmic, RI<0.1: arrhythmic). (N=8, 6, 5; n= 1950, 1728, 913)

The eclosion profiles of the *han*^{5304} mutant had narrow eclosion gates, distinct eclosion peaks and clear lights-on peaks with only a small amount of eclosion during the night (Figure 36 - Figure 39). They had a high similarity with the eclosion profiles of the wildtype (Figure 20 - Figure 24) and the *pdf*^{01} mutant (Figure 31 - Figure 34), but did not resemble those of the clock mutant *per*^{01} (Figure 26 - Figure 29).

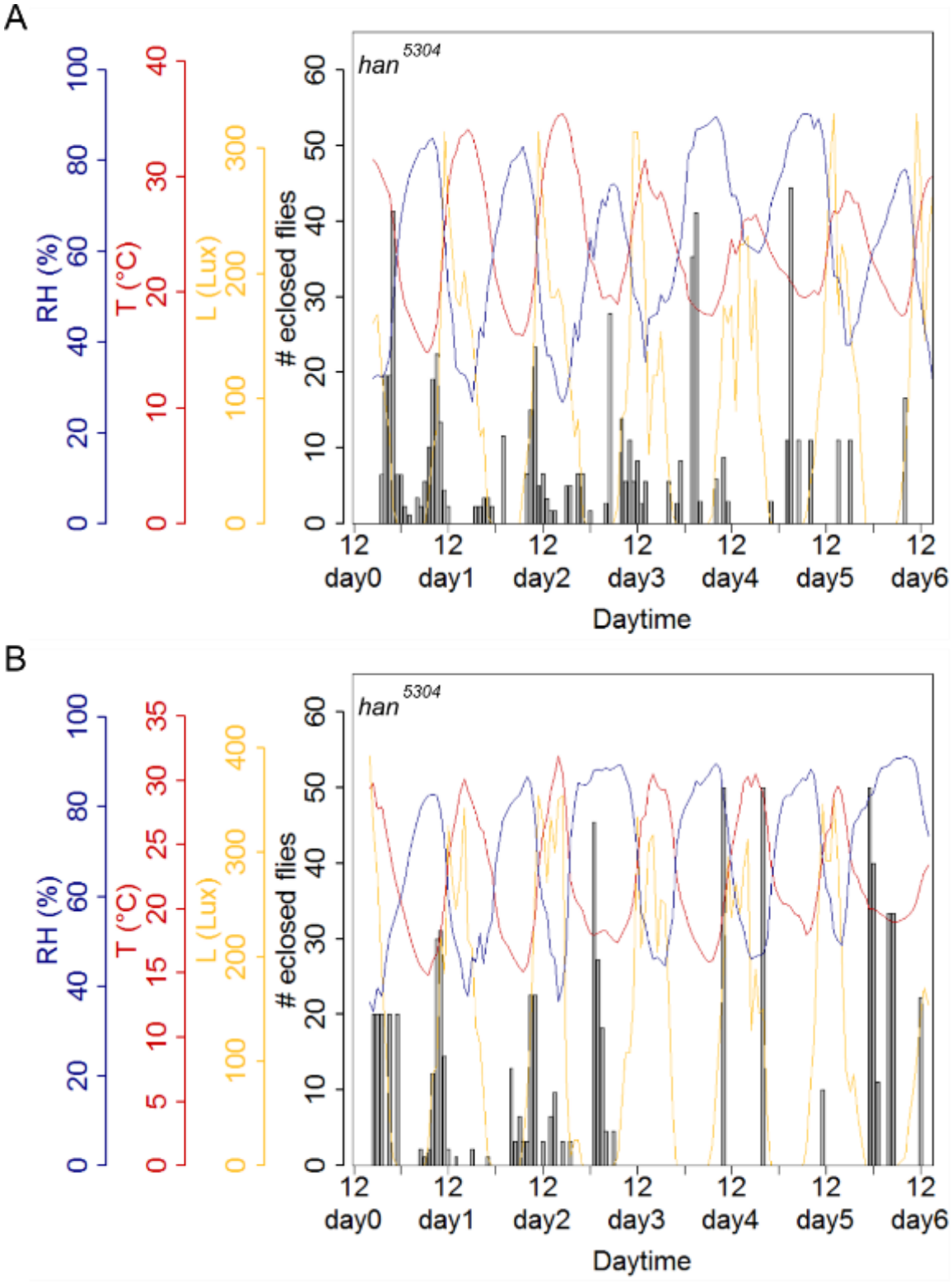

Figure 36: Eclosion rhythms of the *han*^{5304} mutant under natural conditions from 17.07.-31.07.2014

Eclosion profiles for populations of the *han*^{5304} mutant under natural conditions from 17.07.-24.07.2014 (A) and from 24.07.-31.07.2014 (B). Each bar represents the percentage of eclosed flies per hour normalized to the number of eclosed flies per day. Superimposed curves represent abiotic environmental factors measured once every hour: light intensity (yellow), temperature (red) and relative humidity (blue). Experiments were performed under constant red light. (N=1, 1; n: A=280, B=171)

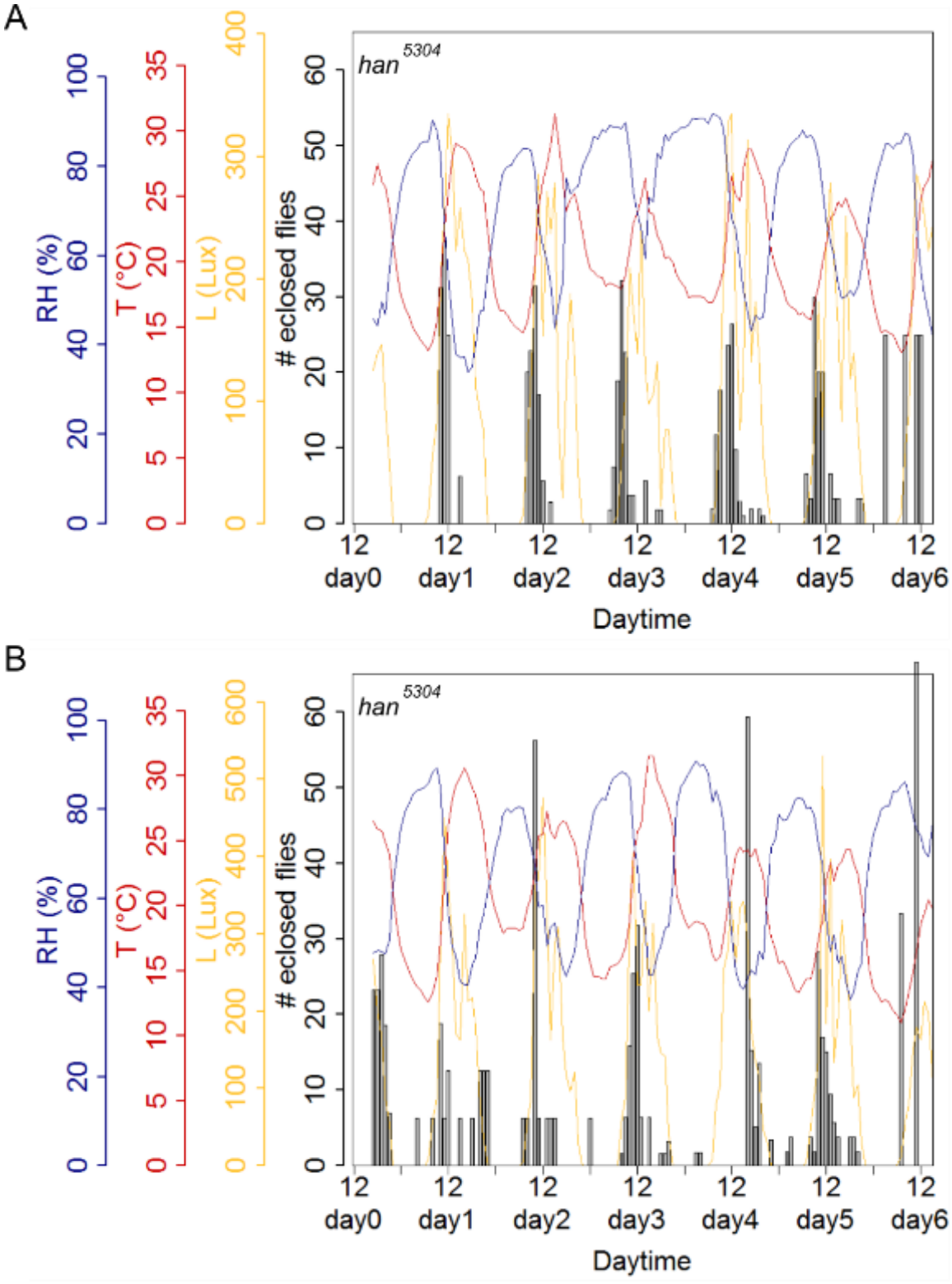

Figure 37: Eclosion rhythms of the *han*^{5304} mutant under natural conditions from 31.07.-14.08.2014

Eclosion profiles for populations of the *han*^{5304} mutant under natural conditions from 31.07.-07.08.2014 (A) and from 07.08.-14.08.2014 (B). Each bar represents the percentage of eclosed flies per hour normalized to the number of eclosed flies per day. Superimposed curves represent abiotic environmental factors measured once every hour: light intensity (yellow), temperature (red) and relative humidity (blue). Experiments were performed under constant red light. (N=1, 1; n: A=241, B=256)

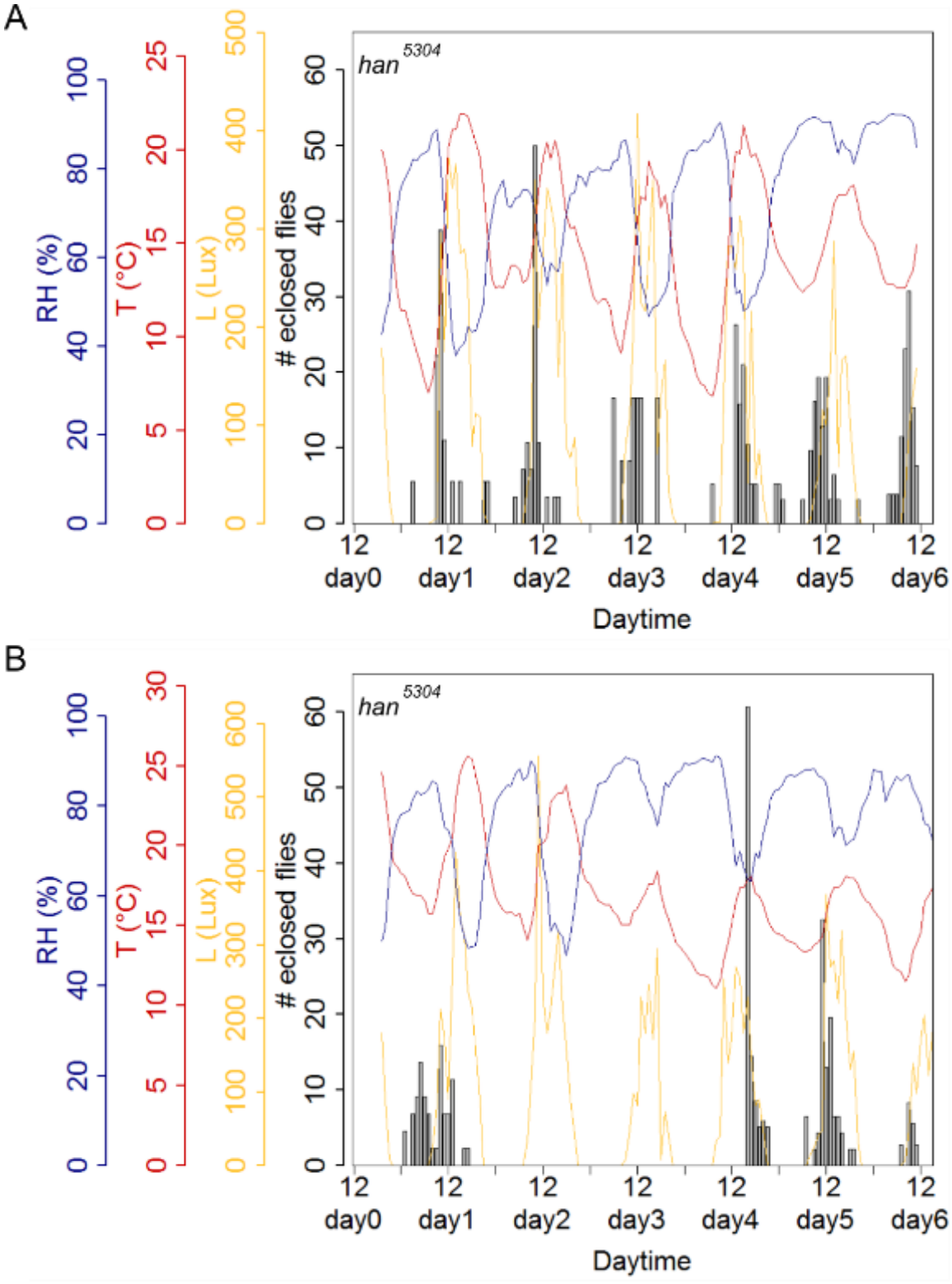

Figure 38: Eclosion rhythms of the *han*^{5304} mutant under natural conditions from 21.08.-04.09.2014

Eclosion profiles for populations of the *han*^{5304} mutant under natural conditions from 21.08.-28.08.2014 (A) and from 28.08.-04.09.2014 (B). Each bar represents the percentage of eclosed flies per hour normalized to the number of eclosed flies per day. Superimposed curves represent abiotic environmental factors measured once every hour: light intensity (yellow), temperature (red) and relative humidity (blue). Experiments were performed under constant red light. (N=1, 1; n: A=135, B=246)

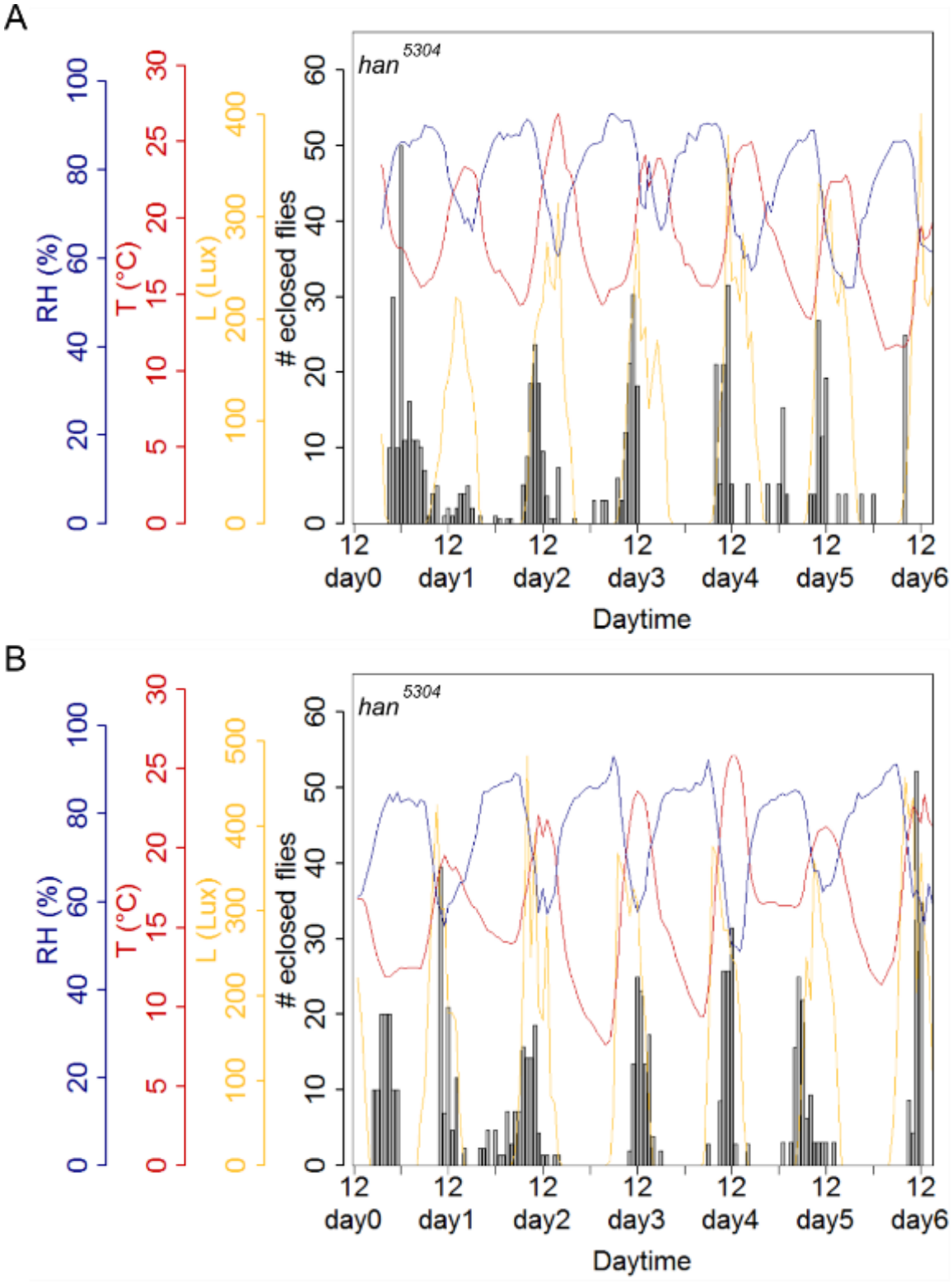

Figure 39: Eclosion rhythms of the *han*^{5304} mutant under natural conditions from 04.09.-02.10.2014

Eclosion profiles for populations of the *han*^{5304} mutant under natural conditions from 04.09.-11.09.2014 (A) and from 25.09.-02.10.2014 (B). Each bar represents the percentage of eclosed flies per hour normalized to the number of eclosed flies per day. Superimposed curves represent abiotic environmental factors measured once every hour: light intensity (yellow), temperature (red) and relative humidity (blue). Experiments were performed under constant red light. (N=1, 1; n: A=330, B=291)

2.7 Comparison of the rhythmicity indices between the genotypes under different conditions

To allow for comparison, the rhythmicity indices for *Canton S*, the per^{01} mutant, the pdf^{01} mutant and the han^{5304} for the experiments under natural as well as under LD and WC conditions were calculated (Figure 40).

Under LD conditions, all tested strains showed mainly rhythmic eclosion (Figure 40 C). While the mutant flies eclosed with a weak rhythmicity in all experiments, wildtype flies showed also experiments with strongly rhythmic (25%) and arrhythmic (25%) eclosion (Figure 40 C). Pdf^{01} mutant flies showed a significantly increased rhythmicity index compared to *Canton S* and per^{01} mutant flies, while there was so significant difference between *Canton S*, per^{01} and han^{5304} mutant flies as well as between the two PDF mutants (Figure 40 D).

Also under WC conditions, the amount of rhythmic experiments in all four genotypes outweighed (*Canton S*: 92 %, $per^{0\,1}$: 67%, $pdf^{0\,1}$: 84%, han^{5304}: 100%) (Figure 40 E). Only *Canton S* and pdf^{01} mutant flies showed experiments with strong rhythmicity (42% each). While there were no arrhythmic experiments in the han^{5304} mutant, the amount was slightly increased in wildtype flies (8%) and pdf^{01} mutant flies (16%) and even more in per^{01} mutant flies (33%) (Figure 40 E). Despite these differences, the rhythmicity showed no significant differences (Figure 40 F).

Under natural conditions, the similarity between the eclosion profiles between *Canton S* and the PDF mutants as well as the differences compared to the clock mutant per^{01} was also reflected in the rhythmicity indices (Figure 40 A). *Canton S*, pdf^{01} and han^{5304} mutant flies showed rhythmic eclosion in the majority of experiments (*Canton S*: 78 %, pdf^{01}: 67%, han^{5304}: 57%). Although the amount was decreased in the PDF mutants compared to the wildtype, they were also the only strains with strongly rhythmic experiments (pdf^{01}: 17%, han^{5304}: 14%). The amount of experiments with arrhythmic eclosion was accordingly increased in the PDF mutants compared to the wildtype and higher in the receptor mutant than in the peptide mutant (*Canton S*: 22 %, pdf^{01}: 33%, han^{5304}: 43%). Per^{01} mutant flies on the other hand showed weakly rhythmic eclosion in only 15% of the experiments, but arrhythmic eclosion in 85% of the experiments (Figure 40 A). Although there was no significant difference between the mean rhythmicity indices of the four genotypes, probably due to the low number of experiments, there was a trend to decreased rhythmicity in the per^{01} mutant flies compared to the other three strains (Figure 40 B).

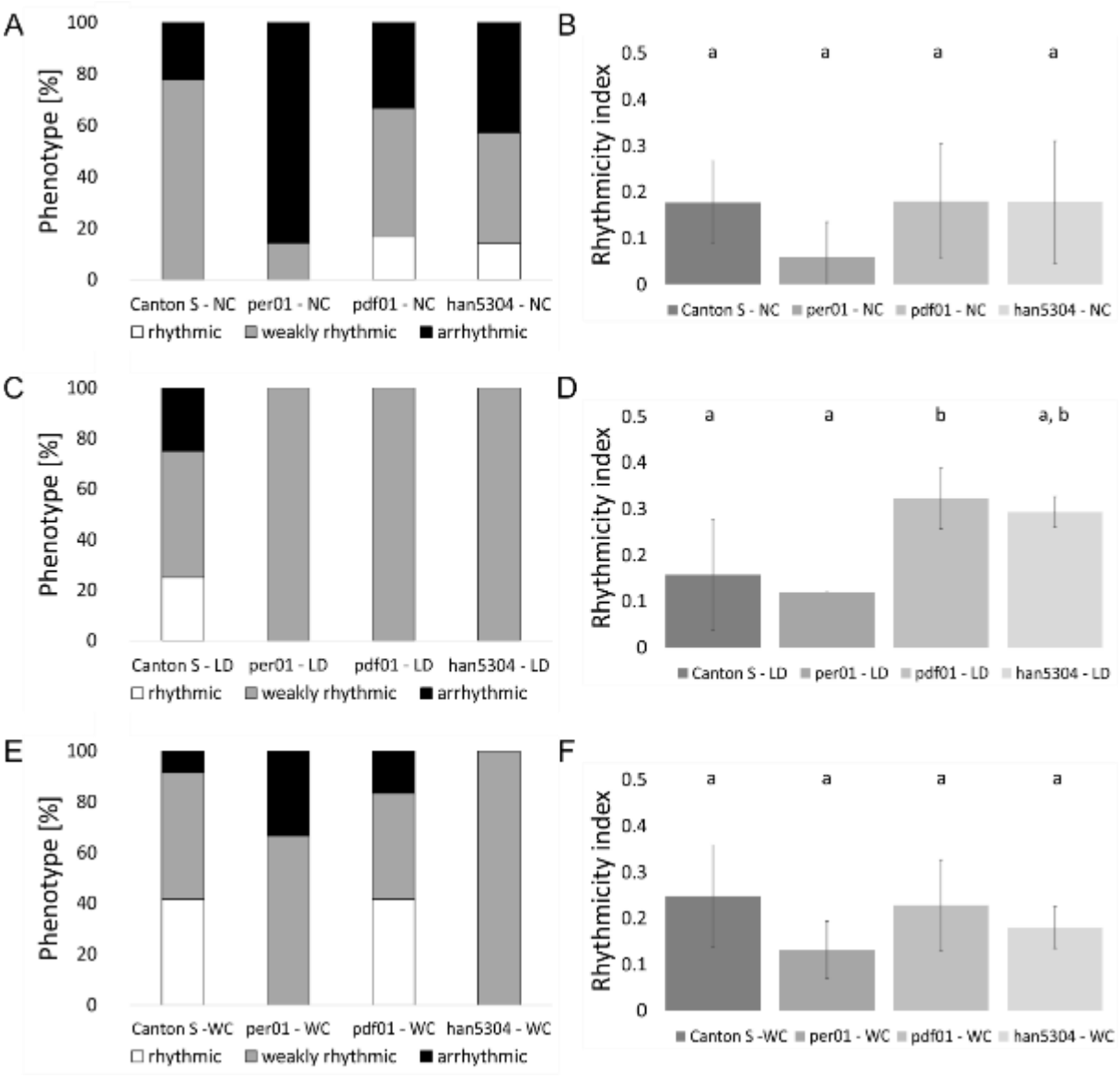

Figure 40: Comparison of the rhythmicity under different conditions

Comparison of the rhythmicity indices of *Canton S*, *per*^{01}, *pdf*^{01} and *han*^{5304} under natural (A, B), LD (C, D) and WC (E, F) conditions. A, C, E show the percentage of experiments with rhythmic (white), weakly rhythmic (gray) and arrhythmic (black) eclosion behavior under the different conditions. The means of the corresponding rhythmicity indices (±SD) are presented in B, D, F. Different letters above columns indicate significant difference ($p<0.05$).

2.8 Statistical modelling of the factors affecting the daily eclosion pattern

Statistical modelling revealed that the two components of the clock, the linear and the quadratic, had a significant effect on the daily pattern of eclosion in *Canton S* wildtype flies (Figure 41 A, A') as well as the two tested abiotic factors temperature (Figure 41 B) and light intensity (Figure 41 C). The effect of light intensity is only about 1/10 of the effect strength of the other factors (Figure 41).

The clock effect on the daily eclosion pattern was significantly reduced in the per^{01} mutant and significantly increased in pdf^{01} mutant flies compared to *Canton S* and han^{5304} mutant (Figure 41 A, A'). Temperature had a stronger effect in the per^{01} and han^{5304} mutant than in the wildtype and the pdf^{01} mutant (Figure 41 B) while light intensity had the same effect in all genotypes (Figure 41 C).

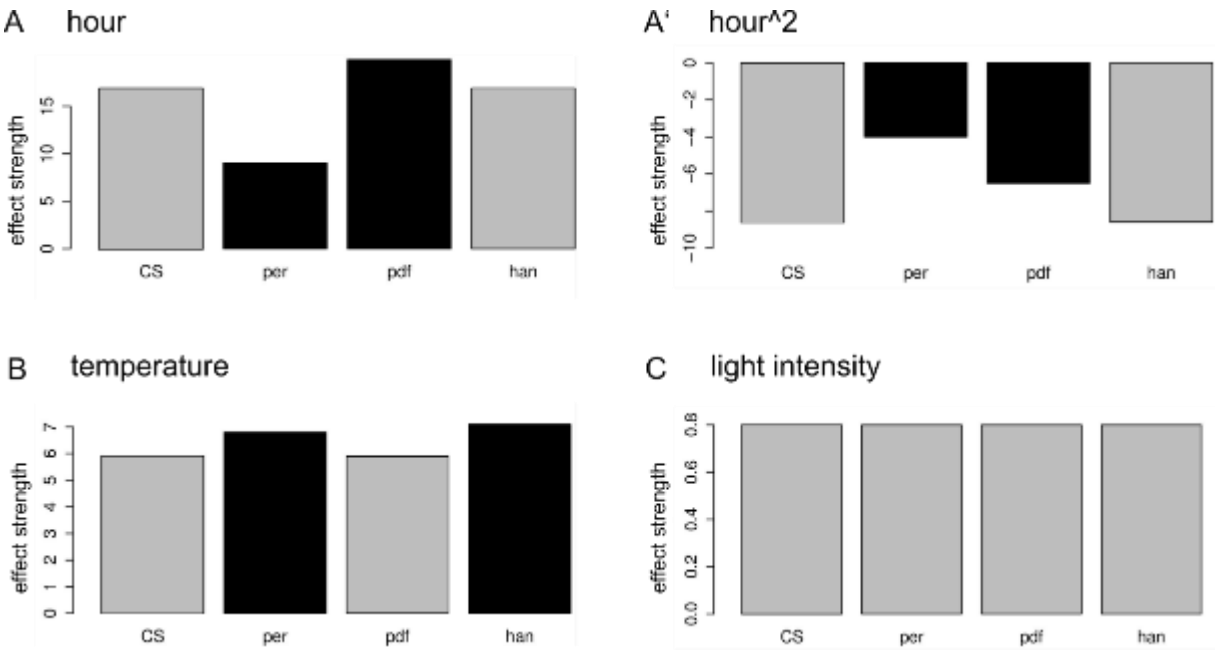

Figure 41: Effect of the clock and abiotic factors on the daily eclosion pattern
Results of the statistical modelling of the effect strength of the clock (A, A') and of the abiotic factors temperature (B) and light intensity (C) on the daily eclosion pattern. Effects in the per^{01} (per), pdf^{01} (pdf) and the han^{5304} (han) mutant were analyzed and compared to the wildtype *Canton S* (CS). Black bars in the mutant stand for a significant difference to *Canton S*, gray bars for no significant difference.

2.9 Theoretical statistical modelling

To better analyze the effects of single factors without influence through interactions with other factors, theoretical statistical modelling was applied. Here, simplified conditions were simulated where single factors were kept constant in a changing manner. All computations and the graphical output were performed by Dr. Oliver Mitesser.

In a first step, the eclosion probability was predicted from a model based on the collected data under natural conditions that only took into account the effect of the clock. The effects of temperature and light intensity were ignored. These results showed that the clock alone lead to a normal distribution of eclosion during the day (Figure 42). The linear clock component promoted eclosion especially early in the day, while later the quadratic component reducedit. This was true for the wildtype *Canton S* (Figure 42 A), the pdf^{01} mutant (Figure 42 C) and the han^{5304} mutant (Figure 42 D). While the general course of the curves was the same in all three genotypes, the amplitude was slightly increased in the pdf^{01} mutant (Figure 42 C) and slightly decreased in the han^{5304} mutant (Figure 42 D) compared to *Canton S* (Figure 42 A). In the per^{01} mutant, however, the effect of the clock alone lead to a distribution of eclosion that was opposite to the normal one (Figure 42 C). The eclosion probability was highest during the night and lowest at midday (Figure 42 C). This increased amount of eclosion during the night could indeed be observed in the eclosion profiles (Figure 26 - Figure 29) and statistical modelling revealed that it is due to an opposite effect of the clock in the per^{01} mutant compared to *Canton S* and the pdf^{01} and han^{5304} mutants.

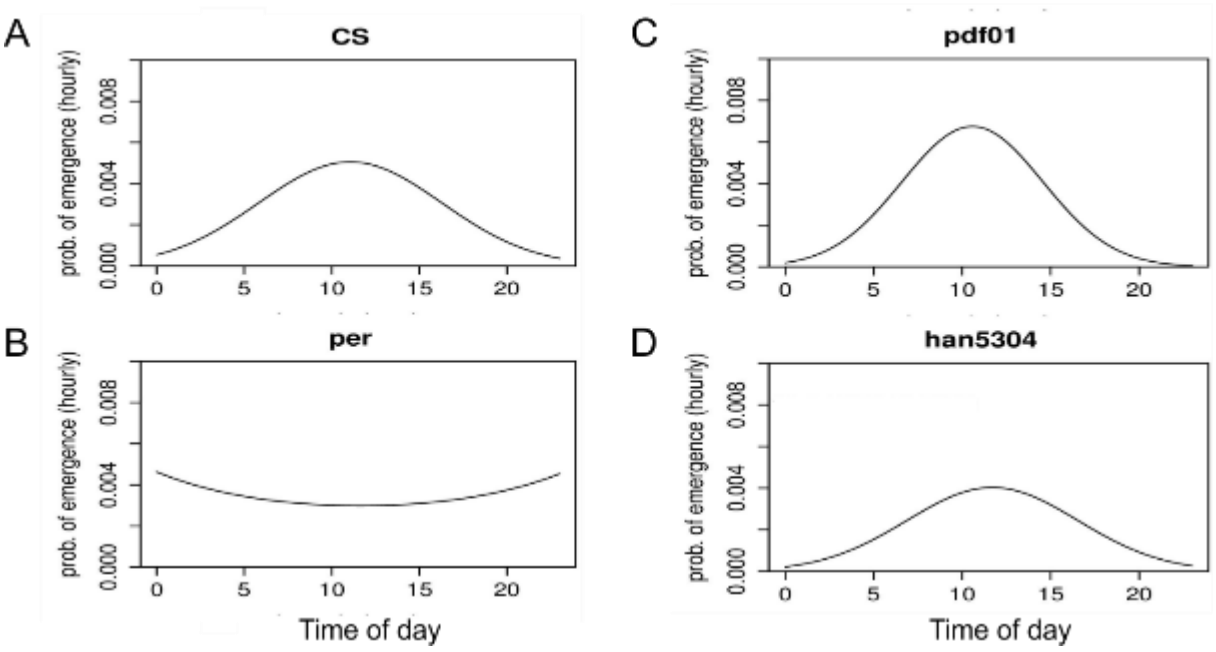

Figure 42: Predicted probability of eclosion from a model based on the clock effect
Theoretical pattern of daily eclosion in a model based on the effect of only the clock (linear and quadratic term) in the wildtype *Canton S* (A; CS), the per^{01} mutant (B; per), the pdf^{01} mutant (C; pdf01) and the han^{5304} mutant (D; han5304). Shown is the probability of eclosion per hour during the day.

In the next scenario, both temperature and light intensity were kept constant at their experimental mean. Additionally, their constant values were either increased (solid line) or decreased (dashed line) by 25% and the effect on the eclosion pattern was simulated (Figure 43). Both the increase and decrease of light intensity lead to an overall reduced eclosion possibility in *Canton S*, the pdf^{01} mutant and the han^{5304} mutant. Especially the eclosion peak around midday was strongly decreased (Figure 43 A, C, D; blue lines). Also in the per^{01} mutant, both increase and decrease of the mean light intensity had the same effect. But while changes in light intensity decreased the eclosion probability in the first half of the day, they increased it during the second half of the day and had nearly no effect in the middle of the day (Figure 43 B; blue lines). A decrease of the mean temperature decreased the probability of eclosion throughout the day in the per^{01} and han^{5304} mutant (Figure 43 B, D; red dashed line). In *Canton S* and the pdf^{01} mutant, it lead to a narrower eclosion curve with a higher amplitude and reduced eclosion probability during the night. The peak was shifted a few hours later (Figure 43 A, C; red dashed line). An increase of the mean temperature also increased the probability of eclosion during the night, especially in *Canton S*, the per^{01} and han^{5304} mutant (Figure 43 A, B, D; red solid line).

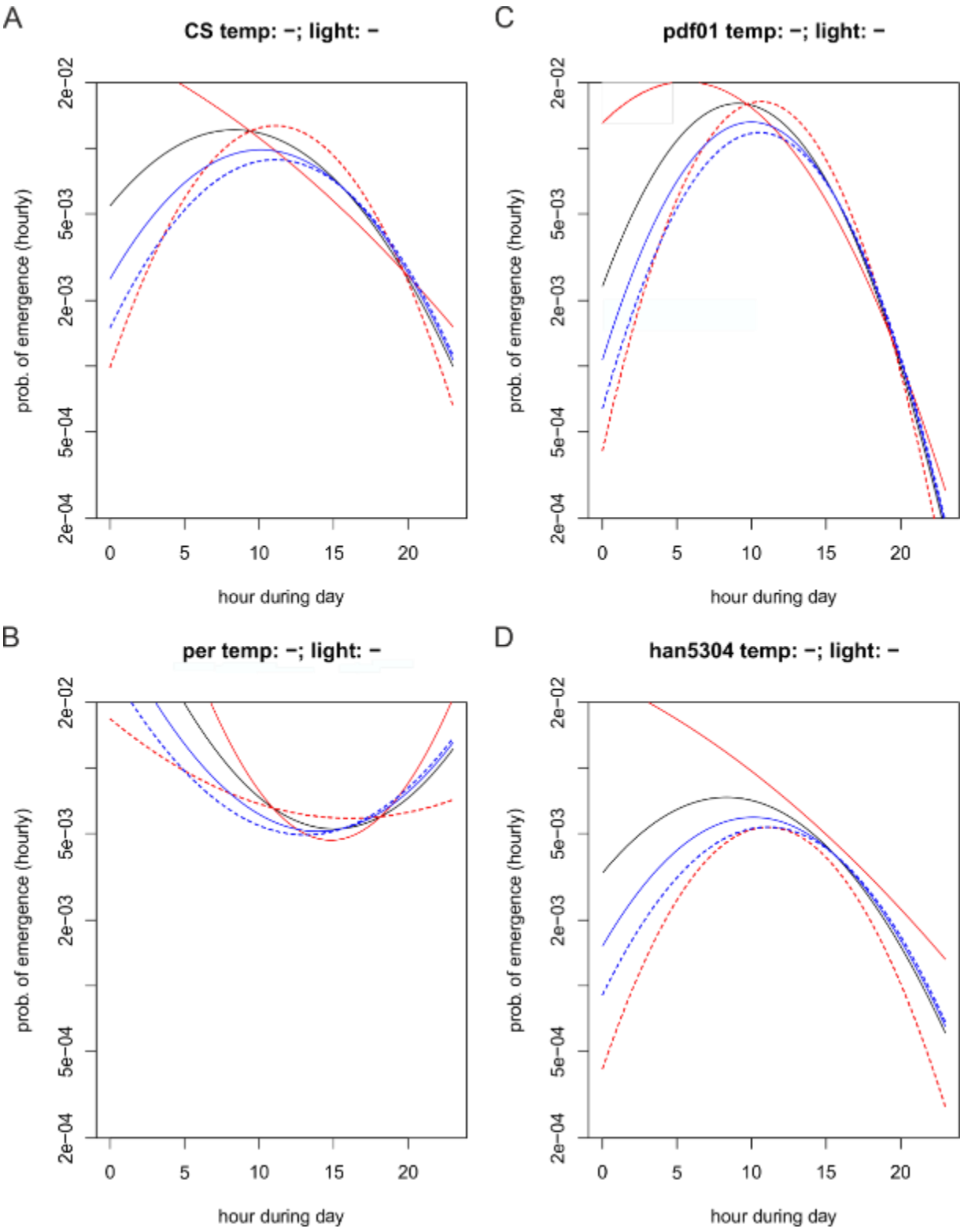

Figure 43: Predicted probability of eclosion in a model with constant mean temperature and light intensity

Theoretical pattern of daily eclosion in a model based on constant mean values of temperature and light intensity in the wildtype *Canton S* (A; CS), the per^{01} mutant (B; per), the pdf^{01} mutant (C; pdf01) and the han^{5304} mutant (D; han5304). Shown is the probability of eclosion per hour during the day. Colored lines represent eclosion pattern after increase (solid lines) or decrease (dashed lines) of temperature (red lines) or light intensity (blue lines).

While it stayed the same around the midday in the *per*^{01} mutant (Figure 43 B; red solid line), it was reduced in the second half of the day in *Canton S* and the *han*^{5304} mutant (Figure 43 A, D; red solid line). In the *pdf*^{01} mutant, the temperature increase increased the amplitude of the eclosion peak and shifted it some hours previous. Again, the eclosion probability was decreased in the second half of the day (Figure 43 C; red solid line).

Next, the temperature was allowed to follow a typical course over the day calculated by taking the mean of every hour, while the light intensity was kept constant at its experimental mean. In *Canton S*, the *pdf*^{01} and the *han*^{5304} mutant this generally lead to the same distribution of eclosion during the day as keeping both factors at a constant mean (Figure 44 A, C, D). The effect of the temperature increase was however weaker and did not promote eclosion during the night as much (Figure 44 A, C, D; red solid line). Temperature decrease still shifted the peak of eclosion a few hours later (Figure 44 A, C, D; red dashed line). For both, an increase or a decrease of temperature, the overall eclosion probability stayed the same in *Canton S* and the *pdf*^{01} mutant (Figure 44 A, C; red lines). In the *han*^{5304} mutant, however, an increase of temperature increased the probability of eclosion (Figure 44 D; red solid line), while a decrease reduced overall eclosion (Figure 44 D; red dashed line). In the *per*^{01} mutant, higher temperatures lead to more eclosion during the night, while the levels stayed the same around midday (Figure 44 B; red solid line). A decrease of temperature also reduced the eclosion probability, except around midday (Figure 44 B; red dashed line). A more natural-like course of temperature promoted the appearance of a slight peak at the beginning of the day in *per*^{01} mutant flies, which could not be seen under complete constant conditions (Figure 44 B). As before, changes in light intensity reduced the overall probability of eclosion in all genotypes (Figure 44; blue lines).

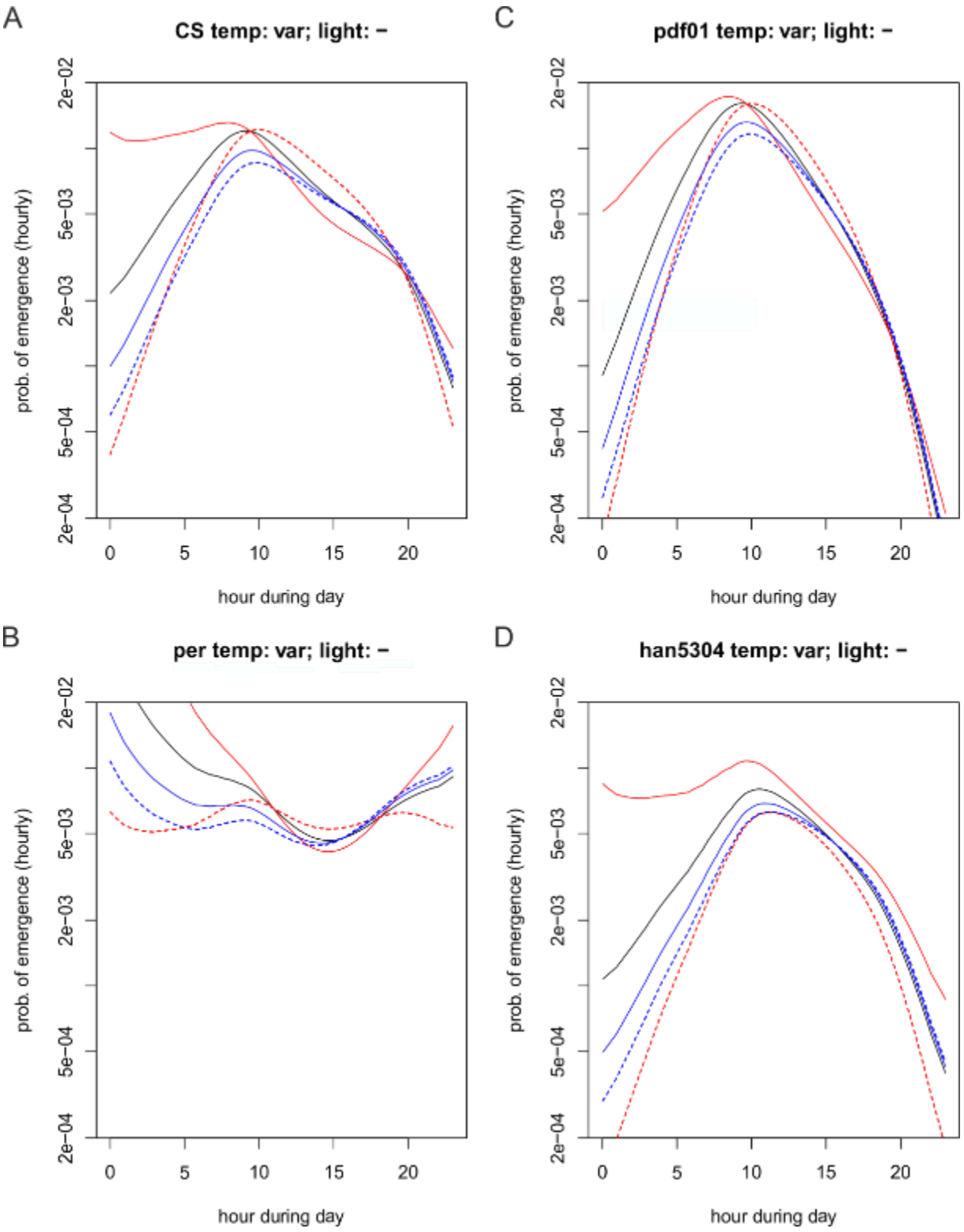

Figure 44: Predicted probability of eclosion in a model with hourly mean temperature and constant mean light intensity

Theoretical pattern of daily eclosion in a model based on hourly mean values of temperature and constant mean values of light intensity in the wildtype *Canton S* (A; CS), the per^{01} mutant (B; per), the pdf^{01} mutant (C; pdf01) and the han^{5304} mutant (D; han5304). Shown is the probability of eclosion per hour during the day. Colored lines represent eclosion pattern after increase (solid lines) or decrease (dashed lines) of temperature (red lines) or light intensity (blue lines).

Allowing the light intensity to change in a natural-like manner while the temperature stayed constant lead to much more distinct eclosion peaks with a higher amplitude in *Canton S*, the *pdf*^{01} and the *han* ^{5304} mutants (Figure 45 A, C, D). Also in *per*^{01} mutant, the eclosion peak, that was already visible under changing temperatures, became more pronounced (Figure 45 B). Increasing the mean of the temperature lead to more eclosion during the night in all strains (Figure 45; red solid line). While eclosion probability was reduced during the rest of the day in *Canton S* and the *pdf*^{01} mutant (Figure 45 A, C; red solid line), it was increased in the first half of the day in the *per*^{01} and *han*^{5304} mutants (Figure 45 B, D; red solid line). A decrease of temperature had the opposite effect and lead to overall increased eclosion in *Canton S* and *pdf*^{01} with a narrower gate and less eclosion during the night (Figure 45 A, C; red dashed line) and to an overall decrease of eclosion in the *per*^{01} and *han*^{5304} mutants (Figure 45 B, D; red dashed line). Changing the level of light intensity again lead to reduced eclosion probability in all genotypes (Figure 45; blue lines).

Giving natural-like temperature and light intensity courses based on the hourly means further enhanced the effects observed before. The eclosion gate was still narrower and the peaks more defined in all genotypes (Figure 46). The temperature effects were the same as in the previous scenario, yet less pronounced. Higher temperatures still lead to more eclosion during the night in all genotypes (Figure 46; red solid line) and both decrease and increase of temperature had an opposite effect in the *Canton S* and *pdf*^{01} mutant (Figure 46 A, C; red lines) compared to the *per*^{01} and *han*^{5304} mutants (Figure 46 B, D; red lines). Changes in light intensity again resulted in a decrease of the overall eclosion probability (Figure 46; blue lines). The additional peak of eclosion in the *per*^{01} mutant was the most pronounced in this scenario (Figure 46 B).

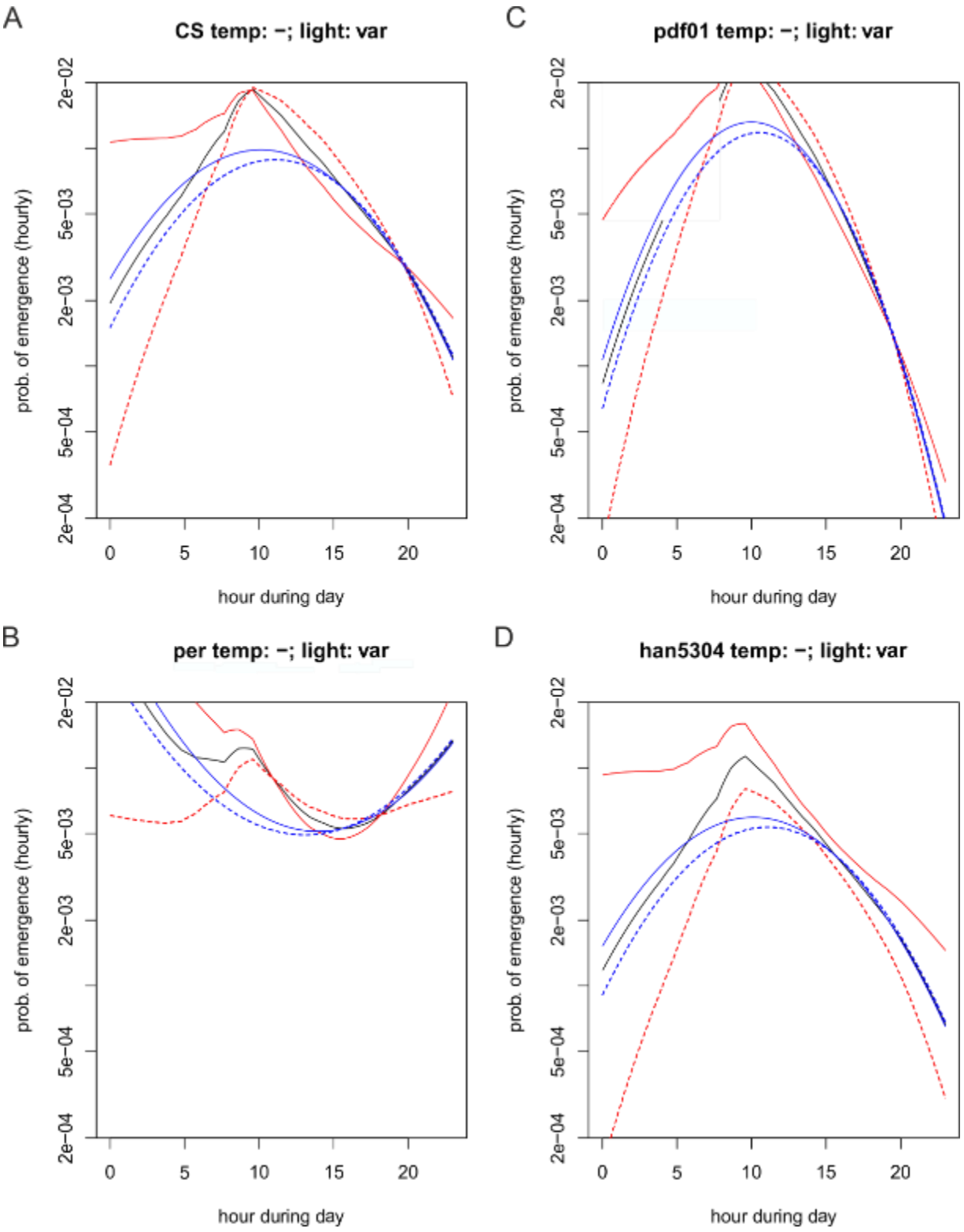

Figure 45: Predicted probability of eclosion in a model with constant mean temperature and hourly mean light intensity

Theoretical pattern of daily eclosion in a model based on constant mean values of temperature and hourly mean values of light intensity in the wildtype *Canton S* (A; CS), the per^{01} mutant (B; per), the pdf^{01} mutant (C; pdf01) and the han^{5304} mutant (D; han5304). Shown is the probability of eclosion per hour during the day. Colored lines represent eclosion pattern after increase (solid lines) or decrease (dashed lines) of temperature (red lines) or light intensity (blue lines).

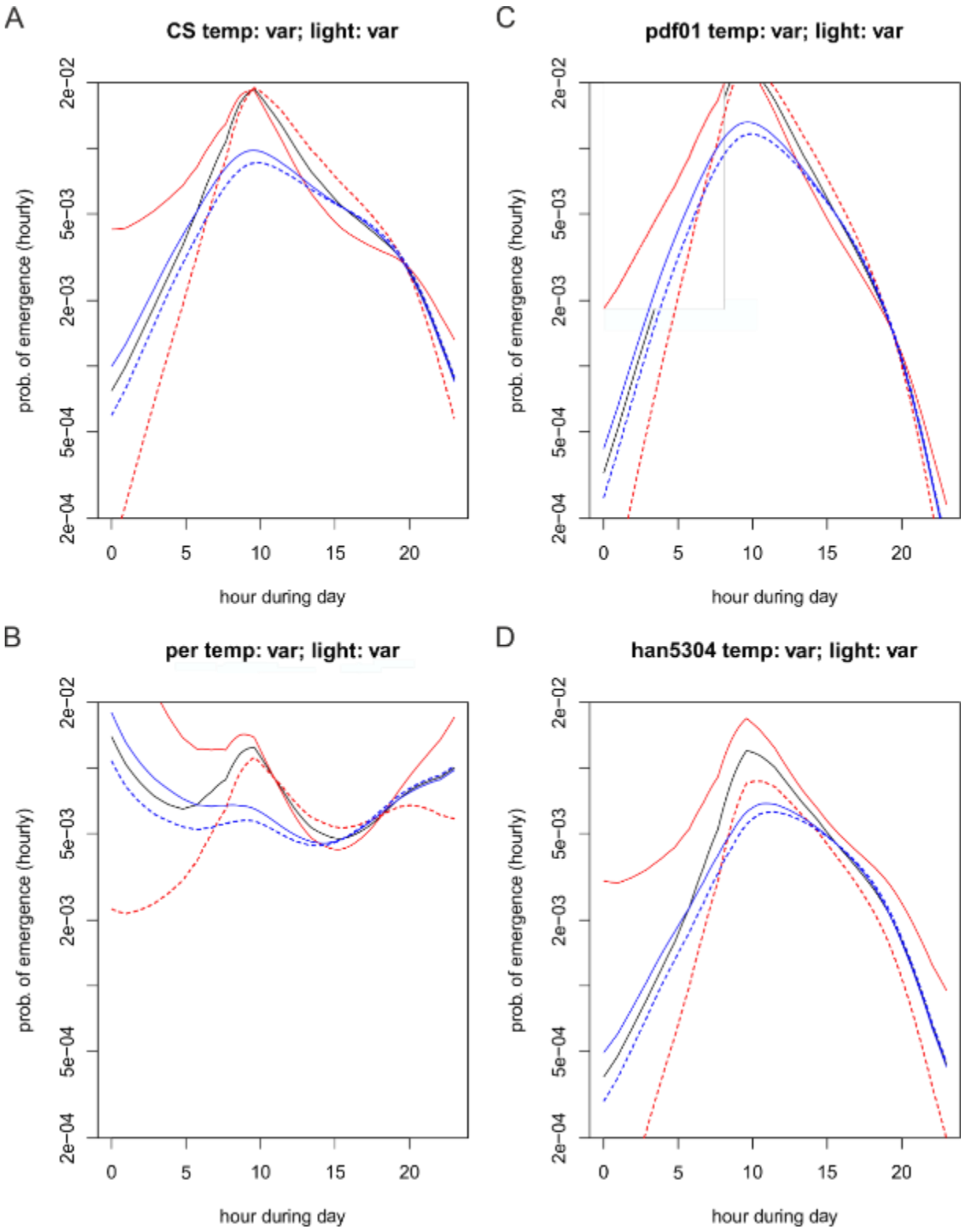

Figure 46: Predicted probability of eclosion in a model with hourly mean temperature and light intensity

Theoretical pattern of daily eclosion in a model based on hourly mean values of temperature and of light intensity in the wildtype *Canton S* (A; CS), the per^{01} mutant (B; per), the pdf^{01} mutant (C; pdf01) and the han^{5304} mutant (D; han5304). The probability of eclosion per hour during the day. Colored lines represent eclosion pattern after increase (solid lines) or decrease (dashed lines) of temperature (red lines) or light intensity (blue lines).

2.10 Eclosion rhythms of the wildtype *Hubland* under laboratory LD conditions

To study the eclosion behavior of free living flies and assess possible differences to laboratory wildtypes, *Drosophila melanogaster* were collected at a pomace heap in Gerbrunn, very close to the campus Hubland, in Würzburg (49°46'45.3"N 9°58'32.1"E). This new strain was named wildtype *Hubland*. The caugth flies were allowed to lay eggs in *Drosophila* culture vials and the resulting first generation was raised under a regime of 12 hours light and 12 hours darkness and a constant temperature of 20°C. After 17 days, their eclosion rhythms were monitored and the results are presented in Figure 47. The flies showed perfectly normal eclosion rhythms with a narrow gate, clear lights-on peaks and only few flies eclosing during the dark phase (Figure 47 A). Analysis revealed that they eclosed weakly rhythmically with a rhythmicity index of 0.27 (Figure 47 B). Overall, their behavior was basically identical to that of the other wildtypes (Figure 12, Figure 14).

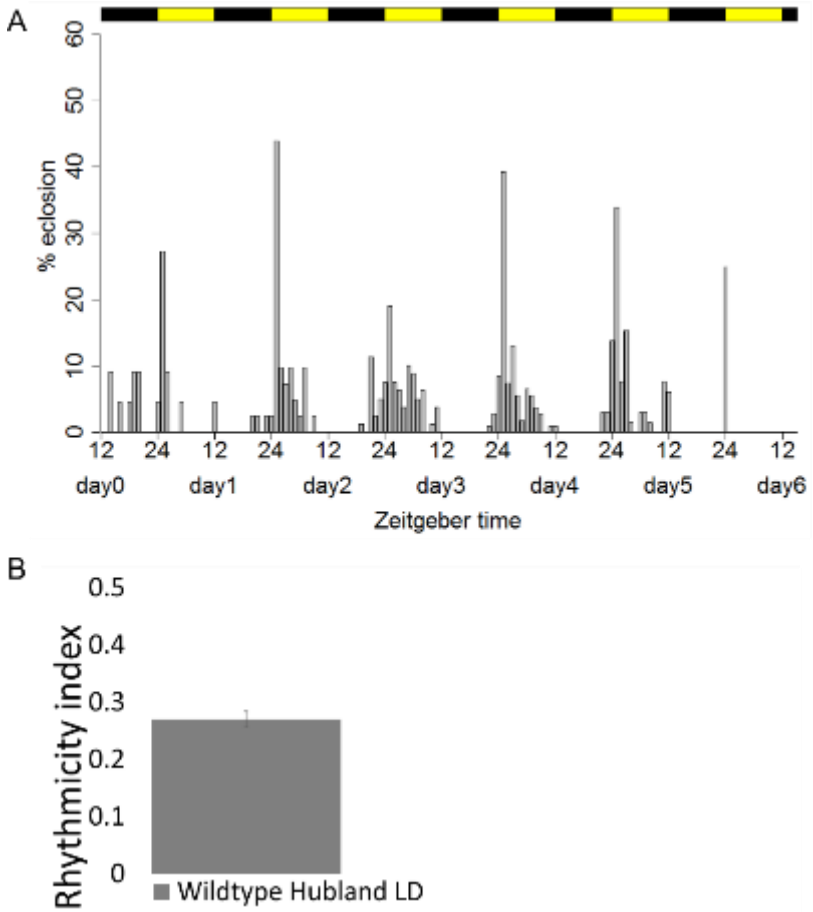

Figure 47: Eclosion rhythms of the wildtype *Hubland* under LD conditions
Eclosion profiles for the wildtype *Hubland* under LD conditions (A). Each bar represents the percentage of eclosed flies per hour normalized to the number of eclosed flies per day. The black and yellow rectangles represent the light regime. (B) shows the mean of the rhythmicity indices (±SD). (N=3; n=319)

3. Discussion

The present dissertation research presents the first results for eclosion monitored under conditions where the pupae were in direct contact with their surrounding environment. Furthermore, it is the first time that statistical modelling was applied to dissect the influence of the clock on the one hand and of the abiotic environmental factors on the other on the eclosion rhythm of *Drosophila melanogaster*.

Temperature and not relative humidity influences the timing of eclosion

It has very early been shown that temperature acts as a Zeitgeber for eclosion entrainment (Zimmerman *et al.*, 1968b), but it was so far not shown for relative humidity. However, keeping wild type flies in cycles of 12 hour 30% and 12 hours 70% relative humidity resulted in non-entrained flies with arrhythmic eclosion. This is in line with the results of other groups that were not able to entrain eclosion (Ralf Stanewsky, personal communication) or locomotor activity (Melanie Horn, CRC 1047, project C5, personal communication) to relative humidity cycles. It is therefore unlikely that relative humidity acts as a Zeitgeber. Pittendrigh hypothesized that eclosion in the morning is an adaptation to the increased humidity levels at this time of day, which would facilitate the spreading of the wings and thereby increase the survival of the flies (Pittendrigh, 1954). Results by Melanie Horn, however, question this long-standing hypothesis, as she could show that flies are still able to eclose and unfold their wings even at only 2% relative humidity. Higher temperatures of already 30°C, on the other hand, impaired both survival and success rate for wing expansion (Melanie Horn, CRC 1047, project C5, personal communication). This is congruent with studies in the onion fly *Delia antiqua* that also showed that high temperatures and not low relative humidity negatively affect viability and wing expansion (Tanaka and Watari, 2009). It is therefore likely that eclosion in the morning is rather an adaption to low temperatures than to high humidity. As flies were shown to be diurnal under seminatural conditions (Vanin *et al.*, 2012), eclosion in the evening or at night, when temperature is also low, is avoided.

PDF is not needed for rhythmic eclosion under natural conditions

As main output factor of the clock, PDF synchronizes cells that express the receptor Han with the main oscillator. Mutants for PDF or its receptor showed rhythmic eclosion under natural

conditions and their rhythmicity indices did not differ from that of the wildtype. This is congruent with results from the lab, where their effect on rhythmicity was only visible under constant conditions (Figure S 10 B, Figure S 11 B, Figure S 12 B, Figure S 13 B). Under natural conditions, as well as under non-constant laboratory conditions, a lack of either PDF or Han has no consequences for rhythmicity since the cells can use the presented Zeitgebers to synchronize.

The clock is essential for rhythmic eclosion under natural conditions

Lack of the clock gene *period,* however, that is part of the central oscillator, resulted in decreased rhythmicity under laboratory conditions (Figure S 8, Figure S 9) and almost complete arrhythmicity under natural conditions. The remaining rhythmicity can be attributed to the fact that per^{01} mutants still possess a residual clock (Dowse *et al.*, 1987; Helfrich and Engelmann, 1987; Helfrich-Förster, 2001; Bywalez *et al.*, 2012). But unlike missing PDF, the absence of a central part of the circadian clock cannot be compensated by re-synchronization to Zeitgebers. While Schlichting *et al.*, 2015 proposed that a functional clock is not needed for rhythmic behavior (Schlichting *et al.*, 2015), the present results show that, at least for eclosion, a functional clock is a prerequisite for rhythmic behavior under natural conditions.

Rhythmicity is decreased under natural conditions

In all four genotypes, a trend to decreased eclosion rhythmicity was observed under natural conditions compared to laboratory conditions. This effect was strongest in the per^{01} mutant, which showed rhythmic eclosion in only one experiment.

Contradicting findings were reported by De *et al.*, 2012: they showed increased general rhythmicity under semi-natural conditions compared to laboratory conditions, especially for the per^{01} mutant, which eclosed rhythmically (De *et al.*, 2012). Moreover, experiments on locomotor activity rhythms under semi-natural (Vanin *et al.*, 2012) or simulated natural-like conditions (Schlichting *et al.*, 2015) reported high rhythmicity levels for per^{01} mutant flies. The general decrease of eclosion rhythmicity and the loss of rhythmicity in per^{01} flies for eclosion under natural conditions in Würzburg can possibly be explained by constantly varying daily conditions throughout the development of the flies within and between experiments. De *et al.*, 2012 conducted their experiments in Bangalore, India under relatively stable climatic conditions throughout the year. These stable conditions, especially during development, could

facilitate a strengthening of the rhythmicity, comparable to constant conditions in the laboratory. To test this hypothesis, simulation experiments were performed. Conditions recorded during the experimental season of the year 2014 were simulated in an incubator and flies were raised and their eclosion monitored under these simulated conditions. In parallel, flies of the same genotype were reared under LD conditions until their eclosion was also monitored under simulated natural conditions. If conditions during the development have an effect on the adult eclosion rhythmicity, the flies raised under laboratory conditions should eclose more rhythmically than these raised under simulated natural conditions. Unfortunately, the eclosion profiles under simulated conditions did not resemble these actually recorded under natural conditions in 2014 (Galliker, 2015). Other studies, however, suggest an effect of the conditions during development on the period of locomotor activity of adult flies (Tomioka *et al.*, 1997). In all the above mentioned studies, conditions were semi-natural or natural-like, where flies were kept in food vials (De *et al.*, 2012) or the behavior of the flies was monitored in glass tubes (Vanin *et al.*, 2012). In these closed conditions, it is not sure whether the measured environmental conditions correspond to those experienced by the flies in the vials. Especially the locomotor activity behavior could be strongly altered by keeping the flies in glass tubes. Schlichting *et al.*, 2015 varied only the light intensities but kept temperature and relative humidity constant, so that the conditions resemble more that in the laboratory (where per^{01} flies were shown to eclose weakly rhythmic) than that in nature.

Temperature influences the daily eclosion profile, light does not

Theoretical statistical modelling revealed that the more natural-like the simulated conditions are, the better the actual eclosion profiles can be describe. Although the effect of the clock alone is sufficient to describe the general course of the daily eclosion pattern, it takes the influence of the abiotic factors light and temperature to sharpen it. Theoretical statistical modelling offers the chance to study the effect of single factors, one by one, which would never be possible under natural conditions where the time of day, light intensity and temperature are highly correlated. It revealed that both increase and decrease of light intensity decrease the probability of eclosion, while they do not affect the daily eclosion profile. This may be interpreted as an adaption of the flies to the natural light regime. Meanwhile, changes in temperature do not affect the overall eclosion probability, but change the daily timing of eclosion. Higher temperatures promote a shift of eclosion into the night

while lower temperature shift eclosion more to midday. These effects are again strongest in the *per*^{01} mutant. Also other studies showed that temperature has a stronger effect on the actual daily behavior rhythm than light (De *et al.*, 2012; Menegazzi *et al.*, 2012; Vanin *et al.*, 2012; Menegazzi *et al.*, 2013) and that flies with an impaired clock respond stronger to temperature changes than wildtype flies (Menegazzi *et al.*, 2012).

Temperature has a stronger effect in *per* mutants than in the wildtype

The shift of eclosion into the night is presumably an adaption to evade high temperatures during the day that would be harmful to the flies. Vanin *et al.*, 2012 described an additional peak of activity during midday under natural conditions that was interpreted as an escape response to high temperatures (Vanin *et al.*, 2012; Green *et al.*, 2015) and was no longer observable under simulated conditions in the wildtype, but still in clock mutants (Menegazzi *et al.*, 2012). Menegazzi *et al.*, 2012 hypothesized that an intact clock suppresses excess activity under increasing temperatures as long as they are tolerable (Menegazzi *et al.*, 2012). This could then also explain why the mutants with defect clocks show more eclosion during the night than the wildtype flies. Another explanation could be the involvement of differential *per* splicing at different temperatures (Low *et al.*, 2008). As the different isoforms adapt their behavior to the current temperature conditions, loss of *per* could also impair this temperature-dependent adaptions. Furthermore it was shown that *per* has an effect on temperature compensation, as flies mutant for the *per* gene had significantly different periods under different temperatures (Konopka *et al.*, 1989), as well as on the circadian rhythm of temperature preference, which is disturbed in clock mutants like *per*^{01} (Kaneko *et al.*, 2012). The stronger effect of temperature in *per*^{01} mutants and their arrhythmic behavior could also be attributed to the defects in behavioral adaption to temperature changes.

Light is the strongest Zeitgeber for eclosion

But even though the daily pattern of activity is mainly regulated by temperature, light remains the most important Zeitgeber for the molecular clock (Menegazzi *et al.*, 2013). Only with a changing light regime are defined eclosion patterns visible and the peaks get much more pronounced in the modelled eclosion patterns. This is in contrast to data from Schlichting *et al.*, 2015, who showed that simulation of natural-like light cycles were enough to produce rhythmicity in *per*^{01} mutant flies and daily locomotor activity patterns that resembled results

from Vanin *et al.*, 2012 under natural conditions. Schlichting *et al.* (2015) concluded that temperature cycles or even a functioning clock are not needed for rhythmicity (Schlichting *et al.*, 2015). However, the simulated data are quite stable, and as mentioned before, per^{01} flies also eclose with weak rhythmicity under laboratory conditions. Also, while light cycles may be enough to induce rhythmic daily behavior, theoretical modelling showed that having both factors, light intensity and temperature, change in a natural way over the course of the day induces behavior that more resembles natural eclosion profiles than changing only one factor.

Conclusions

Taken together, this results in a model for eclosion under natural conditions where light is essential to drive the central pacemaker and define the gate in which eclosion is possible at all, while temperature has more influence on the daily eclosion pattern within the gate.

Outlook

Further experiments have to be done in the coming seasons to confirm and improve the current model, as for now it is based on the data collected in only one year. Analysis of the few data from 2015 so far confirm the current model, as no significant differences of *Canton S* could be detected between the two seasons. Also the wildtype *Lindelbach* showed deviations from *Canton S* from 2014 only for the quadratic term of the hour, while the effect of the other parameters was the same (Figure S 18).

To identify which wavelength of light is important for the entrainment of the clock, different *rhodopsin* and *cry* mutants could be tested under natural conditions.

As it is not possible to change temperature or light intensity under natural conditions without also influencing other factors, mutants for light and/or temperature perception could be tested. First experiments with available mutants showed, however, that the hypomorph temperature blind mutant $nocte^{p}$ (Thibault *et al.*, 2004; Sehadova *et al.*, 2009) had a strongly reduced viability under natural conditions, showed impaired rhythmicity under DD conditions (Figure S 16 A) and was still able to entrain to temperature cycles under laboratory conditions (Figure S 17 A, C). The blind mutant *yw;;* $glass^{60j}$, cry^{b} (Helfrich-Förster *et al.*, 2001) had a higher viability and rhythmicity (Figure S 15 B, C, Figure S 16 B, C, Figure S 17 B, C) and was tested in a few experiments in 2015.

To study the effect of stable conditions on the eclosion rhythmicity, flies could be raised in parallel under natural and laboratory conditions with following monitoring of their eclosion behavior under natural conditions. Differences in rhythmicity would then help to understand the different results from De *et al*., 2012.

To assess if local flies are better adapted to local climate conditions, the wildtype *Hubland* should be tested as well as freshly caught flies in the respective season. This could also show if and how fast differences between laboratory strains and wild flies emerge.

Chapter III. The role of PTTH in the circadian timing of eclosion and eclosion rhythmicity

1. Introduction

The prothoracicotropic hormone (PTTH) is a brain neuropeptide hormone that regulates production of ecdysone in the prothoracic gland (PG), which is the main developmental regulator of molting and ecdysis.

Already at the beginning of the 20th century, head ligation experiments in moths revealed that a factor from the brain was necessary for the induction of molting during critical stages (Kopec, 1922). The same results were later achieved in silkworms (Truman and Riddiford, 1970) and in *Manduca sexta,* where it was shown that the critical period was gated by the photoperiod (Truman, 1972). PTTH was purified in *Bombyx mori* as the factor that induces production of ecdysone from the PG (Kawakami *et al.*, 1990; Kataoka *et al.*, 1991). Only several years later, PTTH was also identified and characterized in *Drosophila melanogaster* (McBrayer *et al.*, 2007). In *Drosophila* larvae, PTTH is expressed in a pair of neurons in the supraoesophageal ganglion that terminates into the PG (Siegmund and Korge, 2001; McBrayer *et al.*, 2007). In adults, *ptth*-GAL4 expression can be observed in several neurons in the brain that innervate the ellipsoid body (McBrayer *et al.*, 2007). PTTH acts through its receptor Torso, a receptor tyrosine kinase that is expressed in the PG and in the adult male accessory glands (Rewitz *et al.*, 2009; Hentze *et al.*, 2013). Binding of PTTH to Torso activates the Ras/Raf/ERK pathway and induces the synthesis of ecdysone (Rewitz *et al*., 2009). Ablation of PTTH neurons leads to a prolongation of development, especially in the phase from the third instar larva to pupariation. The time between pupariation and eclosion is however not changed in these animals. Since the larvae continue feeding in the prolonged stages, pupae and adults are larger in PTTH neuron-ablated flies compared to controls. Overexpression of PTTH on the other hand leads to eclosion of smaller flies. PTTH ablation reduces viability and fecundity in females and leads to male-on-male courtship behavior (McBrayer *et al.*, 2007). The prolonged development is caused by low levels of 20E mainly in the L3 stage (McBrayer *et al.*, 2007). Down-regulation of *torso* in the PG phenocopies the ablation of PTTH neurons and these effects can be completely rescued by feeding 20E (Rewitz *et al.*, 2009). PTTH also plays a role in the regulation of light avoidance in *Drosophila*, which is impaired after silencing of PTTH

neurons or knockdown of its receptor *torso* in the brain. Knockdown of *torso* in the PG does not affect the light avoidance behavior, indicating a functionally different role from ecdysteroidogenesis (Yamanaka *et al*., 2013).

Arborizations of the PDF producing lateral neurons terminate in close proximity to dendrites of the PTTH neurons in larval (McBrayer *et al.*, 2007) and pharate (Selcho *et al.*, unpublished-a) brains of *Drosophila*. McBrayer *et al.*, 2007 showed that the ultradian cycling of the *Ptth* mRNA in L3 larvae was altered in pdf^{01} mutants and that transcript levels were increased compared to controls, implying a role of PDF as a negative regulator of PTTH transcription. Ablation of the PDF-expressing LNs (Myers *et al.*, 2003), as well as disruption of the molecular clock in these neurons (Blanchardon *et al.*, 2001), leads to arrhythmic eclosion, as does the overexpression of PDF (Helfrich-Förster *et al.*, 2000). Yet, the central clock is not sufficient for eclosion rhythmicity, it depends also on the peripheral clock in the PG (Myers *et al.*, 2003). Myers *et al.*, 2003 showed that the PG contains a functioning clock with *per* and *tim* cycling shortly before eclosion and that disruption of this clock leads to arrhythmicity of eclosion, but not locomotor activity (Myers *et al.*, 2003). The PG clock in turn is dependent on input from the central pacemaker cells (Myers *et al.*, 2003). How the clock and the PG are connected remains unclear, but as PTTH neurons are in close proximity to PDF positive cells and terminate onto the PG, they seem to be good candidates to play a role in this connection. It could indeed be shown that silencing of PTTH neurons leads to arrhythmic eclosion under constant conditions (Chen, 2012).

A putative role for PTTH in the circadian timing was recently described by Chen *et al.*, 2014 who found that PTTH activates the miRNA *let-7* via ecdysone. *let-7* inhibites the clock gene *clockwork orange* (*cwo*) (Matsumoto *et al.*, 2007) and thereby represses the transcription of the core clock genes *per* and *tim* (Chen *et al*., 2014). Furthermore, the ecdysone induced nuclear receptor E75 was shown to enhance the CLK/CYC mediated transcription of *per* (Kumar *et al.*, 2014; Jaumouille *et al.*, 2015).

In this chapter, PTTH neurons were ablated to confirm the effect on eclosion timing previously obtained by electrical silencing of the PTTH neurons (Chen 2012). To dissect whether PTTH plays a role in the light reception pathway, the eclosion behavior of the flies was also tested under temperature entrainment. The receptors of the two peptides released by PDF neurons, PDF and sNPF, were knocked-down in the PTTH neurons and eclosion was monitored to study the possible connection between the PDF and the PTTH neurons. As a *torso*-GAL 4 line showed

torso expression not only in the PG, but also in the brain and in the photoreceptor cells of the eye (Mareike Selcho, personal communication), the actual expression pattern of *torso* in pharate flies was analyzed using RT-PCR. Target tissues for PTTH and their relevance for eclosion rhythmicity were further analyzed by knock-down of *torso* in the brain and in the prothoracic gland (PG), followed by eclosion monitoring. As *Ptth* cycling was so far only shown in larvae, mRNA levels in pharate flies under LD and DD conditions were analyzed by qPCR.

2. Results

2.1 Eclosion rhythms under light entrainment after ablation of PTTH neurons

Ablation of the PTTH neurons by expressing UAS-*grim* under the *ptth*-GAL4 driver had only a weak effect under LD conditions and lead to a slightly broader gate compared to the controls, while the lights-on peaks were not affected (Figure 48 A - C). There was no significant difference between the rhythmicity indices of the experimental flies and the control flies (Figure 48 D). Under constant dark conditions, however, ablating the PTTH neurons lead to arrhythmic eclosion after the first day (Figure 49 A), while the controls stayed rhythmic (Figure 49 B, C). Although the effect was not statistically significant, there was a strong trend to reduced rhythmicity in the experimental flies compared to the controls (Figure 49 D). The period lengths showed no significant difference under DD conditions (Figure S 19 A).

2.2 Eclosion rhythms under temperature entrainment after ablation of PTTH neurons

Ablating the PTTH neurons by expressing UAS-*grim* under the *ptth*-GAL4 driver had no effect on the eclosion profiles and rhythmicity indices under WC conditions compared to controls (Figure 50). As in DD conditions, eclosion became arrhythmic under CC conditions (Figure 51 A) while the controls stayed rhythmic (Figure 51 B, C). There was a significant decrease of rhythmicity in flies in which the PTTH neurons had been ablated compared to the controls (Figure 51 D), while the period length was not affected (Figure S 19 B).

2.3 Eclosion rhythms under temperature entrainment after silencing of PTTH neurons

Silencing the PTTH neurons by expressing UAS-*dORKΔ* under the *ptth*-GAL4 driver lead to the same results as ablation. There was no difference observable between the eclosion profiles (Figure 52 A, B) or rhythmicity indices (Figure 52 C) under WC conditions, while eclosion became arrhythmic under CC conditions (Figure 53 A). Although the rhythmicity index in experimental flies was significantly decreased compared to the control (Figure 53 C), the period lengths showed no significant difference (Figure S 19 C).

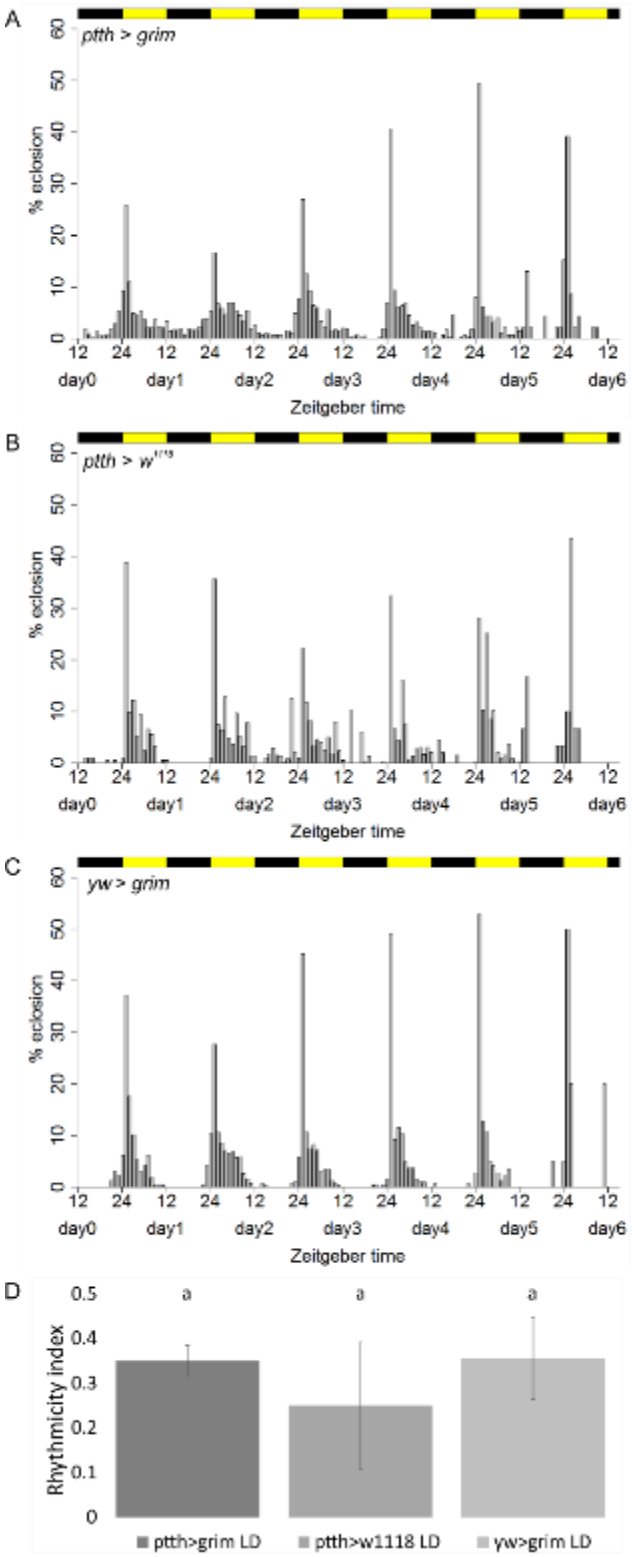

Figure 48: Eclosion rhythms under LD conditions after the ablation of PTTH neurons
Eclosion profiles for populations expressing UAS-*grim* driven by *ptth*-GAL4 (A) and the respective controls (B: GAL4 control, C: UAS control) under LD conditions. Each bar represents the percentage of eclosed flies per hour normalized to the number of eclosed flies per day. The black and yellow rectangles represent the light regime. (D) shows the means of the rhythmicity indices (±SD). Different letters above columns indicate significant difference ($p<0.05$). (N=3, 2, 2; n=2122, 1477, 1223)

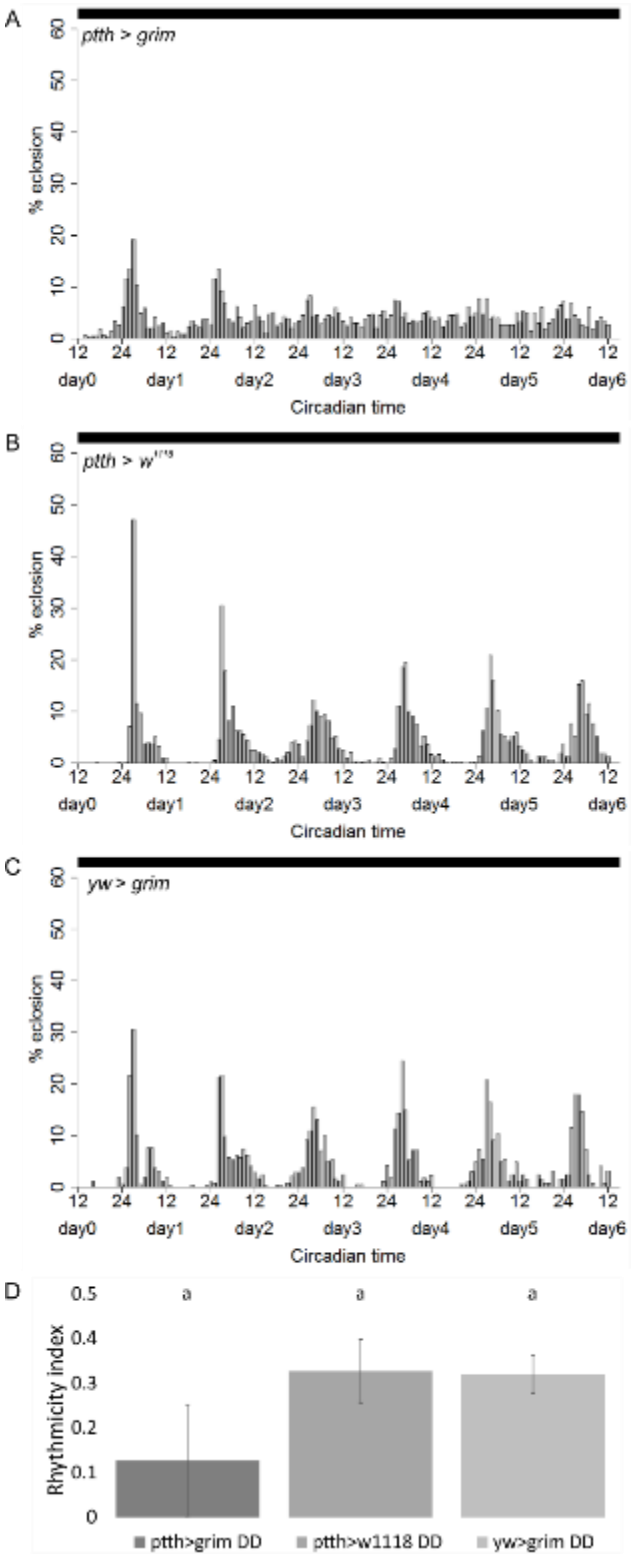

Figure 49: Eclosion rhythms under DD conditions after the ablation of PTTH neurons
Eclosion profiles for populations expressing UAS-*grim* driven by *ptth*-GAL4 (A) and the respective controls (B: GAL4 control, C: UAS control) under DD conditions. Each bar represents the percentage of eclosed flies per hour normalized to the number of eclosed flies per day. The black rectangles represent the light regime. (D) shows the means of the rhythmicity indices (±SD). Different letters above columns indicate significant difference ($p<0.05$). (N=3, 3, 2; n=2569, 2275, 1104)

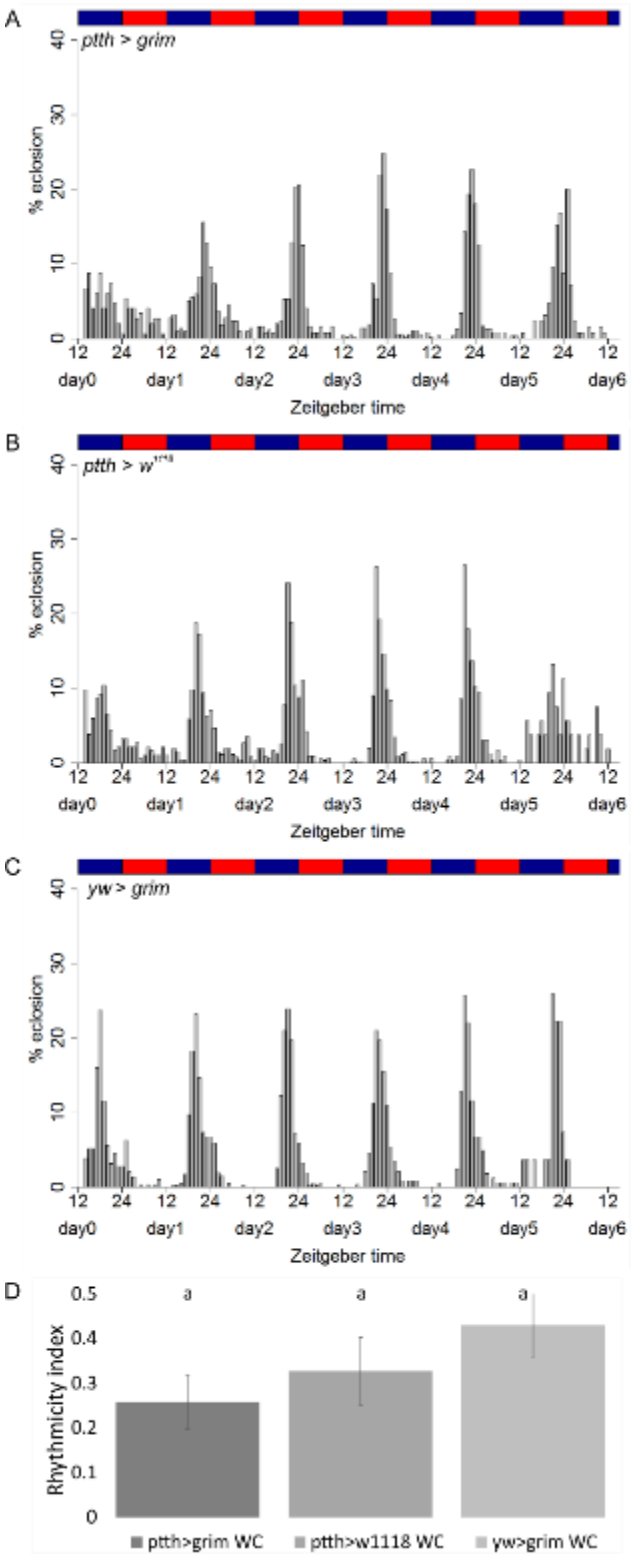

Figure 50: Eclosion rhythms under WC conditions after the ablation of PTTH neurons
Eclosion profiles for populations expressing UAS-*grim* driven by *ptth*-GAL4 (A) and the respective controls (B: GAL4 control, C: UAS control) under WC (25°C:16°C) conditions. Each bar represents the percentage of eclosed flies per hour normalized to the number of eclosed flies per day. The blue and red rectangles represent the temperature regime. (D) shows the means of the rhythmicity indices (±SD). Different letters above columns indicate significant difference ($p<0.05$). (N=6, 6, 4; n=1343, 1380, 1364)

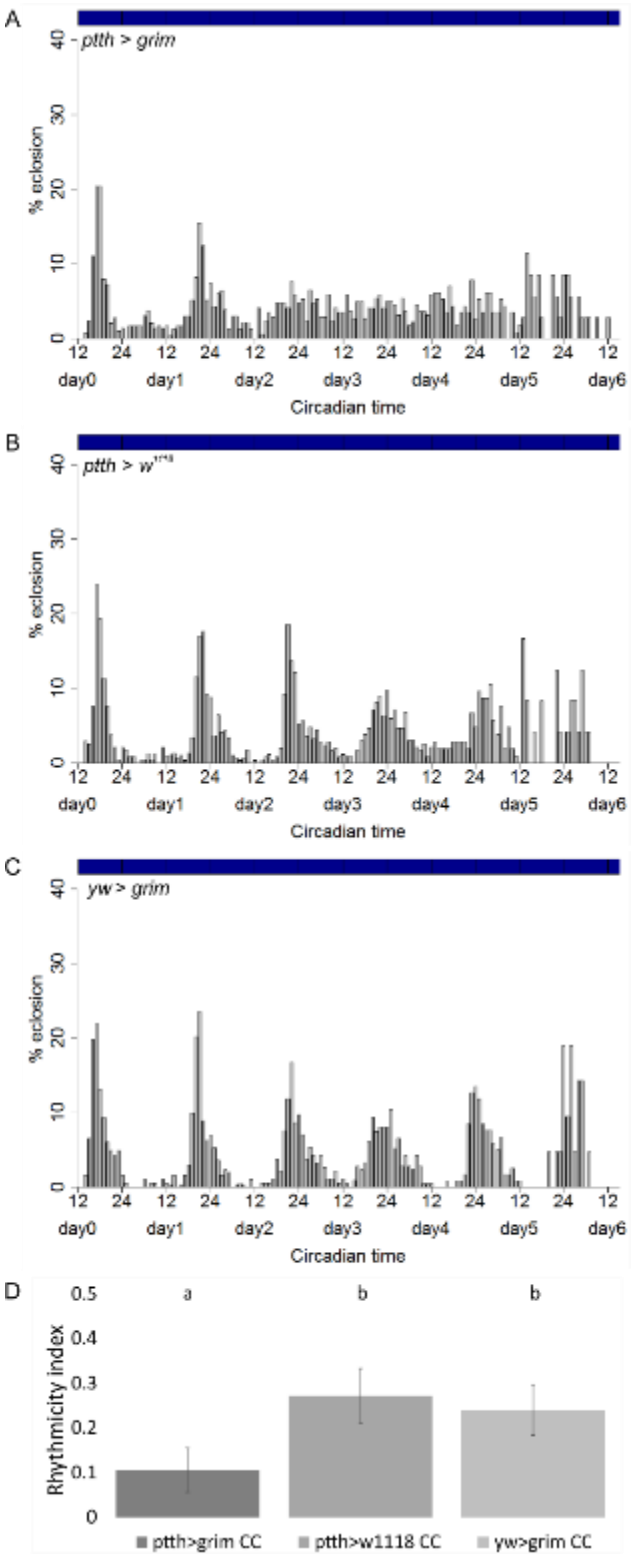

Figure 51: Eclosion rhythms under CC conditions after the ablation of PTTH neurons
Eclosion profiles for populations expressing UAS-*grim* driven by *ptth*-GAL4 (A) and the respective controls (B: GAL4 control, C: UAS control) under CC (20°C) conditions. Each bar represents the percentage of eclosed flies per hour normalized to the number of eclosed flies per day. The blue rectangles represent the temperature regime. (D) shows the means of the rhythmicity indices (±SD). Different letters above columns indicate significant difference ($p<0.05$). (N=7, 7, 6; n=1063, 1146, 1020)

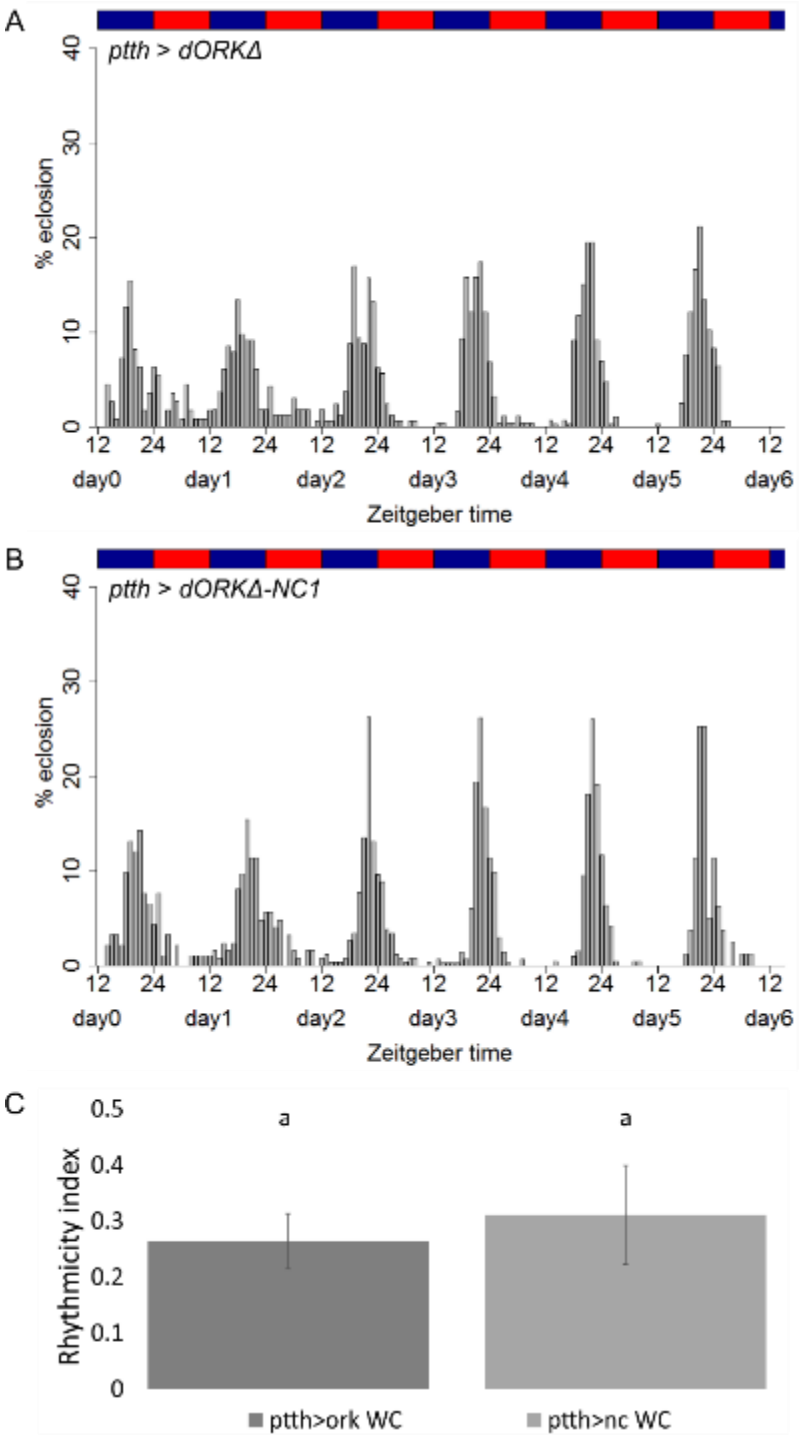

Figure 52: Eclosion rhythms under WC conditions after silencing of PTTH neurons
Eclosion profiles for populations expressing UAS-*dORKΔ* driven by *ptth*-GAL4 (A) and the UAS-*ΔORKΔ-NC1* control (B) under WC (25°C:16°C) conditions. Each bar represents the percentage of eclosed flies per hour normalized to the number of eclosed flies per day. The blue and red rectangles represent the temperature regime. (C) shows the means of the rhythmicity indices (±SD). Different letters above columns indicate significant difference ($p<0.05$). (N=7, 7; n=1116, 1005)

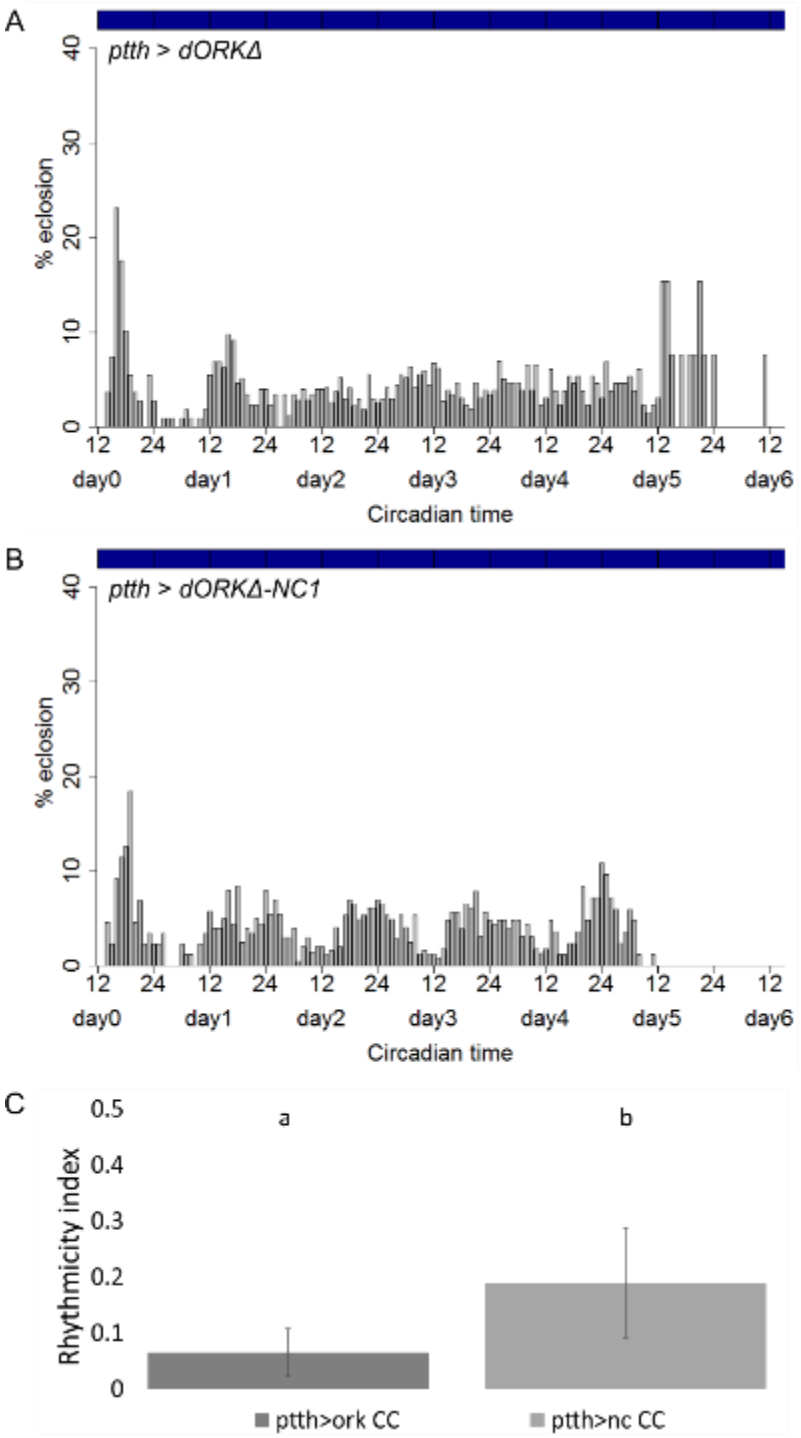

Figure 53: Eclosion rhythms under CC conditions after silencing of PTTH neurons
Eclosion profiles for populations expressing UAS-*dORKΔ* driven by *ptth*-GAL4 (A) and the UAS-*ΔORKΔ-NC1* control (B) under CC (20°C) conditions. Each bar represents the percentage of eclosed flies per hour normalized to the number of eclosed flies per day. The blue rectangles represent the temperature regime. (C) shows the means of the rhythmicity indices (±SD). Different letters above columns indicate significant difference ($p<0.05$). (N=7, 7; n=1139, 1042)

2.4 Eclosion rhythms under light entrainment after knockdown of the PDF receptor in PTTH neurons

The PDF receptor (PDFR) was specifically knocked down in the PTTH neurons by expressing an UAS-*Pdfr* RNAi; UAS-*dicer2* construct under the *ptth*-GAL4 driver. The knockdown of *Pdfr* had no effect on the eclosion profiles (Figure 54 A-C, Figure 55 A-C) or the rhythmicity indices (Figure 54 D, Figure 55 D) compared to the controls, neither under LD (Figure 54) nor under DD conditions (Figure 55). Moreover, no significant difference was observed between the period lenghts (Figure S 20 A).

2.5 Eclosion rhythms under light entrainment after knockdown of the sNPF receptor in PTTH neurons

The sNPF receptor (sNPFR) was specifically knocked down in the PTTH neurons by expressing an UAS-*snpfr* RNAi construct under the UAS-*dicer2*; *ptth*-GAL4 driver. The knockdown of *snpfr* had a weak effect under LD conditions and lead to a reduction of the lights-on peaks and a broader eclosion gate (Figure 56 A) compared to the UAS control (Figure 56 C). Similar effects were observed in the Gal4 control, although the lights-on peaks were not impaired as much from day 3 onwards (Figure 56 B). The flies in all groups showed rhythmic behavior and no statistical difference was observable between the rhythmicity indices under LD conditions (Figure 56 D). Under DD conditions however, both the experimental group (Figure 57 A) and the GAL4 control (Figure 57 B) became arrhythmic, while the UAS control stayed rhythmic (Figure 57 C). This loss of rhythmicity was statistically significant (Figure 57 D). Under DD conditions, the period lengths of the experimental group and the GAL4 control were significantly shorter than that of the UAS control (Figure S 20 B).

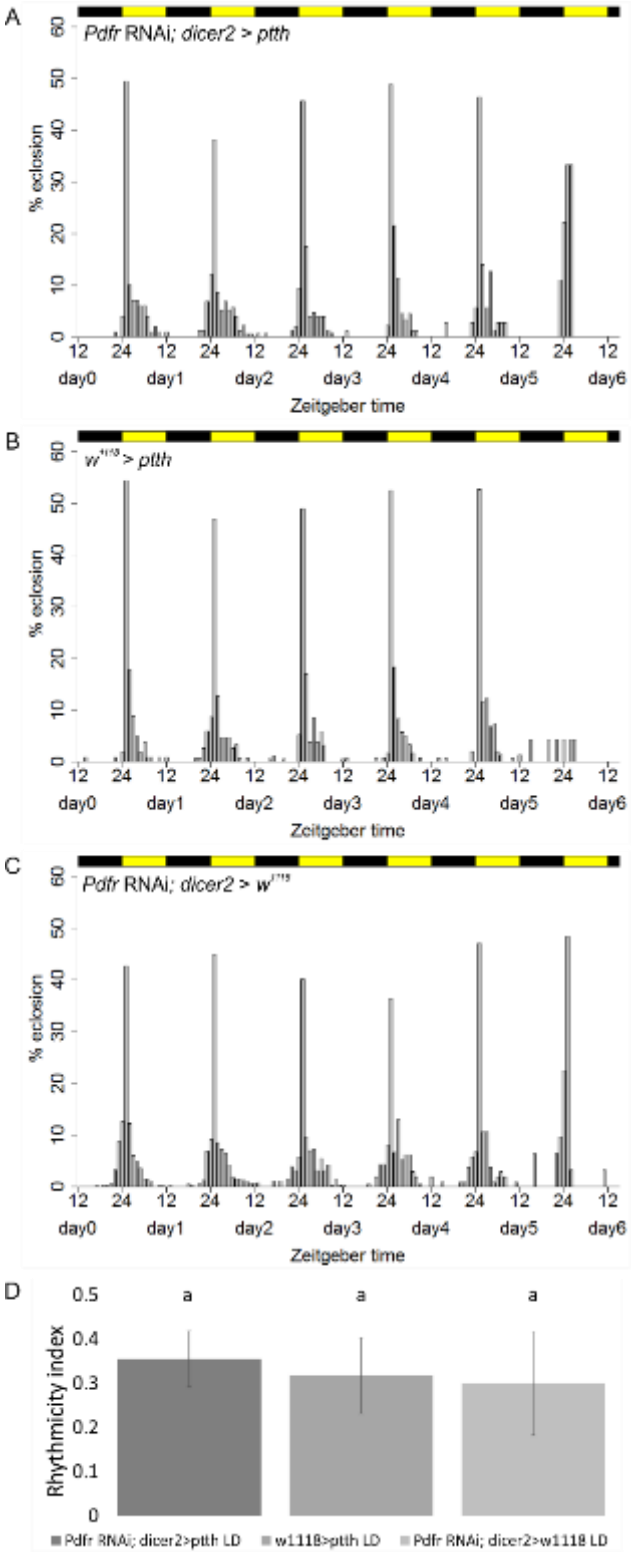

Figure 54: Eclosion rhythms under LD conditions after knockdown of *Pdfr* in PTTH neurons

Eclosion profiles for populations expressing UAS-*Pdfr* RNAi; UAS-*dicer2* driven by *ptth*-GAL4 (A) and the respective controls (B: GAL4 control, C: UAS control) under LD conditions. Each bar represents the percentage of eclosed flies per hour normalized to the number of eclosed flies per day. The black and yellow rectangles represent the light regime. (D) shows the means of the rhythmicity indices (±SD). Different letters above columns indicate significant difference ($p<0.05$). (N=4, 4, 4; n=591, 693, 1241)

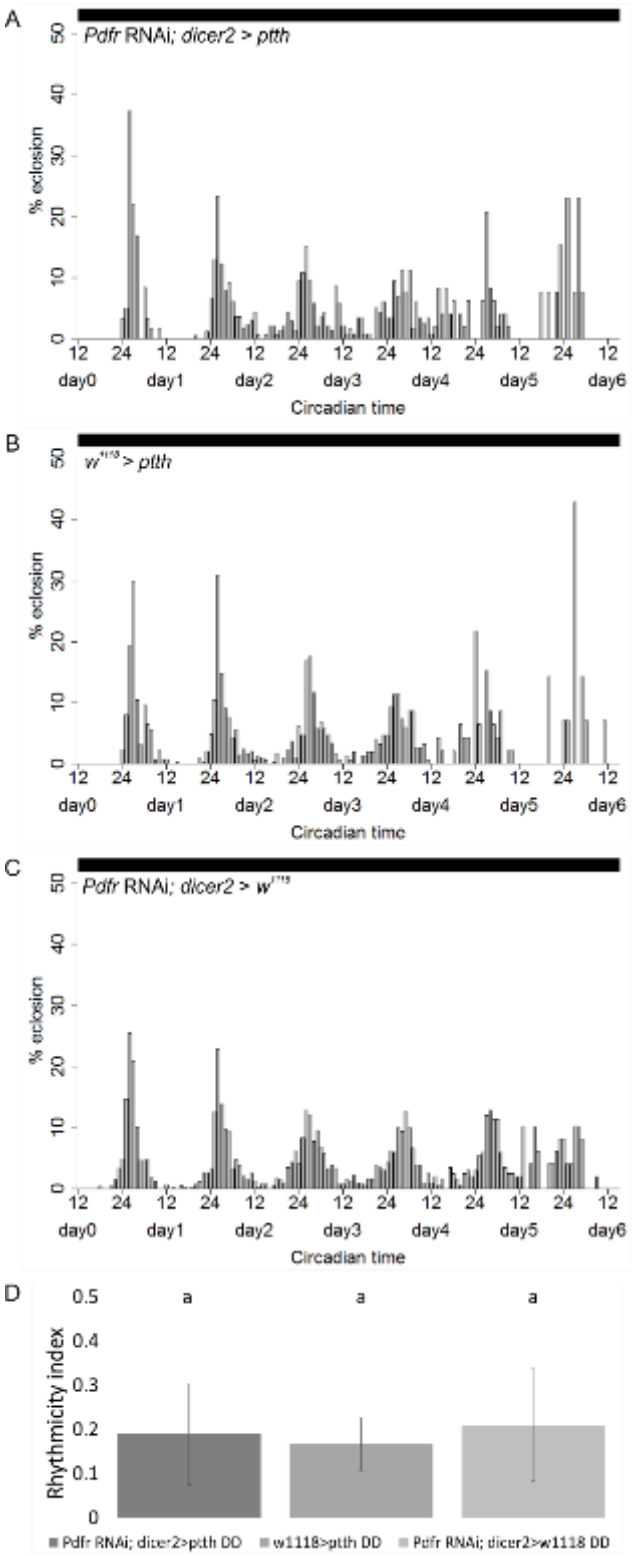

Figure 55: Eclosion rhythms under DD conditions after knockdown of *Pdfr* in PTTH neurons

Eclosion profiles for populations expressing UAS-*Pdfr* RNAi; UAS-*dicer2* driven by *ptth*-GAL4 (A) and the respective controls (B: GAL4 control, C: UAS control) under DD conditions. Each bar represents the percentage of eclosed flies per hour normalized to the number of eclosed flies per day. The black rectangles represent the light regime. (D) shows the means of the rhythmicity indices (±SD). Different letters above columns indicate significant difference ($p<0.05$). (N=4, 4, 4; n=535, 908, 1909)

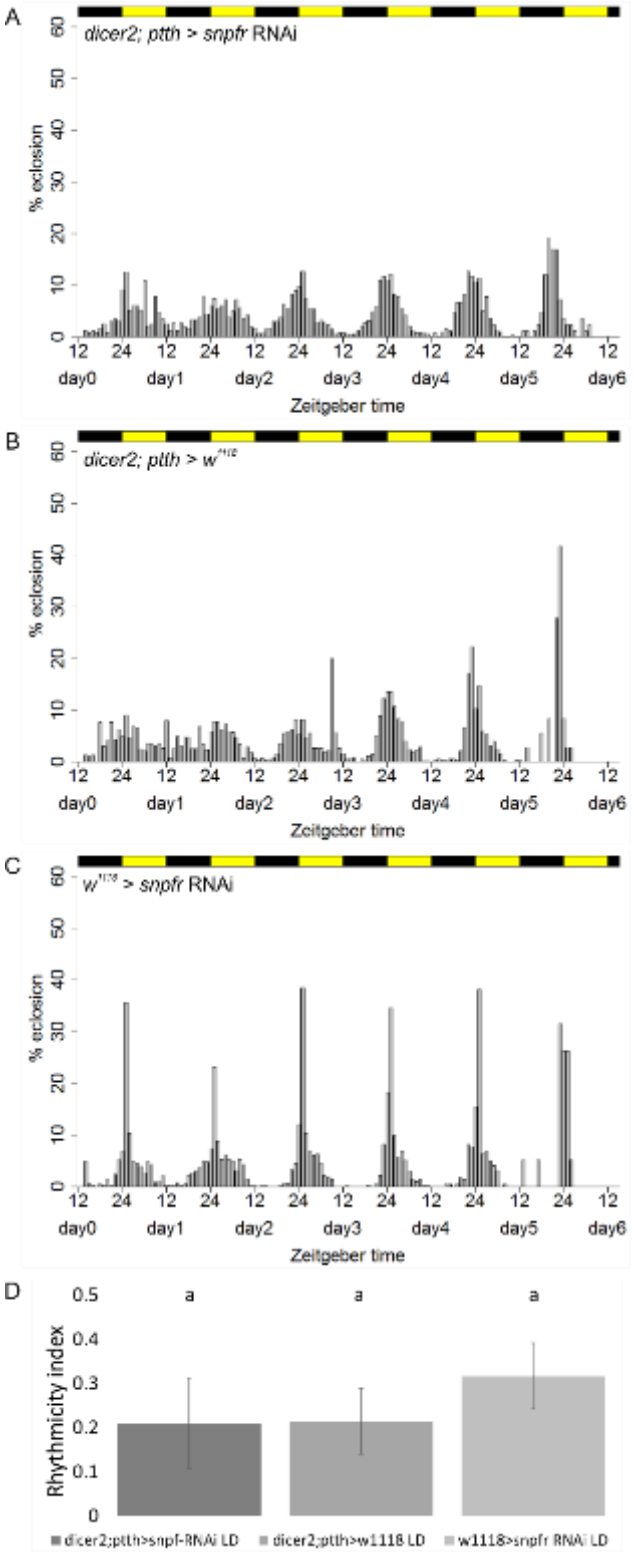

Figure 56: Eclosion rhythms under LD conditions after knockdown of *snpfr* in PTTH neurons

Eclosion profiles for populations expressing UAS-*snpfr* RNAi driven by UAS-*dicer2; ptth*-GAL4 (A) and the respective controls (B: GAL4 control, C: UAS control) under LD conditions. Each bar represents the percentage of eclosed flies per hour normalized to the number of eclosed flies per day. The black and yellow rectangles represent the light regime. (D) shows the means of the rhythmicity indices (±SD). Different letters above columns indicate significant difference ($p<0.05$). (N=6, 5, 5; n=3122, 2984, 2932)

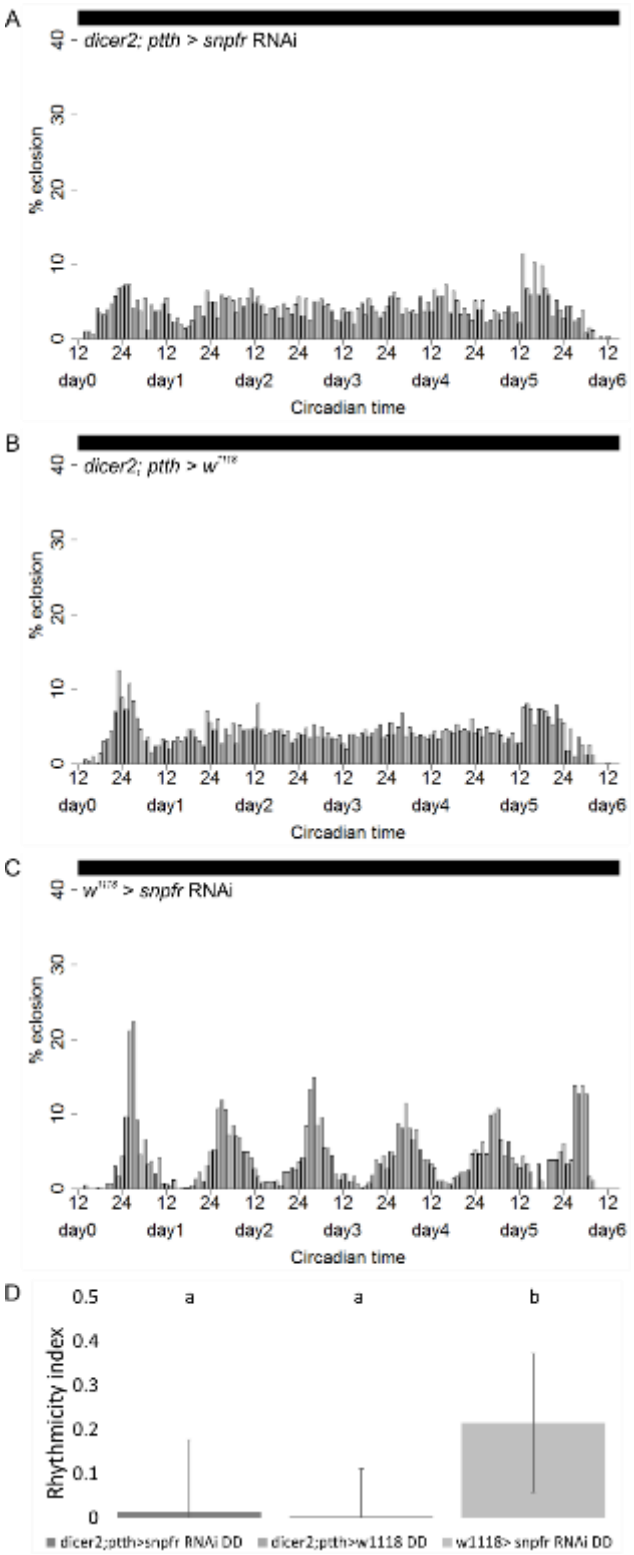

Figure 57: Eclosion rhythms under DD conditions after knockdown of *snpfr* in PTTH neurons

Eclosion profiles for populations expressing UAS-*snpfr* RNAi driven by UAS-*dicer2; ptth*-GAL4 (A) and the respective controls (B: GAL4 control, C: UAS control) under DD conditions. Each bar represents the percentage of eclosed flies per hour normalized to the number of eclosed flies per day. The black rectangles represent the light regime. (D) shows the means of the rhythmicity indices (±SD). Different letters above columns indicate significant difference ($p<0.05$). (N=6, 4, 4; n=4149, 4372, 2877)

2.6 Eclosion rhythms under light entrainment after knockdown of *torso* in the prothoracic gland

The PTTH receptor Torso was specifically knocked down in the PG by expressing an UAS-*torso* RNAi construct under the UAS-*dicer2*; *phm*/TM6B-GAL4 driver. For the experimental group and the GAL4 control, only pupae that were not tubby were used.

The knockdown of *torso* in the PG lead to a prolonged development, an increased size of the lavae and pupae and impaired viability. The flies took about 7 days longer to pupariate than the GAL4 and UAS control as well as the flies carrying the tubby marker instead of the *phm* transgene. Most experimental flies died as pharate flies, while the controls eclosed in a normal way. The experiments were performed in the WEclMon system under constant red light (λ=635 nm). Although flies should not be able to perceive light of this wavelength (Salcedo *et al.*, 1999), the eclosion rhythms of all groups were strongly impaired under both, LD (Figure 58) and DD (Figure 59) conditions. A statistical analysis of the rhythmicity was therefore not possible. While the eclosion profiles of the GAL4 and UAS control exhibit some rhythmicity under both conditions (Figure 58 B, C, Figure 59 B, C), this is not the case in the experimental group (Figure 58 A, Figure 59 A).

2.7 Eclosion rhythms under light entrainment after knockdown of *torso* in the brain

Torso was knocked-down pan-neuronally by expressing an UAS-*torso* RNAi construct under the *elav*-GAL4; UAS-*dicer2* driver. The experiments were conducted in the TriKinetics system. The knockdown of *torso* in the brain had no effect on the eclosion profiles (Figure 60 A-C, Figure 61 A-C) or the rhythmicity index (Figure 60 D, Figure 61 D) compared to the controls, neither under LD (Figure 60) nor under DD conditions (Figure 61). There was also no significant difference observable between the period lengths (Figure S 21).

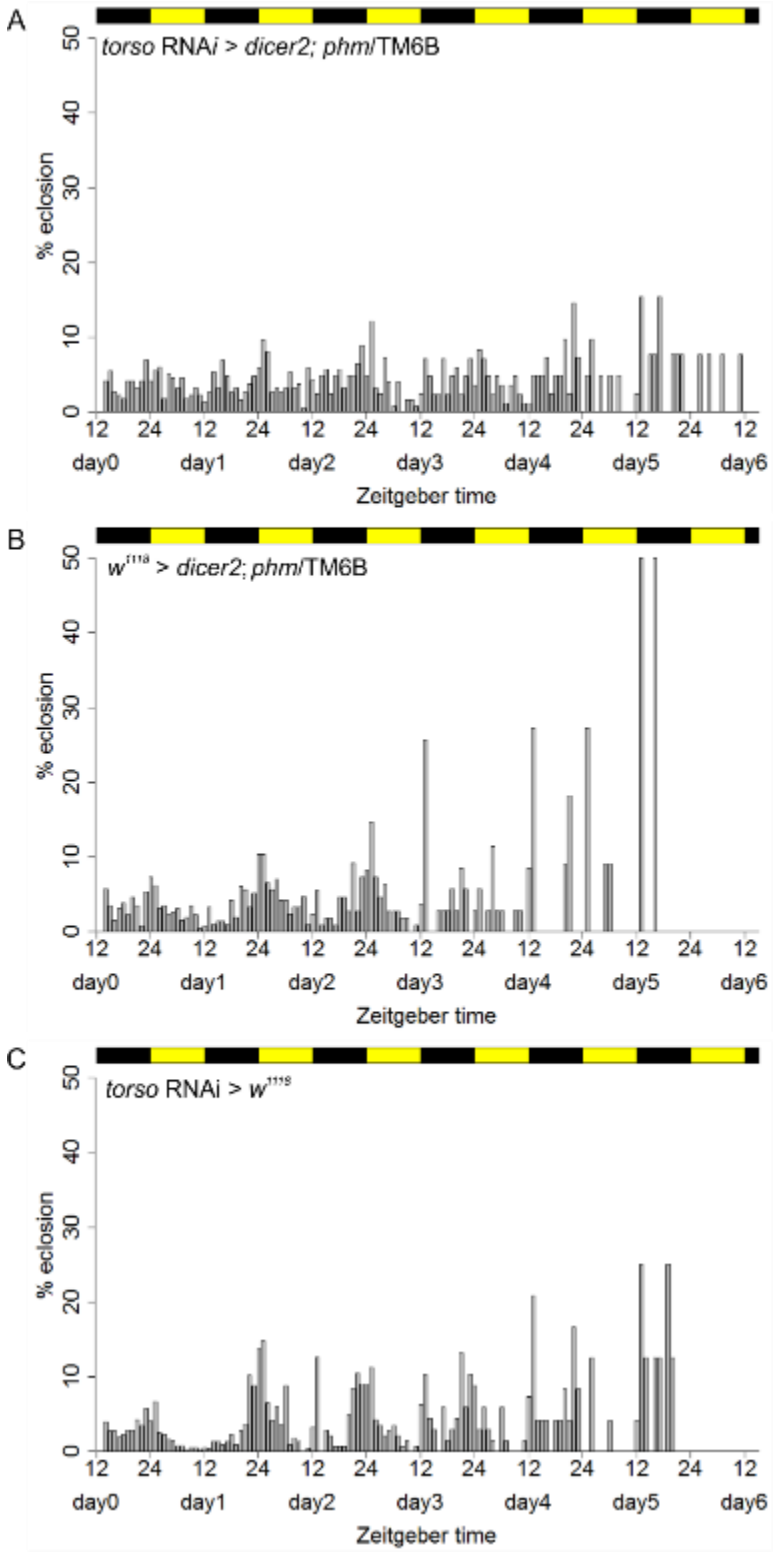

Figure 58: Eclosion rhythms under LD conditions after knockdown of *torso* in the PG
Eclosion profiles for populations expressing UAS-*torso* RNAi driven by UAS-*dicer2; phm*/TM6B-GAL4 (A) and the respective controls (B: GAL4 control, C: UAS control) under LD conditions. Each bar represents the percentage of eclosed flies per hour normalized to the number of eclosed flies per day. The black and yellow rectangles represent the light regime. Experiments were performed in the WEclMon system under constant red light (λ=635 nm). (N=6, 5, 6; n=664, 630, 1202)

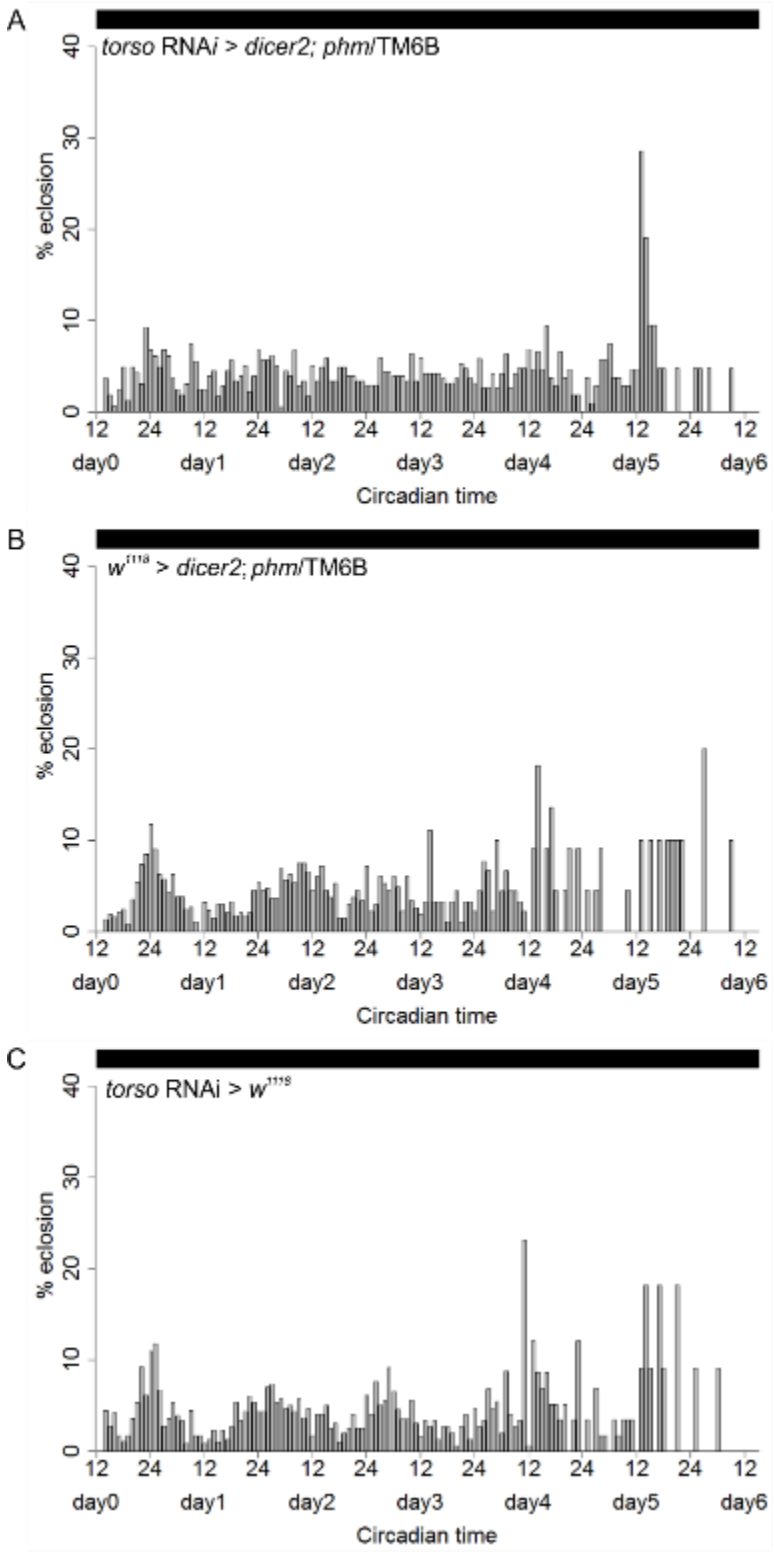

Figure 59: Eclosion rhythms under DD conditions after knockdown of *torso* in the PG
Eclosion profiles for populations expressing UAS-*torso* RNAi driven by UAS-*dicer2; phm*/TM6B-GAL4 (A) and the respective controls (B: GAL4 control, C: UAS control) under DD conditions. Each bar represents the percentage of eclosed flies per hour normalized to the number of eclosed flies per day. The black rectangles represent the light regime. Experiments were performed in the WEclMon system under constant red light (λ=635 nm). (N=7, 7, 7; n=859, 1097, 1068)

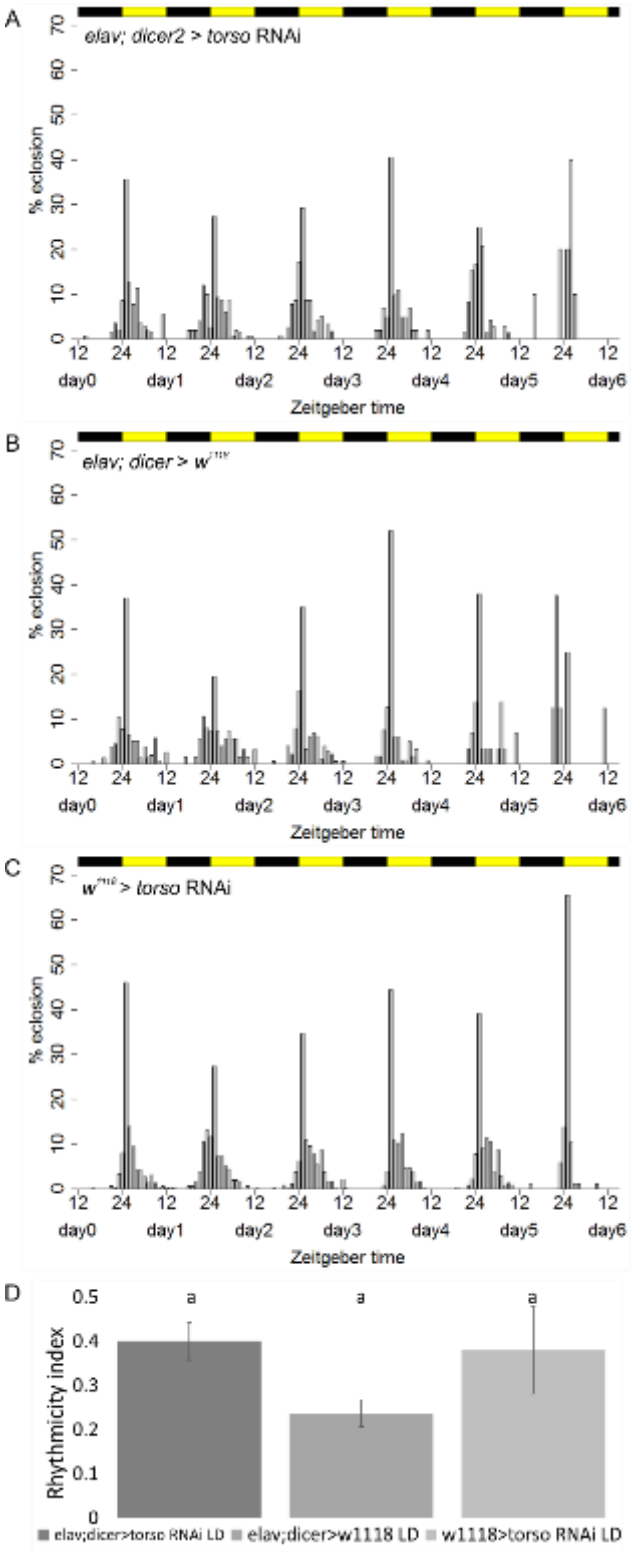

Figure 60: Eclosion rhythms under LD conditions after pan-neuronal knockdown of *torso*
Eclosion profiles for populations expressing UAS-*torso* RNAi driven by *elav*-GAL4; UAS-*dicer2* (A) and the respective controls (B: GAL4 control, C: UAS control) under LD conditions. Each bar represents the percentage of eclosed flies per hour normalized to the number of eclosed flies per day. The black and yellow rectangles represent the light regime. D) shows the means of the rhythmicity indices (±SD). Different letters above columns indicate significant difference ($p<0.05$). Experiments were performed in the TriKinetics system. (N=2, 3, 2; n=589, 617, 1512)

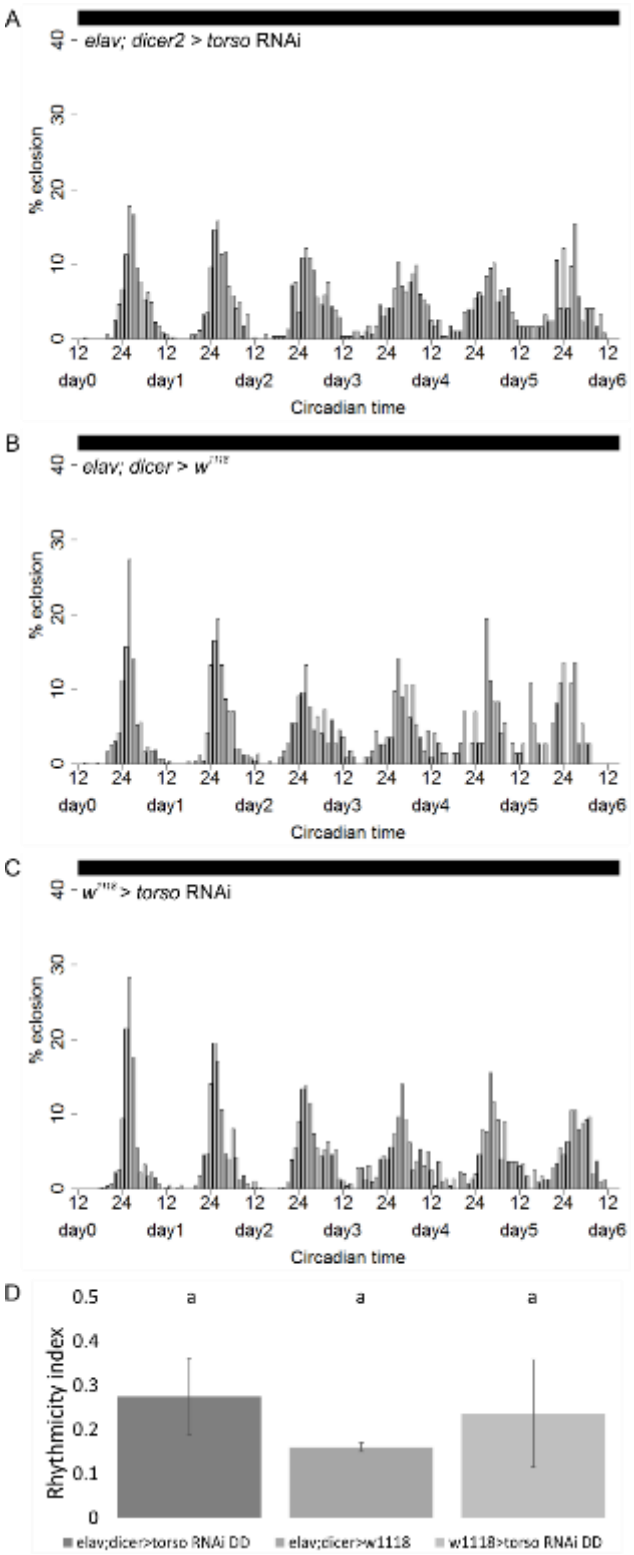

Figure 61: Eclosion rhythms under DD conditions after pan-neuronal knockdown of *torso*
Eclosion profiles for populations expressing UAS-*torso* RNAi driven by *elav*-GAL4; UAS-*dicer2* (A) and the respective controls (B: GAL4 control, C: UAS control) under DD conditions. Each bar represents the percentage of eclosed flies per hour normalized to the number of eclosed flies per day. The black rectangles represent the light regime. D) shows the means of the rhythmicity indices (±SD). Different letters above columns indicate significant difference ($p<0.05$). Experiments were performed in the TriKinetics system. (N=4, 3, 3; n=1782, 1112, 2207)

2.8 Analysis of *torso* expression pattern

To analyze the spatial expression of *torso*, mRNA was isolated from the central brain, the optic lobes and the retina of 10 pharate and adult *Canton S* wildtype flies each, as well as of the gonads or the abdomen of 10 adult or pharate *Canton S* males and females. cDNA was synthesized via reverse transcription of the mRNA, and *torso* cDNA was amplified via PCR. The brains with ring glands of *Canton S* L3 wandering larvae served as positive control and a non-template sample was used as negative control. *torso* expression can be detected in the male and female gonads of adult flies, as well as in the abdomen of male and female pharate flies. *Torso* expression could not be detected in the central brain, the optic lobes or the retina (Figure 62 A).

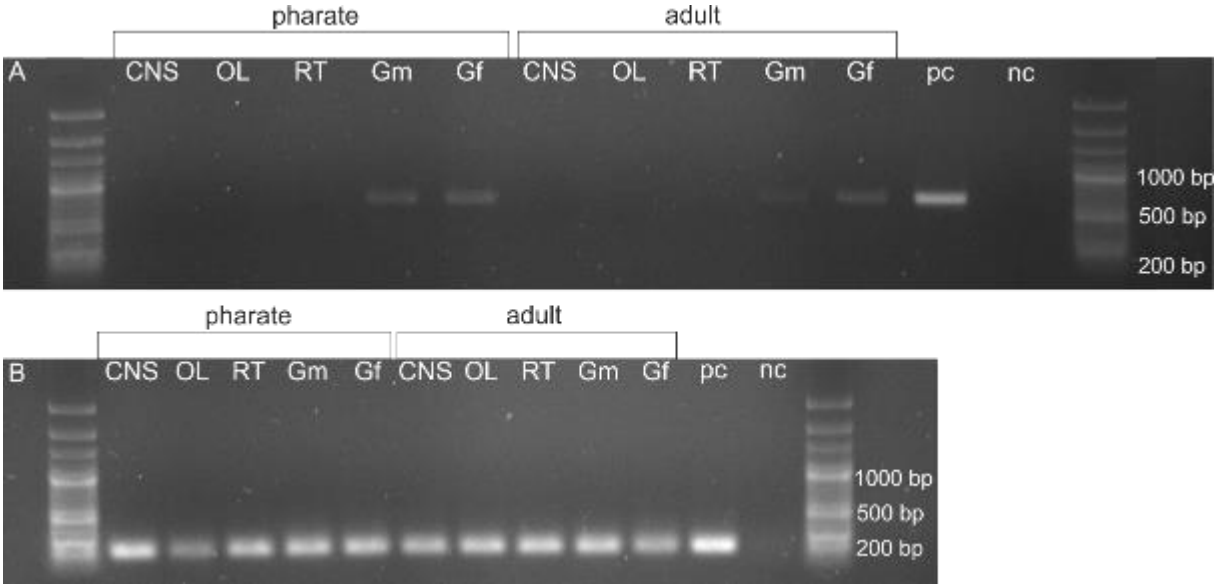

Figure 62: Expression of *torso* mRNA
Expression of *torso* mRNA was analyzed via RT-PCR in the central brain (CNS), the optic lobes (OL), the retina (RT) and the gonads of males (Gm) and females (Gf) of pharate and adult *Canton S* flies (A). As loading control, *α-tubulin* mRNA was amplified (B). Brains with ring glands from *Canton S* L3 wanderer larvae served as positive control (pc) and a non-template sample as negative control (nc). (N=4)

2.9 Analysis of the temporal expression of *Ptth* mRNA

So far, the cycling of *Ptth* mRNA has only been studied in L3 larvae (McBrayer *et al.*, 2007), while nothing is known about the expression in pharate flies. Therefore, *Ptth* mRNA levels were measured via quantitative Real-Time PCR. *Canton S* flies were raised under LD at 20°C. After 11 days, half of the flies were transferred into DD conditions. After 17 days, the heads of pharate flies from both light regimes were collected every 4 hours on 5 consecutive days. The mRNA of the whole heads was isolated and reverse-transcribed into cDNA. Quantitative real-time PCR was performed to compare the *Ptth* mRNA levels between the different timepoints and to identify potential cycling. As reference genes, *α-tubulin* and *Rpl-32* were chosen. *Ptth* mRNA levels were calculated relative to the expression of each of the reference genes. A detailed description of the analysis can be found in Chapter 2.2 of the Materials and Methods.

No significant difference of the *Ptth* mRNA expression levels between the tested time points could be observed, neither under LD nor under DD conditions (Figure 63).

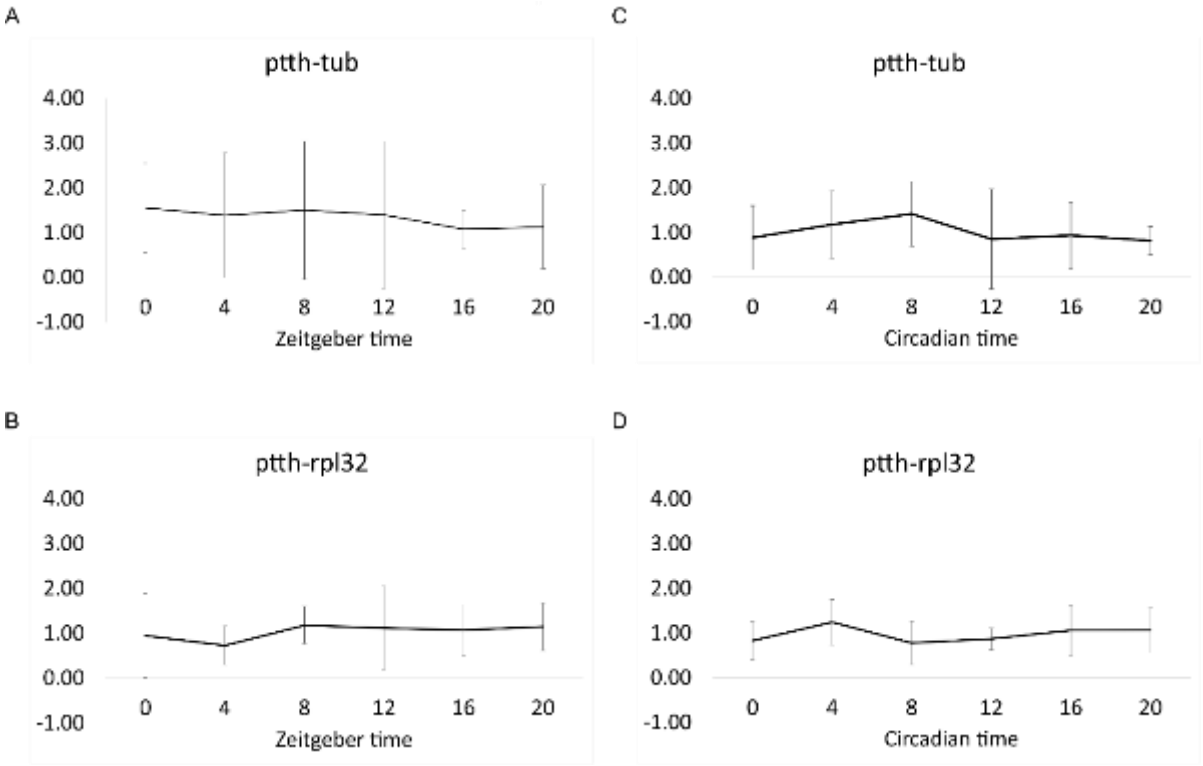

Figure 63: *Ptth* mRNA expression levels after light entrainment
Relative expression of *Ptth* mRNA to the reference genes *α-tubulin* (A, C) and *Rpl-32* (B, D) and the standard deviation under LD (A, B) and DD (C, D) conditions. The mRNA of whole heads of pharate *Canton S* flies was isolated, transcribed into cDNA and levels were measured via quantitative real-time PCR. Comparison of the expression levels between the tested time points by one-way ANOVA revealed no significant difference. (N=5)

3. Discussion

It has been shown for quite some time that there is a connection between the central clock in the brain and the peripheral clock in the prothoracic gland (Emery *et al.*, 1997; Helfrich-Förster *et al.*, 2000; Blanchardon *et al.*, 2001; Myers *et al.*, 2003; McBrayer *et al.*, 2007; Morioka *et al.*, 2012). The results of this chapter suggest that PTTH and the PTTH neurons constitute this connection. Ablation and silencing of PTTH neurons lead to arrhythmic eclosion under constant conditions, which shows that PTTH is necessary for the circadian timing of eclosion. As these flies are still able to eclose, PTTH seems not to be needed for the eclosion behavior and potentially there are redundant ways securing eclosion success. The loss of PTTH neurons phenocopies the effect of ablation of PDF-positive cells (Myers *et al.*, 2003) and pdf^{01} mutants (Figure S 10 B), where flies also become arrhythmic under DD. This suggests a role for PTTH in the synchronization of the central and peripheral clock. Though it was shown that PTTH controls light avoidance in larvae (Yamanaka *et al.*, 2013) and that *per* oscillations in the PG are amplified by CNS-dependent photoreception (Morioka *et al.*, 2012), PTTH seems not to be exclusively in the photic pathway. Flies in which the PTTH neurons were ablated or silenced eclosed arrhythmically under constant conditions after both, light and temperature entrainment. This implies a role for PTTH independent of the kind of presented Zeitgeber.

PTTH neurons show overlaps with the PDF-producing small ventral lateral neurons (sLNv) in larval and pharate flies (McBrayer *et al.*, 2007; Selcho *et al.*, unpublished-a) and ablation or disruption of the clock in these neurons leads to arrhythmic eclosion (Helfrich-Förster *et al.*, 2000; Blanchardon *et al.*, 2001; Myers *et al.*, 2003). Also mutants for PDF or PDFR eclose arrhythmically under constant conditions (Figure S 10 B, Figure S 11 B, Figure S 12 B, Figure S 13 B). This makes PDF a good candidate for a connection between the PDF and PTTH neurons. Knockdown of *Pdfr* in the PTTH neurons had however no effect on the eclosion rhythmicity. Imaging data from Mareike Selcho also showed no effect of PDF on the PTTH neurons in L3 larvae and pharate flies, unless PDFR was ectopically expressed (Selcho *et al.*, unpublished-a). So while PDF is essential for the synchronization of the clock itself and general rhythmicity, there seems to be no immediate effect of PDF on the PTTH neurons. Yet, PDF neurons contain a second neuropeptide, sNPF (Johard *et al.*, 2009). Knockdown of *snpfr* in the PTTH neurons indeed impaired eclosion under LD conditions and caused arrhythmic eclosion under constant conditions. As the same effects could also be observed in the GAL4 control, the results have to be repeated to be confirmed. Knockdown of *snpfr* without dicer showed no loss of

rhythmicity anymore (Figure S 22, Figure S 23), indicating that *dicer* could be crossed with the UAS-*snpfr* instead of the *ptth*-Gal4 driver line. Imaging data from Mareike Selcho confirmed the effect of sNPF on the PTTH neurons, as the application of sNPF stopped calcium oscillations in the PTTH neurons. By combination of the UAS-GAL4 and LexA/LexAop system (Lai and Lee, 2006), she could provide evidence that the inhibiting sNPF signaling comes from the PDF neurons, as optogenetic activation of PDF neurons also lead to a drop of calcium oscillations in the PTTH neurons (Selcho *et al.*, unpublished-a).

The PTTH receptor Torso seems not to be expressed in the brain and knockdown of *torso* had also no effect on eclosion. Knockdown specifically in the PG, however, prolonged especially the last larval stage and reduced viability. The effect of the *torso* knockdown in the PG is stronger than that of ablation or silencing of PTTH neurons, suggesting that PTTH is not the only ligand of Torso. Torso also plays a role during embryogenesis as part of the terminal group, genes that are required for the correct patterning of anterior and posterior structures (Casanova and Struhl, 1989). During this stage, Torso is activated by Trunk (Casali and Casanova, 2001). However, *trunk* is not expressed in the L3 stage anymore and knockdown of *trunk* had no effect on the developmental time (Rewitz *et al.*, 2009). Therefore it remains unclear if there is another ligand in the larval stages and why the knockdown effect is more drastic than the ablation effect. Another possible explanation could be that both, ablation and silencing of PTTH neurons, was not complete and some residual PTTH function remained in these flies, which could be clarified by PTTH stainings in ablated flies. Further, *torso* expression could be shown in the gonads of adult flies and the abdomen of pharate flies. It was already shown that the ovaries are a site of ecdysone production in adult females, where it is needed for normal oogenesis (Warren *et al.*, 2004) and that *torso* is expressed in the male accessory glands (Hentze *et al.*, 2013). It could now be shown that *torso* is also expressed in the adult ovaries and that *torso* expression can already be detected in the abdomen of pharate flies, although the gonads are not yet in an active state. Nothing is so far known about the temporal expression of *torso* and if it is cycling in the PG. Further studies either with stainings or PCR could help to dissect the role of *torso* for eclosion rhythmicity. The temporal analysis of *Ptth* expression showed no cycling of *Ptth* mRNA in pharate flies, while McBrayer *et al.,* (2007) showed an ultradian cycling of *Ptth* transcripts in the L3 stage (McBrayer *et al.*, 2007). First results from Chen, 2012 also showed a rhythmic secretion of PTTH in L3 larvae by PTTH staining (Chen, 2012). It seems therefore that at least the cycling of transcription has stopped

in pharate flies. Further studies could focus on the peptide level and if PTTH translation and synthesis as well as secretion is rhythmic in pharate flies. It is however well possible that PTTH signaling is not needed in pharate stages any more, as its main target for eclosion rhythmicity, the PG, is already degenerating (Dai and Gilbert, 1991).

Although a connection between the central clock in the brain and peripheral clock in the PG could be identified, it remains unclear how eclosion rhythmicity is regulated in pharate stages, as here the PG is already degenerating, and what role ecdysteroids play for rhythmicity. It is known that the regulation of ecdysteroids in the blood feeding bug *Rhodnius prolixus* exhibits many similarities to the system in *Drosophila melanogaster*. In *Rhodnius*, ecdysteroids are released from the PG upon activation by PTTH, which is released by a single paired neuron in the dorsal protocerebrum. These neurons lay close to the brain clock that regulates rhythmic release of neuropeptides. In *Rhodnius*, PTTH is released rhythmically and entrains a second clock in the PG. From the PG, ecdysteroids are released in a rhythmic fashion (Steel and Vafopoulou, 2006). Daily rhythms in ecdysteroid titers have also been shown for *Bombyx mori* (Satake *et al.*, 1998) and *Periplaneta americana* (Richter, 2001). In *Drosophila,* however, no daily cycles in ecdysteroid titers or release have been reported so far and ecdysone could not be detected one day before eclosion (Dai and Gilbert, 1991). In course of the CRC 1047, new and much more sensitive detection methods have been established that now make it possible to detect even small amplitudes of ecdysone cycling and unravel whether PTTH is cycling with a small amplitude in pharate *Drosophila*.

Chapter IV. The role of CCAP in the circadian timing of eclosion and eclosion rhythmicity

1. Introduction

The crustacean cardioactive peptide (CCAP) was first identified in the shore crab *Carcinus maenas* as a factor accelerating the heart rate (Stangier *et al*., 1987). Then it has been characterized in *Drosophila* (Hewes and Taghert, 2001), where a similar cardiostimulatory effects as in crustaceans was described (Dulcis *et al*., 2005). In *Drosophila* larvae, CCAP is expressed in two pairs of neurons in the brain, in five neuron pairs in the subesophageal ganglion, in one to two pairs in at least eight ganglia of the nervous system and in one pair of medial and one pair of lateral descending axons (Ewer and Truman, 1996). In pharate flies, CCAP expression in the brain encompasses two pairs of neurons in the dorsal-median region of the protocerebrum as well as four pairs lateral and one pair ventral to the subesophageal area. In the ventral nerve chord, CCAP is expressed in 24 neurons on the dorsal side of the metathoracic and abdominal ganglia, six to eight neurons in the ventral surface of the thoracic neuromeres and four to six neurons in the abdominal ganglia. The neurons in the ventral nerve cord and the four neuron pairs lateral to the subesophageal area die shortly after eclosion (Draizen *et al.*, 1999; Lee *et al.*, 2013; Selcho *et al.*, unpublished-b). Overlaps of the CCAP synaptic endings and the DN2 clock neurons are observable in the dorsal brain of larval and pharate flies and of the processes of the CCAP neurons and the tritocerebral PDF neurons (Park *et al.*, 2003). These PDF neurons arise in the mid-pupal stage and degrade after eclosion, so that a potential role of the PDF Tri neurons in circadian timing of eclosion is hypothesized (Helfrich-Förster, 1997). Furthermore, CCAP neurons express the RNA-binding protein LARK, which affects eclosion, but not locomotor activity rhythms, when it is expressed in different peptidergic neurons (McNeil *et al.*, 1998; Schroeder *et al.*, 2003; Sundram *et al.*, 2012). In *Manduca sexta*, adding CCAP to isolated nervous systems induces ecdysis motor behavior (Gammie and Truman, 1997), while ablation of CCAP neurons in *Drosophila* causes severe ecdysis defects (Park *et al.*, 2003). 97% of the animals survive until the 3rd instar, although the ecdysis behavior is prolonged compared to controls. The majority of the animals dies at the end of pupariation as pupal ecdysis is severely disrupted and the animals display head evolution defects and shortened appendages. The small percentage of surviving flies able to

eclose take longer than the controls and show impaired inflation of the abdomen. The eclosed flies cannot inflate their wings and their bodies stay soft and white. The eclosion is still rhythmic, yet shows a broader gate with more eclosion during the dark phase and diminished lights-on peaks compared to controls (Park *et al.*, 2003).

CCAP release during ecdysis is induced by EH (Ewer, 2005), and flies in which both neurons are ablated show severe defects already during larval ecdysis (Clark *et al.*, 2004). Later studies with flies mutant for the CCAP gene showed, however, no defects, neither in pupal ecdysis, nor in survival rates or eclosion rhythms (Lahr *et al.*, 2012). This can be explained by the fact that some CCAP neurons co-express the neuropeptides bursicon and myoinhibitory peptide (MIP) (Kim *et al.*, 2006a; Vömel and Wegener, 2007). CCAP and CCAP/MIP neurons are active before and during pupal ecdysis, while the CCAP/MIP/bursicon neurons are active during post-ecdysis (Kim *et al.*, 2006a). Bursicon was already discovered in the blowfly *Calliphora erythrocephala* in the 1960s (Fraenkel and Hsiao, 1962) and was chemically identified in *Drosophila* much later (Dewey *et al.*, 2004; Luo *et al.*, 2005; Peabody *et al.*, 2008). It was shown to be the essential factor for wing spreading as well as cuticle hardening and tanning. Flies mutant for bursicon show severe pupal ecdysis defects and the few eclosing adults fail to unfold their wings and to harden and tan their cuticle. Flies mutant for both, CCAP and bursicon, however, show even more severe effects during pupal ecdysis, comparable to those observed after ablation of CCAP neurons (Lahr *et al.*, 2012). These results indicate a redundant function of CCAP. Myoinhibitory peptides (MIPs) are suspected to regulate together with CCAP the heart beat and blood pressure, as well as the motor program during ecdysis and post-ecdysis (Kim *et al.*, 2006b).

It was so far unclear whether CCAP plays a role in the timing of eclosion, possibly in the entrainment to temperature. The aim was therefore to study the effect of CCAP on the eclosion rhythm under different entrainment conditions to better understand its role in the circadian regulation of eclosion. For this purpose, the CCAP neurons were ablated and silenced to repeat the experiments of Park *et al*. 2003. Furthermore, a CCAP mutant was tested under light and temperature entrainment as well as under natural conditions.

2. Results

2.1 Eclosion rhythms under light entrainment after ablation of CCAP neurons

Ablating the CCAP neurons by expressing UAS-grim under the *ccap*-GAL4 driver decreased the survival rate. The escaper flies showed normal eclosion rhythms under both conditions (Figure 64, Figure 65). No significant difference was observed between the rhythmicity indices under both conditions (Figure 64 D, Figure 65D), although there was a trend to reduced rhythmicity under DD conditions (Figure 65 D). The period lengths showed no significant difference under DD conditions (Figure S 25 A). The lights-on peaks were not affected (Figure 64).

2.2 Eclosion rhythms under light entrainment after silencing of CCAP neurons

Silencing the CCAP neurons by expressing UAS-dORKΔ under the *ccap*-GAL4 driver reduced the number of eclosing flies. However, no effect was observed on the eclosion rhythms under both conditions (Figure 66, Figure 67). Neither the rhythmicity indices under both conditions (Figure 66 D, Figure 67D) nor the period lengths under DD conditions (Figure S 25 B) showed significant differences. Silencing of CCAP expressing neurons had also no effect on the lights-on peaks (Figure 66).

2.3 Eclosion rhythms of the *CCAP^{exc7}* mutant under light entrainment

The *CCAP ^{exc7}* mutant is a null mutation that was created through imprecise excision of a P-element insertion within the *ccap* gene (Lahr *et al.*, 2012). It showed normal eclosion rhythms, under both conditions (Figure 68, Figure 69). Under LD conditions, the rhythmicity indices showed no significant differences between the mutants and the controls (Figure 68 C). Under DD conditions, the period lengths in both strains were similar (Figure S 26 A), while the mutant was significantly more rhythmic than the control (Figure 69 C). The lights-on peaks in the mutants were not affected (Figure 68).

2.4 Eclosion rhythms of the *CCAP^{exc7}* mutant under temperature entrainment

The *CCAP ^{exc7}* mutant showed normal eclosion rhythms under both conditions (Figure 70, Figure 71). There were no significant differences between the rhythmicity indices of mutant and control (Figure 70 C, Figure 71 C). Also the period lengths showed no significant differences under CC conditions (Figure S 26 B). As in wildtypes, the eclosion peaks laid in the cold phase, before the beginning of the temperature increase.

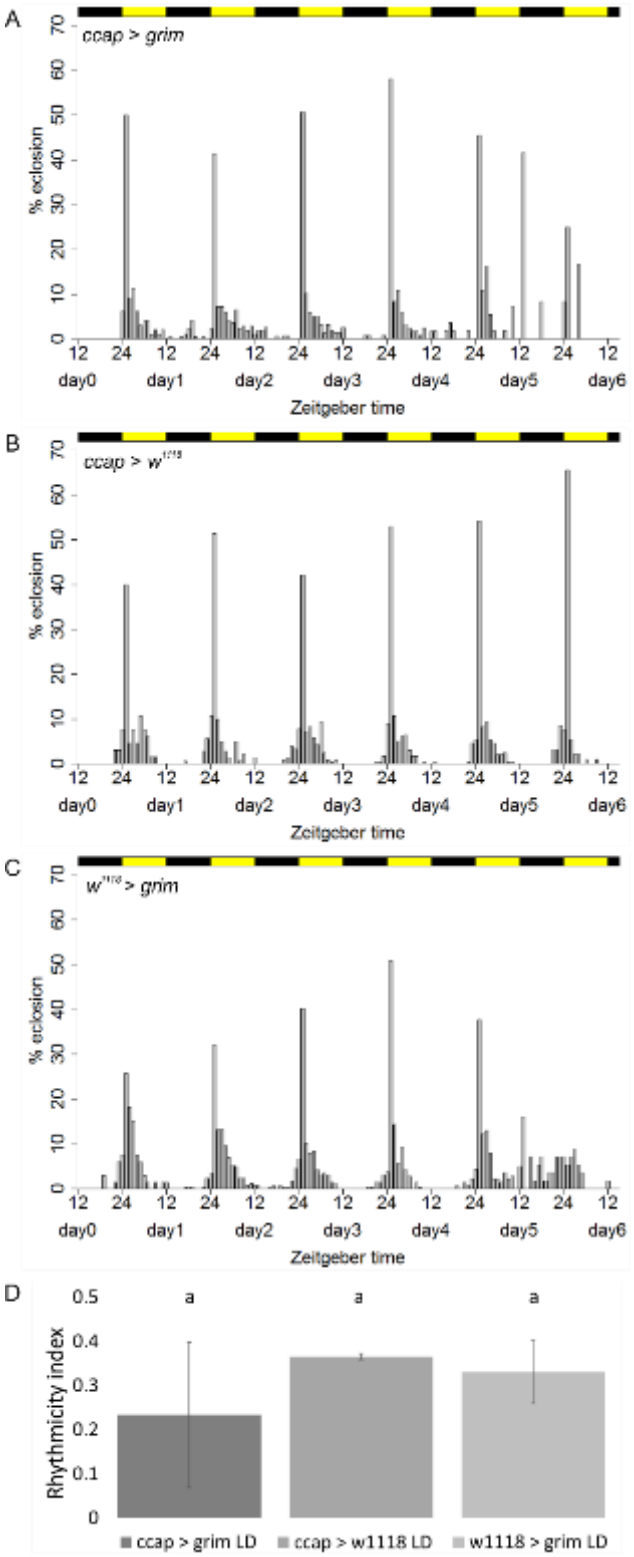

Figure 64: Eclosion rhythms under LD conditions after the ablation of CCAP neurons
Eclosion profiles for populations expressing UAS-*grim* driven by *ccap*-GAL4 (A) and the respective controls (B: GAL4 control, C: UAS control) under LD conditions. Each bar represents the percentage of eclosed flies per hour normalized to the number of eclosed flies per day. The black and yellow rectangles represent the light regime. (D) shows the means of the rhythmicity indices (±SD). Different letters above columns indicate significant difference ($p<0.05$). (N=3, 2, 2; n=609, 1032, 1015)

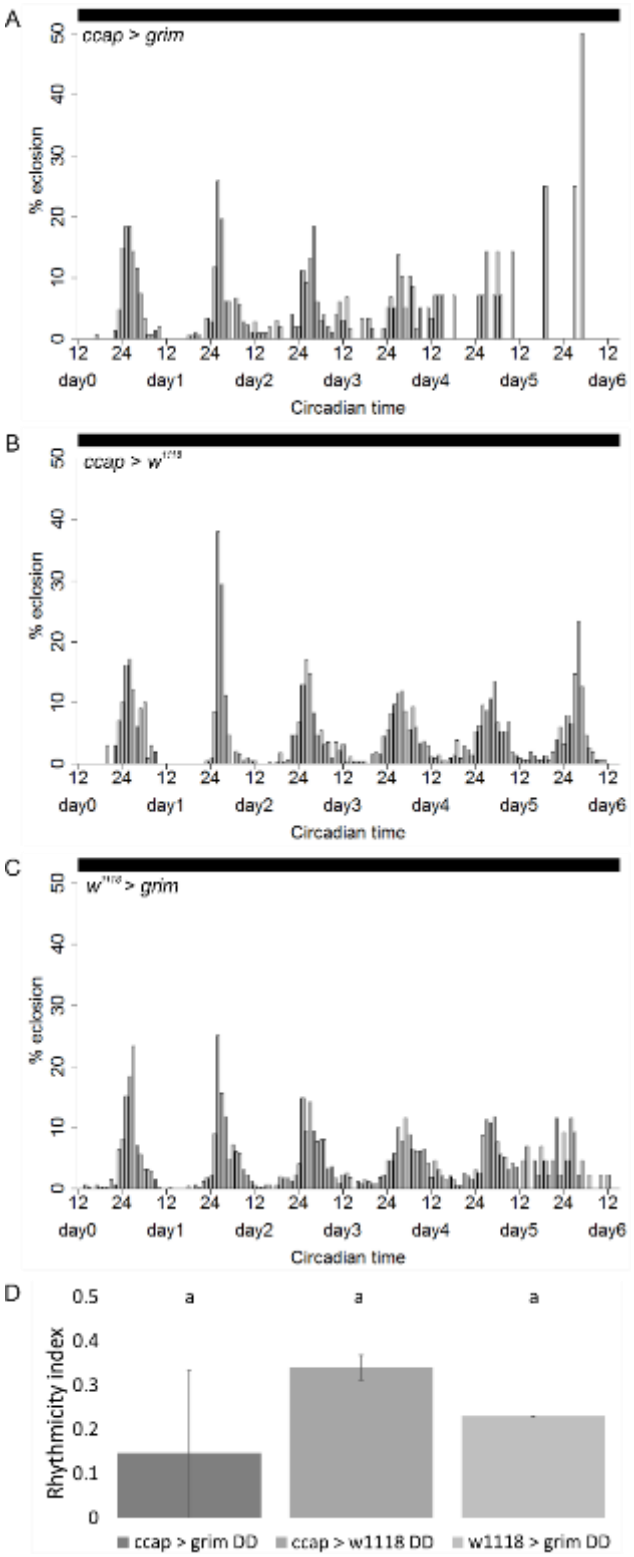

Figure 65: Eclosion rhythms under DD conditions after the ablation of CCAP neurons
Eclosion profiles for populations expressing UAS-*grim* driven by *ccap*-GAL4 (A) and the respective controls (B: GAL4 control, C: UAS control) under DD conditions. Each bar represents the percentage of eclosed flies per hour normalized to the number of eclosed flies per day. The black rectangles represent the light regime. (D) shows the means of the rhythmicity indices (±SD). Different letters above columns indicate significant difference ($p<0.05$). (N=3, 2, 1; n=500, 1189, 1528)

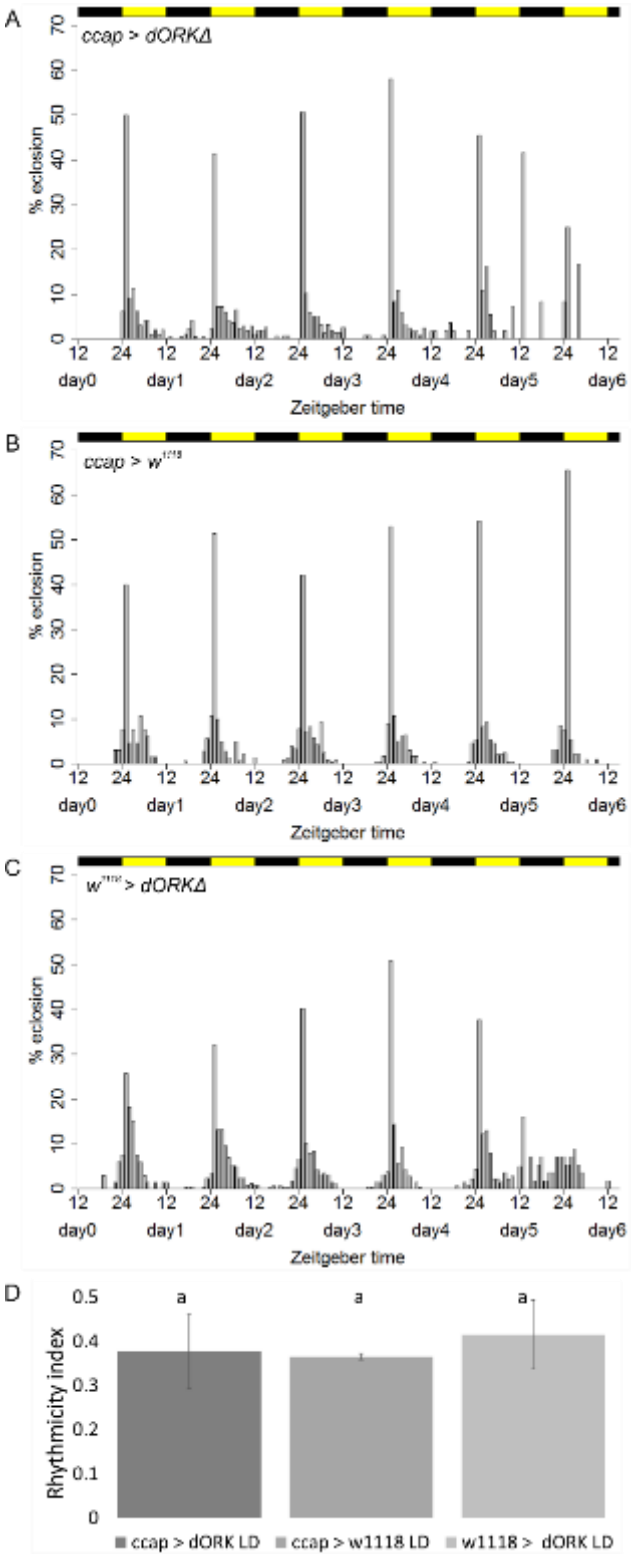

Figure 66: Eclosion rhythms under LD conditions after silencing of CCAP neurons
Eclosion profiles for populations expressing UAS-*dORKΔ* driven by *ccap*-GAL4 (A) and the respective controls (B: GAL4 control, C: UAS control) under LD conditions. Each bar represents the percentage of eclosed flies per hour normalized to the number of eclosed flies per day. The black and yellow rectangles represent the light regime. (D) shows the means of the rhythmicity indices (±SD). Different letters above columns indicate significant difference ($p<0.05$). (N=4, 2, 2; n=689, 1032, 876)

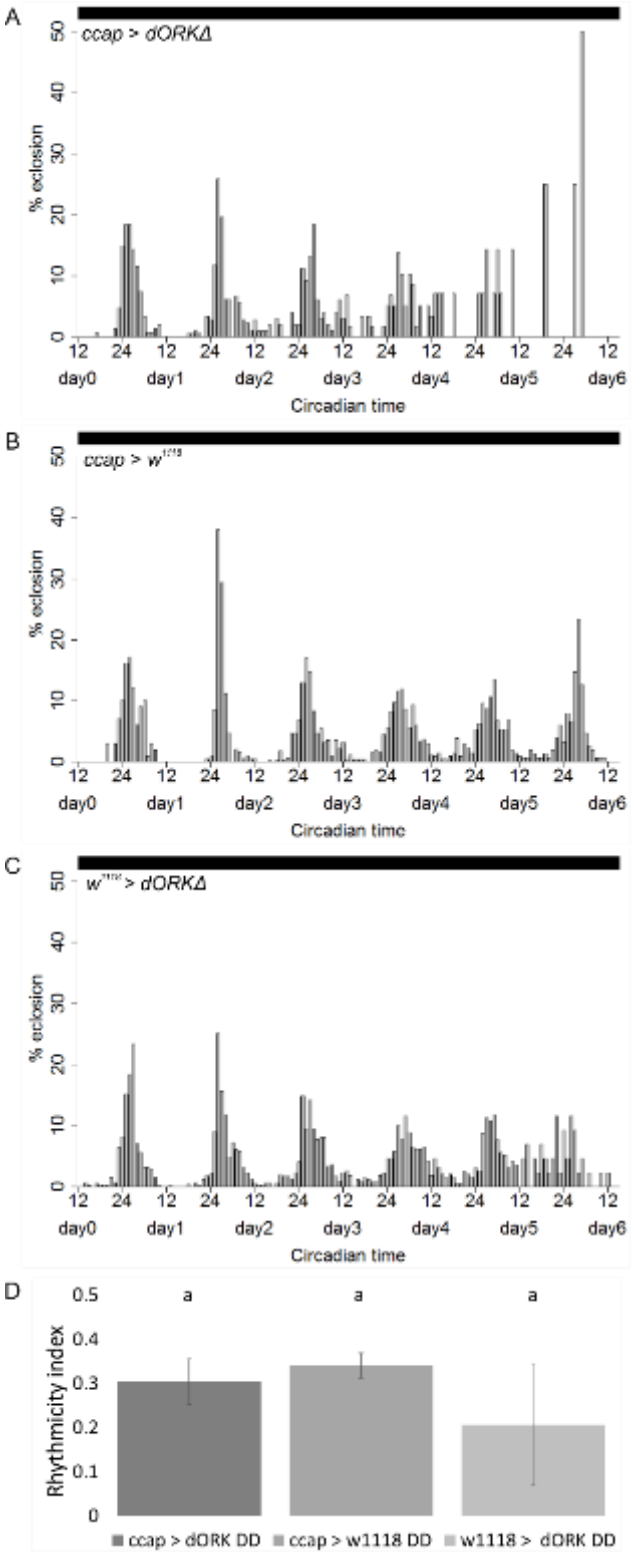

Figure 67: Eclosion rhythms under DD conditions after silencing of of CCAP neurons
Eclosion profiles for populations expressing UAS-*dORKΔ* driven by *ccap*-GAL4 (A) and the respective controls (B: GAL4 control, C: UAS control) under DD conditions. Each bar represents the percentage of eclosed flies per hour normalized to the number of eclosed flies per day. The black rectangles represent the light regime. (D) shows the means of the rhythmicity indices (±SD). Different letters above columns indicate significant difference ($p<0.05$). (N=6, 2, 3; n=1029, 1189, 1093)

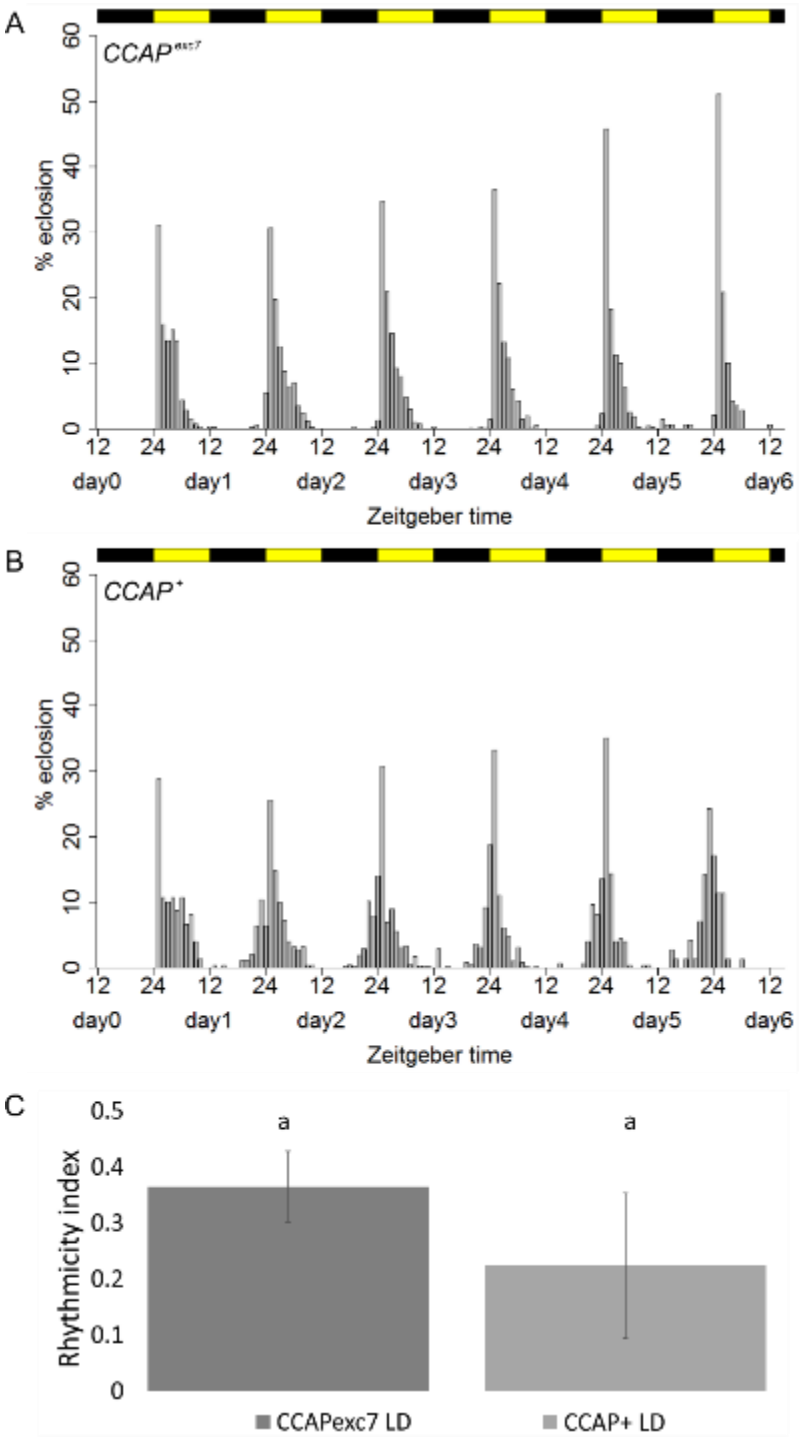

Figure 68: Eclosion rhythms of the *CCAP*^{exc7} mutant under LD conditions
Eclosion profiles for populations of the *CCAP*^{exc7} mutant (A) and the control (B) under LD conditions. Each bar represents the percentage of eclosed flies per hour normalized to the number of eclosed flies per day. The black and yellow rectangles represent the light regime. (C) shows the means of the rhythmicity indices (±SD). Different letters above columns indicate significant difference ($p<0.05$). (N=4, 5; n=2230, 1532)

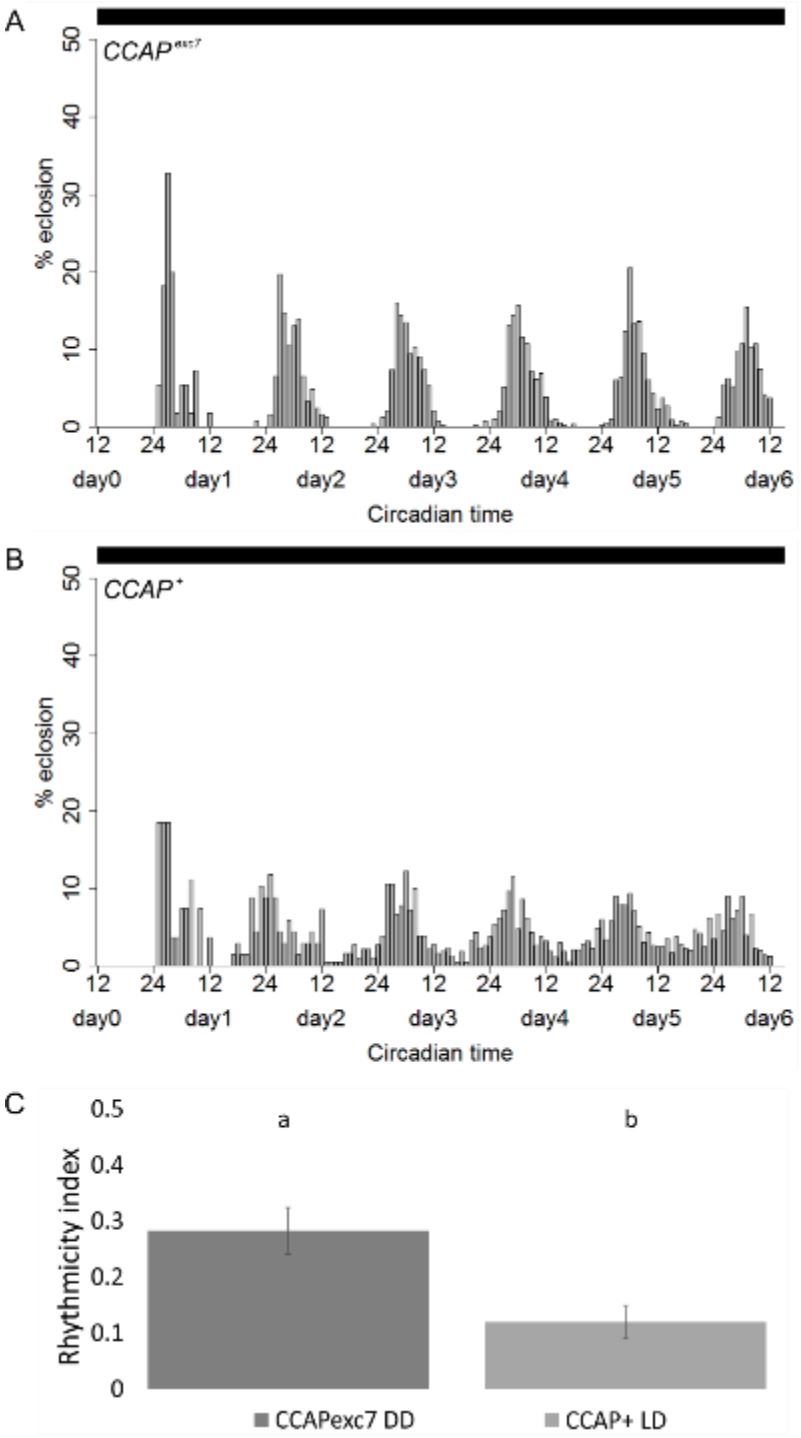

Figure 69: Eclosion rhythms of the *CCAP*^{exc7} mutant under DD conditions
Eclosion profiles for populations of the *CCAP*^{exc7} mutant (A) and the control (B) under DD conditions. Each bar represents the percentage of eclosed flies per hour normalized to the number of eclosed flies per day. The black rectangles represent the light regime. (C) shows the means of the rhythmicity indices (±SD). Different letters above columns indicate significant difference ($p<0.05$). (N=3, 4; n=1747, 1621)

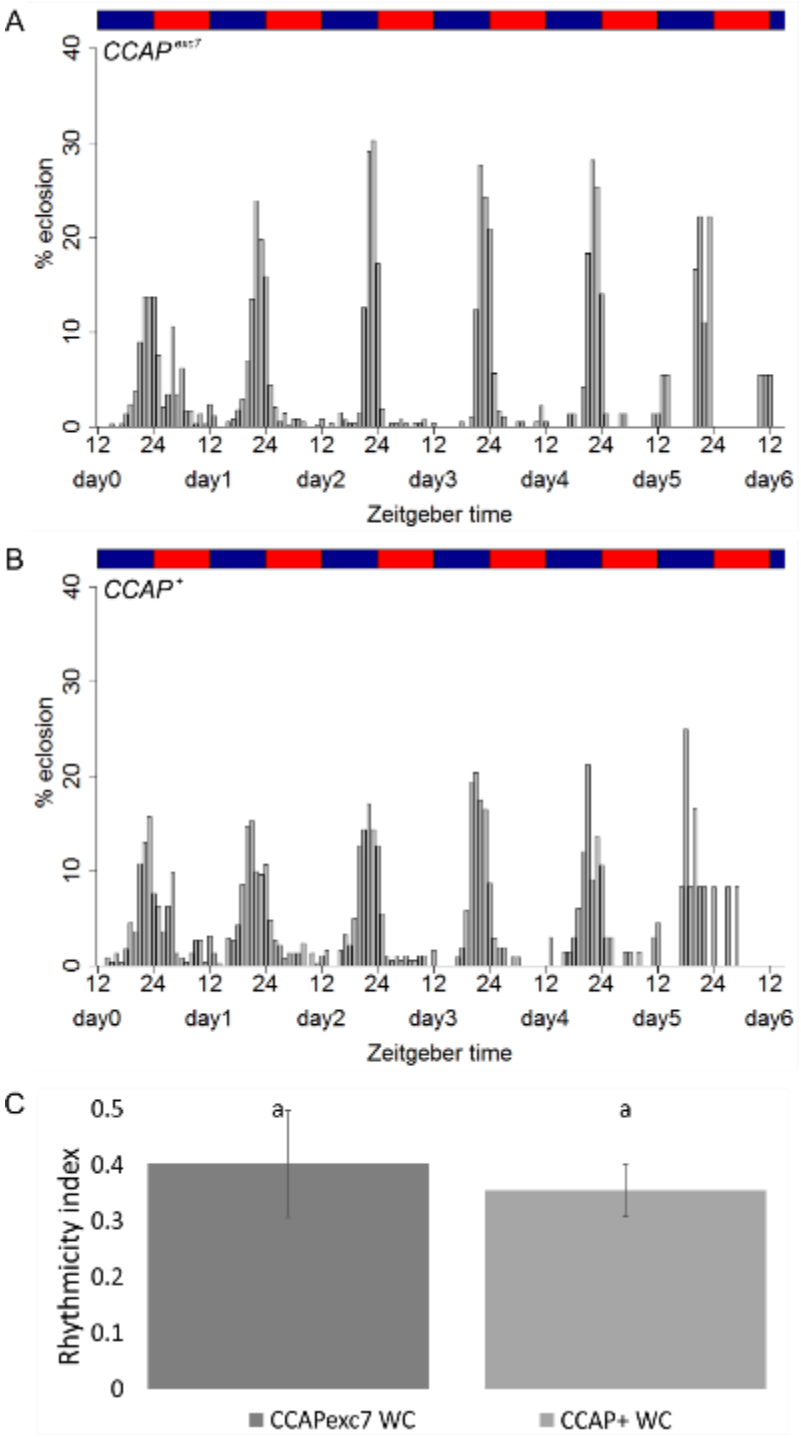

Figure 70: Eclosion rhythms of the *CCAP*^{exc7} mutant under WC conditions
Eclosion profiles for populations of the *CCAP*^{exc7} mutant (A) and the control (B) under WC (25°C:16°C) conditions. Each bar represents the percentage of eclosed flies per hour normalized to the number of eclosed flies per day. The blue and red rectangles represent the temperature regime. (C) shows the means of the rhythmicity indices (±SD). Different letters above columns indicate significant difference ($p<0.05$). Experiments were performed under constant white light. (N=4, 4; n=1160, 963)

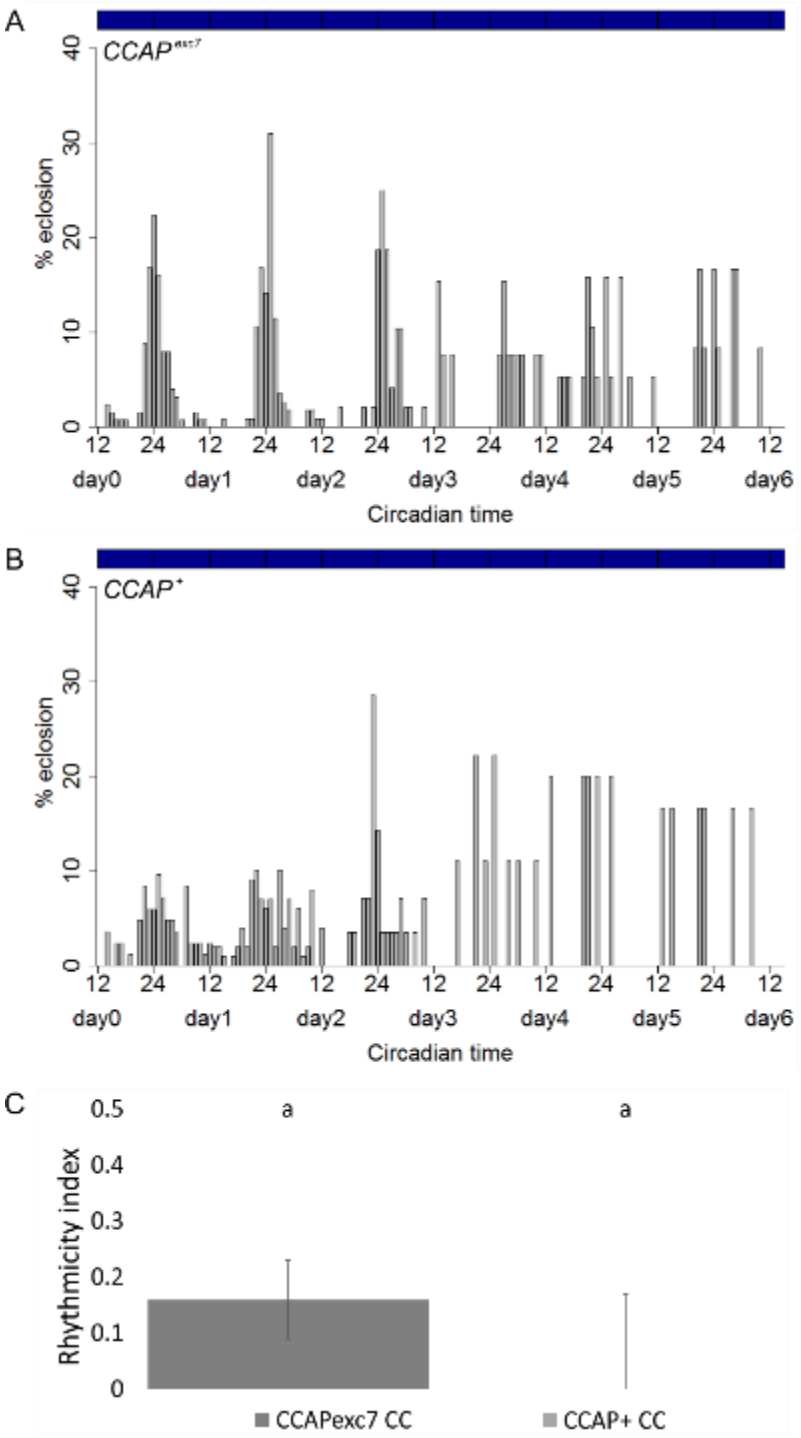

Figure 71: Eclosion rhythms of the *CCAP*^{exc7} mutant under CC conditions
Eclosion profiles for populations of the *CCAP*^{exc7} mutant (A) and the control (B) under CC (20°C) conditions. Each bar represents the percentage of eclosed flies per hour normalized to the number of eclosed flies per day. The blue rectangles represent the temperature regime. (C) shows the means of the rhythmicity indices (±SD). Different letters above columns indicate significant difference ($p<0.05$). Experiments were performed under constant red light. (N=2, 2; n=339, 234)

2.5 Eclosion rhythms of the *CCAP^{exc7}* mutant under natural conditions

Five experiments were conducted with the *CCAP^{exc7}* mutant and the *CCAP^{+}* control under natural conditions during August and September 2014. For each experiment, the rhythmicity index was calculated and the results are summarized in Figure 72.

To allow for comparison, the values of the wildtype *CantonS* (CS) for the same experiments were similarly calculated (Figure 72 C). Under natural conditions, rhythmic, weakly rhythmic and arrhythmic eclosion results were obtained for both the *CCAP^{exc7}* mutant, the *CCAP^{+}* control and *Canton S*. A higher percentage of experiments revealed strong rhythmic behavior in the *CCAP^{exc7}* mutant (40%) than in the *CCAP^{+}* control (0%) and the wildtype (0%), but the percentage of experiments with arrhythmic eclosion behavior was nearly the same for the mutant and the wildtype (20%). For the control, a higher percentage of experiments showed arrhythmic eclosion behavior (40%) (Figure 72 A). However, no significant differences were observed between the means of the rhythmicity indices for all three strains, although the *CCAP^{+}* control showed a trend to decreased rhythmicity (Figure 72 B). The eclosion profiles of the *CCAP^{exc7}* mutant and the *CCAP^{+}* control were very similar for each date (Figure 73 - Figure 77). Also, eclosion profiles of both strains were not different to that of the wildtype *Canton S* (Figure 20-Figure 24). The *CCAP^{exc7}* mutant showed a narrower gate than the control and slightly higher eclosion peaks on some days (Figure 73 - Figure 77). Also, the eclosion rate on the population level was higher in the mutant than in the control, although the same number of pupae were placed on the eclosion plates (Table 8).

Statistical modelling was applied to analyze the effects of the clock and the abiotic parameters temperature and light intensity on the daily eclosion pattern in the *CCAP^{exc7}* mutant and the *CCAP^{+}* control. These effects were then compared to the wildtype *Canton S* (CS) (Figure 78). Temperature and light intensity had the same effect in the mutant and the control as in the wildtype (Figure 78 B, C). The clock, however, had a different effect in the mutant than in the control. No significant difference was observed between the effects on the control and the wildtype (Figure 78 A, A'), while in the *CCAP^{exc7}* mutant the clock had a significantly stronger effect on the eclosion rhythm (Figure 78 A, A').

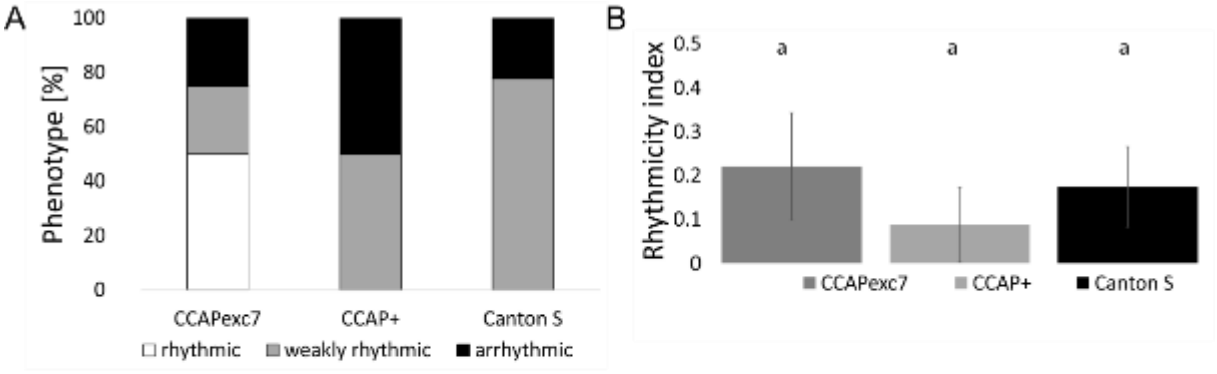

C

	31.07.-07.08.2014	07.08.-14.08.2014	21.08.-28.08.2014	28.08.-04.09.2014	04.09.-11.09.2014
CCAP ^{exc7}	0.33	-	0.3	0.06	0.19
CCAP $^{+}$	0.1	-	0.2	0	0.05
Canton S	0.28	0.1	0.25	0.17	0.07

Figure 72: Rhythmicity of the *CCAP^{exc7}* mutant under natural conditions
Rhythmicity indices of the *CCAP^{exc7}*, the *CCAP^{+}* control and the wildtype *Canton S* for the experiments conducted under natural conditions. In **A**, the percentage of experiments with rhythmic (white), weakly rhythmic (gray) and arrhythmic (black) eclosion behavior for each genotype is shown. The means (±SD) of the rhythmicity indices are presented in **B**. Different letters above columns indicate significant difference ($p<0.05$). The rhythmicity indices for each genotype and experiment are listed in **C** ($RI>0.3$: rhythmic, $0.1<RI<0.3$: weakly rhythmic, $RI<0.1$: arrhythmic). (N=5)

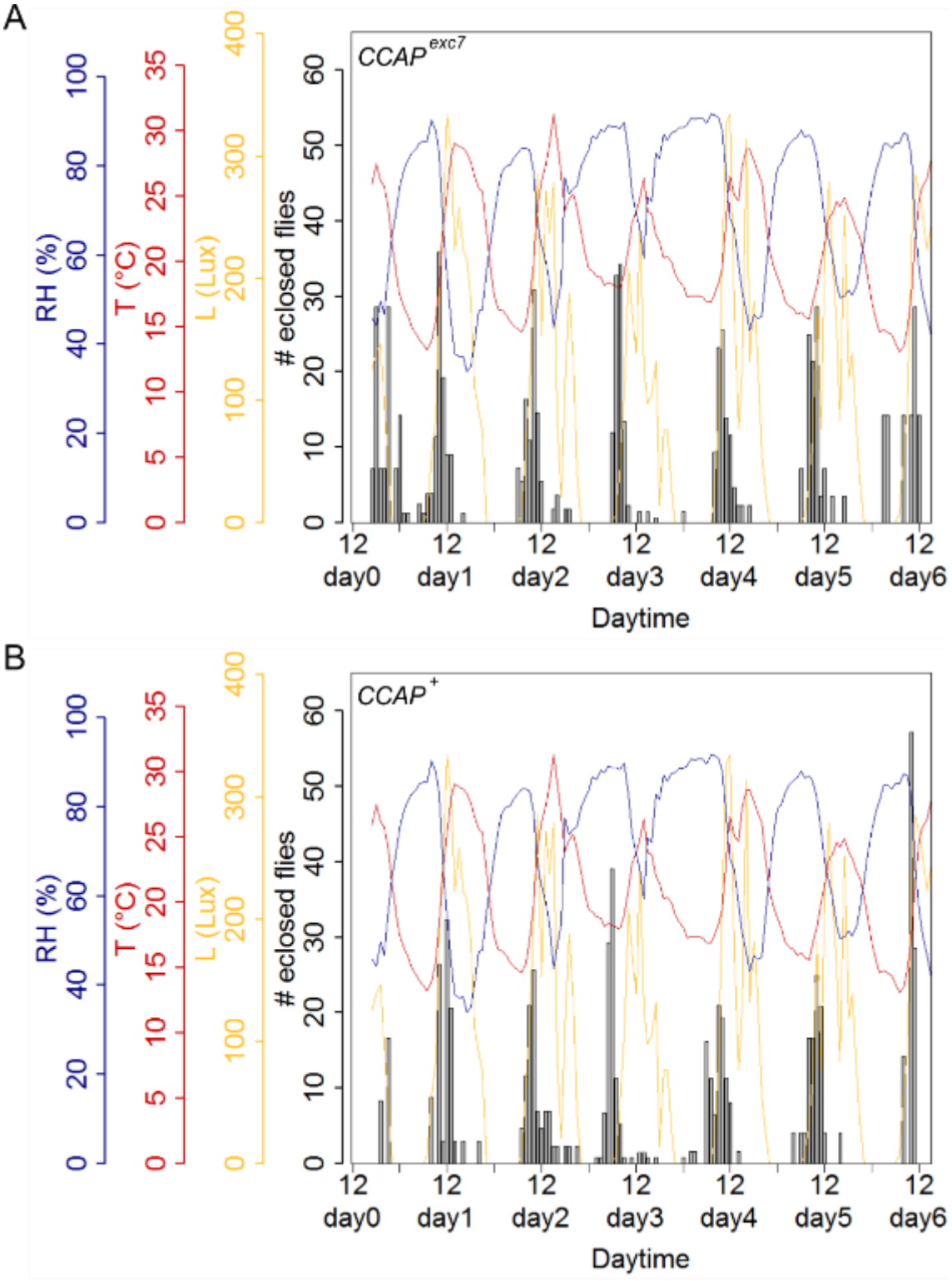

Figure 73: Eclosion rhythms of the *CCAP*^{exc7} mutant under natural conditions from 31.07.-07.08.2014

Eclosion profiles for populations of the *CCAP*^{exc7} mutant (A) and the control (B) under natural conditions. Each bar represents the percentage of eclosed flies per hour normalized to the number of eclosed flies per day. Superimposed curves represent abiotic environmental factors measured once every hour: light intensity (yellow), temperature (red) and relative humidity (blue). Experiments were performed under constant red light. (N=1, 1; n: A=362, B=317)

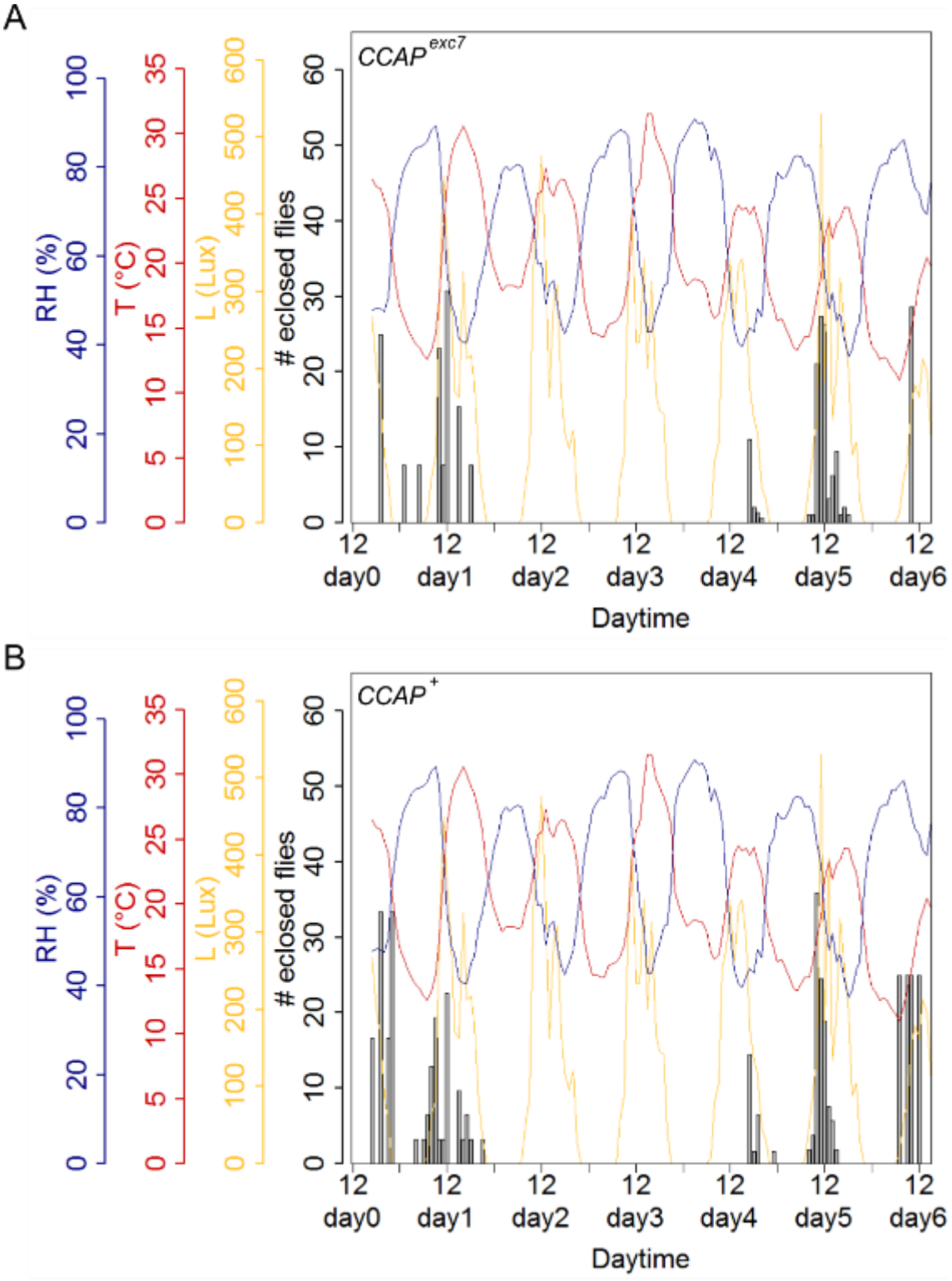

Figure 74: Eclosion rhythms of the *CCAP*^{exc7} mutant under natural conditions from 07.08.-14.08.2014

Eclosion profiles for populations of the *CCAP*^{exc7} mutant (A) and the control (B) under natural conditions. Each bar represents the percentage of eclosed flies per hour normalized to the number of eclosed flies per day. Superimposed curves represent abiotic environmental factors measured once every hour: light intensity (yellow), temperature (red) and relative humidity (blue). Experiments were performed under constant red light. (N=1, 1; n: A=263, B=158)

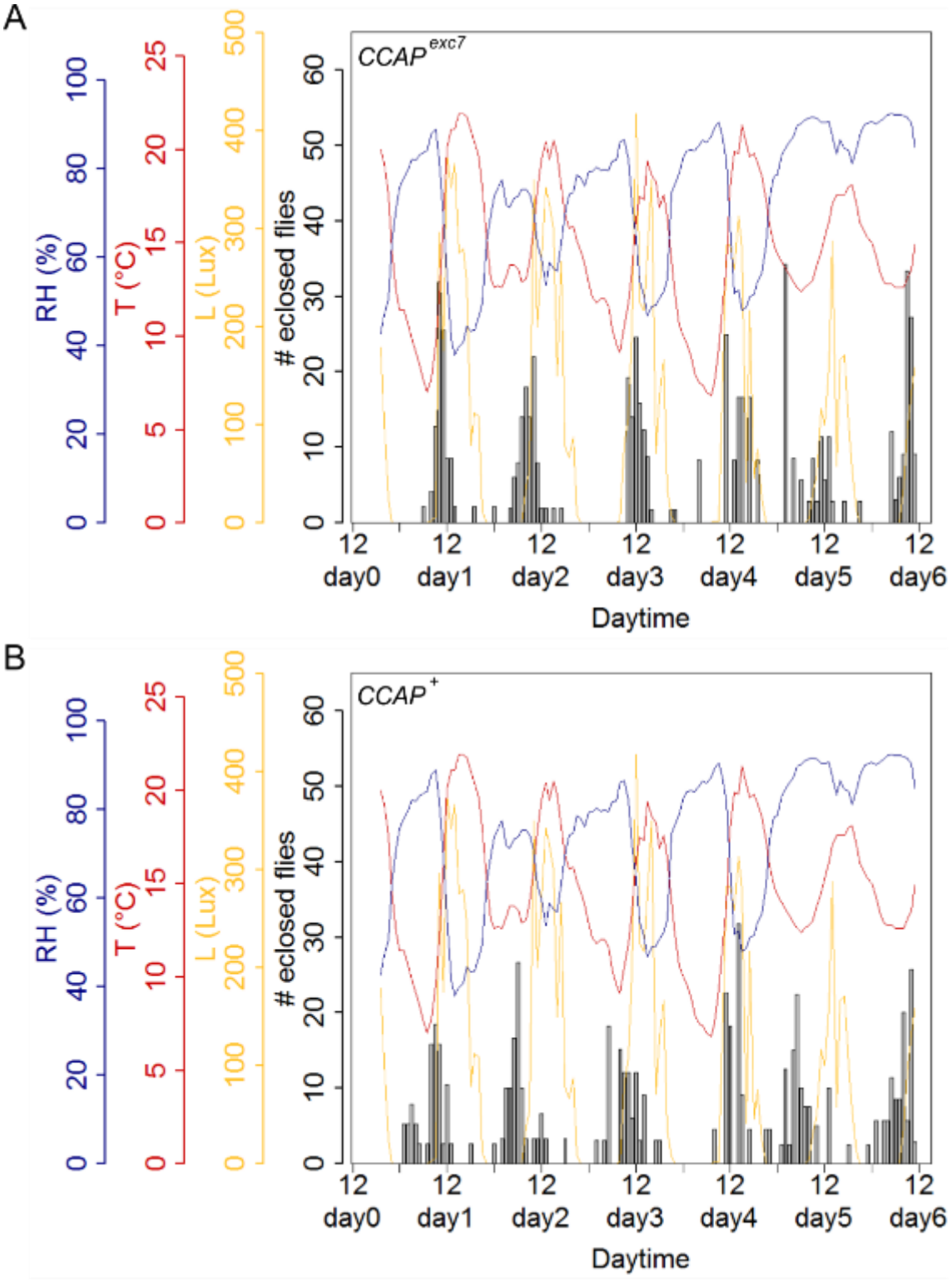

Figure 75: Eclosion rhythms of the *CCAP*^{exc7} mutant under natural conditions from 21.08.-28.08.2014

Eclosion profiles for populations of the *CCAP*^{exc7} mutant (A) and the control (B) under natural conditions. Each bar represents the percentage of eclosed flies per hour normalized to the number of eclosed flies per day. Superimposed curves represent abiotic environmental factors measured once every hour: light intensity (yellow), temperature (red) and relative humidity (blue). Experiments were performed under constant red light. (N=1, 1; n: A=235,, B=199)

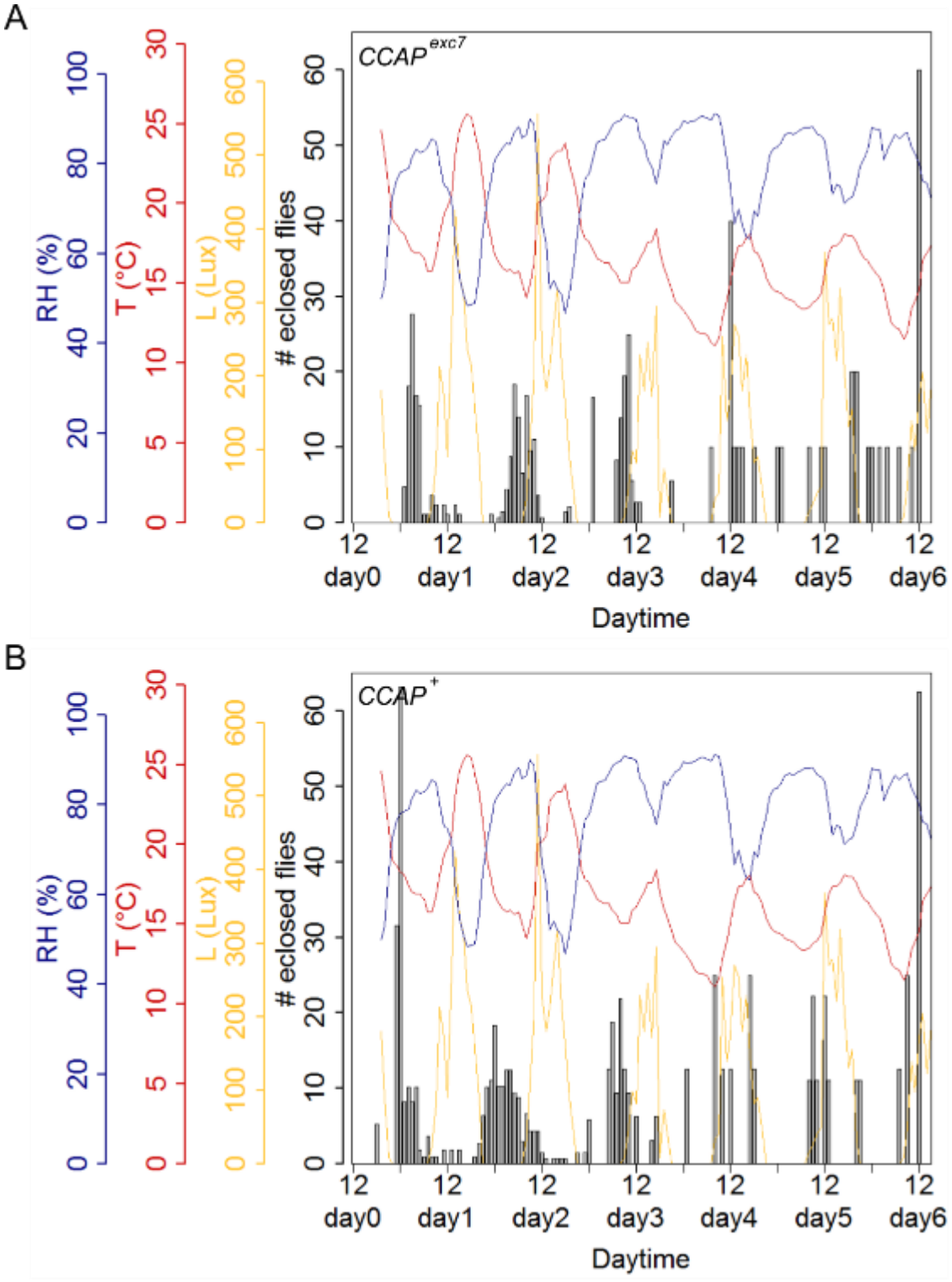

Figure 76: Eclosion rhythms of the *CCAP*^{exc7} mutant under natural conditions from 28.08.-04.09.2014

Eclosion profiles for populations of the *CCAP*^{exc7} mutant (A) and the control (B) under natural conditions. Each bar represents the percentage of eclosed flies per hour normalized to the number of eclosed flies per day. Superimposed curves represent abiotic environmental factors measured once every hour: light intensity (yellow), temperature (red) and relative humidity (blue). Experiments were performed under constant red light. (N=1, 1; n: A=289, B=322)

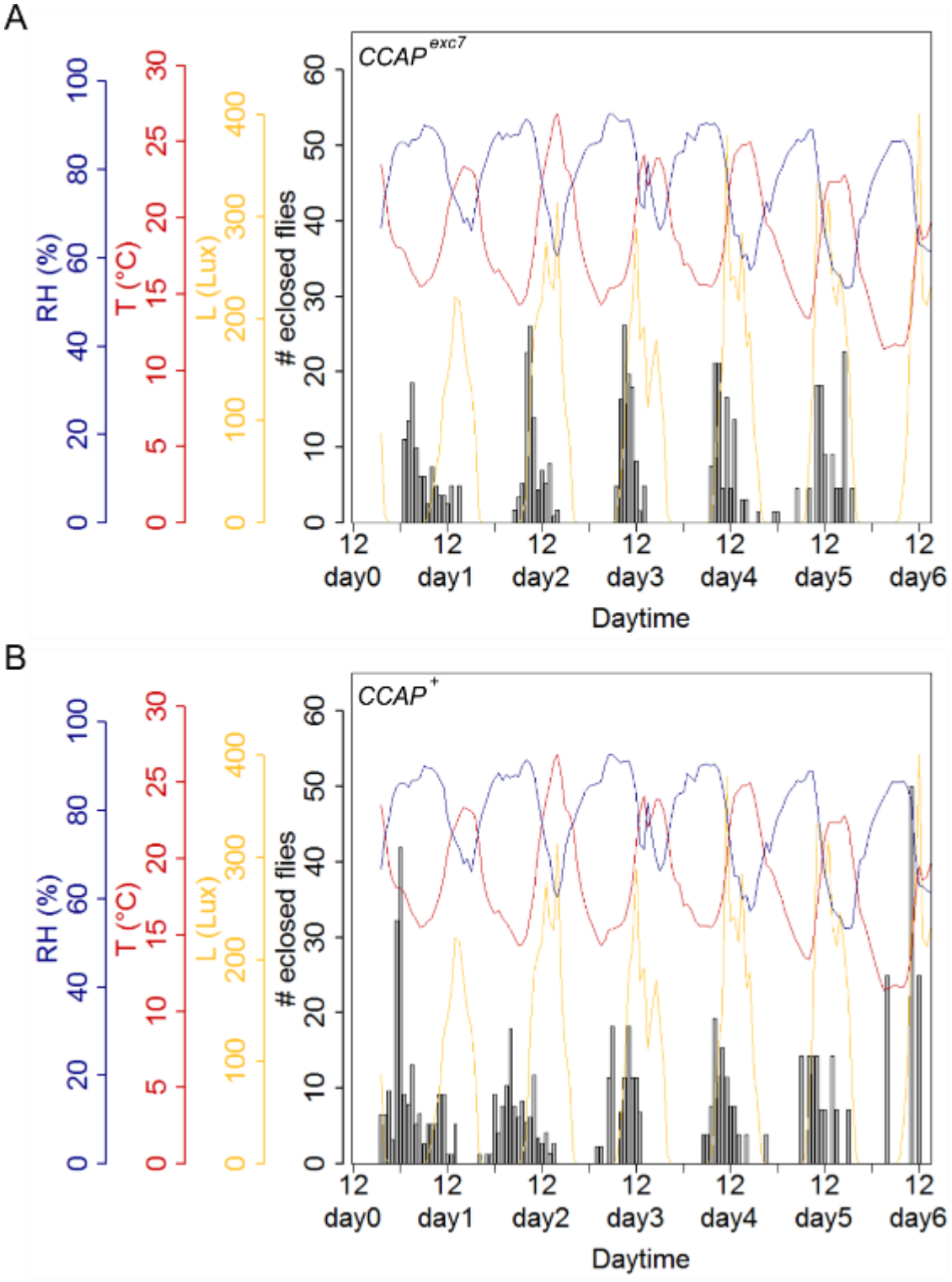

Figure 77: Eclosion rhythms of the *CCAP*^{exc7} mutant under natural conditions from 04.09.-11.09.2014

Eclosion profiles for populations of the *CCAP*^{exc7} mutant (A) and the control (B) under natural conditions. Each bar represents the percentage of eclosed flies per hour normalized to the number of eclosed flies per day. Superimposed curves represent abiotic environmental factors measured once every hour: light intensity (yellow), temperature (red) and relative humidity (blue). Experiments were performed under constant red light. (N=1, 1; n: A=351, B=343)

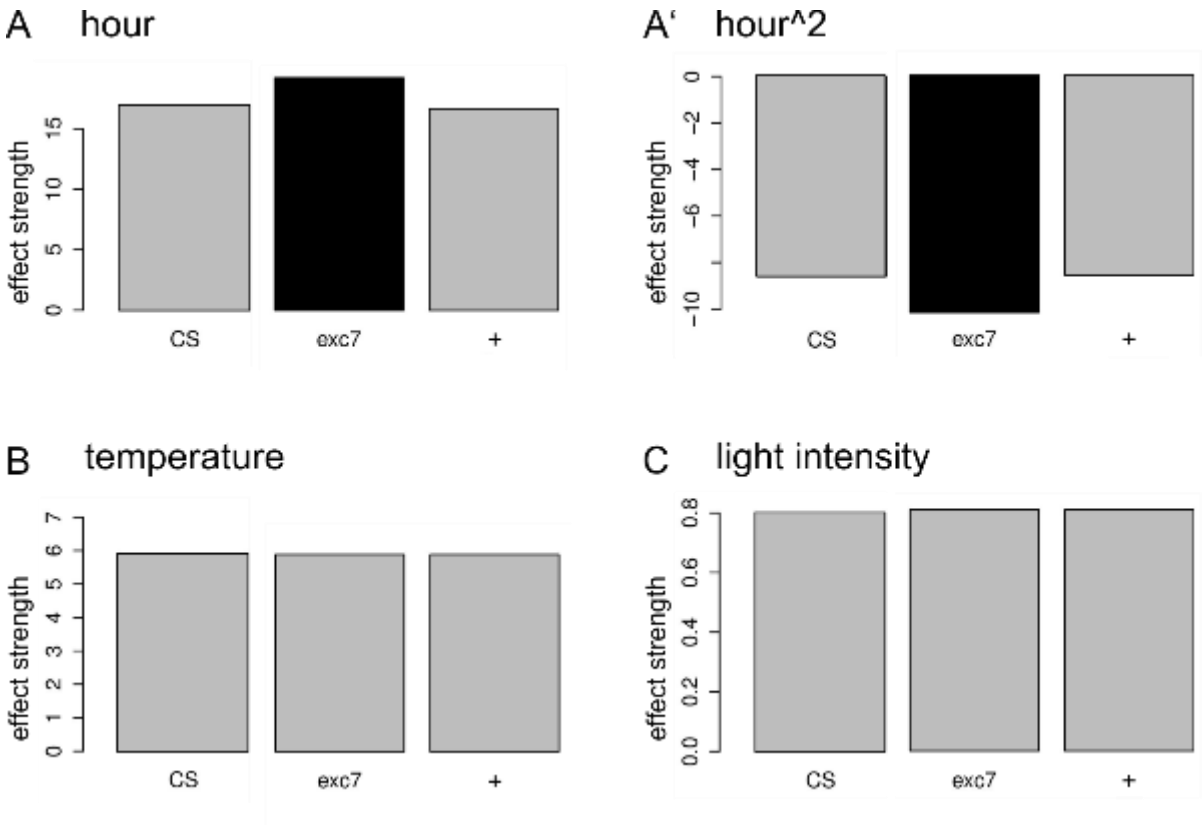

Figure 78: Statistical modelling of the *CCAP^{exc7}* mutant under natural conditions
Results obtained from statistical modelling of the effect of the clock (A, A') and of the abiotic factors temperature (B) and light intensity (C) on the daily eclosion pattern. Effects in the *CCAP^{exc7}* mutant (exc7) and the *CCAP^{+}* control (+) were analyzed and compared to the wildtype *Canton S* (CS). Black bars in mutant and control stand for a significant difference to *Canton S*, gray bars for no significant difference.

3. Discussion

Ablation and silencing of the CCAP neurons delivered similar phenotypes to Park *et al.* 2003, for example a reduced number of flies surviving pupal ecdysis. In contrast, however, no effect on the lights-on peak was observed and the eclosion rhythm was not different to that of the controls. A possible explanation is that the ablation and silencing was incomplete, so that the residual CCAP was enough to attenuate the phenotype.

Besides CCAP, CCAP neurons also express MIP (Kim *et al.*, 2006b) and bursicon (Dewey *et al.*, 2004). Selcho *et al.* showed that the *ccap*-Gal4 line additionally includes the EH cells (Figure 79) (Selcho *et al.*, unpublished-b). After ablation of EH neurons, only one third of the flies survive until adulthood (McNabb *et al.*, 1997b), while flies mutant for *Eh* die at the first larval ecdysis (Krüger *et al.*, 2015). The EH neurons also mediatie the lights-on response (McNabb and Truman, 2008), so that they are probably responsible for the effect observed in Park *et al.*, 2003. This co-expression further impedes the interpretation of the ablation and silencing data of CCAP neurons as the observed effects cannot be clearly assigned to either CCAP, MIP, bursicon or EH.

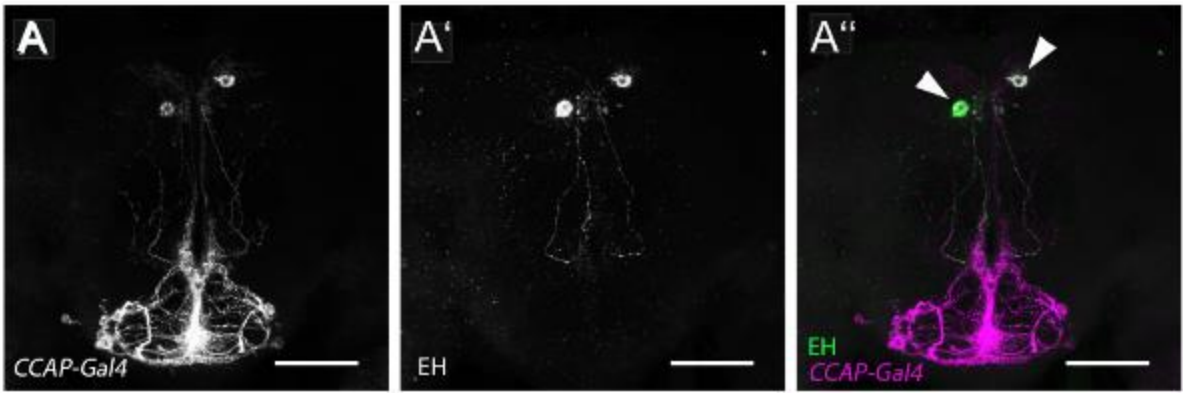

Figure 79: EH cells are present in the *ccap*-GAL4 driver line
The expression pattern of the *ccap*-GAL4 line (A) and immunostaining for EH (A') are shown and superimposed in A''. From Selcho *et al*., unpublished

Therefore, the *CCAP*^{exc7} mutant was used for further experiments. It showed normal eclosion rhythms under both LD and DD conditions, which confirms the data from Lahr *et al*. 2012. Under temperature entrainment, both mutant and control flies eclosed perfectly rhythmic and there were no significant differences between rhythmicity and period length. This contradicts the idea that CCAP could play a role in the temperature entrainment of the eclosion rhythm. CCAP synaptic endings overlap with DN2 clock neurons in the dorsal brain of

larval and pharate flies (Park *et al.*, 2003). These cells do not express CRY and cannot receive light inputs directly, but play an important role in the entrainment to temperature (Yoshii *et al.*, 2005; Busza *et al.*, 2007; Miyasako *et al.*, 2007; Picot *et al.*, 2009). However, as the mutants show normal eclosion rhythms under temperature conditions, CCAP seems to play no role in the temperature perception and entrainment of the clock.

Under both entrainments, the mutants achieved significantly higher values for the rhythmicity indices under constant conditions and a trend under entrainment conditions, indicating that flies eclose even more rhythmic without CCAP than with. This effect can also be observed under natural conditions. Both the mutant and the control showed general rhythmic eclosion and eclosion profiles similar to that of the wildtype. Although the differences were not statistically significant, the means of the rhythmicity indices were increased in the $CCAP^{exc7}$ mutant and they had a higher percentage of experiments with strongly rhythmic eclosion behavior. Statistical modelling further revealed that the effect of the clock on the eclosion rhythm is significantly stronger in flies mutant for *ccap* than in the control or the wildtype. The abiotic factors temperature and light intensity had the same effect in all three strains. This could imply a dampening role of CCAP on the clock or on the clock output. Analysis of the expression pattern of the CCAP receptor, especially in clock cells, or fluorescent imaging with CCAP in the clock cells in pharate adults could help to dissect a possible influence of CCAP and exclude effects of different genetic backgrounds. Although ablation or silencing of the CCAP neurons reduces viability strongly, CCAP itself is not necessary for eclosion rhythmicity, neither under light or temperature nor under natural conditions. A possible explanation is that as eclosion is a crucial event in the life of the fly, there are several redundant pathways controlling eclosion timing and behavior. This way, losing one peptide would not prevent the fly from emerging as an adult and secure its survival. Loss of also the other peptides expressed in CCAP neurons, however, cannot be compensated so easily. A role for CCAP in the entrainment of the eclosion rhythm via light or temperature can be ruled out.

Chapter V. Screen for candidate peptides regulating eclosion behavior and rhythmicity

1. Introduction

Eclosion starts with an initiatial release of ETH from the Inka cells, which induces the release of EH. EH then induces the complete depletion of the Inka cells, and ETH and EH together activate peptides regulating the ecdysis behavior (reviewed in Nässel and Winther, 2010). It was also shown that injection of ETH induces premature eclosion (Park *et al.*, 1999). While it was shown in *Manduca* that Corazonin induces the initial release of ETH from the Inka cells (Kim *et al.*, 2004), the starting signal for ETH release and eclosion in *Drosophila* is so far unknown. It was therefore the aim of this chapter to identify this starting signal and other candidate peptides that play a role in the regulation of eclosion. To this end, a direct approach was chosen, where different peptide-expressing cells were transiently activated by blue light at a defined time point using the newly developed Channelrhodopsin-2-XXL (Dawydow *et al.*, 2014).

Channelrhodopsins (ChR) are sensory photoreceptors of green algae. The first channelrhodopsins, *Channelrhodopsin-1 and -2 (ChR-1, ChR-2),* were discovered in *Chlamydomonas reinhardtii (Nagel, 2002; Sineshchekov et al., 2002; Nagel et al., 2003).* Like the rhodopsins of vertebrates, they are retinylidene proteins with seven transmembrane domains and contain the chromophore all-*trans*-retinal. Whereas rhodopsins are G protein-coupled receptors that open other ion channels indirectly via second messengers, channelrhodopsins directly form ion channels and are light-inducible. When the all-*trans*-retinal absorps a photon, it undergoes a conformational change to 13-*cis*-retinal. This also induces a structural change of the proteins and thereby directly opens the channel (Nagel *et al.*, 2003). ChR-1 and -2 have their absorption maxima around 510 nm and 480 nm respectively (Nagel, 2002; Sineshchekov *et al.*, 2002; Nagel *et al.*, 2003). Most channelrhodopsins are unselective cation-channels, so that they can be used to optogenetically influence many cellular processes in target cells (Nagel *et al.*, 2003). The first channelrhodopsin used in *Drosophila* was ChR-2 (Zhang *et al.*, 2007). The thick cuticle of *Drosophila* impeded the transmission of the stimulating light to deep laying cells and addition of all-*trans*-retinal in a high dose to the food was necessary. There are several modified versions of ChR-2 and several

channelrhodopsins of other algae, partly with yellow- to red-shifted absorption maxima (Zhang *et al.*, 2008; Govorunova *et al.*, 2011; Lin *et al.*, 2013). Channnelrhodopsin-2-XXL (ChR2-XXL) is a variant of ChR-2 and was created by substituting the aspartic acid with cysteine at position 156. This led to an exceptionally high expression of the channelrhodopsin and a long open state of the channel after activation. Addition of retinal to the food of the flies is therefore no longer necessary (Dawydow *et al.*, 2014). Using the UAS-GAL4-system together with ChR2-XXL provides an ideal means of controlling the activity of cells with high spatial and temporal control in a non-invasive way.

The time point of optogenetic activation was chosen after Pittendrigh. He proposed a model were eclosion could only happen in an allowed phase. Under an entrainment of a 24 hour period, this timeframe would last about 6 hours (Pittendrigh, 1954; Saunders, 2002). To clearly identify eclosion peaks induced by the activation of candidate peptidergic cells, the earliest possible time point for the activation was chosen. This would then be 6 hours before the expected eclosion peak time based on eclosion rhythms of wildtype flies under temperature entrainment.

2. Results

To study the role of different peptides as starting factors for eclosion or in the regulation of eclosion rhythmicity, defined peptidergic neurons were optogenetically activated by combining the ChR2-XXL with specific GAL4 driver lines. The results of this screen are summarized in Table 10 at the end of this chapter. The effects of the activation of the peptidergic neurons are described in detail in the following chapters.

2.1 Ecdysis-triggering hormone (ETH)

The role of ETH as an ecdysis-inducing factor was first discovered in *Manduca sexta*, where it is expressed in the epitrachael glands (=Inka cells) of pharate pupa (Zitnan *et al.*, 1996). In *Drosophila*, the *eth* gene encodes for the two peptides ETH1 and ETH2. Both induce premature eclosion upon injection into pharate adults (Park *et al.*, 1999). Flies mutant for *eth* nearly all die during transition from first to second instar and show the buttoned-up phenotype of incomplete ecdysis. The phenotype can be rescued by injection of ETH at precise time points (Park *et al.*, 2002). High levels of ecdysteroids shortly before ecdysis induce the expression of ETH in Inka cells and increase the sensitivity of the CNS for ETH. The subsequent decline of ecdysteroid titers increases the secretory competence of the Inka cells and is required for the release of ETH into the hemolymphe (Zitnan *et al.*, 1999; Kingan and Adams, 2000; Cho *et al.*, 2013). Also incubation with eclosion hormone (EH) induces release of ETH from Inka cells, but only in a window of about 8 hours prior to ecdysis (Kingan *et al.*, 1997). The *Drosophila* ETH carries an ecdysone-response element (Park *et al.*, 1999). EH and ETH are in a positive feedback loop, where ETH induces release of EH and EH induces complete depletion of the Inka cells. ETH than induces together with EH the release of other peptides like CCAP and promotes the ecdysis behavior (reviewed in Nässel and Winther, 2010).

To verify the experimental setup and the chosen activation time point of 6 hours before the expected peak of eclosion, ChR2-XXL was first expressed in Inka cells using the *eth*-GAL4 driver line. Since ETH triggers the subsequent peptide cascade leading to eclosion (Park *et al.*, 2002; Clark *et al.*, 2004), it is the starting point for eclosion behavior and thus defines the earliest possible time point of activation via ChR2-XXL and blue light. In addition, a second time point 8 hours before the expected eclosion peak was tested as a control.

Activation of the ETH expressing cells 6 hours before the expected eclosion peak lead to an additional eclosion peak during the activation period in the experimental group (Figure 81 A),

but not in the controls (Figure 81 B, C). Activation 2 hours earlier, however, did not lead to an additional peak of eclosion in either experimental or control flies (Figure 82).

A higher temporal resolution of the time point of the blue light activation showed that most of the flies (about 55%) eclosed within the first 20 minutes. This proves that the additional eclosion peak is a direct response to the activation of the Inka cells and the induced secretion of ETH (Figure 80).

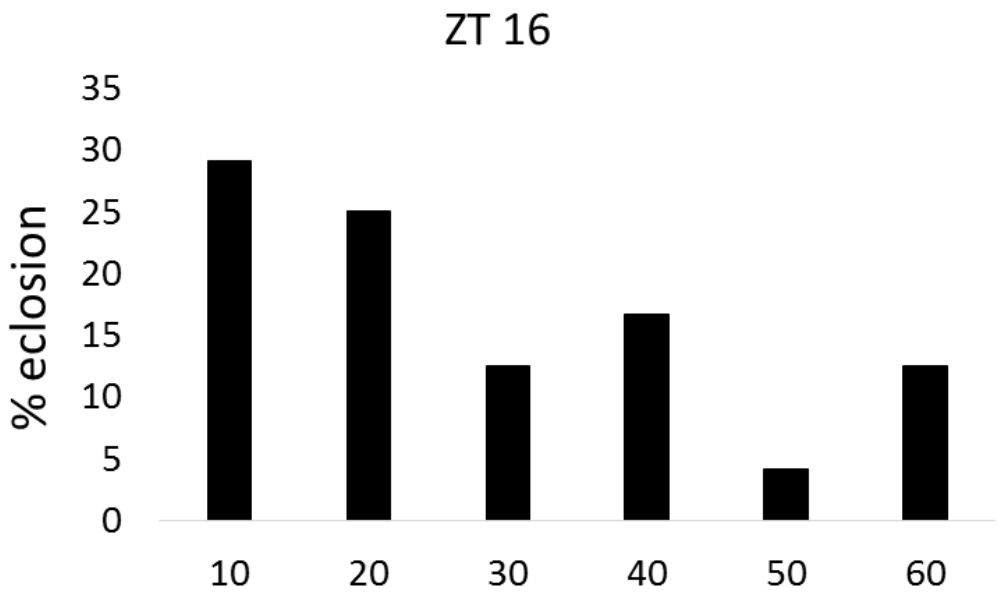

Figure 80: Temporal distribution of eclosion during the optogenetic activation of the Inka cells

The bars represent the percentage of flies that eclosed in 10 minute intervals during the one hour activation with blue light in cells expressing ChR2-XXL driven by *eth*-GAL4

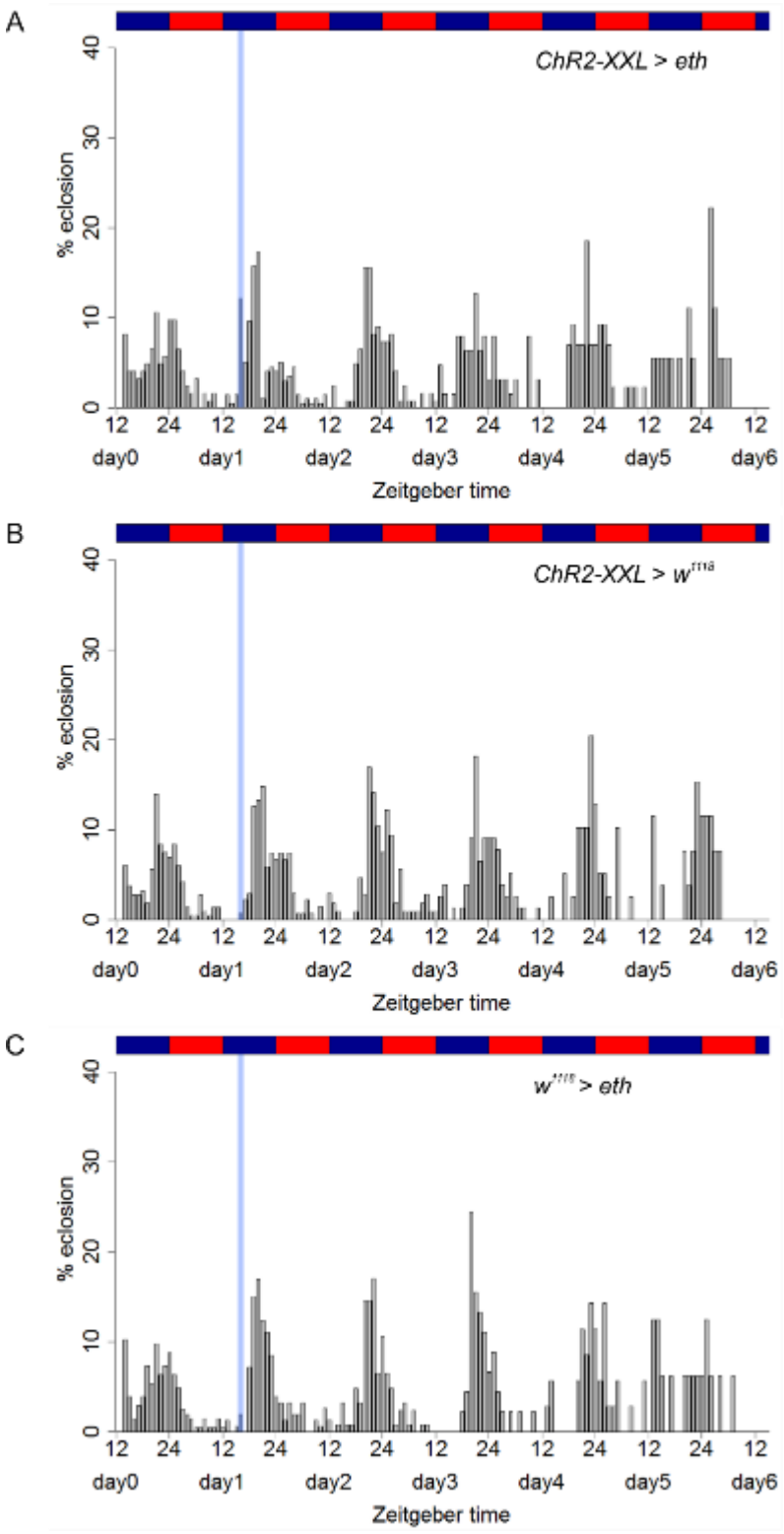

Figure 81: Eclosion rhythms after the activation of ETH-expressing cells 6 hours before the main peak.

Eclosion profiles for populations expressing ChR2-XXL driven by *eth*-GAL4 (A) and the respective controls (B: UAS control, C: GAL4 control) under temperature entrainment (25°C:16°C). Each bar represents the percentage of eclosed flies per hour normalized to the number of eclosed flies per day. The blue and red rectangles represent the temperature regime. The blue bars mark the time point of activation with blue light. (N=3, 3, 3; n=565, 597, 576)

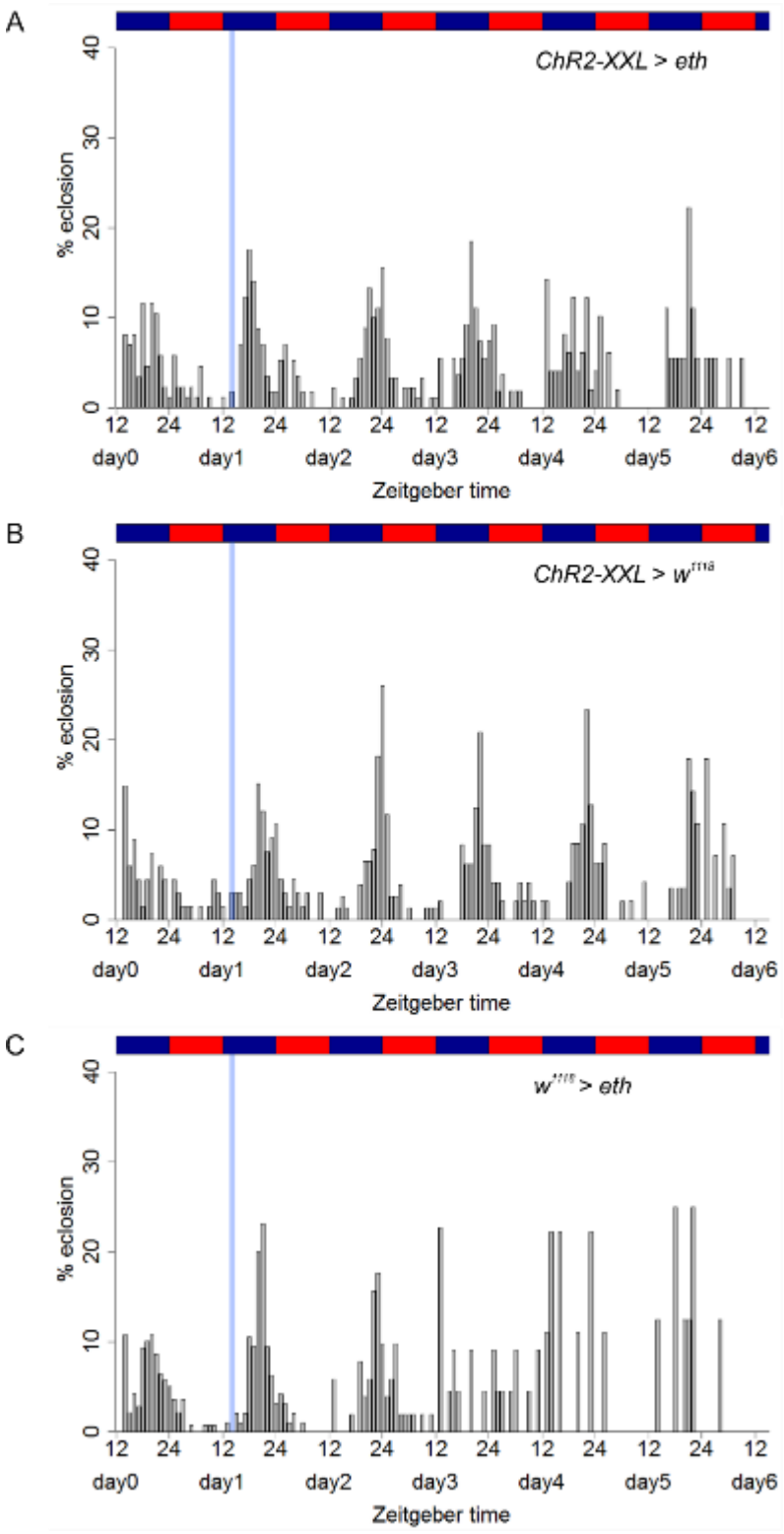

Figure 82: Eclosion rhythms after the activation of ETH-expressing cells 8 hours before the main peak.

Eclosion profiles for populations expressing ChR2-XXL driven by *eth*-GAL4 (A) and the respective controls (B: UAS control, C: GAL4 control) under temperature entrainment (25°C:16°C). Each bar represents the percentage of eclosed flies per hour normalized to the number of eclosed flies per day. The blue and red rectangles represent the temperature regime. The blue bars mark the time point of activation with blue light. (N=2, 2, 2; n=354, 333, 324)

2.2 Apterous (Ap)

The *ap* gene is a so-called selector gene that plays an essential role in the development of both, the wing compartments and the wing and haltere imaginal discs in *Drosophila*. It is expressed in the central and peripheral nervous system (Cohen *et al.*, 1992), and a subset of AP-neurons, which express enzymes for neuropeptide biosynthesis and are suggested to play a role in the regulation of the ecdysis behavior (Park *et al.*, 2004).

The activation of cells expressing ChR2-XXL under control of the *ap/cyo*-GAL4 driver line did not lead to an additional peak of eclosion in either the experimental group or the controls (Figure 83). An effect on the eclosion rhythm could not be observed.

2.3 Capability (Capa)

The Capa peptide family has myostimulatory and osmoregulatory functions in many different insect families (Davies *et al.*, 2013). In *Drosophila*, the CAPA propeptide codes for two periviscerokins , CAPA-PVK-1 and 2, and one pyrokinin, called CAPA-PK (Nässel and Winther, 2010). They are diuretic hormones that act on the Malpighian tubules and are important for fluid homeostasis (Nässel and Winther, 2010; Davies *et al.*, 2013). *Capa* expression is regulated by Clk (McDonald and Rosbash, 2001).

The activation of cells expressing ChR2-XXL under control of the *capa*-GAL4 driver lines did not lead to an additional peak of eclosion in the experimental group or the controls in either of the two tested lines (Figure 84, Figure 85). Moreover, an effect on the eclosion rhythm was not detectable.

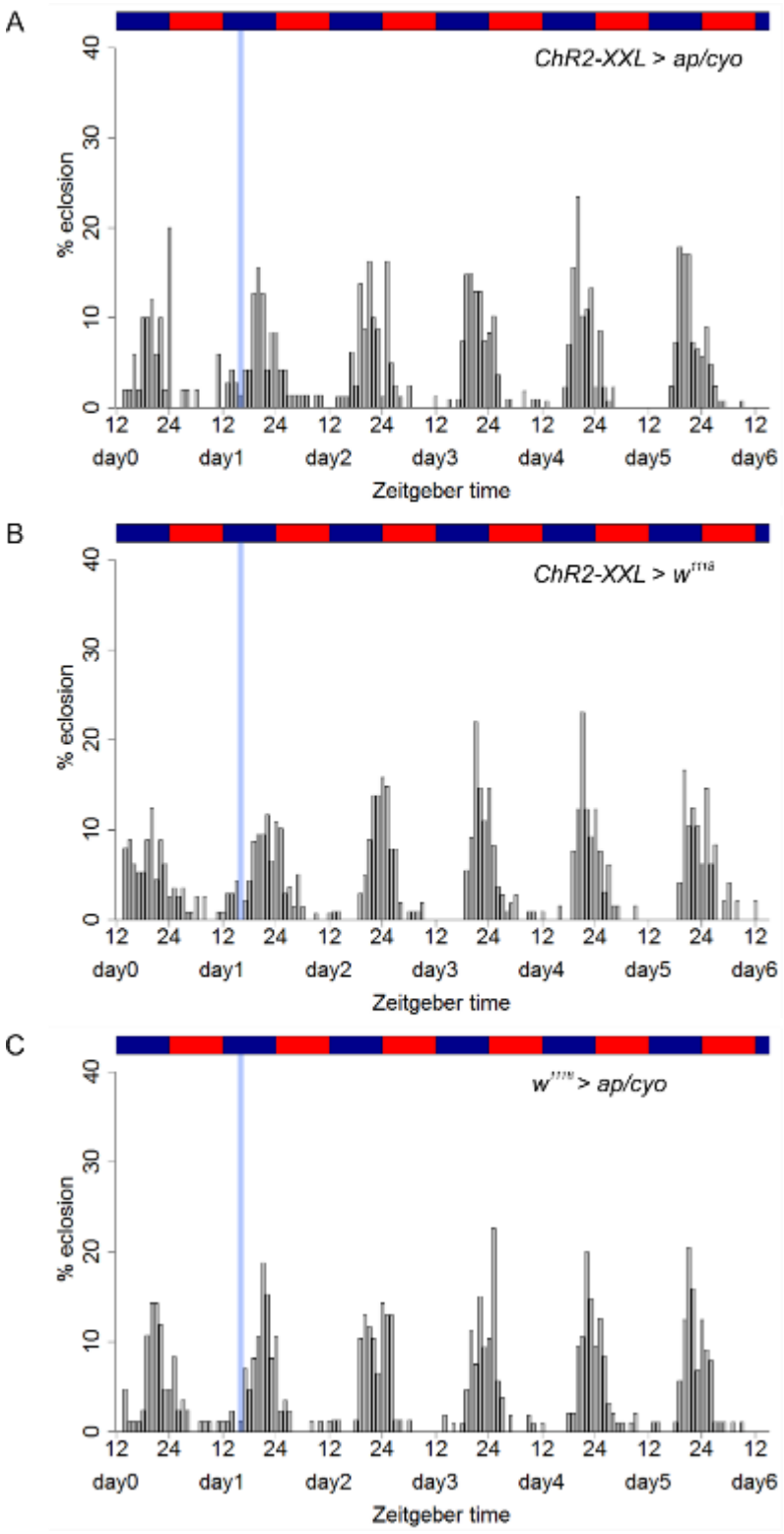

Figure 83: Eclosion rhythms after the activation of ap-expressing cells 6 hours before the main peak.

Eclosion profiles for populations expressing ChR2-XXL driven by *ap/cyo*-GAL4 (A) and the respective controls (B: UAS control, C: GAL4 control) under temperature entrainment (25°C:16°C). Each bar represents the percentage of eclosed flies per hour normalized to the number of eclosed flies per day. The blue and red rectangles represent the temperature regime. The blue bars mark the time point of activation with blue light. (N=3, 3, 3; 560, 573, 535)

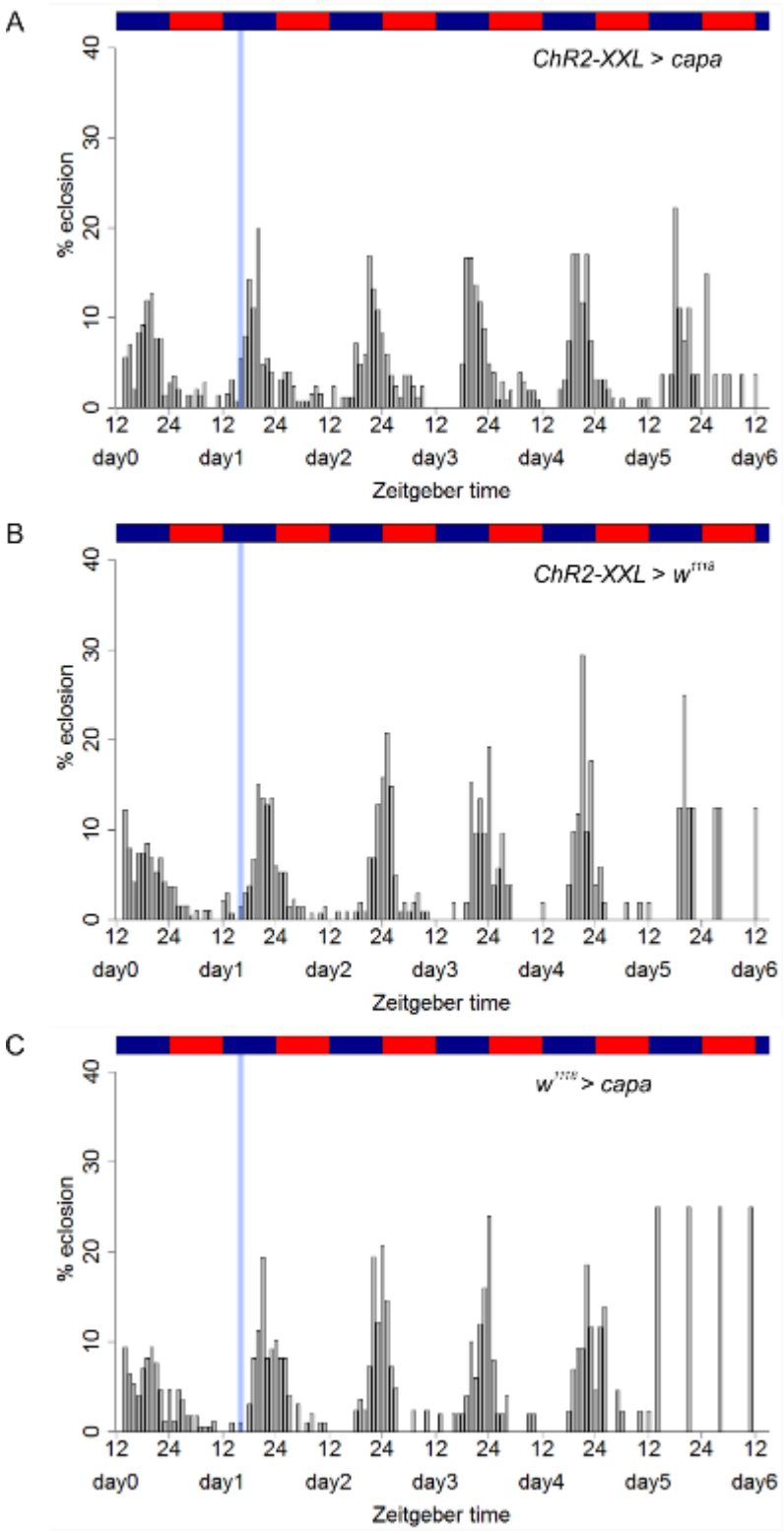

Figure 84: Eclosion rhythms after the activation of Capa-expressing neurons 6 hours before the main peak.

Eclosion profiles for populations expressing ChR2-XXL driven by *capa*-GAL4 (#51969) (A) and the respective controls (B: UAS control, C: GAL4 control) under temperature entrainment (25°C:16°C). Each bar represents the percentage of eclosed flies per hour normalized to the number of eclosed flies per day. The blue and red rectangles represent the temperature regime. The blue bars mark the time point of activation with blue light. (N=4, 4, 4; n=577, 534, 453)

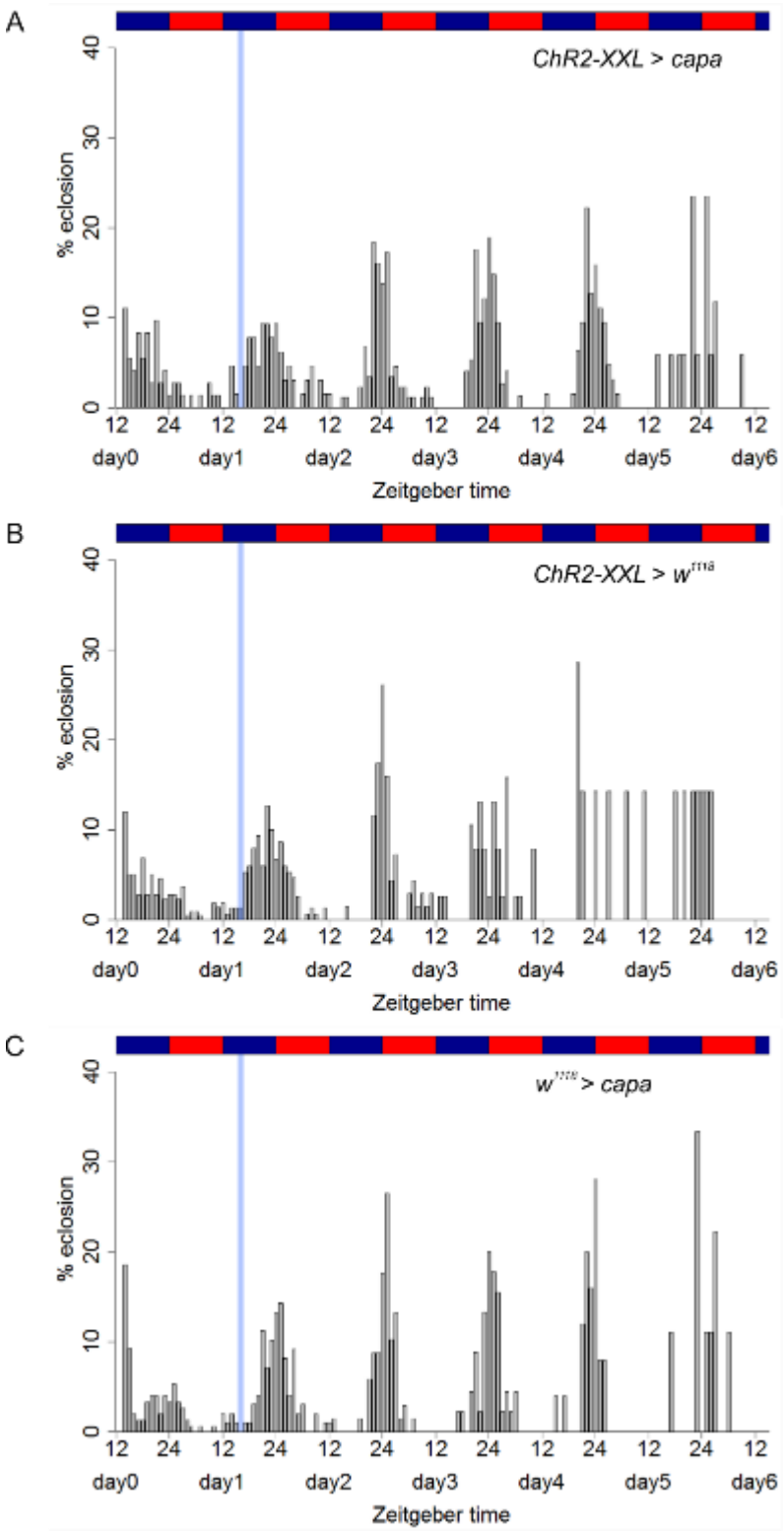

Figure 85: Eclosion rhythms after the activation of Capa-expressing neurons 6 hours before the main peak.

Eclosion profiles for populations expressing ChR2-XXL driven by *capa*-GAL4 (#51970) (A) and the respective controls (B: UAS control, C: GAL4 control) under temperature entrainment (25°C:16°C). Each bar represents the percentage of eclosed flies per hour normalized to the number of eclosed flies per day. The blue and red rectangles represent the temperature regime. The blue bars mark the time point of activation with blue light. (N=3, 3, 3; n=377, 488, 396)

2.4 Corazonin (Crz)

Crz is highly sequence-conserved but has diverse functions in different insect families. For example, it is cardiostimulatory in cockroaches (Veenstra, 1989) and induces gregarious black patterns and cuticle tanning in locusts (Tawfik *et al.*, 1999). In *Manduca sexta*, it directly induces the release of ETH from the Inka cells and starts ecdysis (Kim *et al.*, 2004). In *Drosophila,* Crz neurons express receptors for the diuretic hormones DH31 and DH44 and the peptide AstA (Veenstra, 2009). Crz is also a candidate to be under Clk regulation (McDonald and Rosbash, 2001). Another function is the mediation of stress responses in a sex-dependant way (Veenstra, 2009; Zhao *et al.*, 2010).

The activation of cells expressing ChR2-XXL under control of the *crz*-GAL4 driver line lead to a small additional peak of eclosion in the experimental group (Figure 86 A), but it could also be found in the GAL4 control (Figure 86 C). However, a clear effect of the activation of the Crz neurons on the eclosion rhythm could be seen: it was dampened compared to both controls, showed a broader distribution of eclosion and more eclosion during the warm phase (Figure 86). This effect could still be observed on the following days, although the neurons were not activated again (Figure 86 A). To further study the effect of Crz on the eclosion rhythm, the Crz neurons were ablated or silenced and the eclosion rhythm was monitored after LD entrainment. The ablation of Crz neurons by UAS-*grim* lead to reduced eclosion peaks and a broader distribution of eclosion under LD conditions (Figure 87). The same effect could be observed under DD conditions, but here it was less pronounced (Figure 88). No significant difference between the mean of the rhythmicity indices was observable under LD conditions (Figure 87 D), nor under DD conditions (Figure 88 D) or between the means of the period lengths (Figure S 27 A). Silencing the Crz neurons via UAS-*dORKΔ* lead to the same but less pronounced effect as the ablation. There were no differences between the eclosion rhythms (Figure 89, Figure 90), the rhythmicity indices (Figure 89 C, Figure 90 C) or the period lengths (Figure S 27 B) under either condition.

The ablation experiments were performed by Jana Schmitz (Schmitz, 2014) and the silencing experiments by Ruben Trapp (Trapp, 2014) , both supervised by Franziska Ruf.

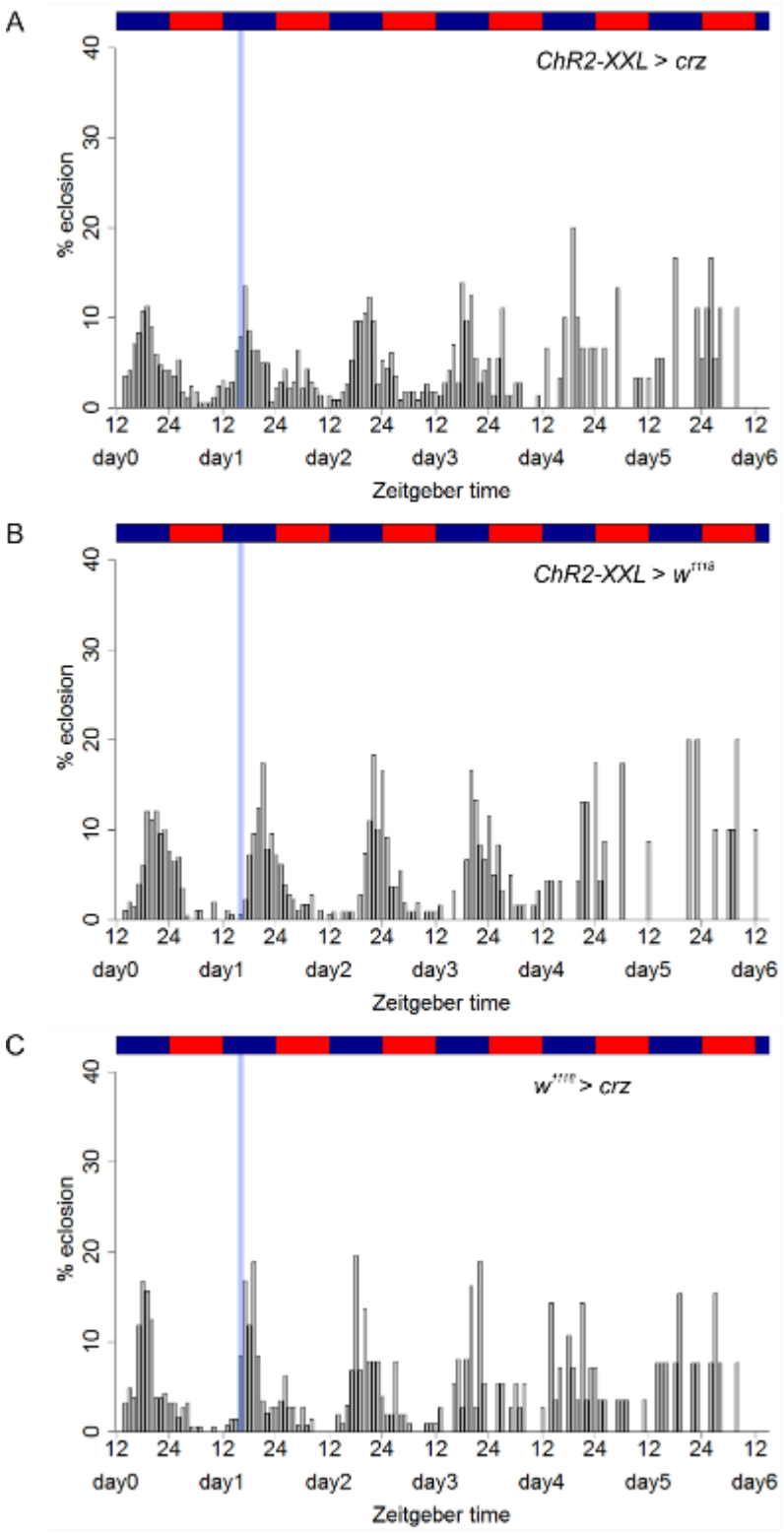

Figure 86: Eclosion rhythms after the activation of Crz-expressing neurons 6 hours before the main peak.

Eclosion profiles for populations expressing ChR2-XXL driven by *crz*-GAL4 (A) and the respective controls (B: UAS control, C: GAL4 control) under temperature entrainment (25°C:16°C). Each bar represents the percentage of eclosed flies per hour normalized to the number of eclosed flies per day. The blue and red rectangles represent the temperature regime. The blue bars mark the time point of activation with blue light. (N=3, 3, 3; n=544, 580, 511)

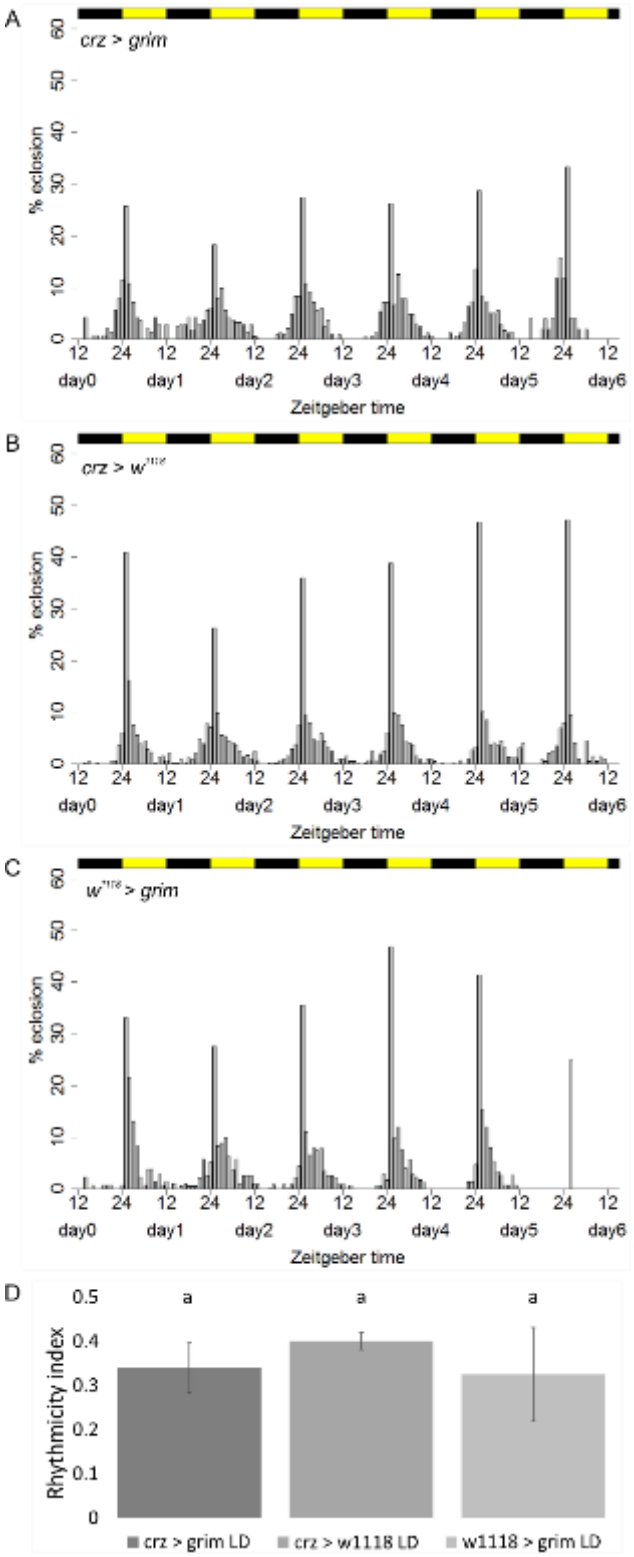

Figure 87: Eclosion rhythms after the ablation of Crz-expressing neurons under LD conditions

Eclosion profiles for populations expressing UAS-*grim* driven by *crz*-GAL4 (A) and the respective controls (B: GAL4 control, C: UAS control) under LD conditions. Each bar represents the percentage of eclosed flies per hour normalized to the number of eclosed flies per day. The black and yellow rectangles represent the light regime. (D) shows the means of the rhythmicity indices (±SD). Different letters above columns indicate significant difference ($p<0.05$). Data from Schmitz, 2014. (N=2, 3, 2; n=1354, 2569, 1755)

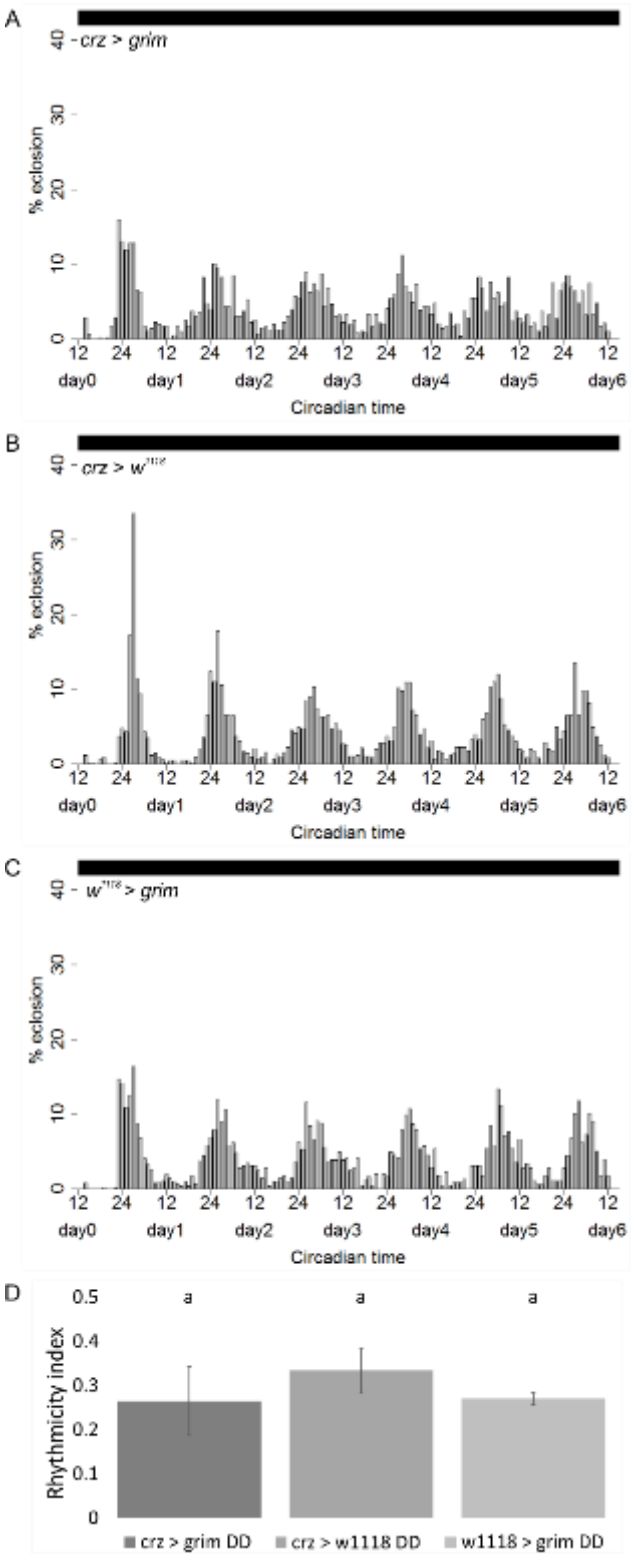

Figure 88: Eclosion rhythms after the ablation of Crz-expressing neurons under DD conditions

Eclosion profiles for populations expressing UAS-*grim* driven by *crz*-GAL4 (A) and the respective controls (B: GAL4 control, C: UAS control) under DD conditions. Each bar represents the percentage of eclosed flies per hour normalized to the number of eclosed flies per day. The black rectangles represent the light regime. (D) shows the means of the rhythmicity indices (±SD). Different letters above columns indicate significant difference ($p<0.05$). Data from Schmitz, 2014 (N=2, 3, 2; n=2011, 2388, 1612)

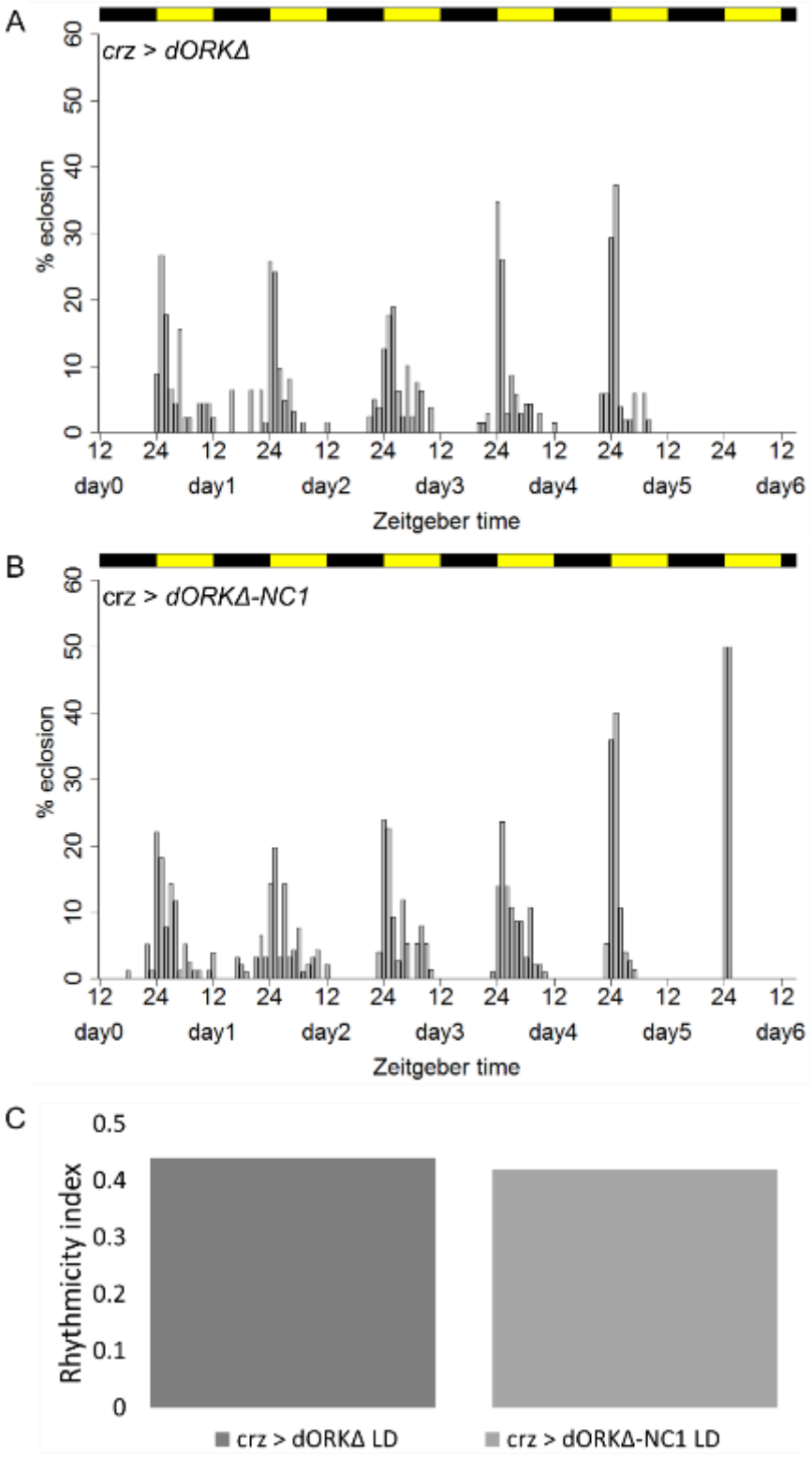

Figure 89: Eclosion rhythms after silencing Crz-expressing neurons under LD conditions
Eclosion profiles for populations expressing UAS-*dORKΔ* driven by *crz*-GAL4 (A) and the UAS-*ΔORKΔ-NC1* control (B) under LD conditions. Each bar represents the percentage of eclosed flies per hour normalized to the number of eclosed flies per day. The yellow and black rectangles represent the light regime. (C) shows the means of the rhythmicity indices (±SD). Data from Trapp, 2014. (N=1, 1; n=308, 413)

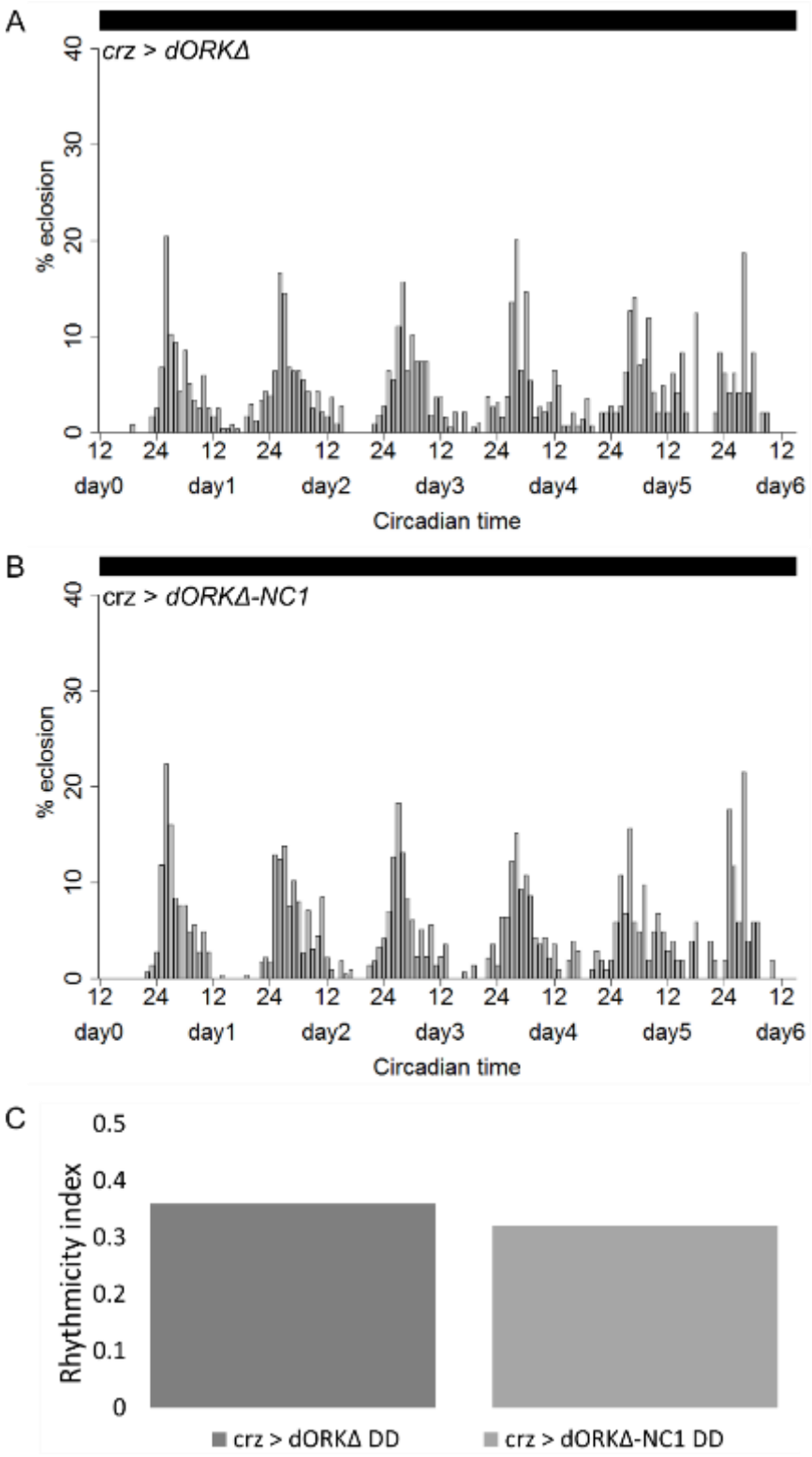

Figure 90: Eclosion rhythms after silencing Crz-expressing neurons under DD conditions
Eclosion profiles for populations expressing UAS-*dORKΔ* driven by *crz*-GAL4 (A) and the UAS-*ΔORKΔ-NC1* control (B) under DD conditions. Each bar represents the percentage of eclosed flies per hour normalized to the number of eclosed flies per day. The black rectangles represent the light regime. (C) shows the means of the rhythmicity indices (±SD). Data from Trapp, 2014. (N=1, 1; n=836, 873)

2.5 Diuretic hormone 31 (DH31)

DH31 is a diuretic peptide hormone that regulates the secretion of fluid from the Malpighian tubules (Coast *et al.*, 2001), increases gut contractions (Vanderveken and O'Donnell, 2014) and acts as a circadian wake-promoting signal (Kunst *et al.*, 2014).

The activation of cells expressing ChR2-XXL under control of the *dh31*-GAL4 driver lines did not lead to an additional peak of eclosion in the experimental group or the controls in either of the two tested lines (Figure 91, Figure 92). There was also no effect on the eclosion rhythm.

2.6 Diuretic hormone 44 (DH44)

DH44 is a diuretic peptide hormone that stimulates fluid production and secretion in Malpighian tubules of *Drosophila* via cAMP increase (Cabrero *et al.*, 2002). It was shown to play a role in the selection of nutritive sugars and the frequency of excretion (Dus *et al.*, 2015), as well as in the timing of retaining sperm from the uterus (Lee *et al.*, 2015). Furthermore, it was shown to act as a circadian output of cells of the pars intercerebralis and to be required for normal locomotor activity rhythms (Cavanaugh *et al.*, 2014).

The activation of cells expressing ChR2-XXL under control of the *dh44*-GAL4 driver lines did not lead to an additional peak of eclosion in the experimental group or the controls in either of the two tested lines (Figure 93, Figure 94). There was also no effect on the eclosion rhythm.

2.7 Dromyosuppressin (DMS)

In *Drosophila*, DMS is found in the brain, heart and gut (McCromick and Nichols, 1993) and was shown to decrease gut and heart contractions dose-dependently (Dickerson *et al.*, 2012). The knockdown of the DMS receptor decreases the velocity of locomotion in *Drosophila* (Kiss *et al.*, 2013). In *Bombyx mori*, it acts as a prothoracicostatic factor and inhibits ecdysteroidogenesis in the prothoracic gland (Yamanaka *et al.*, 2005).

The activation of cells expressing ChR2-XXL under control of the *dms*-GAL4 driver line lead to distinct additional eclosion peaks (Figure 95 A). This was also observed in the GAL4 control on the third day (Figure 95 C), but not in any of the remaining controls (Figure 95 B). The effect of activation was strongest on the first and third day, with the additional eclosion peak surmounting the expected eclosion peak, but was also clearly distinguishable on the successive days (Figure 95 A).

Although the activation through blue light had no influence on the eclosion rhythm, ablation experiments using UAS-*grim* were conducted to investigate the influence of DMS on the

rhythmicity of eclosion. The ablation of the DMS-expressing cells did however not influence the rhythms eclosion profiles, neither under LD conditions (Figure 96) nor under DD conditions (Figure 97). There was only a significant difference between the means of the rhythmicity indices of the two controls under LD conditions, but not between the experimental crossing and the two controls (Figure 96 D). Under DD conditions, there were no differences between the means of the rhythmicity indices (Figure 97 D) or the period lengths (Figure S 28).

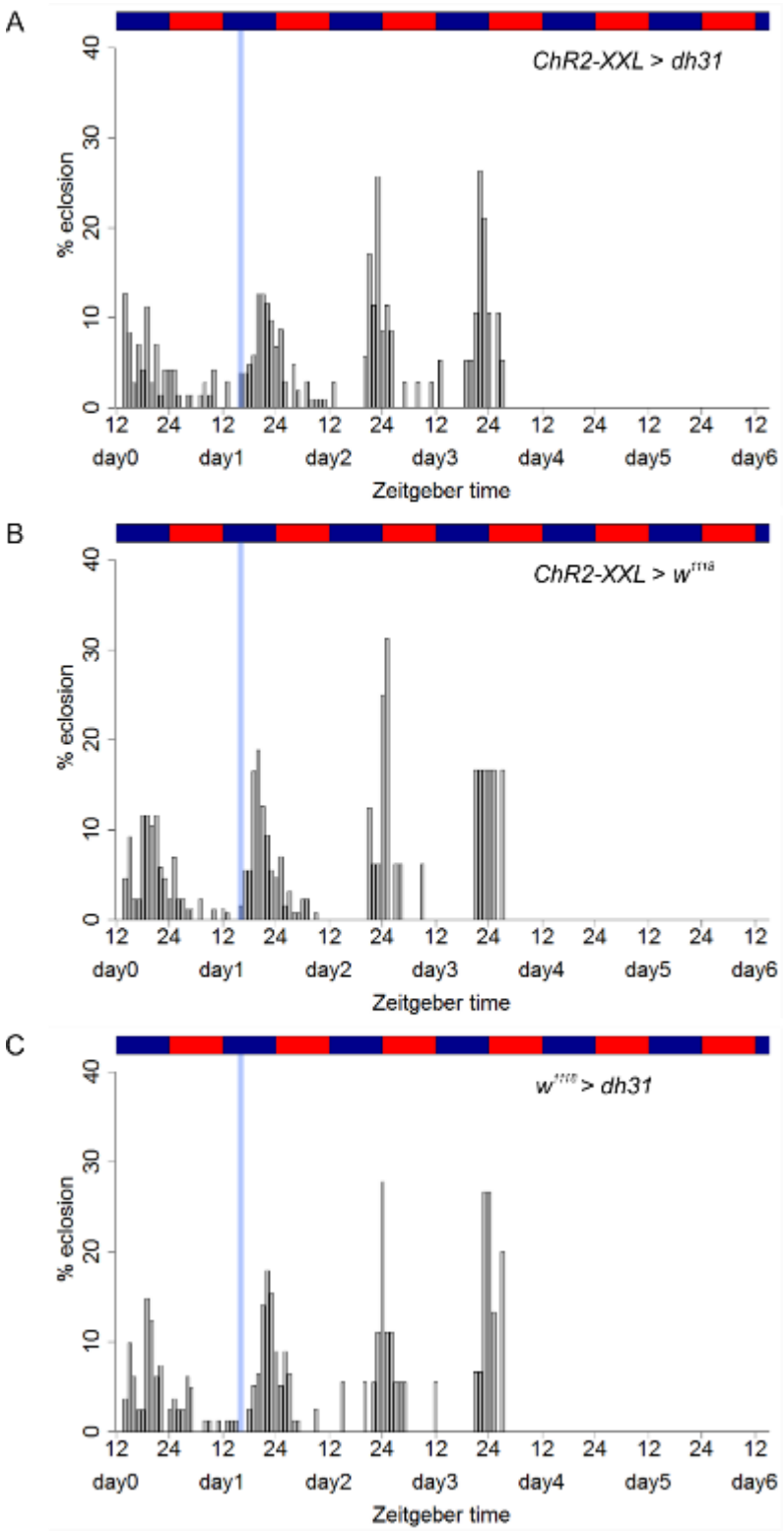

Figure 91: Eclosion rhythms after the activation of DH31-expressing neurons 6 hours before the main peak.

Eclosion profiles for populations expressing ChR2-XXL driven by *dh31*-GAL4 (#51988) (A) and the respective controls (B: UAS control, C: GAL4 control) under temperature entrainment (25°C:16°C). Each bar represents the percentage of eclosed flies per hour normalized to the number of eclosed flies per day. The blue and red rectangles represent the temperature regime. The blue bars mark the time point of activation with blue light. (N=2, 2, 2; n=228, 235, 192)

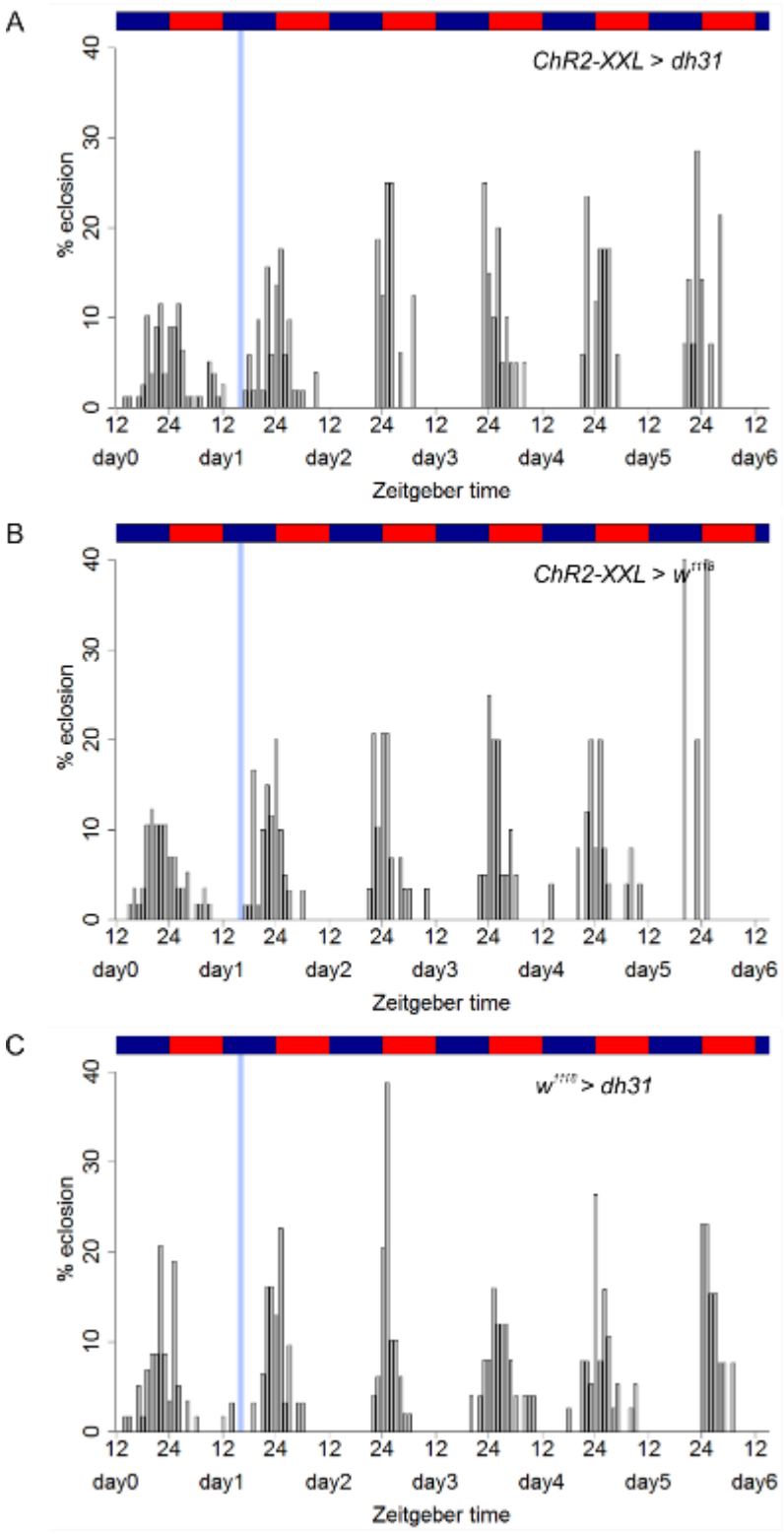

Figure 92: Eclosion rhythms after the activation of DH31-expressing neurons 6 hours before the main peak.

Eclosion profiles for populations expressing ChR2-XXL driven by *dh31*-GAL4 (#51989) (A) and the respective controls (B: UAS control, C: GAL4 control) under temperature entrainment (25°C:16°C). Each bar represents the percentage of eclosed flies per hour normalized to the number of eclosed flies per day. The blue and red rectangles represent the temperature regime. The blue bars mark the time point of activation with blue light. (N=2, 2, 2; n=196, 196, 214)

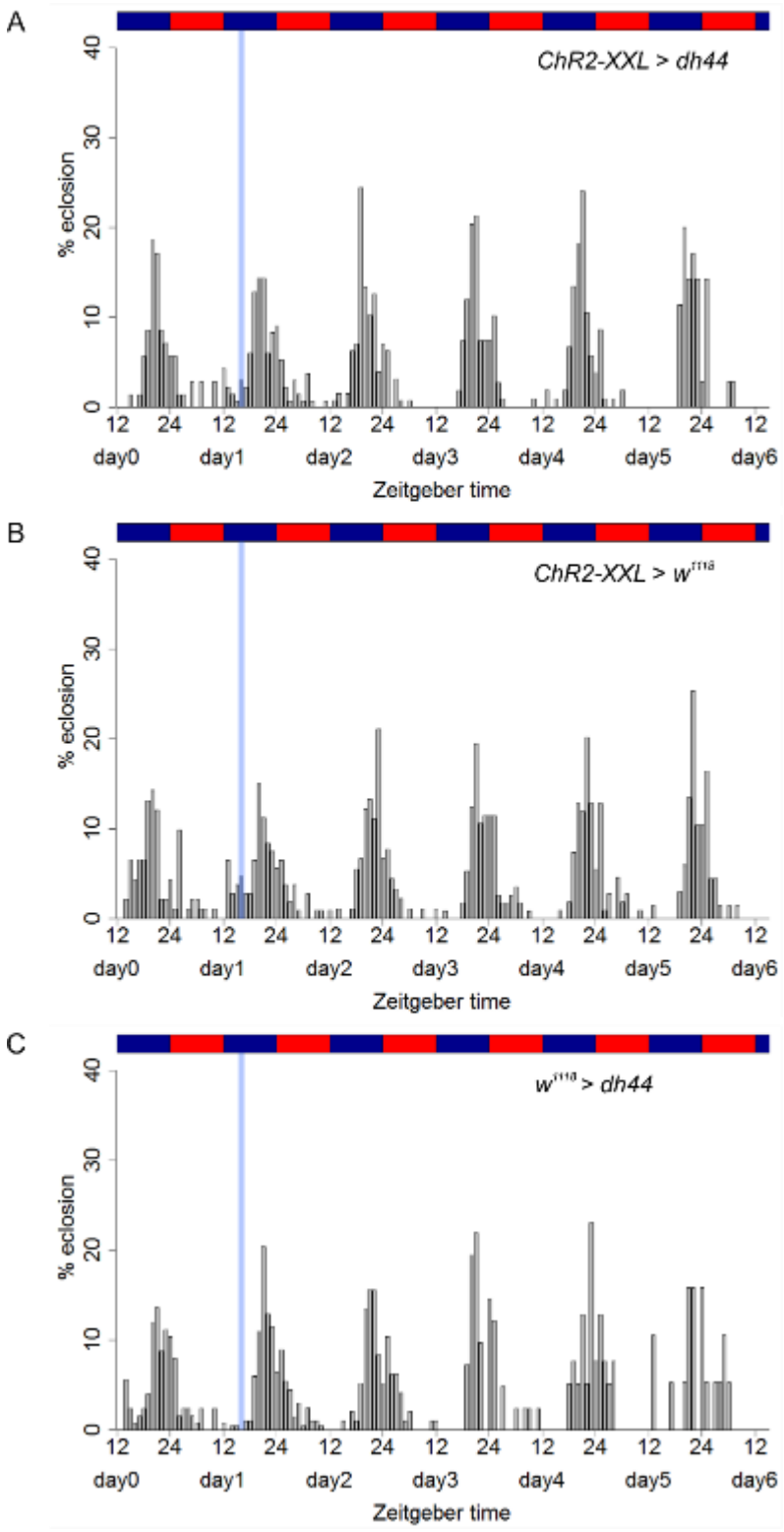

Figure 93: Eclosion rhythms after the activation of DH44-expressing neurons 6 hours before the main peak.

Eclosion profiles for populations expressing ChR2-XXL driven by *dh44*-GAL4 (#39347) (A) and the respective controls (B: UAS control, C: GAL4 control) under temperature entrainment (25°C:16°C). Each bar represents the percentage of eclosed flies per hour normalized to the number of eclosed flies per day. The blue and red rectangles represent the temperature regime. The blue bars mark the time point of activation with blue light. (N=3, 3, 3; n=576, 577, 521)

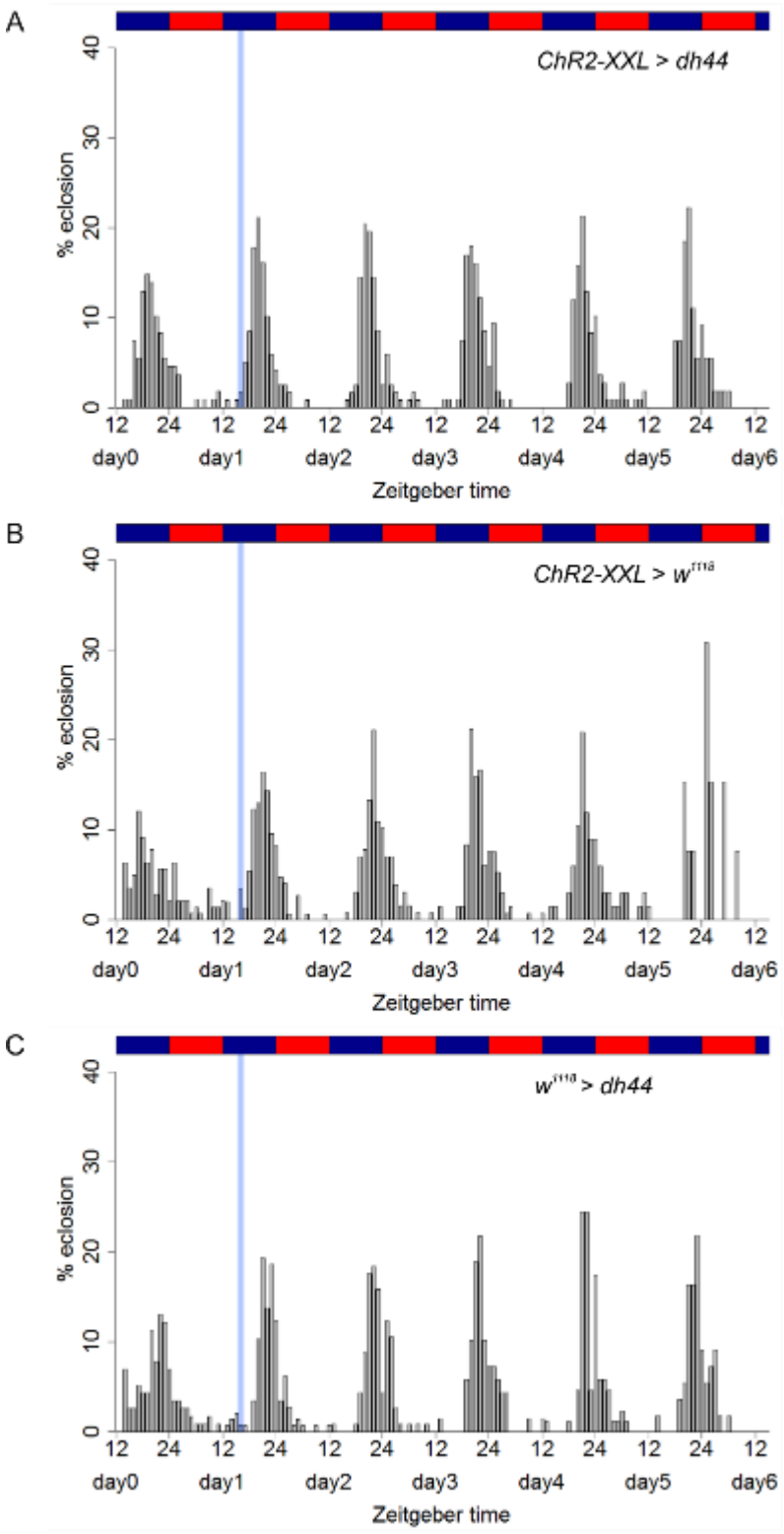

Figure 94: Eclosion rhythms after the activation of DH44-expressing neurons 6 hours before the main peak.

Eclosion profiles for populations expressing ChR2-XXL driven by *dh44*-GAL4 (VT039046) (A) and the respective controls (B: UAS control, C: GAL4 control) under temperature entrainment (25°C:16°C). Each bar represents the percentage of eclosed flies per hour normalized to the number of eclosed flies per day. The blue and red rectangles represent the temperature regime. The blue bars mark the time point of activation with blue light. (N=3, 3, 3; n=611, 627, 584)

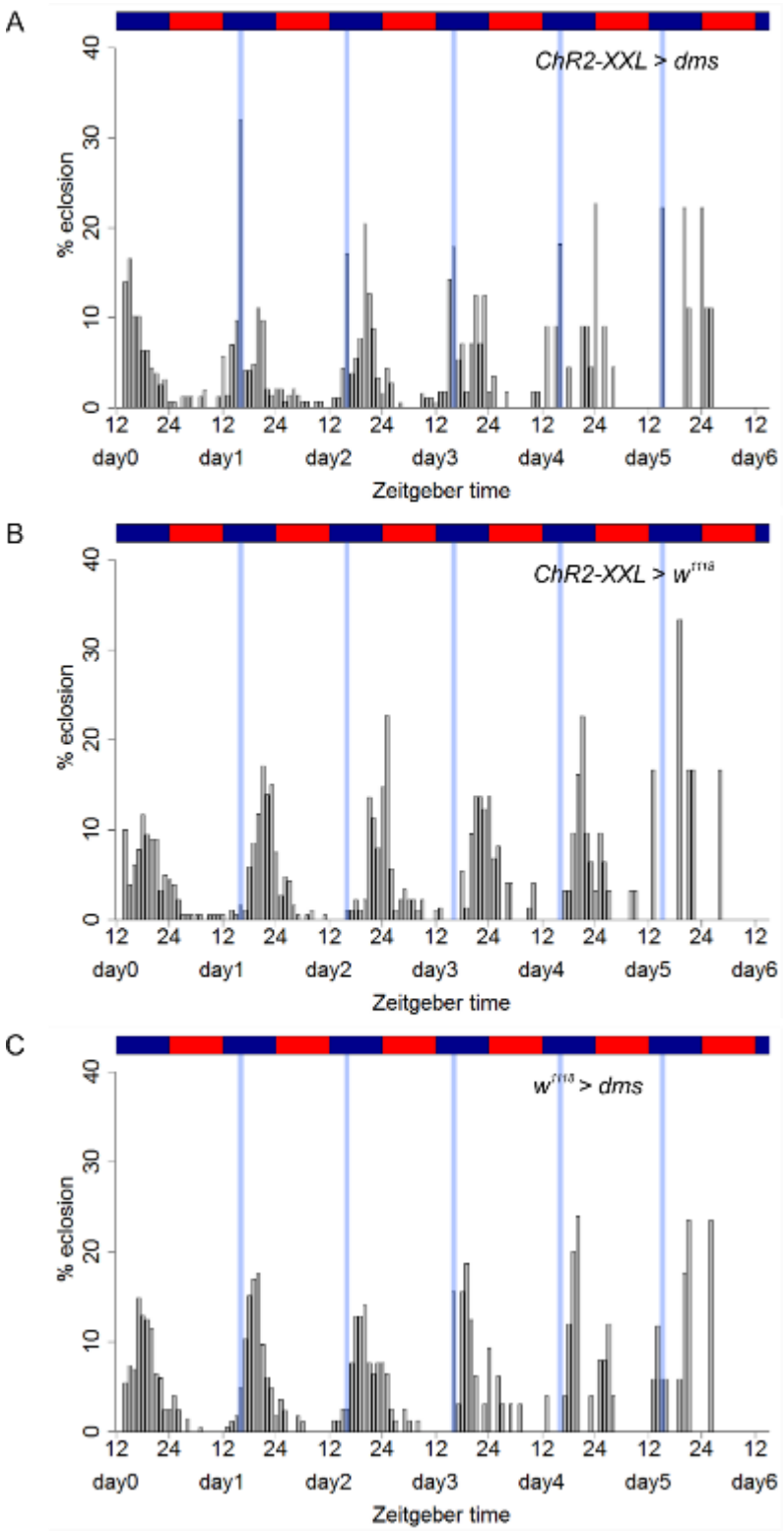

Figure 95: Eclosion rhythms after frequent repeats of the light-induced activation of DMS-expressing neurons 6 hours before the main peak.
Eclosion profiles for populations expressing ChR2-XXL driven by *dms*-GAL4 (A) and the respective controls (B: UAS control, C: GAL4 control) under temperature entrainment. Each bar represents the percentage of eclosed flies per hour normalized to the number of eclosed flies per day. The blue and red rectangles represent the temperature regime (25°C:16°C). The blue bars mark the time points of activation with blue light. (N=3, 3, 3; n=569, 564, 518)

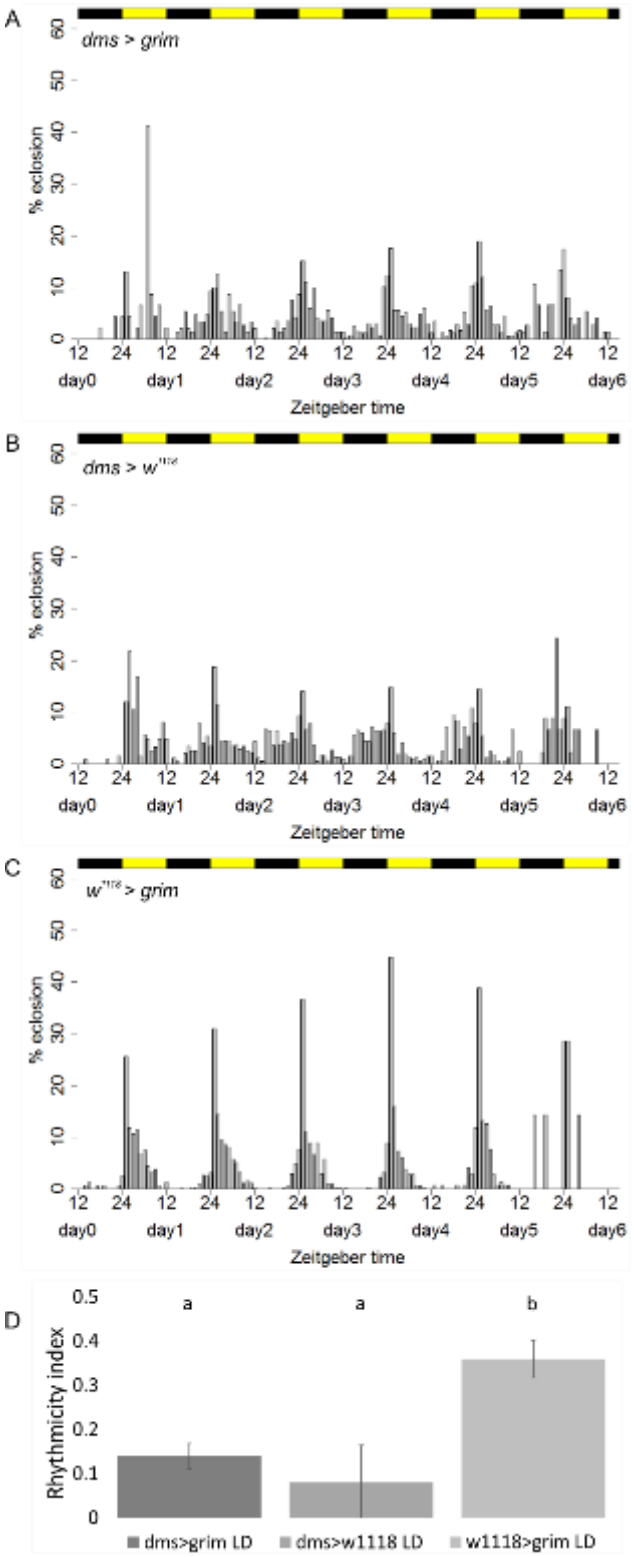

Figure 96: Eclosion rhythms after the ablation of DMS-expressing neurons under LD conditions

Eclosion profiles for populations expressing UAS-*grim* driven by *dms*-GAL4 (A) and the respective controls (B: GAL4 control, C: UAS control) under LD conditions. Each bar represents the percentage of eclosed flies per hour normalized to the number of eclosed flies per day. The black and yellow rectangles represent the light regime. (D) shows the means of the rhythmicity indices (±SD). Different letters above columns indicate significant difference ($p<0.05$). (N=2, 2, 2; n=1018, 1451, 1199)

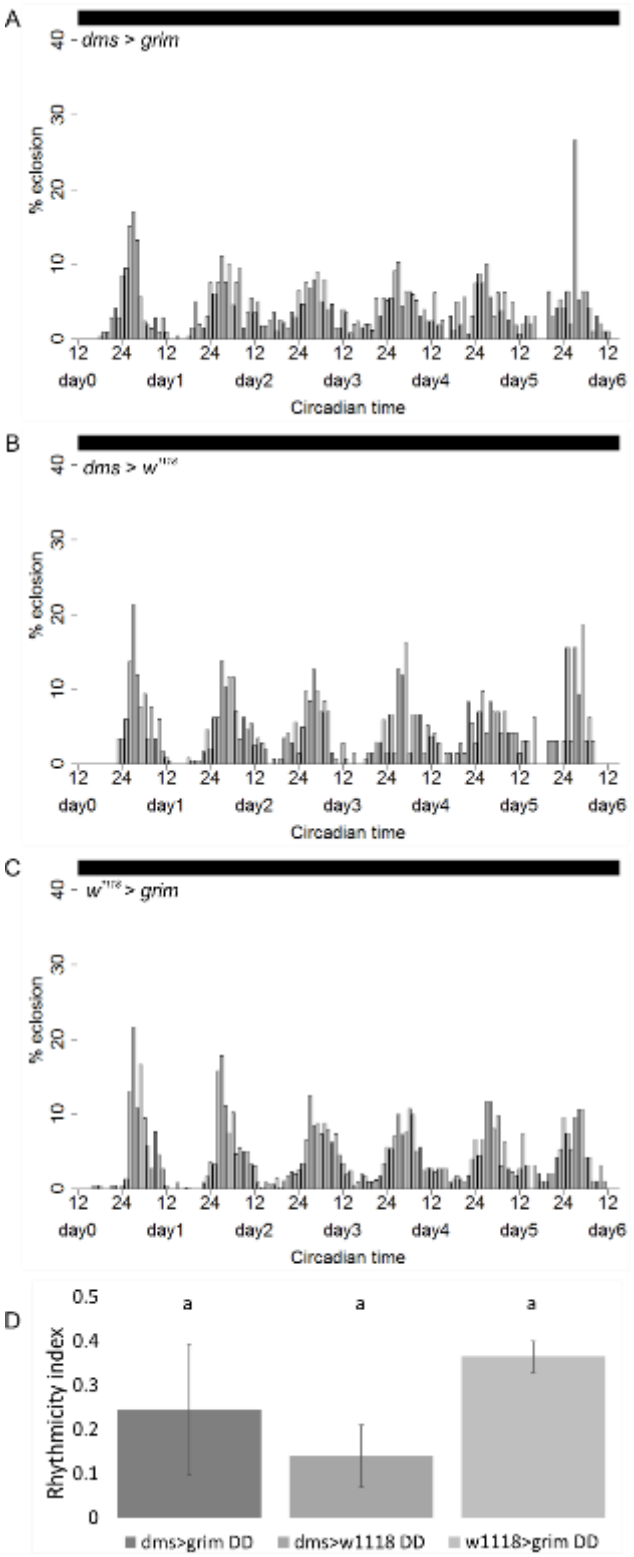

Figure 97: Eclosion rhythms after the ablation of DMS-expressing neurons under DD conditions

Eclosion profiles for populations expressing UAS-*grim* driven by *dms*-GAL4 (A) and the respective controls (B: GAL4 control, C: UAS control) under DD conditions. Each bar represents the percentage of eclosed flies per hour normalized to the number of eclosed flies per day. The black rectangles represent the light regime. (D) shows the means of the rhythmicity indices (±SD). Different letters above columns indicate significant difference ($p<0.05$). (N=2, 2, 2; n=1210, 741, 1666)

2.8 Eclosion hormone (EH)

EH was first discovered in transplantation experiments in silkworms as the hormonal factor that is released from the brain to induce the ecdysis motor behavior (Truman and Riddiford, 1970). In *Drosophila*, EH is produced in a single neuron pair in the cerebral ganglia called VM cells that have terminations on the corpora cardiaca of the ring gland (Horodyski *et al.*, 1993). EH is a main peptide hormone initiating the peptide cascade that orchestrates ecdysis motor behavior, which starts with the release of ETH from the Inka cells. ETH induces the release of EH from the VM neurons in the brain which leads to further and complete release of ETH. ETH and EH together induce the secretion of further peptides, especially CCAP, that initiate the ecdysis behavior (Ewer, 2005). Regarding the exact function of EH in *Drosophila*, partly contradictory studies were reported: while the ablation of EH neurons lead to the survival of one third of the animals into adults (McNabb *et al.*, 1997b), *Eh* null mutants were lethal in early larval stages (Krüger *et al.*, 2015). It is however clear that EH neurons are needed for the lights-on response in eclosion (McNabb and Truman, 2008). EH also regulates the responsiveness of other target cells to ETH, as in animals without EH neurons ETH is not released and its injection does not induce ecdysis (McNabb *et al.*, 1997b; Krüger *et al.*, 2015). The activation of cells expressing ChR2-XXL under control of the *Eh*-GAL4 driver line lead to an additional peak of eclosion (Figure 98 A) which could not be seen in the controls (Figure 98 B, Figure 98 C). This peak, however, was not as pronounced as could be expected. The effect of activating the EH neurons seems to be weaker than the effect of activation of the ETH cells (Figure 81 A). There was no effect on the eclosion rhythm compared to the controls and viability was not impeded. To investigate the effect of EH on eclosion rhythmicity, EH neurons were silenced using UAS-*dORKΔ* driven by the *Eh*-GAL4 driver. Silencing the EH neurons lead to a broader distribution of the eclosion events and less defined eclosion peaks (Figure 99 A) compared to the control (Figure 99 B) under DD conditions. However, no significant differences between the means of the rhythmicity indices (Figure 99 C) or period lengths (Figure S 29) were observed, although there was a trend to reduced rhythmicity indices in the experimental flies (Figure 99 C).

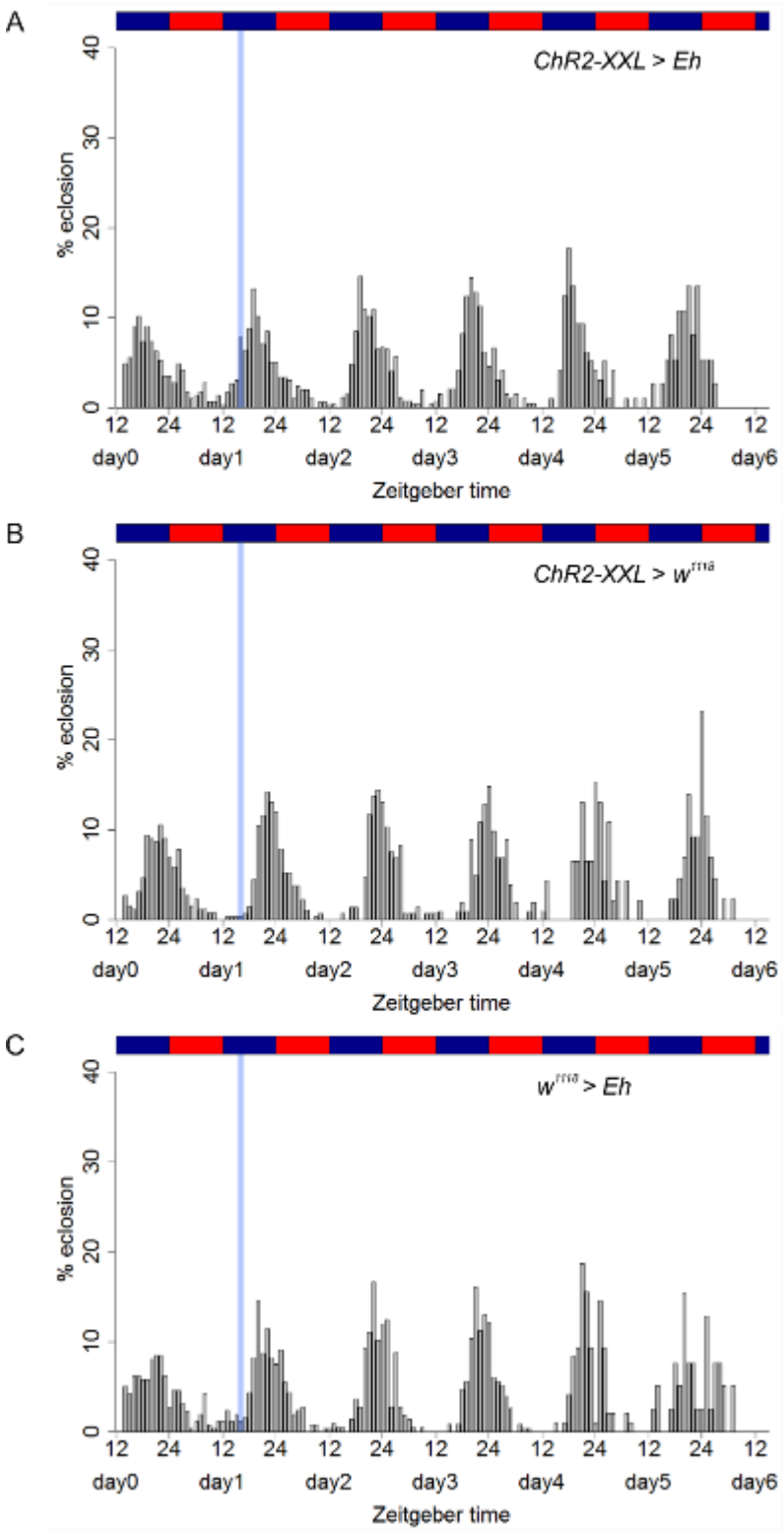

Figure 98: Eclosion rhythms after the activation of EH-expressing neurons 6 hours before the main peak.

Eclosion profiles for populations expressing ChR2-XXL driven by *Eh*-GAL4 (A) and the respective controls (B: UAS control, C: GAL4 control) under temperature entrainment (25°C:16°C). Each bar represents the percentage of eclosed flies per hour normalized to the number of eclosed flies per day. The blue and red rectangles represent the temperature regime. The blue bars mark the time points of activation with blue light. (N=6, 6, 6; 1152, 857, 1093)

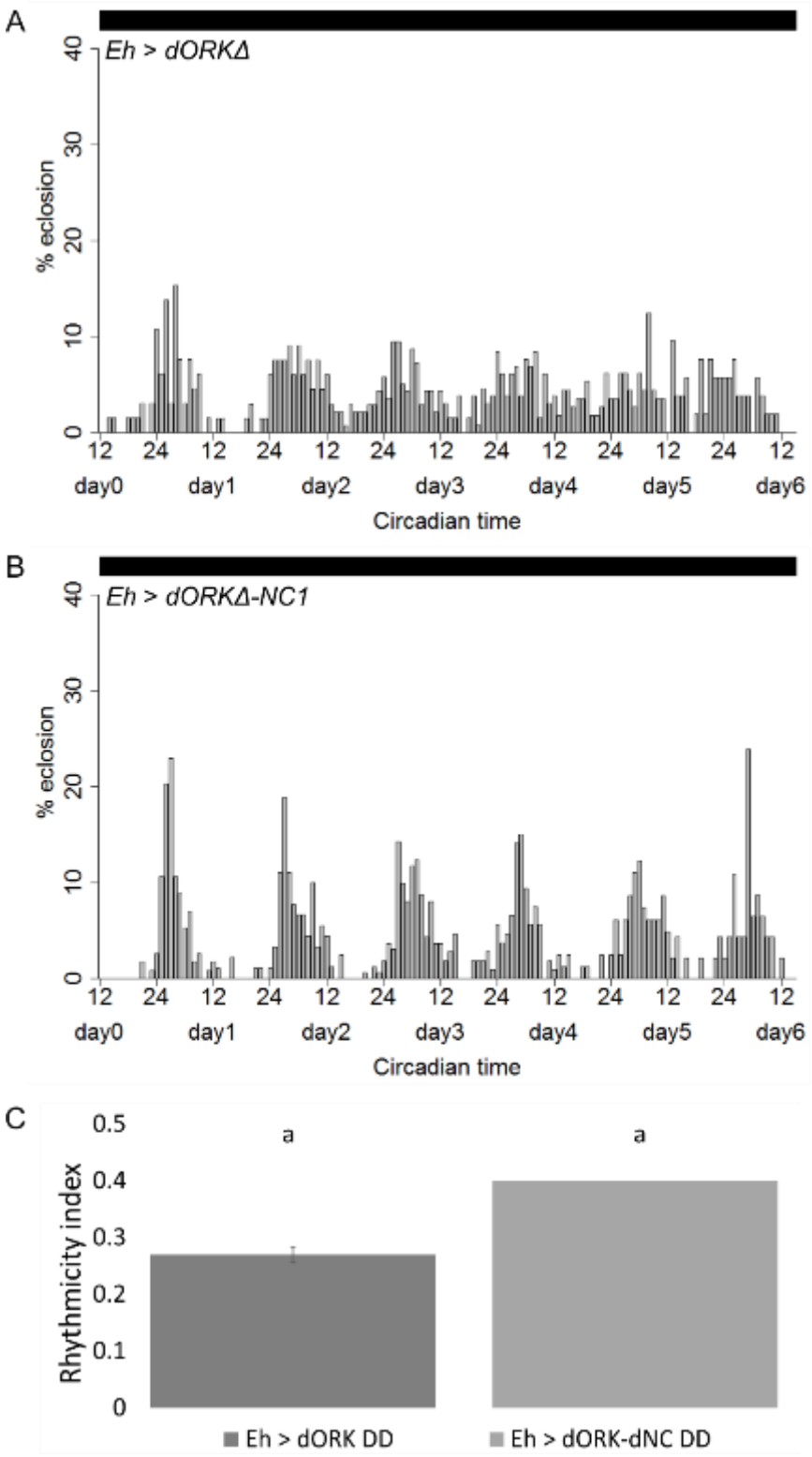

Figure 99: Eclosion rhythms after silencing EH-expressing neurons under DD conditions
Eclosion profiles for populations expressing UAS-*dORKΔ* driven by *Eh*-GAL4 (A) and the UAS-*ΔORKΔ-NC1* control (B) under DD conditions. Each bar represents the percentage of eclosed flies per hour normalized to the number of eclosed flies per day. The black rectangles represent the light regime. (C) shows the means of the rhythmicity indices (±SD). Different letters above columns indicate significant difference ($p<0.05$). (N=2, 1; n=567, 597)

2.9 Hugin (hug)

Hug was discovered in a genetic screen in *Drosophila* as a propeptide that encodes for one pyrokinin (PK). Hug-PK has a myostimulatory effect on the *Drosophila* heart muscle (Meng *et al.*, 2002) and plays a role as modulator in chemosensory signal-dependent feeding behavior (Melcher and Pankratz, 2005). Ectopic expression of hug resulted in larval death, mostly around the ecdysis from second to third instar (Meng *et al.*, 2002).

The activation of cells expressing ChR2-XXL under control of the *hug*-GAL4 driver line did not lead to an additional peak of eclosion in the experimental group or the controls. There was also no effect on the eclosion rhythm (Figure 100).

2.10 Mai316

The *Mai316*-GAL4 line was created by mobilizing an enhancer-trap element in a screen for neurons innervating the ring gland. It comprises expression in PG-LPs (prothoracic gland innervating neurosecretory neurons of the lateral protocerebrum = PTTH neurons), the EH expressing VM cells, CC-MS2 (corpora cardiaca innvervating neurosecretory neurons of the medial subesophageal ganglion 2 = CAPA neurons) and sPDFMe (small pigment dispersing factor neurons in the medulla = sLNvs) (Siegmund and Korge, 2001).

The activation of cells expressing ChR2-XXL under control of the *Mai316*-GAL4 driver line did not lead to an additional peak of eclosion in the experimental group or the controls. Also, an effect on the eclosion rhythm was not detectable (Figure 101).

Ablation of Mai316 neurons using UAS-*grim* lead to severe developmental defects. Only few L1 larvae were visible, but the majority of animals was not able to hatch out of the egg. Therefore it was impossible to monitor the eclosion timing of these flies.

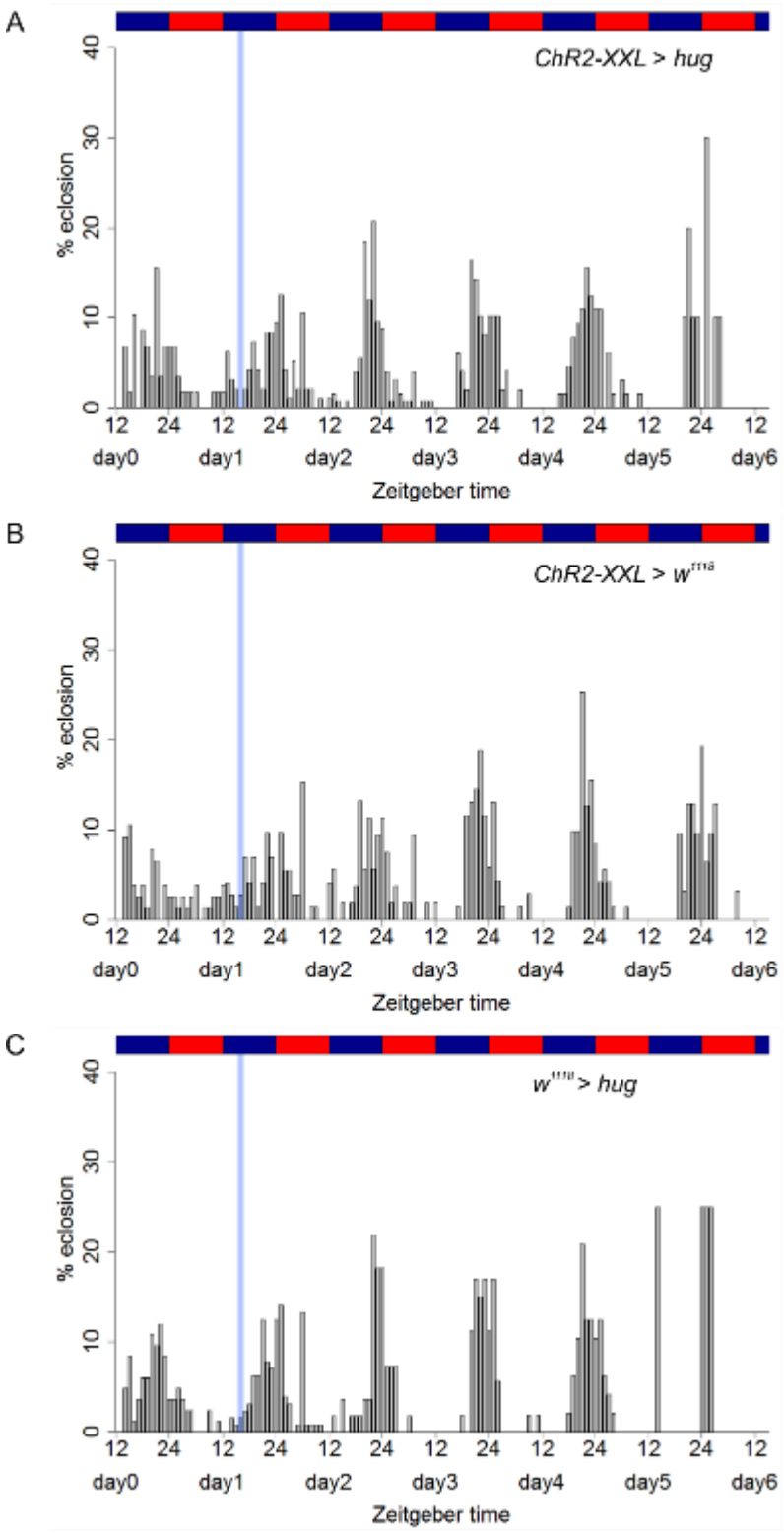

Figure 100: Eclosion rhythms after the activation of hug-expressing neurons 6 hours before the main peak.

Eclosion profiles for populations expressing ChR2-XXL driven by *hug*-GAL4 (A) and the respective controls (B: UAS control, C: GAL4 control) under temperature entrainment (25°C:16°C). Each bar represents the percentage of eclosed flies per hour normalized to the number of eclosed flies per day. The blue and red rectangles represent the temperature regime. The blue bars mark the time points of activation with blue light. (N=3, 3, 3; n=401, 372, 371)

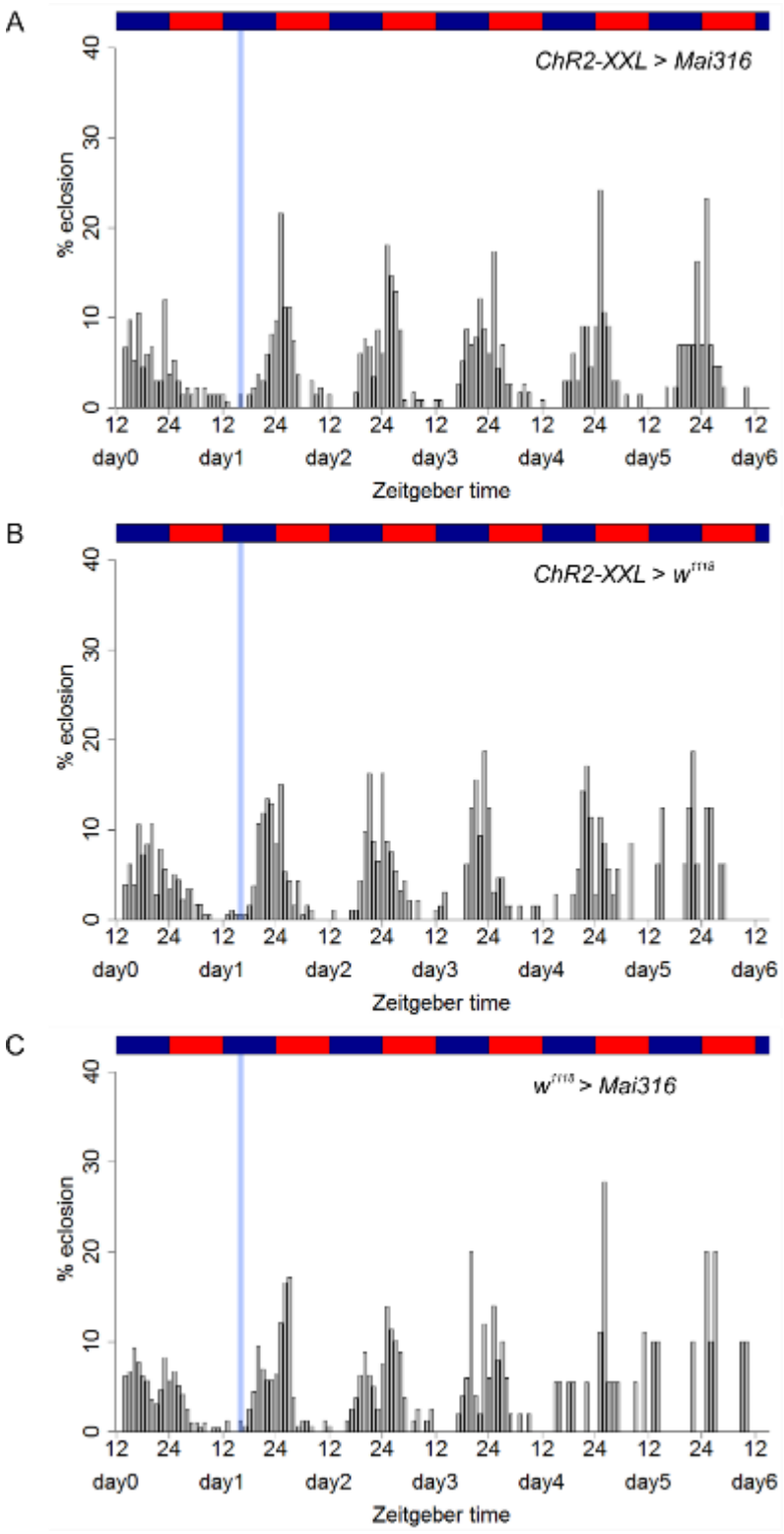

Figure 101: Eclosion rhythms after the activation of Mai316 neurons 6 hours before the main peak.

Eclosion profiles for populations expressing ChR2-XXL driven by *Mai316*-GAL4 (A) and the respective controls (B: UAS control, C: GAL4 control) under temperature entrainment (25°C:16°C). Each bar represents the percentage of eclosed flies per hour normalized to the number of eclosed flies per day. The blue and red rectangles represent the temperature regime. The blue bars mark the time points of activation with blue light. (N=2, 2, 2; n=613, 573, 511)

2.11 Myoinhibitory Peptide (MIP)

MIPs, also termed B-type allatostatins, were first discovered in *Locusta micgratoria* as suppressors of the spontaneous contractions of the hindgut and oviduct (Schoofs *et al.*, 1991). The *mip* gene encodes for five MIPs in *Drosophila* and is expressed in the CNS and the gut (Williamson *et al.*, 2001). The CCAP/MIP neurons play an important role in the initiation and execution of the ecdysis motor behavior (Kim *et al.*, 2006a; Kim *et al.*, 2006b). In *Bombyx mori*, the expression of the MIP receptor in the PG is coupled to the titers of ecdysteroids, implying a role in the fine-tuning of ecdysteroid production (Yamanaka *et al.*, 2005).

The activation of cells expressing ChR2-XXL under control of the *mip*-GAL4 driver line lead to distinct additional eclosion peaks (Figure 102 A) which could not be seen in the controls (Figure 102 B, C). The expected peak was less pronounced than the peaks of the following days (Figure 102 A). There was no effect of activation through blue light on the eclosion rhythm (Figure 102).

To verify the effect of the activation of MIP expressing neurons, the *mip*-GAL4 line was combined with the *nSyb*GAL80 line. Here, ChR2-XXL should be expressed only in cells that are not in the central or peripheral nervous system, like for example midgut cells (Nässel and Winther, 2010; Harris *et al.*, 2015). Activation of ChR2-XXL only in peripheral cells did not lead to an additional eclosion peak any more (Figure 103).

2.12 Neuropeptide F (NPF)

NPFs are similar to the vertrebrate neuropeptide Y (NPY) and are expressed in interneurons of the brain and enteroendocrine cells of the gut in *Drosophila* (Brown *et al.*, 1999). Males additionally express NPF in a subset of the LNds, and males mutant for *npf* exhibit reduced courtship activity, indicating a role in a clock-controlled sexual dimorphism (Lee *et al.*, 2006). NPF has diverse functions that are reviewed in Nässel and Wegener (2011).

The activation of cells expressing ChR2-XXL under control of the *npf*-GAL4 driver line did not lead to an additional peak of eclosion in the experimental group or the controls and had no effect on the eclosion rhythm (Figure 104).

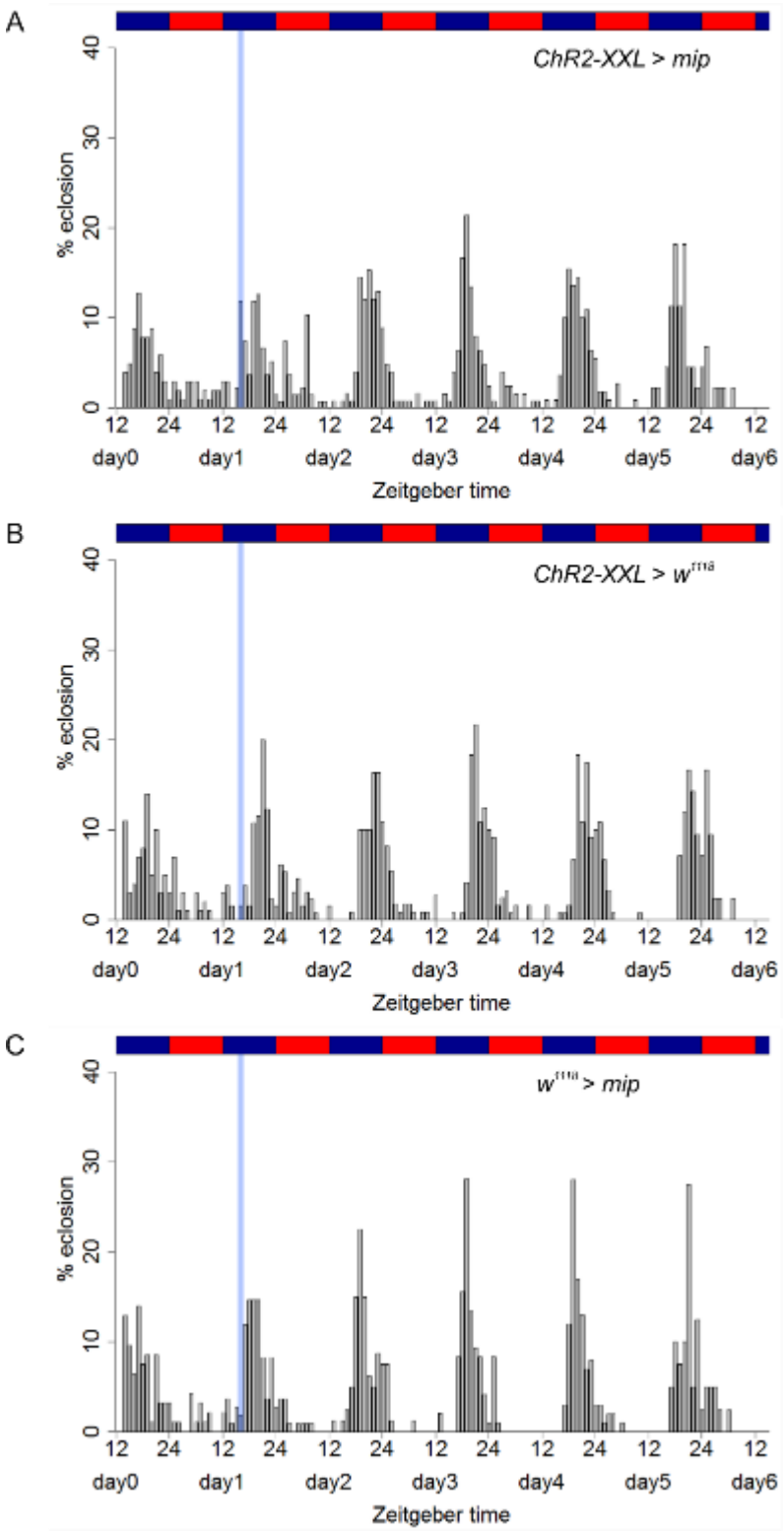

Figure 102: Eclosion rhythms after the activation of MIP-expressing neurons 6 hours before the main peak.

Eclosion profiles for populations expressing ChR2-XXL driven by *mip*-GAL4 (A) and the respective controls (B: UAS control, C: GAL4 control) under temperature entrainment (25°C:16°C). Each bar represents the percentage of eclosed flies per hour normalized to the number of eclosed flies per day. The blue and red rectangles represent the temperature regime. The blue bars mark the time points of activation with blue light. (N=3, 3, 3; n=641, 622, 518)

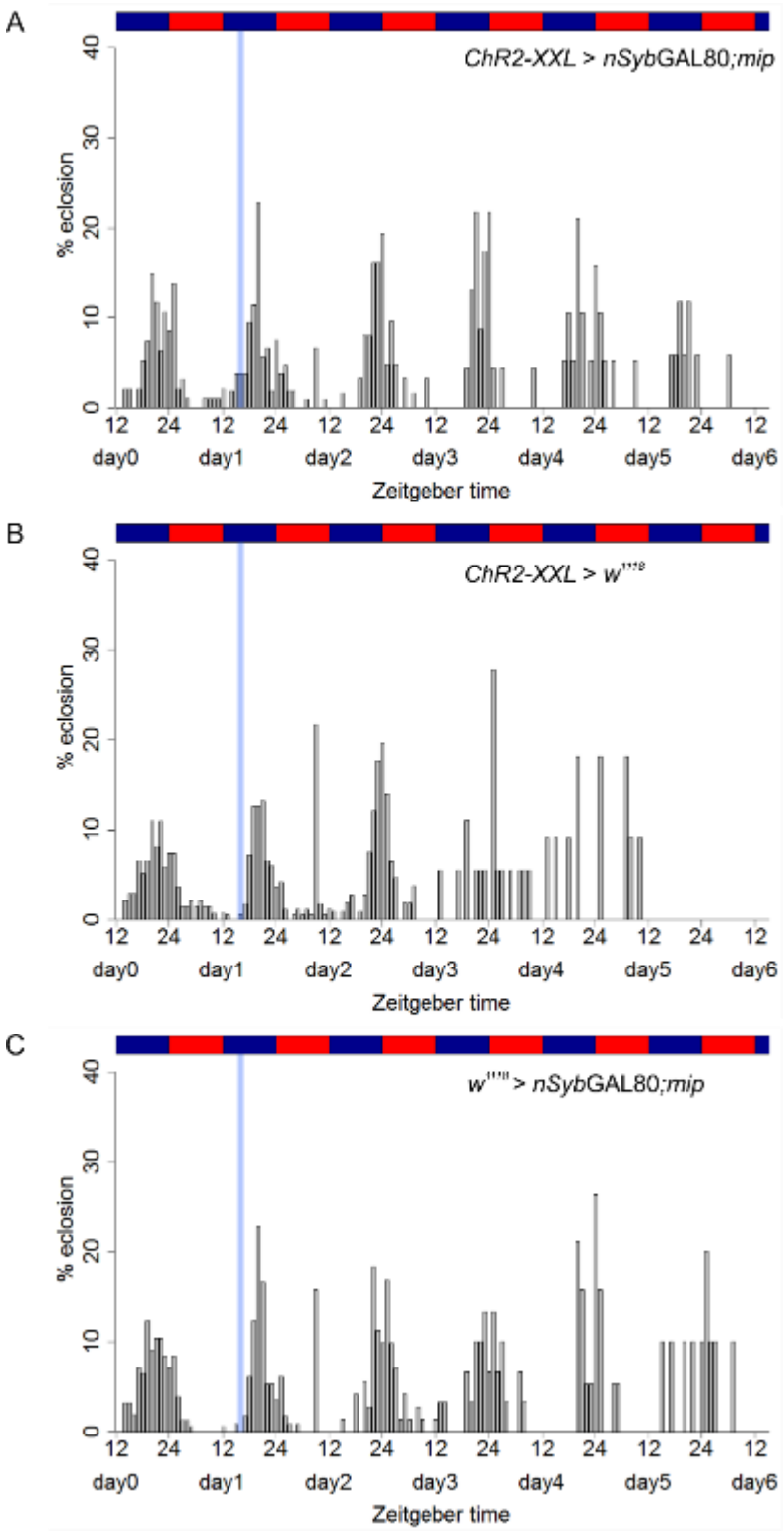

Figure 103: Eclosion rhythms after the activation of nSybGAL80; MIP-expressing neurons 6 hours before the main peak.

Eclosion profiles for populations expressing ChR2-XXL driven by *nSyb*GAL80; *mip*-GAL4 (A) and the respective controls (B: UAS control, C: GAL4 control) under temperature entrainment (25°C:16°C). Each bar represents the percentage of eclosed flies per hour normalized to the number of eclosed flies per day. The blue and red rectangles represent the temperature regime. The blue bars mark the time points of activation with blue light. (N=3, 3, 3; n=320, 442, 398)

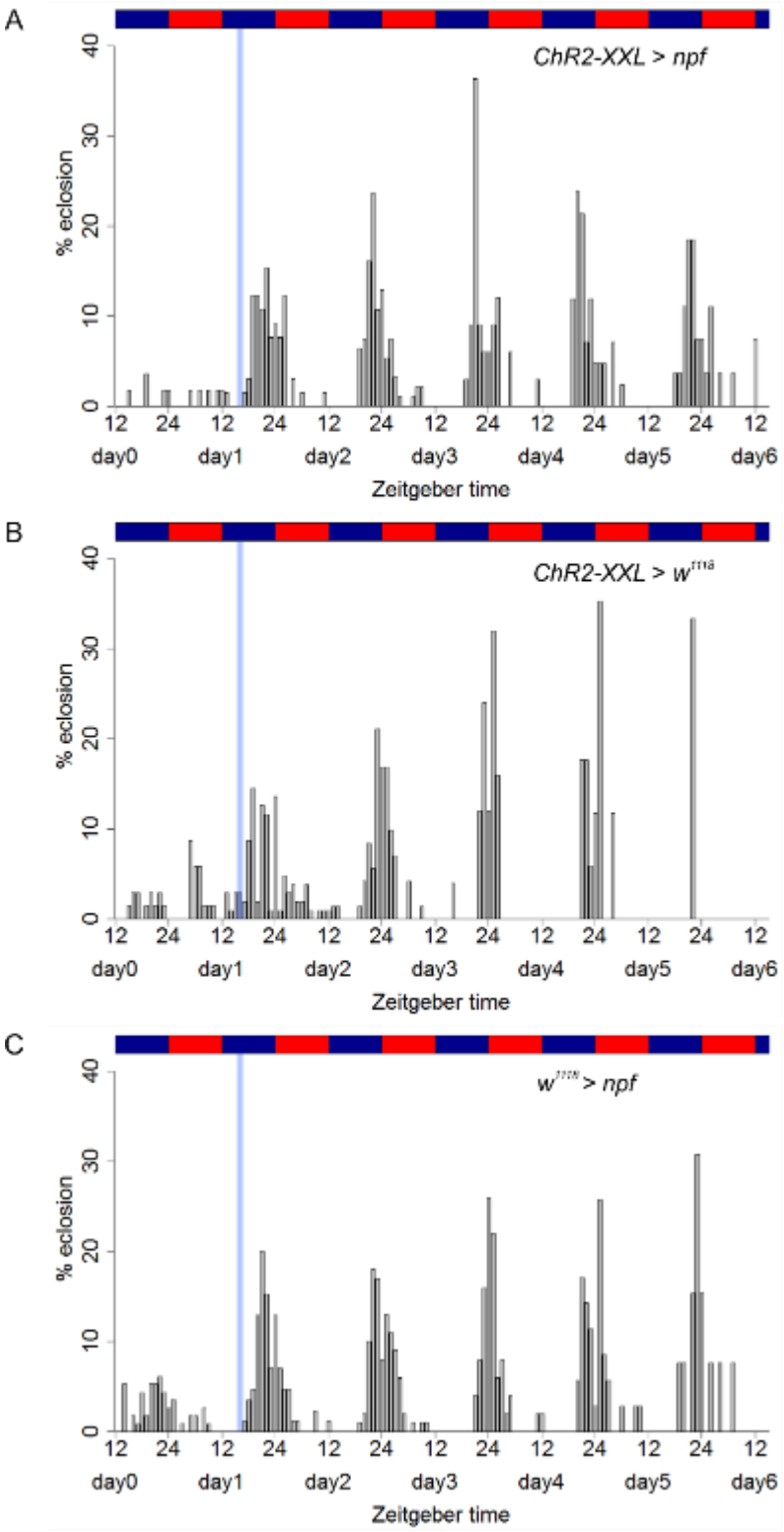

Figure 104: Eclosion rhythms after the activation of NPF-expressing neurons 6 hours before the main peak.

Eclosion profiles for populations expressing ChR2-XXL driven by *npf*-GAL4 (A) and the respective controls (B: UAS control, C: GAL4 control) under temperature entrainment (25°C:16°C). Each bar represents the percentage of eclosed flies per hour normalized to the number of eclosed flies per day. The blue and red rectangles represent the temperature regime. The blue bars mark the time points of activation with blue light. (N=3, 3, 3; n=315, 288, 397)

2.13 Pigment dispersing factor (PDF)

PDF is the main output factor of the clock cells in the brain (Renn *et al*., 1999; Helfrich-Förster *et al.*, 2000). For a detailed description of PDF and its functions see Chapter 2.4 in the Introductions.

The activation of cells expressing ChR2-XXL under control of the *pdf*-GAL4 driver line did not lead to an additional peak of eclosion in the experimental group or the controls. Additionally, no effect on the eclosion rhythm was found (Figure 105).

2.14 Phantom (Phm) / Ecdysone

Phm is one of the Halloween genes, P450 enzymes that mediate the biosynthesis of ecdysteroids from cholesterol in the PG. Ecdysone is released from the PG and in a last step converted into its active form 20-hydroxyecdysone (20E) right at the target tissue (Rewitz *et al.*, 2006b). The production of ecdysone is induced by PTTH that is secreted from the brain upon environmental stimuli (Vedeckis *et al.*, 1976; Bollenbacher *et al.*, 1979)

The activation of cells expressing ChR2-XXL under control of the *phm*-GAL4 driver line did not lead to an additional peak of eclosion in the experimental group or the controls. The eclosion rhythm was slightly shifted earlier compared to the controls (Figure 106).

2.15 Prothoracicotropic hormone (PTTH)

PTTH regulates the production and release of ecdysteroids from the PG (Vedeckis *et al.*, 1976; Bollenbacher *et al.*, 1979). For a detailed description of PTTH and its functions see Chapter III.

The activation of cells expressing ChR2-XXL under control of the *ptth*-GAL4 driver line did not lead to an additional peak of eclosion in the experimental group or the controls. There was also no effect on eclosion rhythmicity (Figure 107).

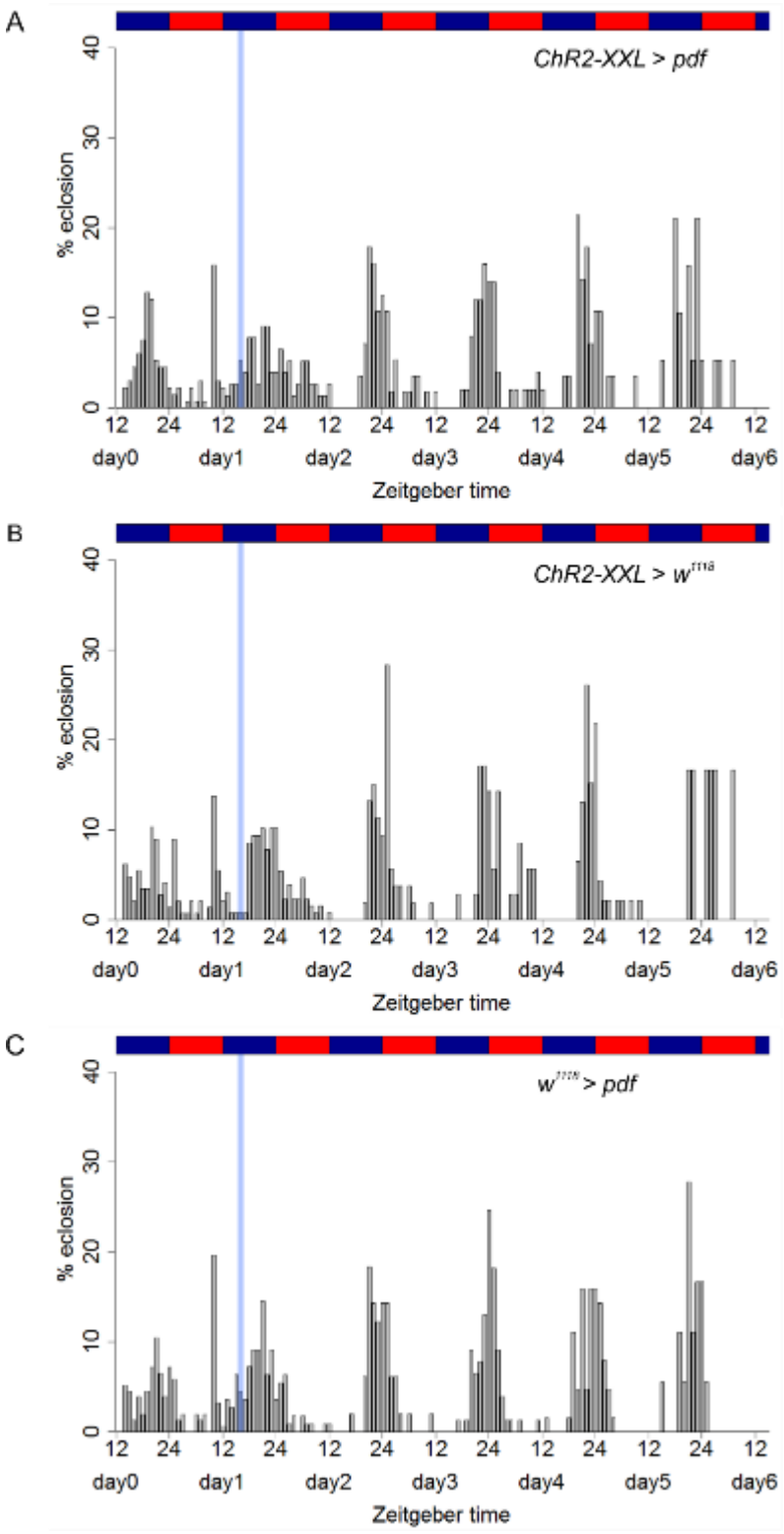

Figure 105: Eclosion rhythms after the activation of PDF-expressing neurons 6 hours before the main peak.

Eclosion profiles for populations expressing ChR2-XXL driven by *pdf*-GAL4 (A) and the respective controls (B: UAS control, C: GAL4 control) under temperature entrainment (25°C:16°C). Each bar represents the percentage of eclosed flies per hour normalized to the number of eclosed flies per day. The blue and red rectangles represent the temperature regime. The blue bars mark the time points of activation with blue light. (N=4, 4, 4; n=362, 413, 470)

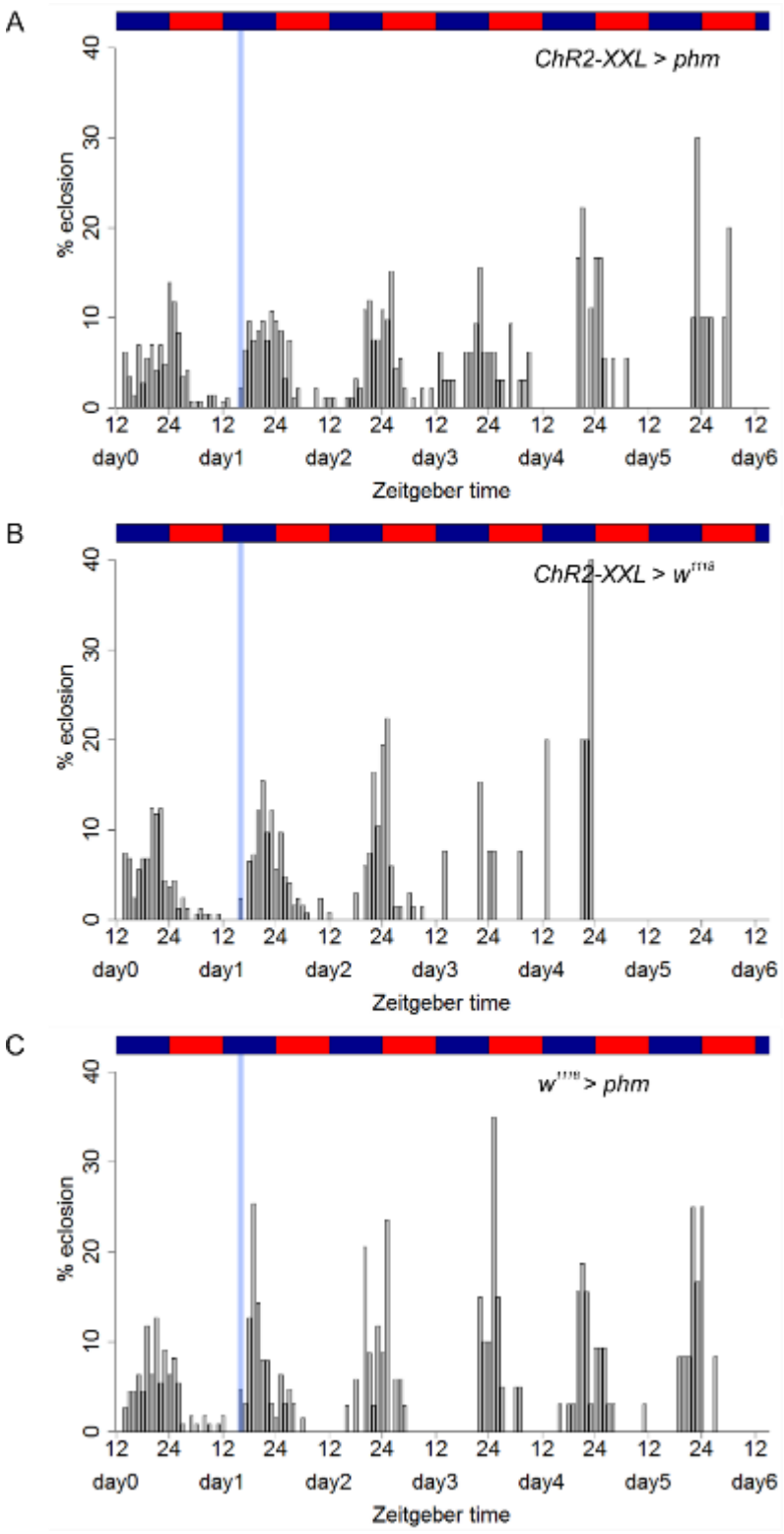

Figure 106: Eclosion rhythms after the activation of Phm-expressing cells 6 hours before the main peak.

Eclosion profiles for populations expressing ChR2-XXL driven by *phm*-GAL4 (A) and the respective controls (B: UAS control, C: GAL4 control) under temperature entrainment (25°C:16°C). Each bar represents the percentage of eclosed flies per hour normalized to the number of eclosed flies per day. The blue and red rectangles represent the temperature regime. The blue bars mark the time points of activation with blue light. (N=4, 3, 3; n=389, 370, 271)

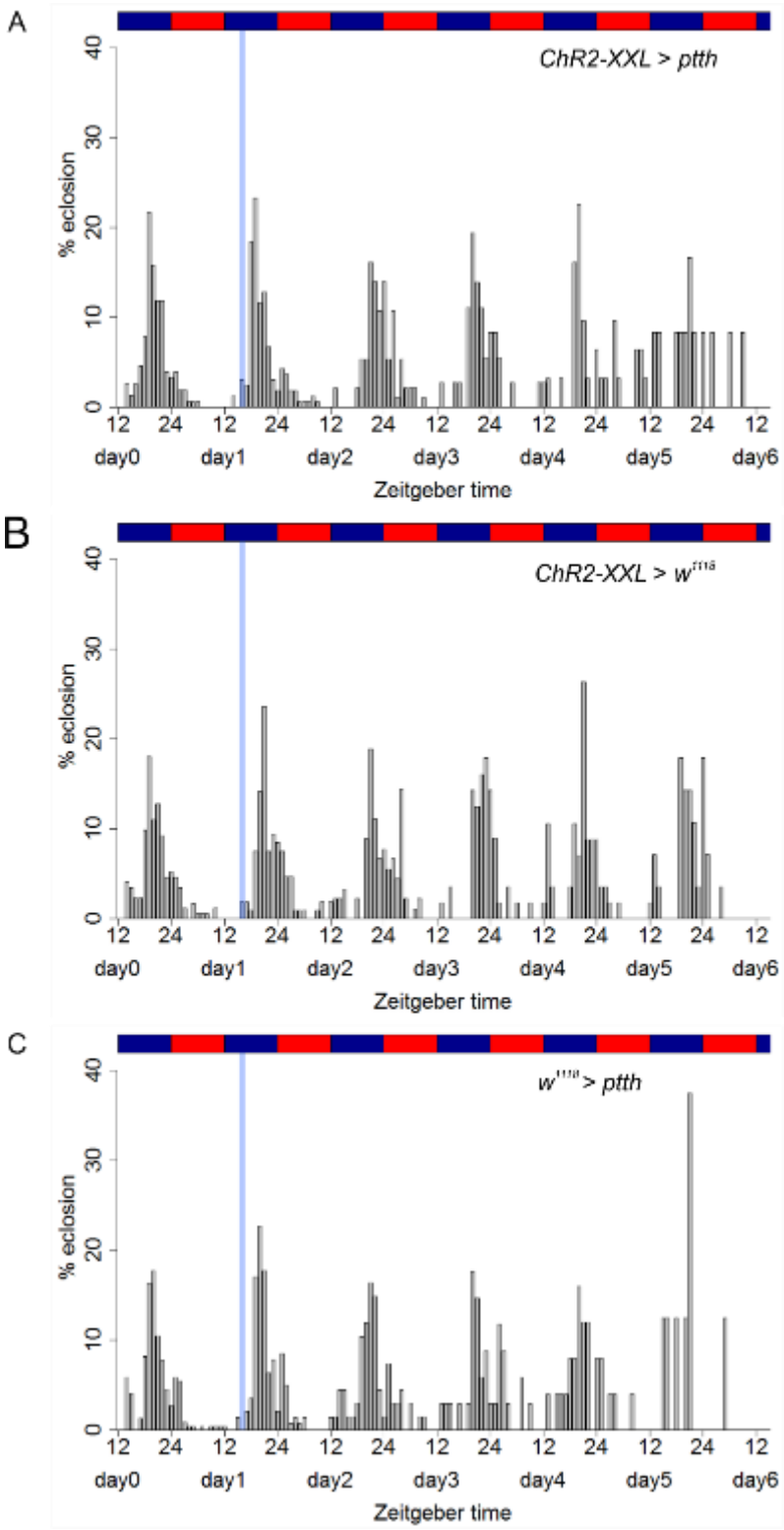

Figure 107: Eclosion rhythms after the activation of PTTH-expressing neurons 6 hours before the main peak.

Eclosion profiles for populations expressing ChR2-XXL driven by *ptth*-GAL4 (A) and the respective controls (B: UAS control, C: GAL4 control) under temperature entrainment (25°C:16°C). Each bar represents the percentage of eclosed flies per hour normalized to the number of eclosed flies per day. The blue and red rectangles represent the temperature regime. The blue bars mark the time points of activation with blue light. (N=3, 3, 3; n=488, 510, 495)

2.16 Short Neuropeptide F (sNPF)

The *snpf* gene encodes for four different peptides in *Drosophila* (Wegener *et al.*, 2006; Yew *et al.*, 2009) that are expressed in a large number of diverse cells in the brain (Lee *et al.*, 2004; Nässel *et al.*, 2008). Most prominent among these are the Kenyon cells of the mushroom bodies (Nässel *et al.*, 2008). sNPF is also expressed in some clock cells, the sLNvs and subsets of LNds (Johard *et al.*, 2009). sNPF functions are quite diverse and are reviewed in Nässel and Wegener (2011).

The activation of cells expressing ChR2-XXL under control of the *snpf*-GAL4 driver line did not lead to an additional peak of eclosion in the experimental group or the controls. There was also no effect on the eclosion rhythm (Figure 108).

2.17 Adipokinetic hormone (AKH)

Drosophila has only one AKH (Schaffer *et al.*, 1990; Noyes *et al.*, 1995). It is expressed only in the endocrine cells of the the corpora cardiaca which have projections to the brain and the prothoracic gland (Lee and Park, 2004). Among the diverse functions of AKH are the mobilization of lipids from the fat body (Mayer and Candy, 1969), the increase of trehalose levels in the hemolymph (Lee and Park, 2004) and acceleration of the heart beat (Noyes *et al.*, 1995).

Silencing of AKH-expressing cells by expressing UAS-*dORKΔ* under the *akh*-GAL4 did not influence the rhythms eclosion profiles, neither under LD conditions (Figure 109) nor under DD conditions (Figure 110). Experiments were performed by Katharina Endres and supervised by Franziska Ruf (Endres, 2013).

2.18 Allatostatin A (AstA)

In *Drosophila*, the AstA preprohormone encodes four AstA peptides (Lenz *et al.*, 2000). It is expressed in the adult CNS and the optic lobes, in the thoracic ganglion and in endocrine cells of the midgut (Yoon and Stay, 1995). It plays an important role in the regulation of feeding and feeding related behaviors (Hergarden *et al.*, 2012; Hentze *et al.*, 2015).

Silencing of AstA-expressing cells by expressing UAS-*dORKΔ* under the *AstA*-GAL4 did not influence the rhythms eclosion profiles, neither under LD conditions (Figure 111) nor under DD conditions (Figure 112). Experiments were performed by Elena Dillmann and supervised by Franziska Ruf (Dillmann, 2014).

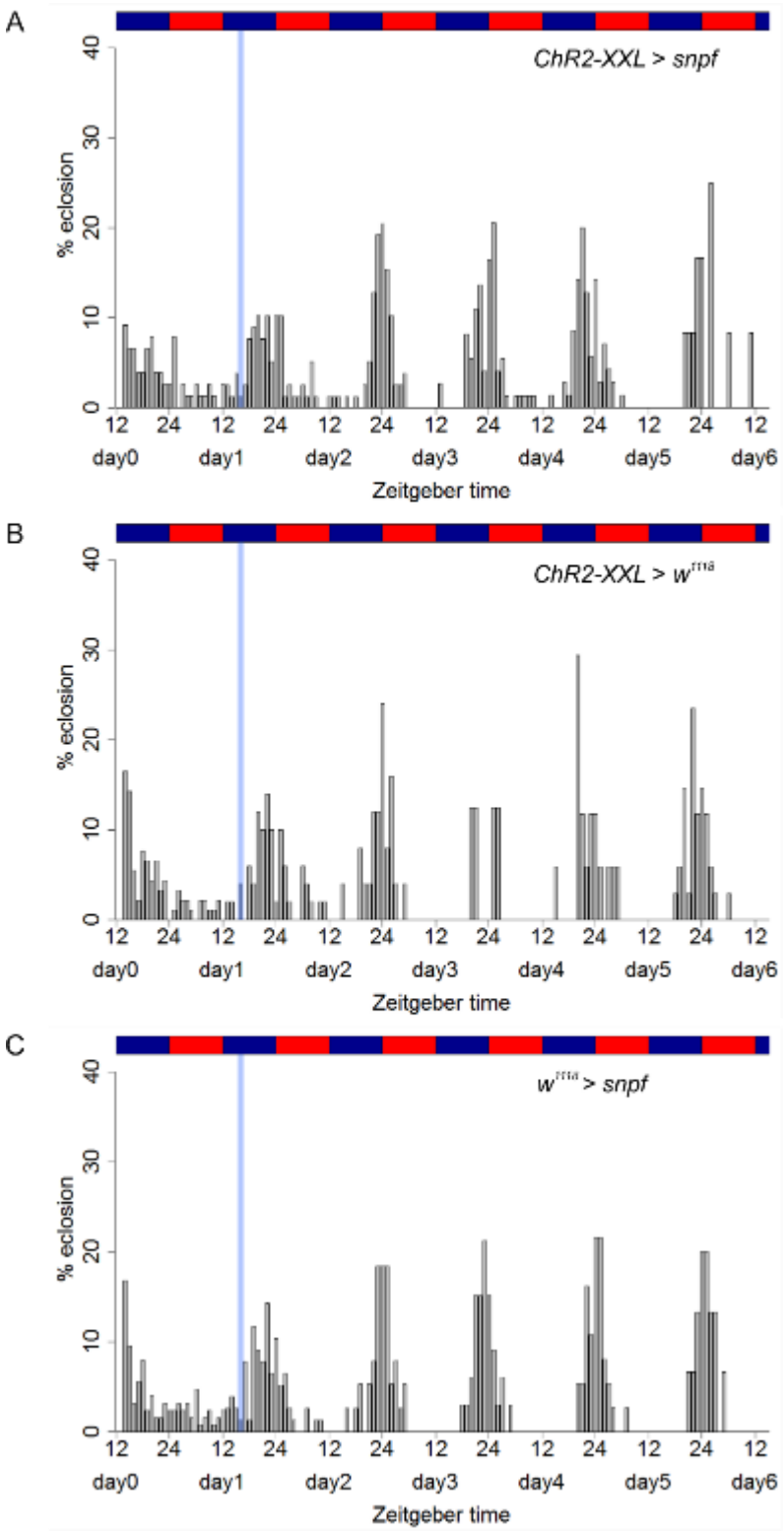

Figure 108: Eclosion rhythms after the activation of sNPF-expressing neurons 6 hours before the main peak.

Eclosion profiles for populations expressing ChR2-XXL driven by *snpf*-GAL4 (A) and the respective controls (B: UAS control, C: GAL4 control) under temperature entrainment (25°C:16°C). Each bar represents the percentage of eclosed flies per hour normalized to the number of eclosed flies per day. The blue and red rectangles represent the temperature regime. The blue bars mark the time points of activation with blue light. (N=3, 3, 3; n=387, 225, 325)

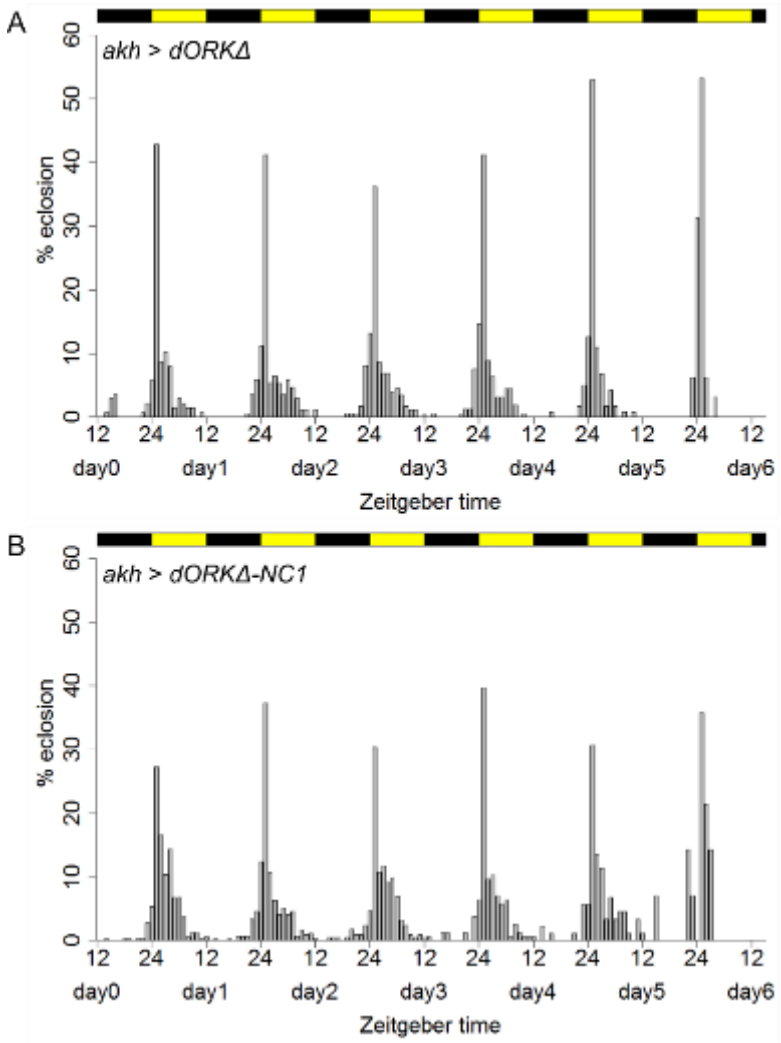

Figure 109: Eclosion rhythms after silencing of AKH-expressing neurons under LD conditions

Eclosion profiles for populations expressing UAS-*dORKΔ* driven by *akh*-GAL4 (A) and the UAS-*ΔORKΔ-NC1* control (B) under LD conditions. Each bar represents the percentage of eclosed flies per hour normalized to the number of eclosed flies per day. The black and yellow rectangles represent the light regime. Data from Endres, 2013. (N=6, 7; n=798, 1242)

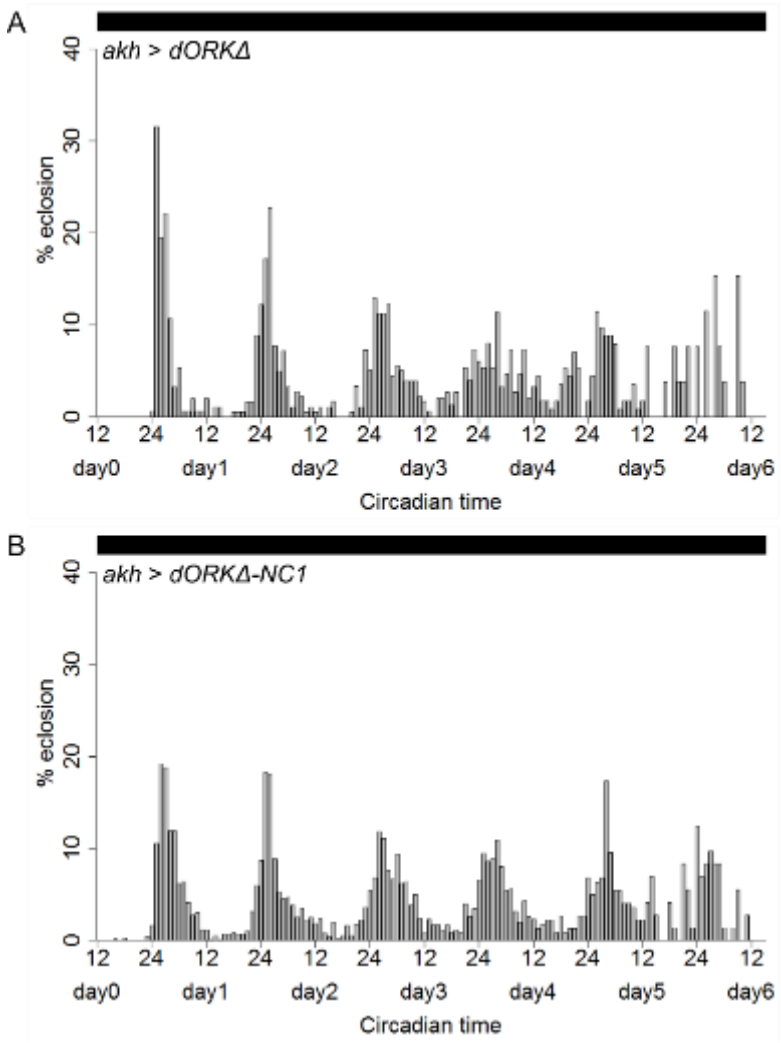

Figure 110: Eclosion rhythms after silencing of AKH-expressing neurons under DD conditions

Eclosion profiles for populations expressing UAS-*dORKΔ* driven by *akh*-GAL4 (A) and the UAS-*ΔORKΔ-NC1* control (B) under DD conditions. Each bar represents the percentage of eclosed flies per hour normalized to the number of eclosed flies per day. The black rectangles represent the light regime. Data from Endres, 2013. (N=6, 7; n=796, 2117)

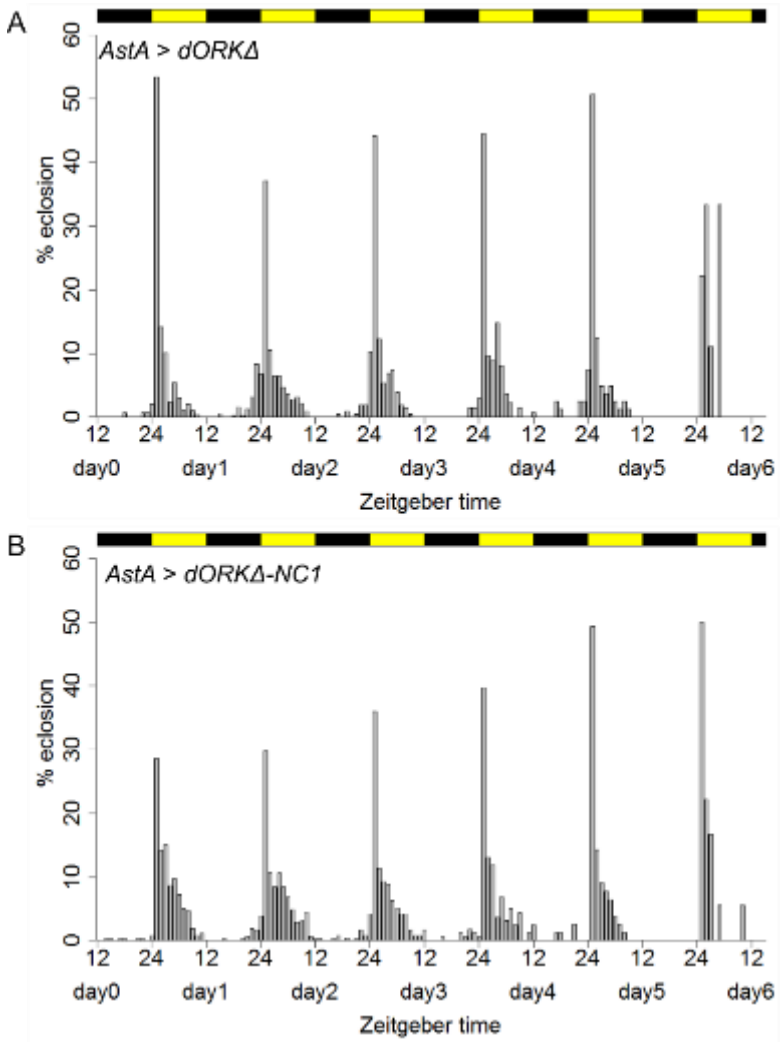

Figure 111: Eclosion rhythms after silencing of AstA-expressing neurons under LD conditions

Eclosion profiles for populations expressing UAS-*dORKΔ* driven by *AstA*-GAL4 (A) and the UAS-*ΔORKΔ-NC1* control (B) under LD conditions. Each bar represents the percentage of eclosed flies per hour normalized to the number of eclosed flies per day. The black and yellow rectangles represent the light regime. Data from Dillmann, 2014. (N=5, 6; n=1051, 1259)

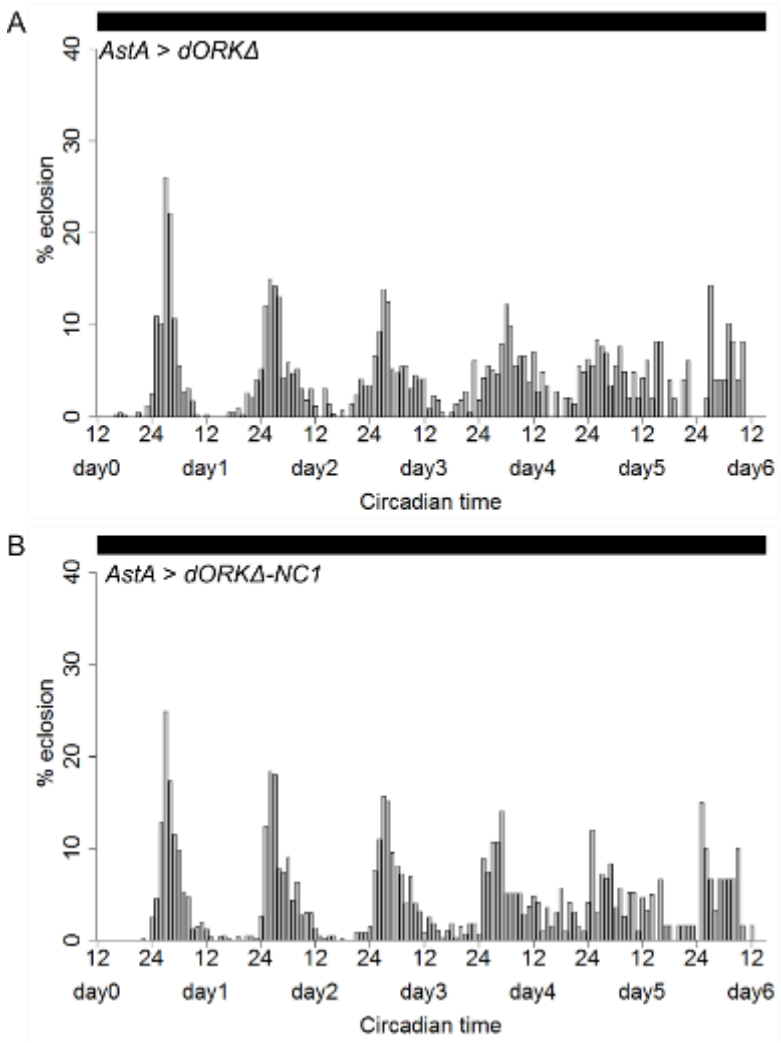

Figure 112: Eclosion rhythms after silencing of AstA expressing neurons under DD conditions

Eclosion profiles for populations expressing UAS-*dORKΔ* driven by *AstA*-GAL4 (A) and the UAS-*ΔORKΔ-NC1* control (B) under DD conditions. Each bar represents the percentage of eclosed flies per hour normalized to the number of eclosed flies per day. The black rectangles represent the light regime. Data from Dillmann, 2014. (N=7, 6; n=1507, 1768)

2.19 Tyrosine decarboxylase (Tdc) / Octopamine

Octopamine is a metabolite of tyramine, which is synthesized from tyrosine by the enzyme tyrosine decarboxylase (Tdc) (Figure 113). Octopamine shows a high structural similarity to the vertebrate norepinephrine. In *Drosophila*, two *tdc* genes have been identified. In contrast to *tdc1*, which is expressed nonneuronally, *tdc2* is expressed in neuronal cells, and both gene products seem to have different functions (Cole *et al.*, 2005). Among other functions, octopamines play important roles in oviposition (Cole *et al.*, 2005), the induction of starvation-induced hyperactivity (Yang *et al.*, 2015), the modulation of male aggressiveness (Hoyer *et al.*, 2008), in associative learning and in larval locomotion (Selcho *et al.*, 2012). The octopamine

receptor is highly express in the mushroom bodies, the ellipsoid body of central complex, in larval muscles and in the tracheal system (Han *et al.*, 1998; El-Kholy *et al.*, 2015). Furthermore, it plays a role in the biosynthesis of ecdysteroids in the PG and the induction of metamorphosis (Ohhara *et al.*, 2015).

The activation of cells expressing ChR2-XXL under control of the *tdc2*-GAL4 driver line did not lead to an additional peak of eclosion in the experimental group or the controls. There was also no effect on the eclosion rhythm (Figure 114).

2.20 Tyrosine hydroxylase (TH) / Dopamine

Dopamine is synthesized from tyrosine by the enzymes tyrosine hydroxylase (TH) and dopa decarboxylase (DDC) (Figure 113). It has diverse functions for example in the regulation of sleep and arousal (Kume *et al.*, 2005), learning (Berry *et al.*, 2012), locomotion, aversive olfactory learning, sugar preference and phototaxis behavior (Selcho *et al.*, 2009; Riemensperger *et al.*, 2011). Furthermore, it plays a role in the tanning of the cuticula during post-ecdysis (Neckameyer and White, 1993; Davis *et al.*, 2007).

The activation of cells expressing ChR2-XXL under control of the *th*-GAL4 driver line did not lead to an additional peak of eclosion in the experimental group or the controls. There was also no effect on the eclosion rhythm (Figure 115).

2.21 Tryptophan hydroxylase (TRH) / Serotonin

Serotonin is synthesized from L-tryptophan by the tryptophan hydroxylase (TRH) and the dopa decarboxylase (DDC) with 5-hydroxy-tryptophan as a metabolite (Figure 113). It has diverse functions, for example as inhibitory modulator of locomotor activity (Pooryasin and Fiala, 2015), in the promotion of sleep (Yuan *et al.*, 2006), as modulator of olfactory processing (Dacks *et al.*, 2009), in memory formation (Sitaraman *et al.*, 2008; Sitaraman *et al.*, 2012), in courtship and mating (Becnel *et al.*, 2011) and in aggression (Dierick and Greenspan, 2007). Furthermore, serotonin plays a role in the circadian system: serotonergic neurons are close to the dendrites and dorsal terminals of the sLN_vs and converge with the terminals of the lLNvs in the distal medulla (Hamasaka and Nässel, 2006). The serotonin receptor d5-HT1B is expressed in the small and large LNvs and modulates the behavioral responses of the clock to light (Yuan *et al.*, 2005). There are serotonergic neurons innervating the PG (Shimada-Niwa and Niwa, 2014) and serotonin signaling regulates ecdysteroid biosynthesis (Shimada-Niwa and Niwa, 2014).

The activation of cells expressing ChR2-XXL under control of the *trh*-GAL4 driver line did not lead to an additional peak of eclosion in the experimental group or the controls. There was also no effect on the eclosion rhythm (Figure 116).

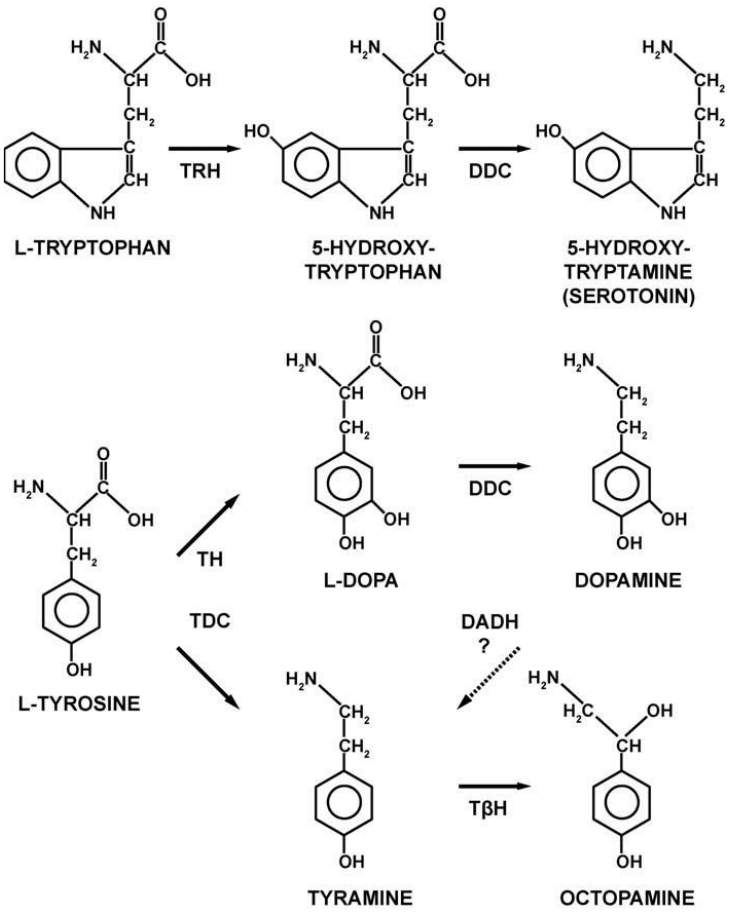

Figure 113: Biosynthesis of biogenic amines
Serotonin is synthesized from L-Tryptophan by the tryptophan hydroxylase (TRH) and the dopa decarboxylase (DDC). Both dopamine and octopamine are synthesized from tyrosine. The tyrosine hydroxylase (TH) and dopa decarboxylase (DDC) mediate the conversion to dopamine. The tyrosine decarboxylase (TDC) and the tyramine ß-Hydroxylase (TßH) catalysis the reaction to octopamine. (Vömel and Wegener, 2008)

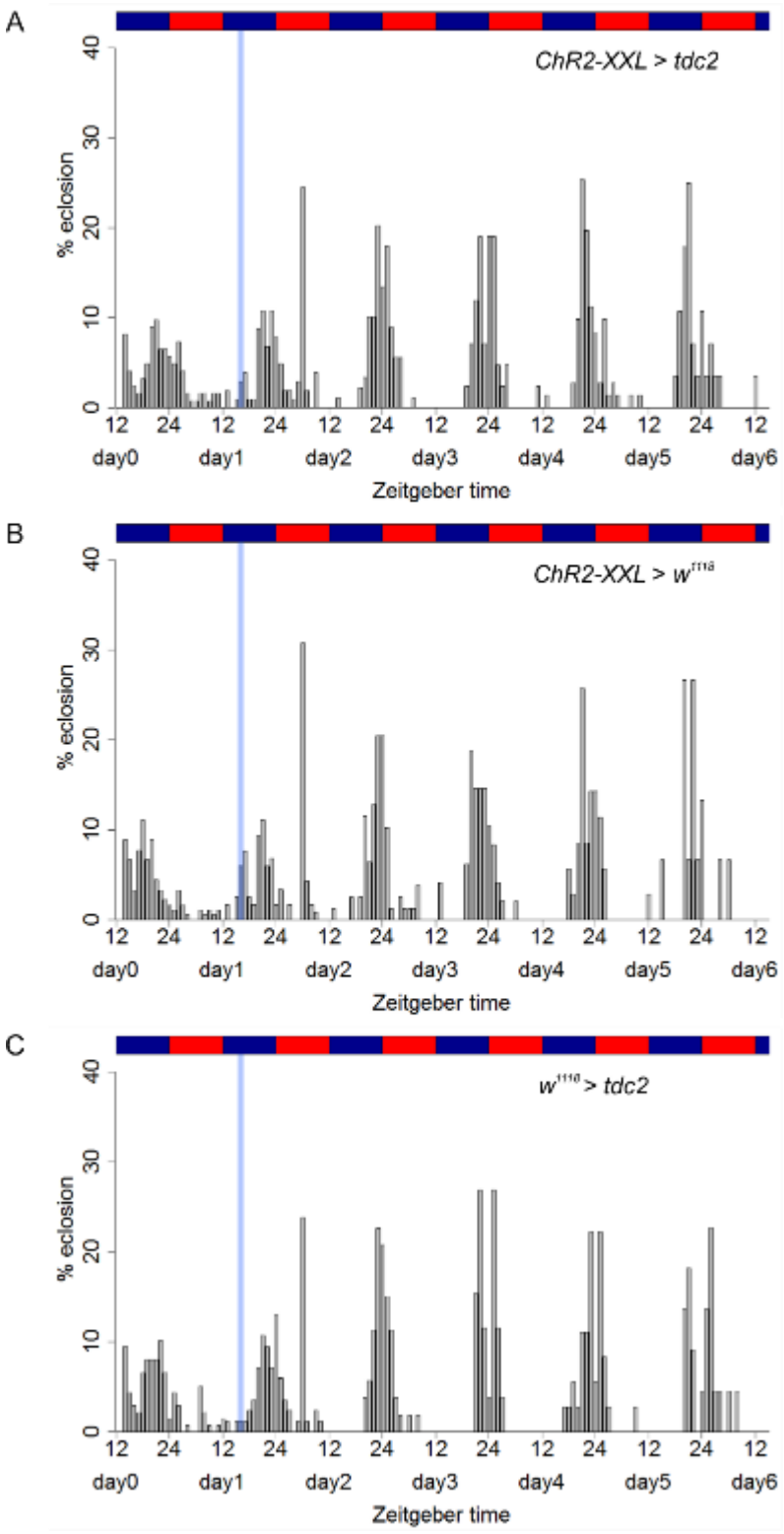

Figure 114: Eclosion rhythms after the activation of Tdc2-expressing neurons 6 hours before the main peak.

Eclosion profiles for populations expressing ChR2-XXL driven by *tdc2*-GAL4 (A) and the respective controls (B: UAS control, C: GAL4 control) under temperature entrainment (25°C:16°C). Each bar represents the percentage of eclosed flies per hour normalized to the number of eclosed flies per day. The blue and red rectangles represent the temperature regime. The blue bars mark the time points of activation with blue light. (N=3, 3, 3; n=465, 478, 360)

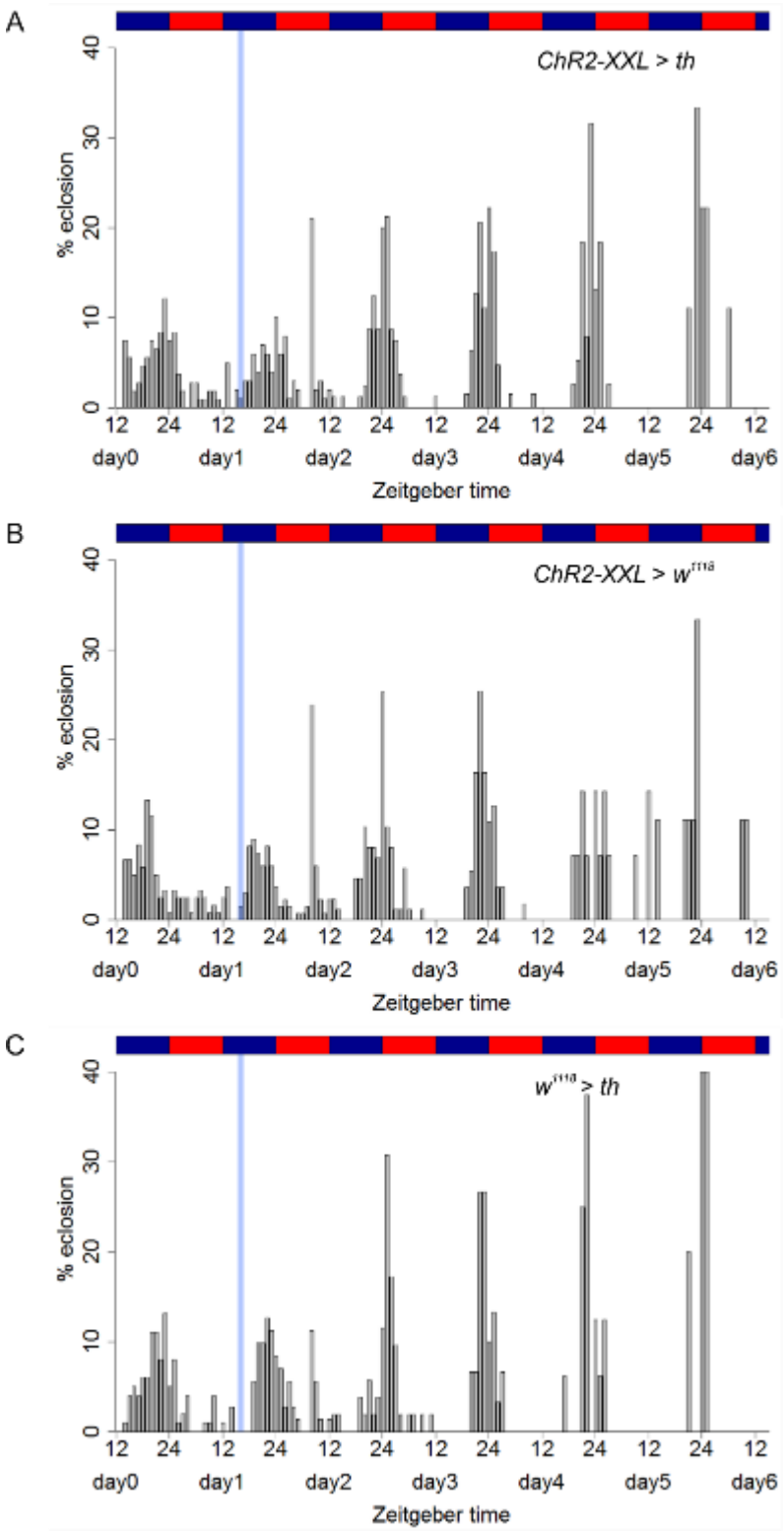

Figure 115: Eclosion rhythms after the activation of TH expressing neurons 6 hours before the main peak.

Eclosion profiles for populations expressing ChR2-XXL driven by *th*-GAL4 (A) and the respective controls (B: UAS control, C: GAL4 control) under temperature entrainment (25°C:16°C). Each bar represents the percentage of eclosed flies per hour normalized to the number of eclosed flies per day. The blue and red rectangles represent the temperature regime. The blue bars mark the time points of activation with blue light. (N=3, 3, 3; n=402, 428, 277)

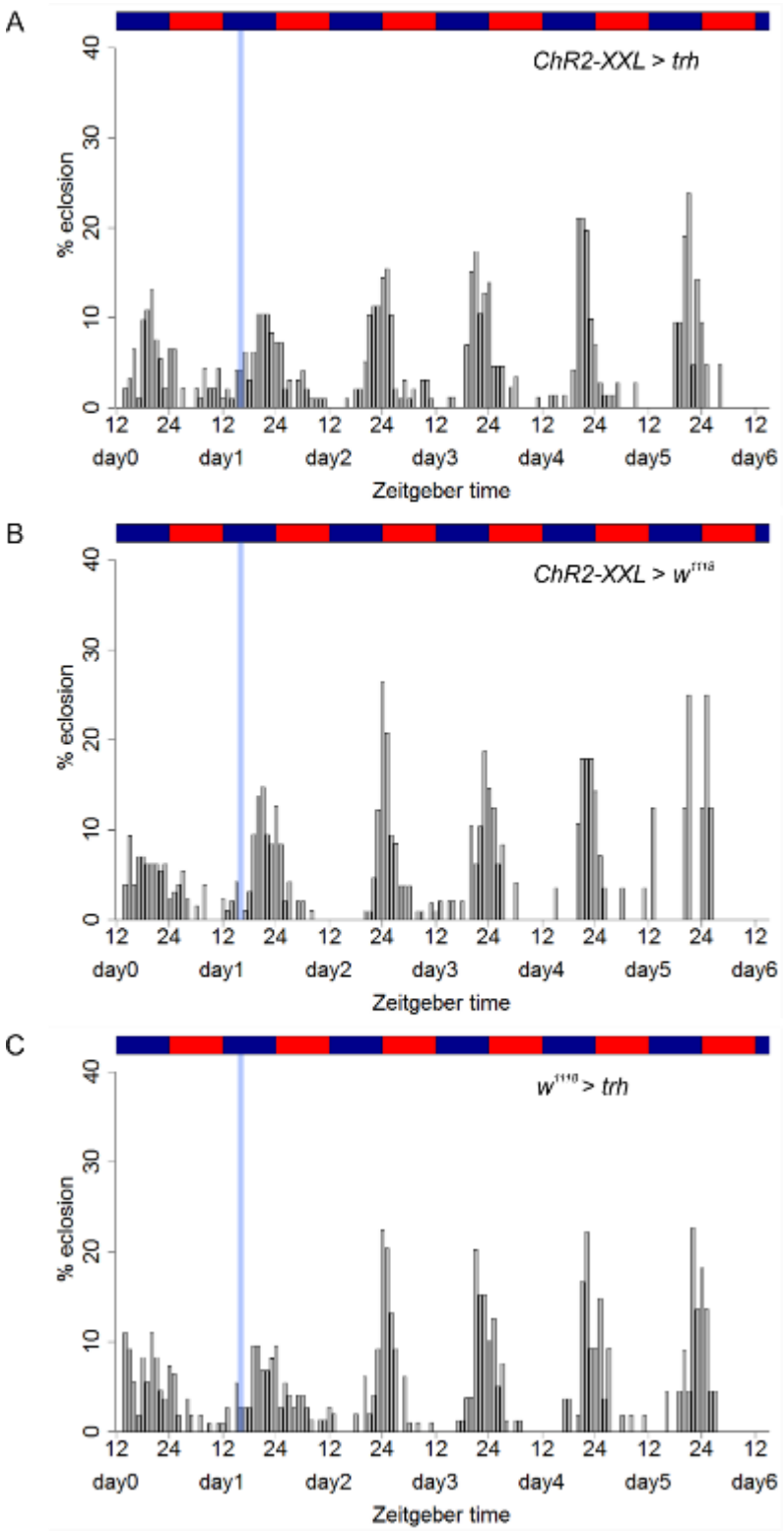

Figure 116: Eclosion rhythms after the activation of TRH-expressing neurons 6 hours before the main peak.

Eclosion profiles for populations expressing ChR2-XXL driven by *trh*-GAL4 (A) and the respective controls (B: UAS control, C: GAL4 control) under temperature entrainment (25°C:16°C). Each bar represents the percentage of eclosed flies per hour normalized to the number of eclosed flies per day. The blue and red rectangles represent the temperature regime. The blue bars mark the time points of activation with blue light. (N=3, 3, 3; n=463, 413, 435)

2.22 Summary

Table 10: Summary of the results of the screen for new candidates in the regulation of eclosion

Driver line	Optogenetic activation six hours before eclosion	Effect of ablation/silencing on eclosion rhythmicity
akh-GAL4	not tested	no effect (#)
AstA-GAL4	not tested	no effect (+)
ap-GAL4/cyo	no effect	not tested
capa-GAL4 #51969	no effect	not tested
capa-GAL4 #51970	no effect	not tested
ccap-GAL4	not tested	no effect
crz-GAL4	effect	effect (‡)
dh31-GAL4 #51988	no effect	not tested
dh31-GAL4 #51989	no effect	not tested
dh44-GAL4 #39347	no effect	not tested
dh44-GAL4 VT039046	no effect	not tested
dms-GAL4	effect	no effect
Eh-GAL4	effect	effect
eth-GAL4	effect	not tested
hug-GAL4	no effect	not tested
Mai316-GAL4	no effect	not tested
mip-GAL4	effect	not tested
*nSyb*GAL80; *mip*-GAL4	no effect	not tested

npf-GAL4	no effect	not tested
pdf-GAL4	no effect	effect (*)
phm-GAL4	no effect	not tested
ptth-GAL4	no effect	effect
snpf-GAL4	no effect	not tested
tdc-GAL4	no effect	not tested
th-GAL4	no effect	not tested
trh-GAL4	no effect	not tested

(#) Data from Katharina Endres

(+) Data from Elena Dillmann

(‡) Data from Jana Schmitz and Ruben Trapp

(*) Data from Jiangtian Chen

3. Discussion

The transient optogenetic activation of peptidergic neurons proved to be a suitable screen to identify candidate peptides that have a direct effect on eclosion. It is now possible to exclude several of the approximately 80 predicted peptides in *Drosophila* (Nässel and Winther, 2010; Pauls *et al.*, 2014) as candidates that induce the peptide cascade orchestrating eclosion behavior (Table 10).

The optogenetic activation of ETH and EH neurons immediately and reliably induced eclosion, as long as it happened maximal 6 hours prior to the expected eclosion peak. This confirms Pittendrigh's hypothesis of an allowed gate for eclosion of about 6 hours. During this time, the system is ready for eclosion, but waits for the Zeitgeber or clock signal (Pittendrigh, 1954). Silencing of EH neurons lead to reduced eclosion success as well as to a broader eclosion gate and less defined peaks compared to controls. These results are in accordance with results from McNabb *et al*., 1997. But as Krüger *et al.*, 2015 could show that complete loss of EH results in lethality at early larval stages, the silencing in our results was probably incomplete and some residual EH function was left.

The tested biogenic amines dopamine, octopamine and serotonin showed no effect, although serotonin has connections to clock cells (Yuan *et al.*, 2005; Hamasaka and Nässel, 2006). The two diuretic hormones DH31 and DH44 also had no inducing effect, although their osmoregulatory effects in close proximity to Inka cells could hint at a role in the ecdysis behavior (Coast *et al.*, 2001; Cabrero *et al.*, 2002). There was also no effect upon activation of ap, capa, hug or NPF on eclosion. Silencing of AKH and AstA neurons had no effect on eclosion rhythmicity and survival rate, so they are apparently not needed for the eclosion timing and process.

The activation of Crz, DMS and MIP induced immediate eclosion additional to the expected eclosion peak six hours later.

In *Manduca sexta*, Crz induces the release of ETH from the Inka cells and therefore is the starting signal for eclosion (Kim *et al.*, 2004). The activation of Crz neurons in *Drosophila* induced eclosion only weakly, but had a strong dampening effect on the eclosion rhythm of experimental flies with a broadening of the eclosion gate and reduction of the peaks, even on the days following the activation. The ablation and silencing of Crz neurons had no effect on eclosion success, but the ablation also lead to broader distribution of eclosion events and reduced peaks, especially under LD conditions. In contrast to that, silencing of the Crz neurons

did not lead to an effect on the eclosion rhythm, possibly due to an incomplete silencing. The residual function would then maybe be enough to maintain the function of Crz. The results show that Crz is not a starting signal for eclosion in *Drosophila* as it is in *Manduca*. It is also not necessary for eclosion in *Drosophila*, but has strong dampening effects on the shape of the eclosion rhythm. This could hint at modulator effects, maybe even on the clock output, as Crz neurons are in close vicinity to terminals of the PDF expressing sLNvs (Choi *et al.*, 2005). Anatomical characterization of connections between Crz neurons and clock neurons, as well as other peptidergic neurons involved in eclosion regulation, could help to further dissect the effect of Crz on the eclosion rhythm and reveal possible effects on clock outputs.

Activation of DMS neurons induced eclosion strongly and repeatedly. Ablation of DMS neurons however had no effect on the eclosion rhythm or on viability. It therefore seems that while DMS is sufficient to start eclosion, it is not necessary and plays no role in the circadian timing. So far, the only known function for DMS in *Drosophila* is the decrease of heart contractions (Dickerson *et al.*, 2012). This is unlikely to play a role for the ecdysis behavior, as contrary an increased heart rate would distribute peptides faster and broader and be more helpful for eclosion. In *Bombyx mori,* however, DMS inhibits ecdysteroidogenesis in the larval PG (Yamanaka *et al.*, 2010). It is not known if DMS has the same function in *Drosophila* or if its receptors are expressed in the PG. Further experiments like the knockdown of the DMS receptor in the Inka cells and the PGd could help to dissect the role of DMS in eclosion.

MIP is the third newly identified candidate for starting eclosion. It is sufficient for the induction of eclosion, as its activation immediately started eclosion. This effect is due to only the neuronal MIP cells and not peripheral ones. MIP neurons are known to promote ecdysis and post-ecdysis behavior *in Drosophila* (Kim *et al.*, 2006a; Kim *et al.*, 2006b), but so far nothing is known about a role in pre-ecdysis behavior. In *Bombyx mori,* the MIP receptor is expressed in the PG and its expression is coupled to the titers of ecdysteroids (Yamanaka *et al.*, 2005). It is not known if this is the case in *Drosophila* and if MIP has a role in ecdysteriodogenesis. To rule out that the effect of MIP activation is based on the co-expression of CCAP (Kim *et al.*, 2006b), the experiments should be repeated with a combination of the *mip*-GAL4 line and *ccap* RNAi. Further studies must show if MIP is also necessary for eclosion, for example by ablation or silencing the MIP neurons. These experiments would also disclose a role of MIP in the circadian timing of eclosion. Knockdown of the MIP receptor in the Inka cells could show if MIP or

another peptide expressed in the MIP neurons is inducing eclosion. Knockdown in the PG could reveal a function in the production and regulation of ecdysteroid levels.

Activation of Phm and thereby expression of ecdysone, which plays an essential role in ecdysis and pupariation (Garen *et al.*, 1977), did not induce eclosion directly, but seems to have a slight effect on eclosion rhythmicity. A direct role of ecdysone as inducer of eclosion in *Drosophila* is however unlikely, as the physiological ecdysteroid titers are very low in pharate adults (Handler, 1982; Bainbridge and Bownes, 1988). As was however already described in Chapter III, new detecting methods could reveal if there is still enough ecdysone left shortly before eclosion to initiate ETH release and eclosion.

Although this screen can be used to identify direct activators of eclosion, it is not suited to identify peptides that play a role in the circadian rhythmicity of eclosion, as these have generally long-term effects. This is the case for PDF, PTTH and sNPF (via its receptor in PTTH neurons), who show clear effects on eclosion rhythmicity (Myers *et al.*, 2003) (Selcho *et al.*, unpublished; see Chapter III), but did not induce direct eclosion upon activation.

Although the blue light was given at a high intensity of 586 $\mu W/cm^2$ for one hour, no masking effects on the actual eclosion rhythm could be observed

To further identify candidate peptides in eclosion regulation and timing, it would be interesting to study the expression of peptide receptors in the PG and the Inka cells. A temporal analysis of their expression patterns would help to understand the events leading to eclosion and the peptides involved. Further ablation and silencing experiments could be done to find new peptides in the circadian timing of eclosion.

Synopsis

Numerous cooperating components orchestrate the precise timing and execution of the motor behavior that facilitate successful eclosion in flies. The main components comprise the circadian clock in the brain, the peripheral clock in the prothoracic gland and the peptides regulating the ecdysis behavior. Collaboration of these systems results in a behavior that is well adapted to the environment and thereby is presumed to increase the chance of survival (Beaver *et al.*, 2002; Saunders, 2002). The present dissertation research focused on the different levels of eclosion organization: in Chapters III and IV, the connection between the central clock and the peripheral clock, as well as the peptides regulating eclosion behavior, is investigated. In Chapter V, the peptides starting the eclosion behavior and their connection to the clock are addressed. The eclosion rhythmicity under natural conditions and the influence of different Zeitgebers were investigated in Chapter II. To this end, a new eclosion monitoring system was developed and is described in Chapter I.

PTTH connects the central clock in the brain with the peripheral clock in the PG

Chapter III focuses on PTTH, which regulates production and release of ecdysteroids from the prothoracic gland (Vedeckis *et al.*, 1976; Bollenbacher *et al.*, 1979; Rewitz *et al.*, 2006a). Silencing and ablation of PTTH neurons resulted in arrhythmic eclosion under constant conditions after both, light and temperature entrainment. Knockdown of the PTTH receptor Torso in the PG phenocopied these results with stronger effect on the length of development. A reduced viability was observed following *torso* knockdown, but not after ablation of the PTTH neurons. Moreover, it was shown that *torso* is expressed neither in the brain nor by the photoreceptors in the compound eyes of pharate flies, refuting a role for PTTH in the light detection pathway. PDF neurons do not signal to PTTH neurons via PDF, which could be shown by knockdown of the receptor and be proved by imaging data from Mareike Selcho (Selcho *et al.*, unpublished-a). Instead, sNPF emerged as a candidate signaling peptide between the neurons (Selcho *et al.*, unpublished-a). The data show that the PTTH neurons form indeed a link between the circadian clock and the peripheral clock in the PG. Further experiments will have to dissect the role of the connection between the PG and the eclosion regulating peptides, as well as the role of ecdysone for eclosion rhythmicity.

CCAP has no role in the circadian regulation of eclosion rhythmicity

Although much is known about the organization of the circadian clock (reviewed in Peschel and Helfrich-Förster, 2011) and the regulation of eclosion behavior (reviewed in Ewer, 2007), it remains unknown how the central clock in the brain, which regulates eclosion rhythmicity, and the peptide cascade orchestrating eclosion behavior are interconnected. The PDF expressing lateral neurons (LNs) have been identified as main oscillators for eclosion rhythmicity in the fly brain (Myers *et al.*, 2003), and CCAP neurons are suggested as possible connector between the central clock and the peptides orchestrating eclosion behavior based on the proximity of their projections to LN arborizations (Park *et al.*, 2003) and their role in promoting the eclosion motor behavior (Gammie and Truman, 1997; Park *et al.*, 2003). In Chapter IV, the influence of CCAP, which promotes ecdysis behavior, on eclosion rhythmicity is investigated. The results confirmed earlier studies that reported a decrease in viability when CCAP neurons were ablated (Park *et al.*, 2003), while loss of the CCAP peptide had no effect on viability or eclosion rhythmicity under light entrainment (Lahr *et al.*, 2012). A potential role of CCAP in temperature entrainment, hypothesized due to the proximity of CCAP neurons to DN2 clock neurons (Busza *et al.*, 2007; Miyasako *et al.*, 2007; Picot *et al.*, 2009), could also be refuted. Under natural conditions, CCAP mutants showed no deficits in rhythmicity and behaved wildtype-like. Therefore it can be concluded that CCAP plays no role in eclosion rhythmicity and does not constitute the molecular connection between the central pacemaker and the behavioral output.

DMS and MIP as new candidates in the regulation of eclosion behavior

To identify a starting signal for eclosion behavior comparable to Crz in *Manduca* (Kim *et al.*, 2004), a screen for candidate peptides has been conducted and is described in Chapter V. Three new candidate peptides have been evaluated: Crz, DMS and MIP. Crz could not directly induce eclosion, but had a dampening effect on the eclosion rhythm. While DMS could induce eclosion, ablation of DMS neurons had no effect on eclosion rhythmicity. MIP also induced eclosion and further studies will have to show if it also has an effect on rhythmicity or if the effects are induced by CCAP. All other tested peptides and amines could not directly induce eclosion, although they still might play a role in modulating eclosion rhythmicity or motor behavior.

The clock is the most important factor for rhythmic eclosion under natural conditions

Eventually, in Chapter II, the role of different Zeitgebers on eclosion rhythmicity under natural conditions is studied. For this purpose a new monitoring system was developed in Chapter I: the WEclMon is an open monitoring system that allows direct exposure of the pupae to abiotic environmental factors. Comparing the results to experiments conducted under laboratory conditions showed that rhythmicity strength was decreased under natural conditions, which is in contrast to previous studies (De *et al.*, 2012; Vanin *et al.*, 2012). The differences could be explained by different oscillators involved in locomotor activity and eclosion (Sheeba *et al.*, 2001) and the influence of the entrainment conditions during development (Tomioka *et al.*, 1997). While wildtype, pdf^{01} and han^{5304} flies showed rhythmic eclosion under natural conditions, the per^{01} mutant became almost completely arrhythmic. These results reflect the different functions of PDF and PER. PDF is the main output factor of the clock and is needed for synchronization, while PER is part of the transcriptional feedback loop that constitutes the endogenous clock. Under natural conditions, the flies are able to synchronize their clock each day anew by the Zeitgebers and therefore the loss of PDF or its receptor can be compensated. Without an intact clock, however, it is impossible for the flies to eclose rhythmically. To untangle the correlations between the abiotic factors and their influence on eclosion rhythmicity, a statistical model that describes the daily eclosion pattern under natural conditions was developed in cooperation with Prof. Dr. Thomas Hovestadt and Dr. Oliver Mitesser. This is the first time that statistical modelling was applied to assess the influence of the clock, light intensity and temperature on the eclosion rhythm. Relative humidity was not included into the statistical modelling, as experimental data revealed no evidence that it acts as a Zeitgeber for eclosion rhythmicity. However, the strong negative correlation of humidity and temperature is hard to disentangle in these calculations. The analysis, which was performed by Dr. Oliver Mitesser, shows a clear hierarchy of the analyzed factors. The clock appears as the main factor determining the daily eclosion pattern, followed by temperature. The light intensity has the lowest impact. This results in a model where the clock defines the temporal boundaries (=gate) in which eclosion is possible and temperature adapts the eclosion to the current environmental conditions by moving eclosion activity within the gate. While for example normally no eclosion occurs during the night, high temperatures can shift eclosion in the night where temperatures are more bearable. Light intensity had a very low influence on the daily eclosion pattern but still is the main factor entraining the clocks and

thereby defines the eclosion gate. Laboratory conditions confirmed that light is a stronger Zeitgeber for eclosion than temperature, as many genotypes showed a decline or even a loss of rhythmicity under constant temperatures. The *per*^{01} mutant again showed the strongest deviations from the wildtype, as here the loss of functional clocks lead to a high amount of eclosion during the night independent of the temperature. This confirms that the clock is the most important factor for rhythmic eclosion.

Eclosion in the morning is an adaption to low temperature and not high relative humidity

It is a long standing hypothesis that eclosion represents an adaptation to high relative humidity in the morning (Pittendrigh, 1954). Results by Melanie Horn however provide strong evidence that it is rather an adaption to avoid high temperatures. High temperatures decrease eclosion success and the rate of wing expansion, while low humidity has nearly no phenotypic effects (Melanie Horn, personal communication). This was also shown in studies on *Delia antiqua* (Tanaka and Watari, 2009). Studies by Pittendrigh and Minis (1972) showed that flies are adapted to the period of their environment so well that raising them under periods that differ from 24 hours decreased their survival (Pittendrigh and Minis, 1972). Having an intact clock that allows eclosion at the right time of day therefore increases the viability and leads to higher fitness.

The dual-oscillator model for eclosion

The results from Chapter II, especially the effects revealed by the statistical modelling of the data, fit very well into the dual-oscillator model. This model was first postulated by Pittendrigh to explain phase-shifts in eclosion rhythms after light pulses in *Drosophila pseudoobscura* (Pittendrigh, 1957). He described a light-sensitive A-oscillator (master oscillator) and a temperature-sensitive B-oscillator (slave oscillator) that is insensitive to light. The A-oscillator as a central pacemaker would drive the coupled peripheral B-oscillator, while the phase of the B-oscillator would control eclosion (Pittendrigh and Bruce, 1959a). Since then, other behaviors have been found to be also driven by B-oscillators, so that the model was expanded to a multi-oscillator model. Here, different functions are controlled by separate circadian oscillators that are coupled and influence each other (Sheeba *et al.*, 2001). It has been shown that under the same conditions, the free-running periods of locomotor activity, eclosion and oviposition in *D. pseudoobscura* (Engelmann and Mack, 1978) and *D. melanogaster* (Sheeba *et al.*, 2001) are

significantly different from each other, implying that they are controlled by different oscillators. Additionally, there are mutants that affect the period of either locomotor activity (*ebony*) or eclosion (*lark*) (Jackson, 1993; Wülbeck *et al.*, 2005). For eclosion, the A oscillator is the circadian clock in the brain, while the peripheral clock in the PG is the B oscillator. Not all peripheral clocks are the same: while some function autonomously, like the clock in the Malphigian tubules, others are under the control of or driven by the central clock, like the clock in the PG (Ito and Tomioka, 2016). Most overt rhythms are correlated with *per* cycling (Hardin, 1994), which was also found in the PG (Emery *et al.*, 1997). However, while the B oscillator was hypothesized to be insensitive to light (Pittendrigh and Bruce, 1959a), it was shown that the cycling of *per* in the PG can be entrained by light, although this effect might be amplified by photoreception from the CNS (Emery *et al.*, 1997; Morioka *et al.*, 2012). Also *tim* is cycling in the PG, and disruption of this cycling lead to arrhythmic eclosion (Myers *et al.*, 2003). Furthermore, the *per* and *tim* cycling in the central clock can be entrained by temperature (Stanewsky *et al.*, 1998), refuting a strict constraint of the Zeitgebers light and temperature to one oscillator. Experiments by John Ewer show that the central clock does dominate over the peripheral clock as it was predicted by Pittendrigh (Pittendrigh and Bruce, 1959a): manipulating specifically the speed of the central clock also changed the period of eclosion, while manipulating only the speed of the PG clock had no effect on the eclosion period (Selcho *et al.*, unpublished-a). The results on the effect of temperature on the daily eclosion pattern indicate that the PG might have a more direct role on the daily eclosion pattern. To test this, it would be interesting to study the *per* and *tim* cycling in the PG under temperature entrainment and compare the results to the cycling of the clock genes in the brain.

Taken all together, the results of this dissertation lead to a model for eclosion where light is essential to drive the central pacemaker and define the gate in which eclosion is at all possible. Temperature however seems to have more influence on the peripheral oscillator in the prothoracic gland and therefore directly controls the daily eclosion pattern within the gate. Both clocks are coupled by PTTH and its receptor Torso via sNPF from the LNs. How the clocks influence the eclosion behavior remains unknown, but EH emerged as possible candidate (summarized in Figure 117).

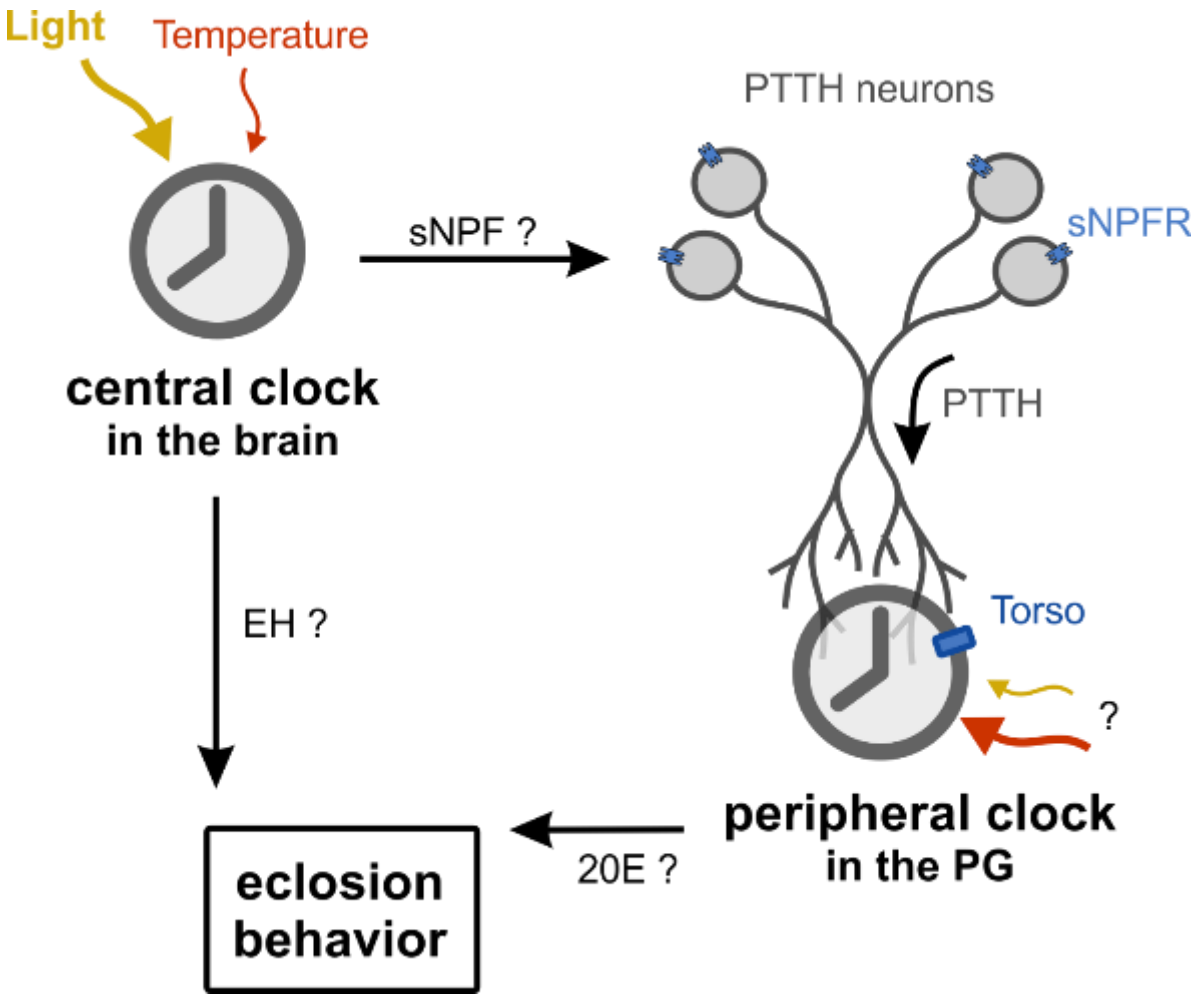

Figure 117: Current model for the connection between the central and peripheral clock and the role of the Zeitgebers light and temperature for eclosion timing

Appendix

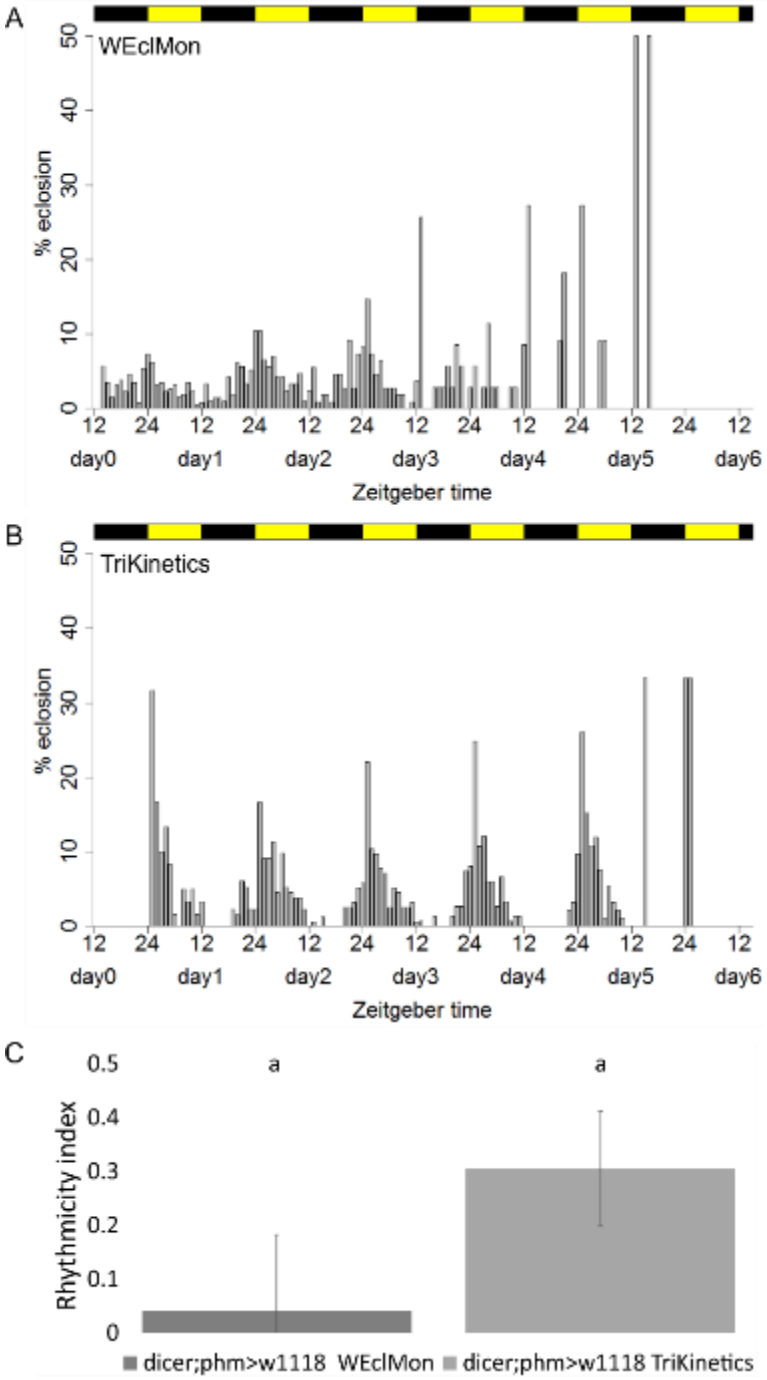

Figure S 1: Comparison between the WEclMon with constant red light and the TriKinetics system under LD conditions

Eclosion profiles for populations of w^{1118} > *dicer2*; *phm* recorded in the WEclMon (A) and the TriKinetics system (B) under LD conditions. Each bar represents the percentage of eclosed flies per hour normalized to the number of eclosed flies per day. The black rectangles represent the light regime. (C) shows the means of the rhythmicity indices (±SD). Different letters above columns indicate significant difference ($p<0.05$). Experiments in the WEclMon were performed under constant red light (λ=635 nm). (N=5, 2; n=630, 590)

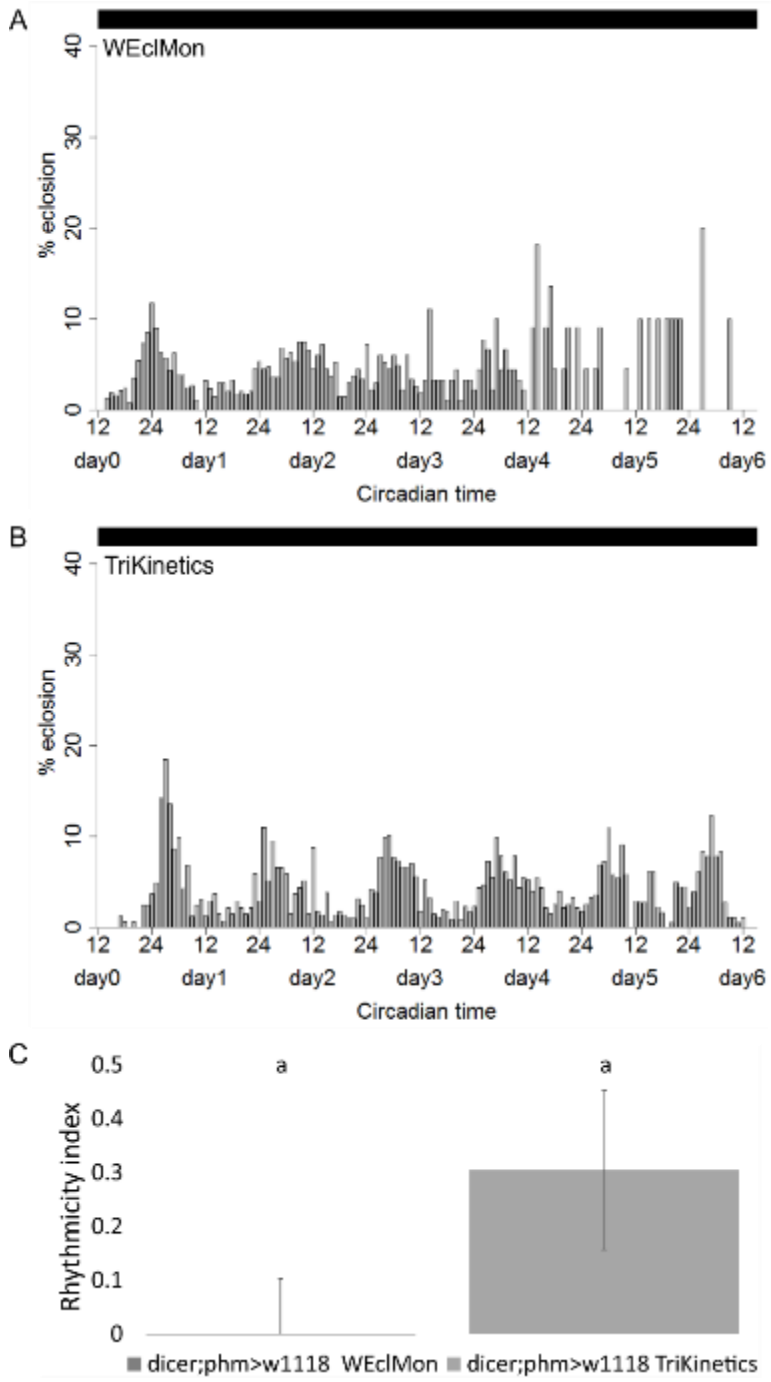

Figure S 2: Comparison between the WEclMon with constant red light and the TriKinetics system under DD conditions

Eclosion profiles for populations of w^{1118} > *dicer2*; *phm* recorded in the WEclMon (A) and the TriKinetics system (B) under DD conditions. Each bar represents the percentage of eclosed flies per hour normalized to the number of eclosed flies per day. The black rectangles represent the light regime. (C) shows the means of the rhythmicity indices (±SD). Different letters above columns indicate significant difference ($p<0.05$). Experiments in the WEclMon were performed under constant red light (λ=635 nm). (N=7, 2; n=1097, 1427)

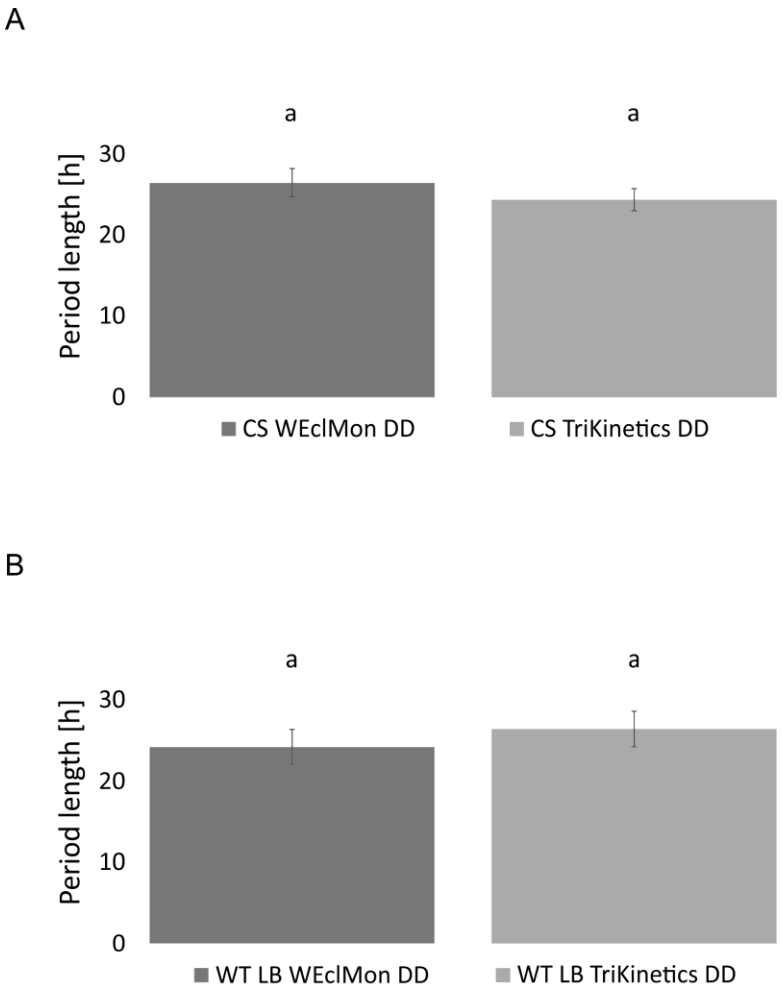

Figure S 3: Period lengths of the wildtypes *Canton S* and *Lindelbach* under DD conditions
Means of the period lengths (±SD) of the wildtypes *Canton S* (A) and *Lindelbach* (B) recorded with the WEclMon and the TriKinetics system under DD conditions. Different letters above columns indicate significant difference ($p<0.05$). (N=5, 4; 5, 3)

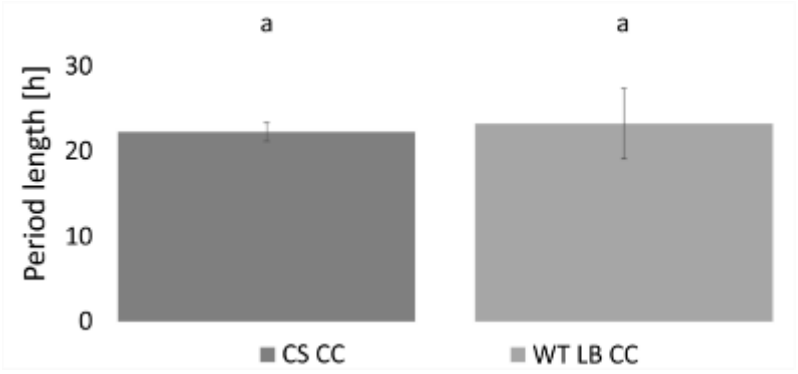

Figure S 4: Period lengths of the wildtypes *Canton S and Lindelbach* under CC conditions
Means of the period lengths (±SD) of the wildtypes *Canton S* (A) and *Lindelbach* (B) recorded with the WEclMon system under CC conditions. Different letters above columns indicate significant difference ($p<0.05$). (N=8, 6)

Figure S 5: Enclosure for the monitoring of eclosion under natural conditions at the bee station of the University of Würzburg (Theodor-Boveri-Weg 6, 97074 Würzburg; 49°46'46.8"N 9°58'30.6"E)

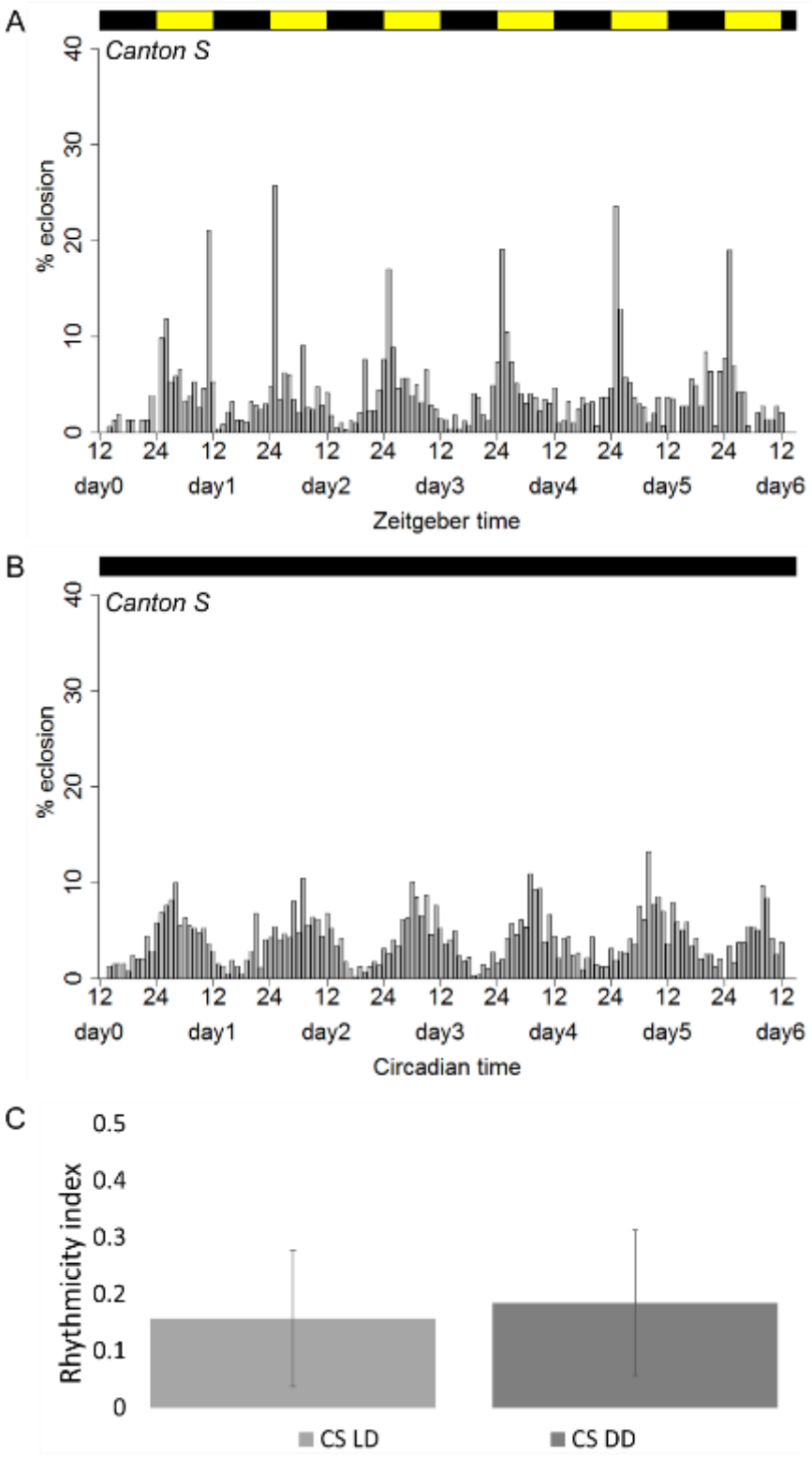

Figure S 6: Eclosion rhythms of *Canton S* under light entrainment
Eclosion profiles of *Canton S* under LD conditions (A) and DD conditions (B). Each bar represents the percentage of eclosed flies per hour normalized to the number of eclosed flies per day. The black and yellow rectangles represent the light regime. (C) shows the means of the rhythmicity indices (±SD). (N=4, 4; n=2223, 2648)

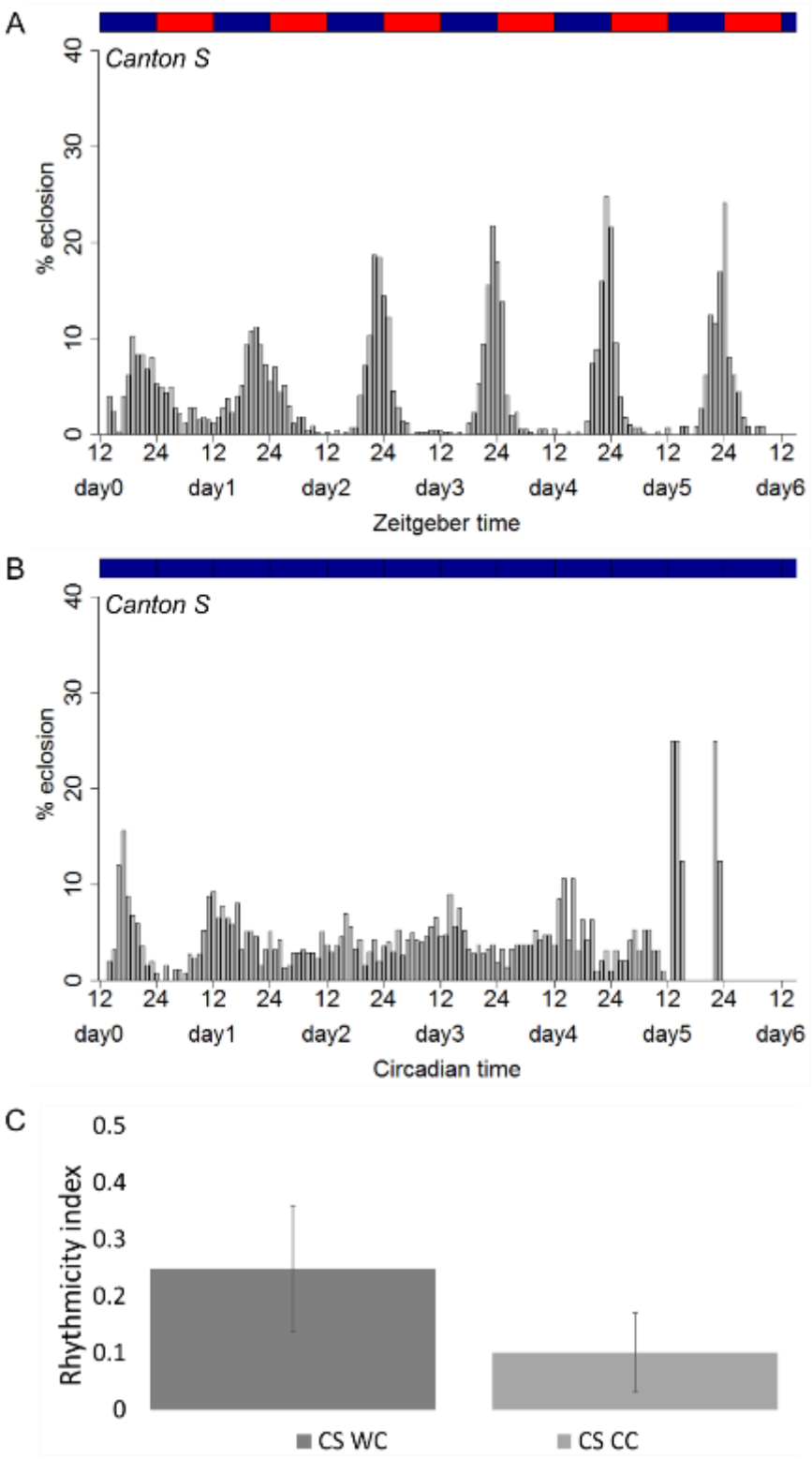

Figure S 7: Eclosion rhythms of *Canton S* under temperature entrainment
Eclosion profiles of *Canton S* under WC conditions (A) and CC conditions (B). Each bar represents the percentage of eclosed flies per hour normalized to the number of eclosed flies per day. The blue and red rectangles represent the temperature regime. (C) shows the means of the rhythmicity indices (±SD). (N=12, 8; n=1907, 1234)

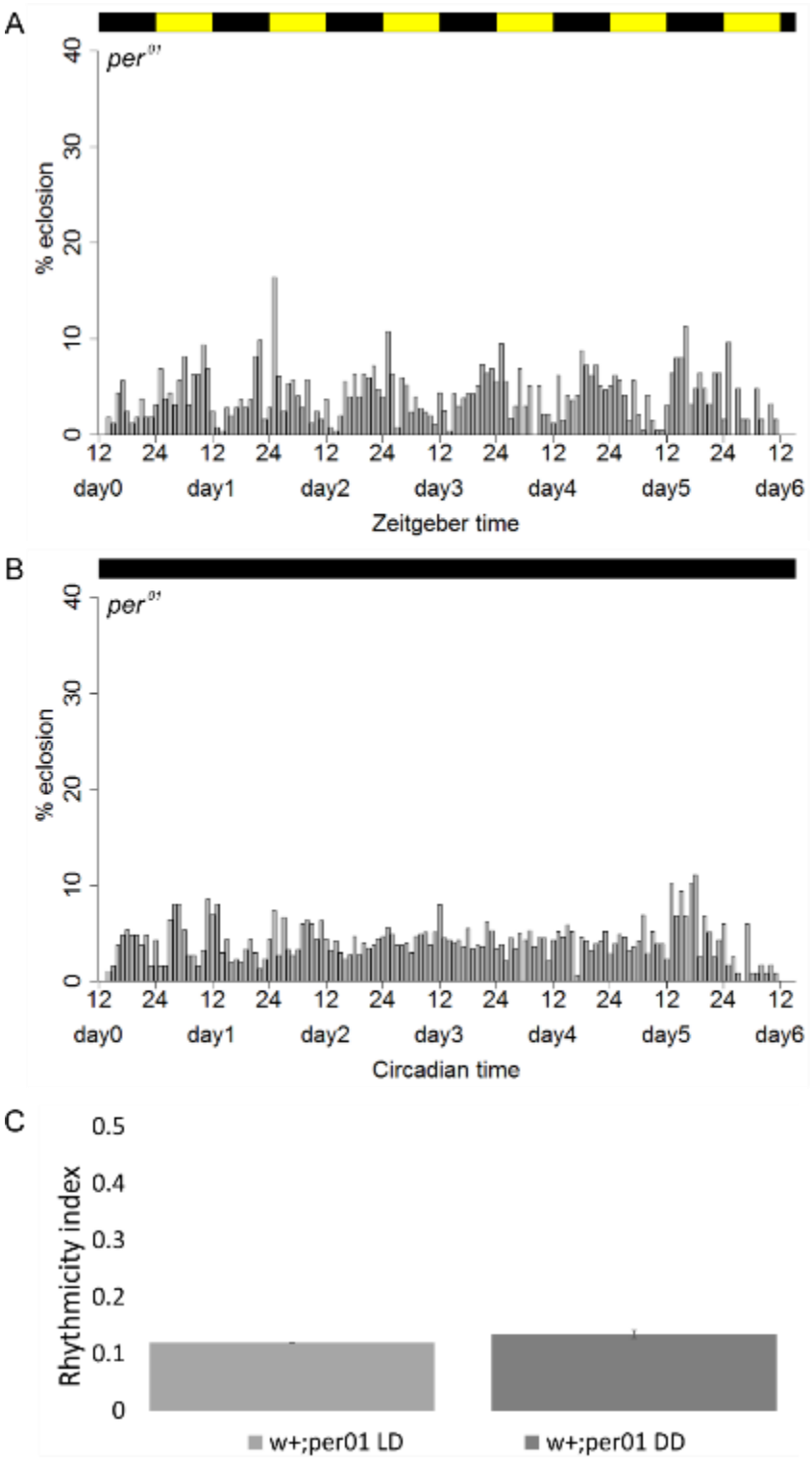

Figure S 8: Eclosion rhythms of the *per*^{01} mutant under light entrainment
Eclosion profiles of *per*^{01} under LD conditions (A) and DD conditions (B). Each bar represents the percentage of eclosed flies per hour normalized to the number of eclosed flies per day. The black and yellow rectangles represent the light regime. (C) shows the means of the rhythmicity indices (±SD). (N=2, 2; n=1148, 1756)

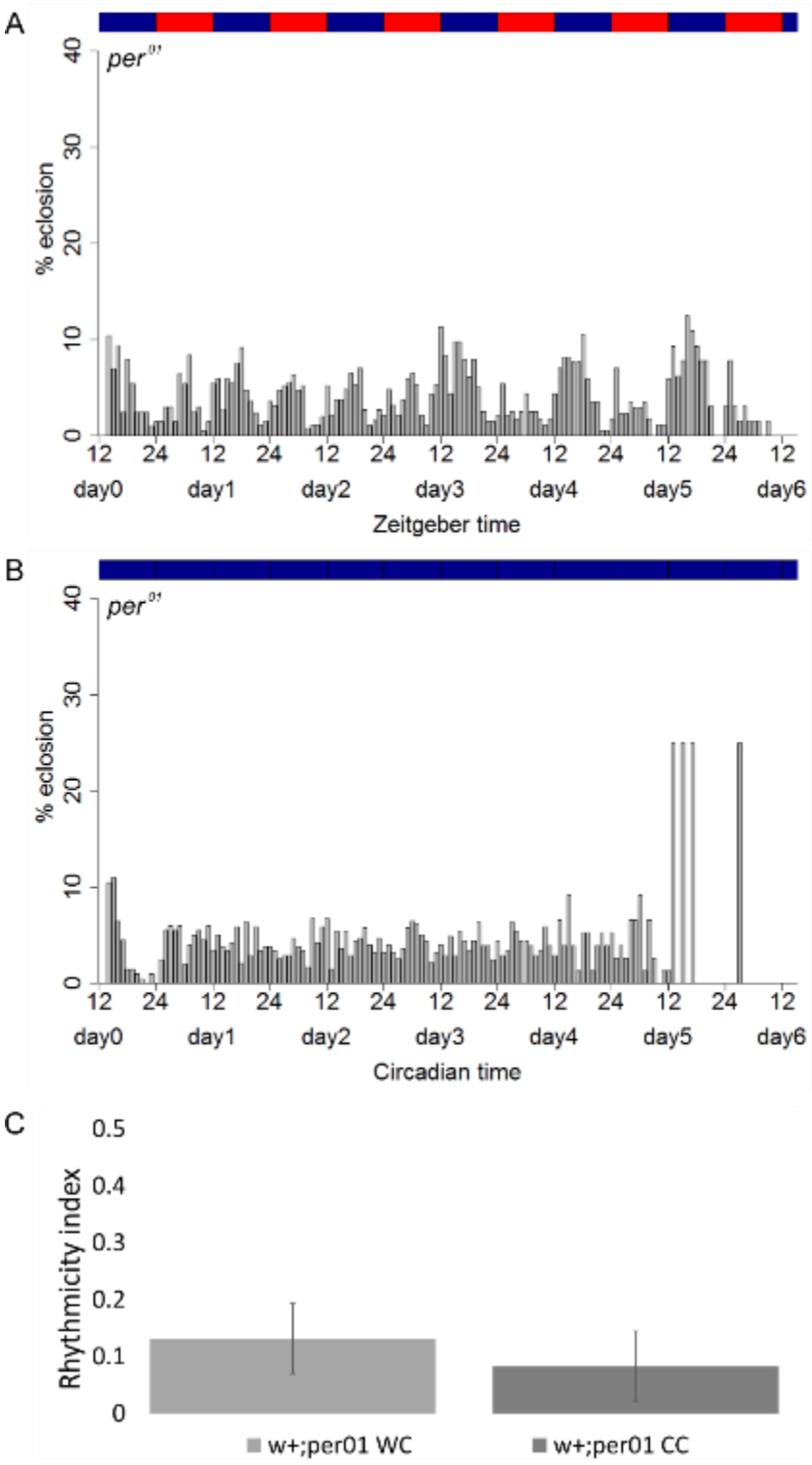

Figure S 9: Eclosion rhythms of the *per*^{01} mutant under temperature entrainment
Eclosion profiles of *per*^{01} under WC conditions (A) and CC conditions (B). Each bar represents the percentage of eclosed flies per hour normalized to the number of eclosed flies per day. The blue and red rectangles represent the temperature regime. (C) shows the means of the rhythmicity indices (±SD). (N=6, 6; n=1146, 995)

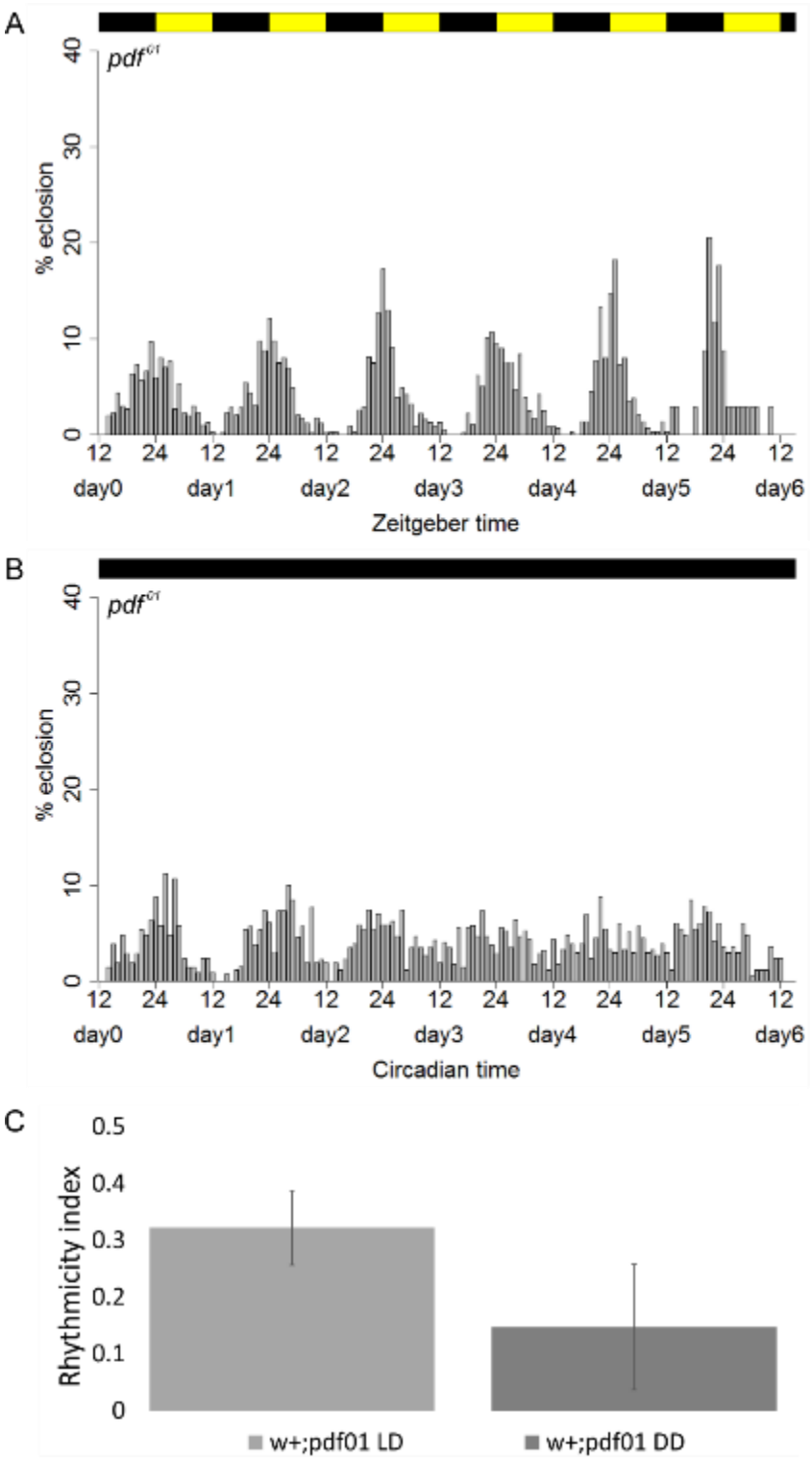

Figure S 10: Eclosion rhythms of the *pdf*^{01} mutant under light entrainment
Eclosion profiles of *pdf*^{01} under LD conditions (A) and DD conditions (B). Each bar represents the percentage of eclosed flies per hour normalized to the number of eclosed flies per day. The black and yellow rectangles represent the light regime. (C) shows the means of the rhythmicity indices (±SD). (N=4, 4; n=1672, 1556)

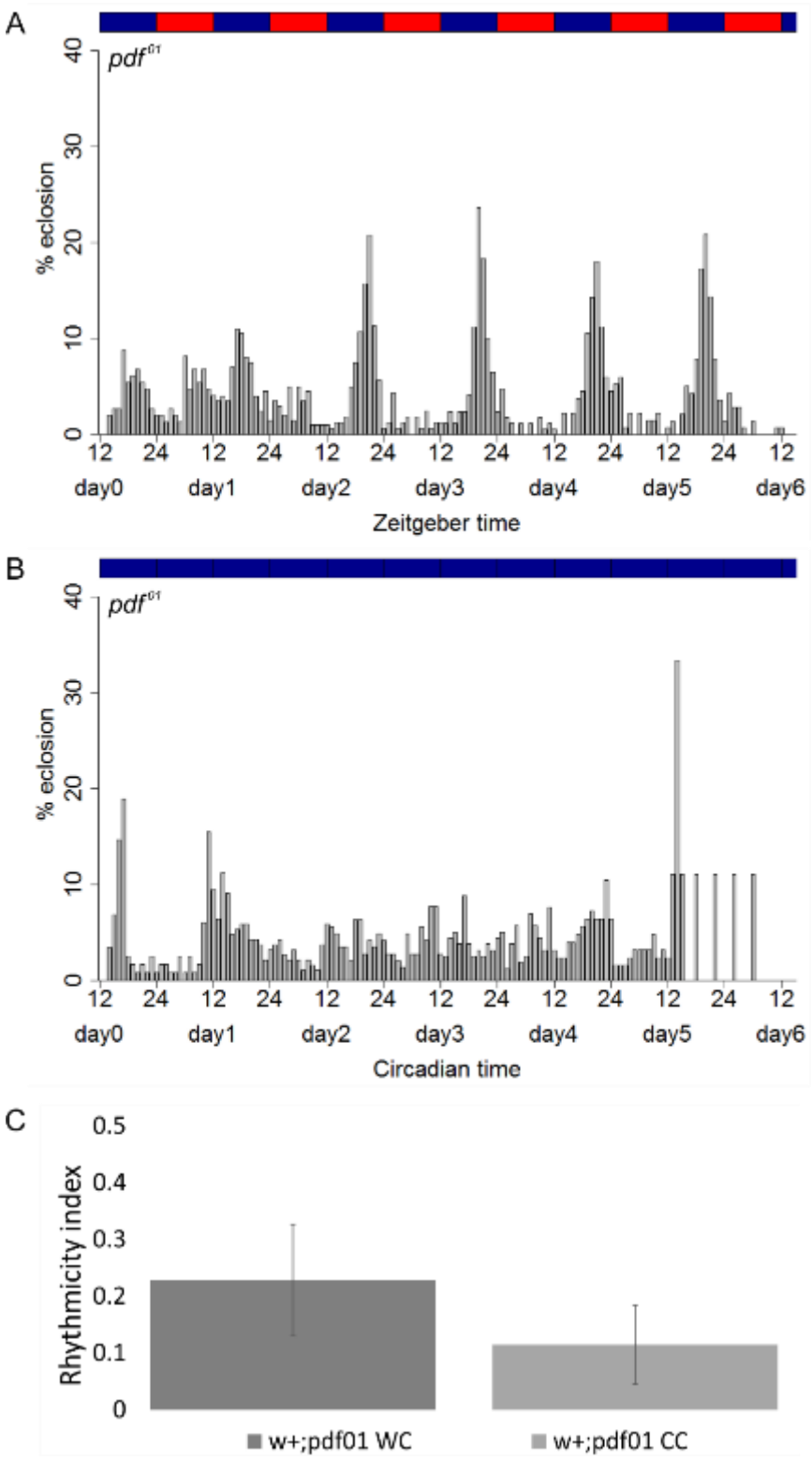

Figure S 11: Eclosion rhythms of the *pdf*^{01} mutant under temperature entrainment
Eclosion profiles of *pdf*^{01} under WC conditions (A) and CC conditions (B). Each bar represents the percentage of eclosed flies per hour normalized to the number of eclosed flies per day. The blue and red rectangles represent the temperature regime. (C) shows the means of the rhythmicity indices (±SD). (N=12, 8; n=948, 735)

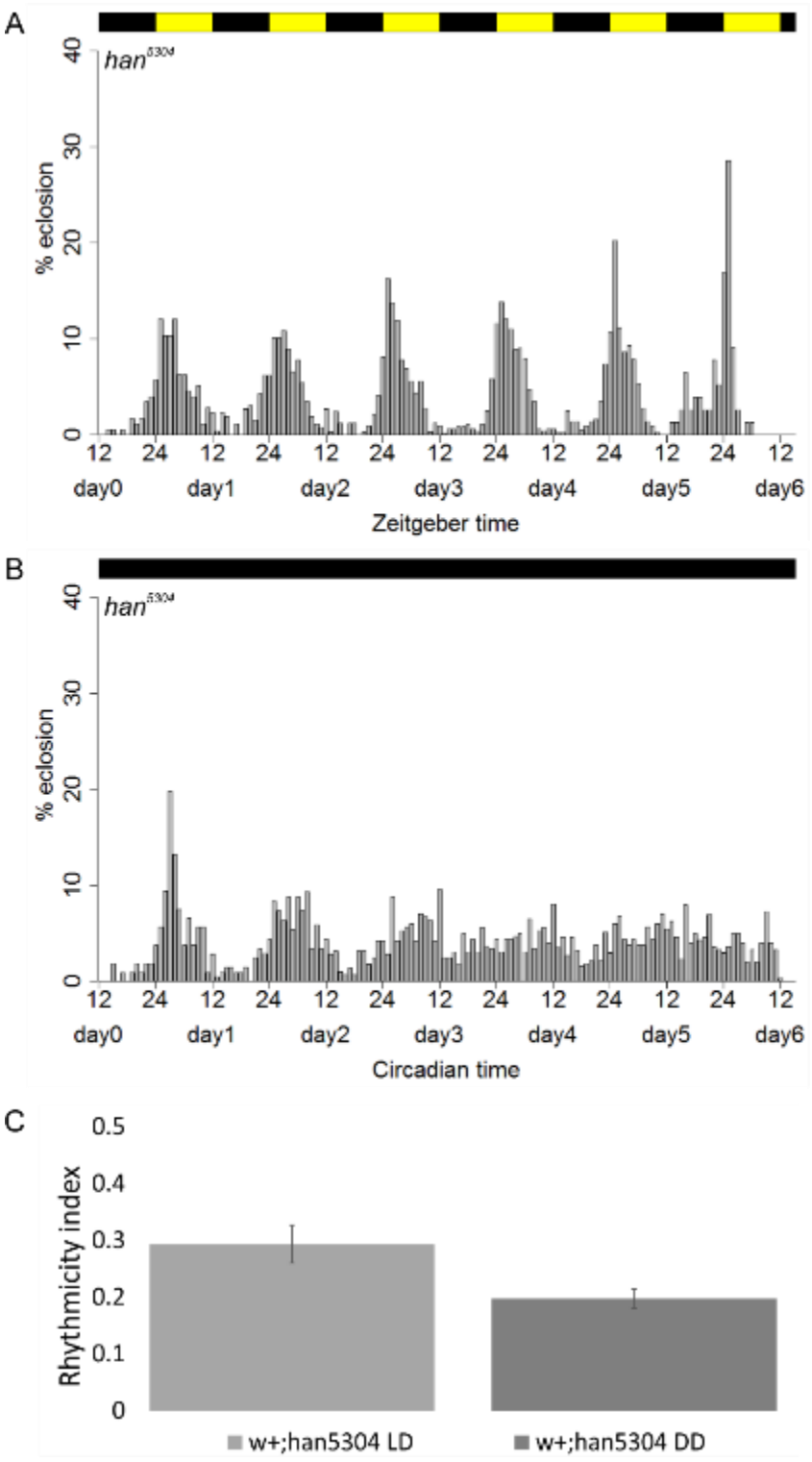

Figure S 12: Eclosion rhythms of the *han^{5304}* mutant under light entrainment
Eclosion profiles of *han^{53041}* under LD conditions (A) and DD conditions (B). Each bar represents the percentage of eclosed flies per hour normalized to the number of eclosed flies per day. The black and yellow rectangles represent the light regime. (C) shows the means of the rhythmicity indices (±SD). (N=6, 4; n=1724, 1707)

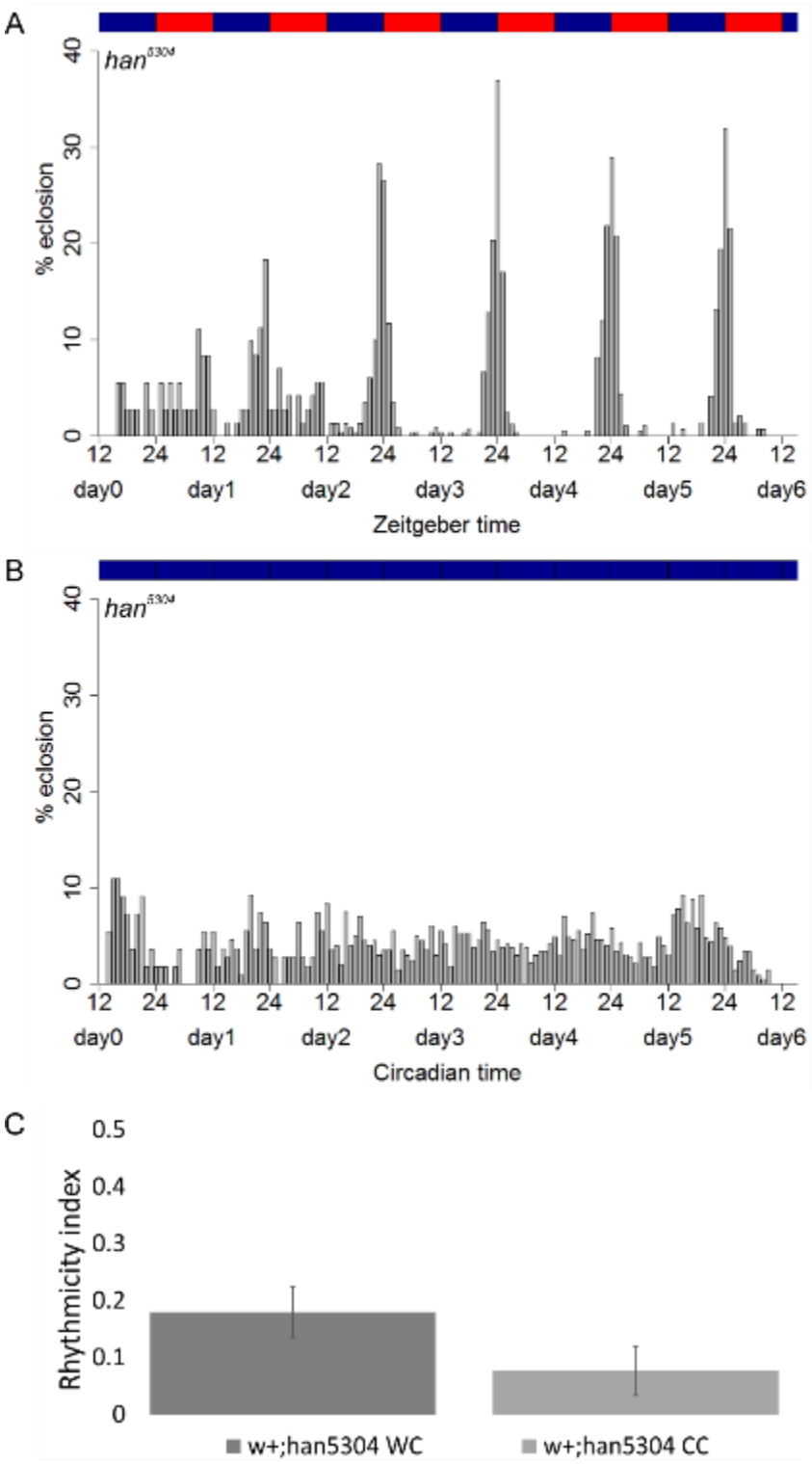

Figure S 13: Eclosion rhythms of the *han^{5304}* mutant under temperature entrainment
Eclosion profiles of *han^{5304}* under WC conditions (A) and CC conditions (B). Each bar represents the percentage of eclosed flies per hour normalized to the number of eclosed flies per day. The blue and red rectangles represent the temperature regime. (C) shows the means of the rhythmicity indices (±SD). (N=5, 7; n=905, 1157)

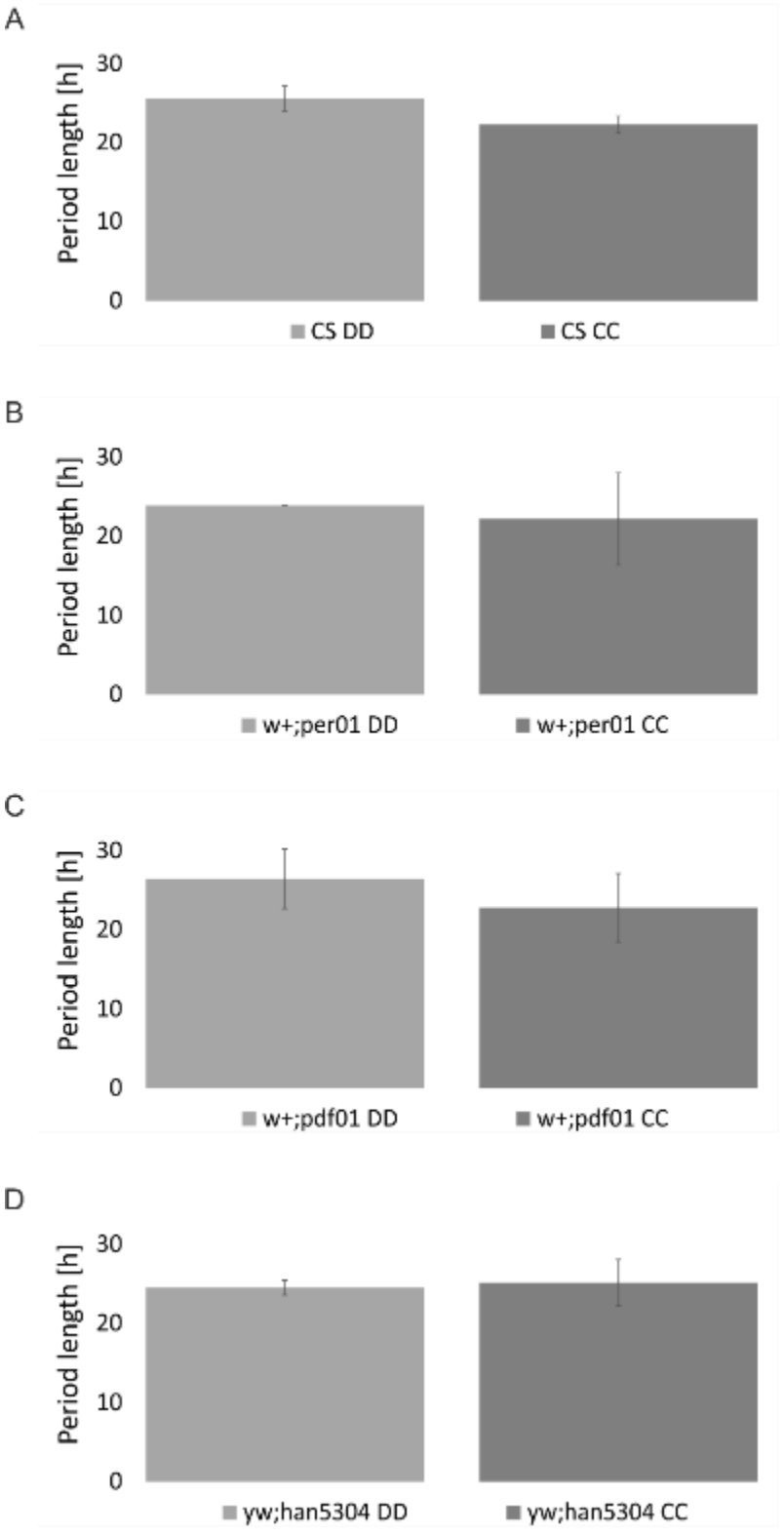

Figure S 14: Period lengths of *Canton S*, *per*^{01}, *pdf*^{01} and *han*^{5304} under DD and CC conditions

Means of the period lengths (±SD) under DD and CC conditions of *Canton S* (A), *per*^{01} (B), *pdf*^{01} (C) and *han*^{5304} (D).

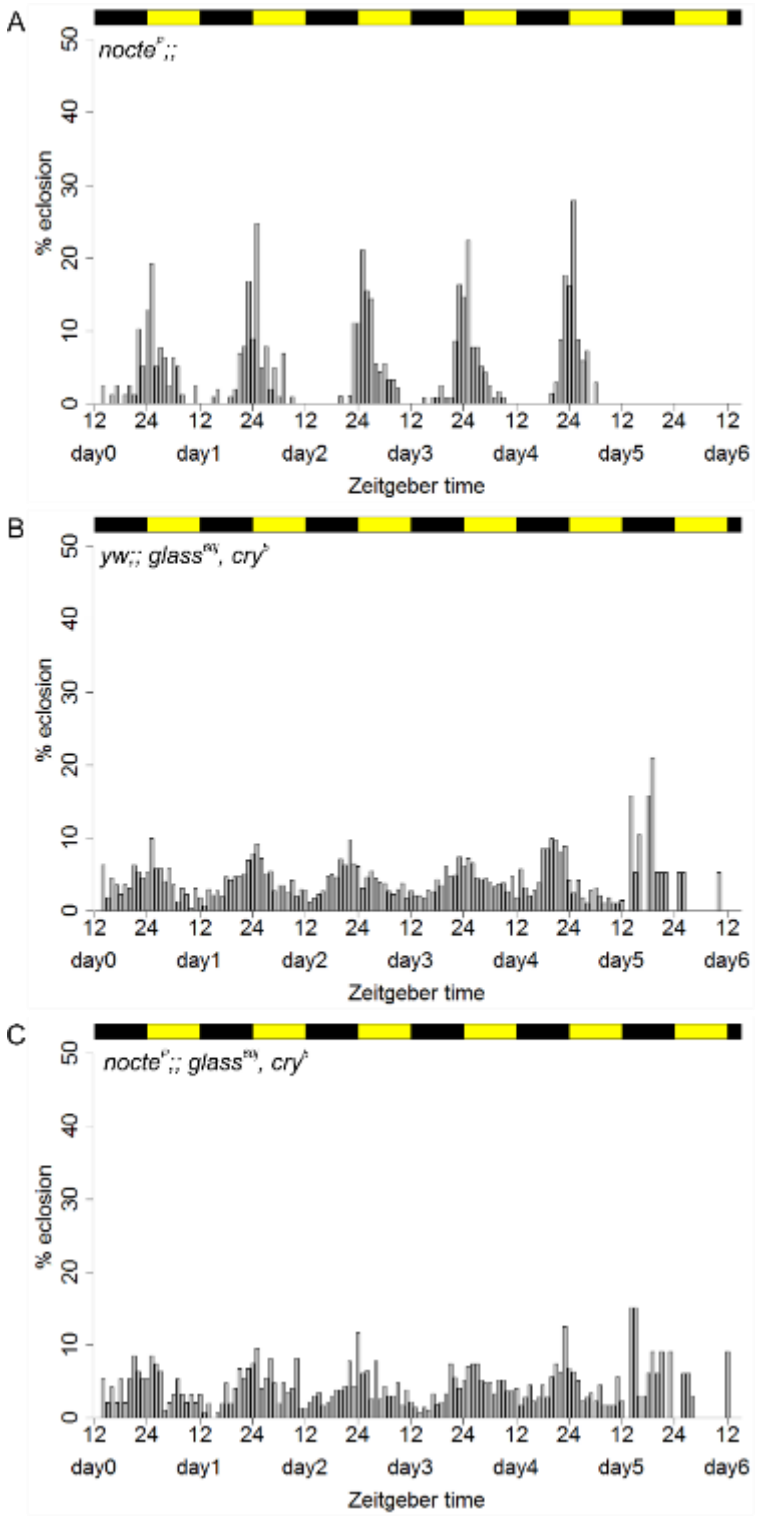

Figure S 15: Eclosion rhythms of temperature and light detection mutants under LD conditions

Eclosion profiles for populations of the temperature defective *nocte*^{P} mutant (A), the blind *yw;; glass*^{60j}*, cry*^{b} mutant (B) and the *nocte*^{P}*;; glass*^{60j}*, cry*^{b} double mutant (C) under LD conditions. Each bar represents the percentage of eclosed flies per hour normalized to the number of eclosed flies per day. The black and yellow rectangles represent the light regime. (N=1, 3, 2; n=455, 1888, 951)

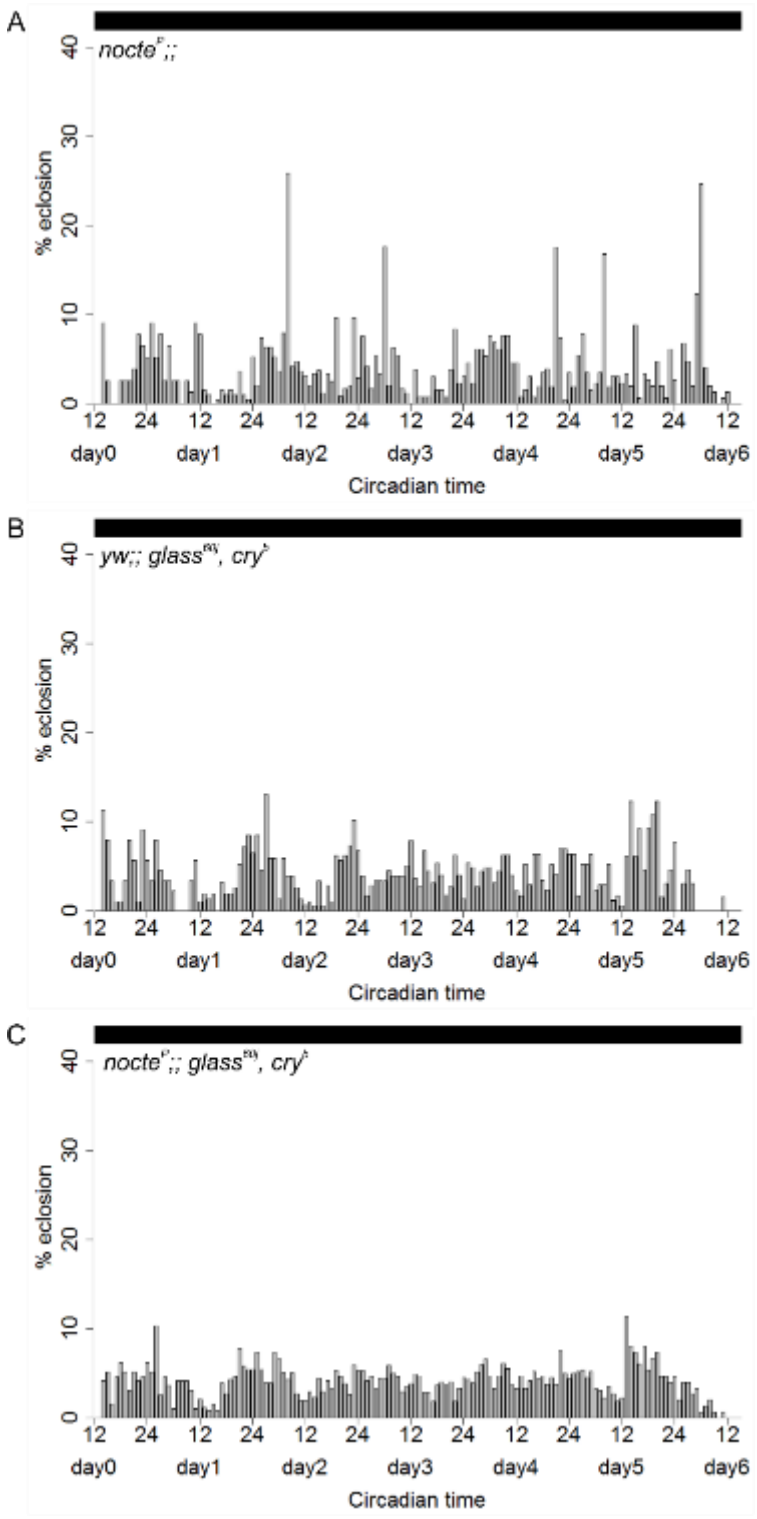

Figure S 16: Eclosion rhythms of temperature and light detection mutants under DD conditions

Eclosion profiles for populations of the temperature defective *nocte*^{P} mutant (A), the blind *yw;; glass*^{60j}*, cry*^{b} mutant (B) and the *nocte*^{P}*;; glass*^{60j}*, cry*^{b} double mutant (C) under DD conditions. Each bar represents the percentage of eclosed flies per hour normalized to the number of eclosed flies per day. The black rectangles represent the light regime. (N=2, 1, 2; n=1056, 879, 1908)

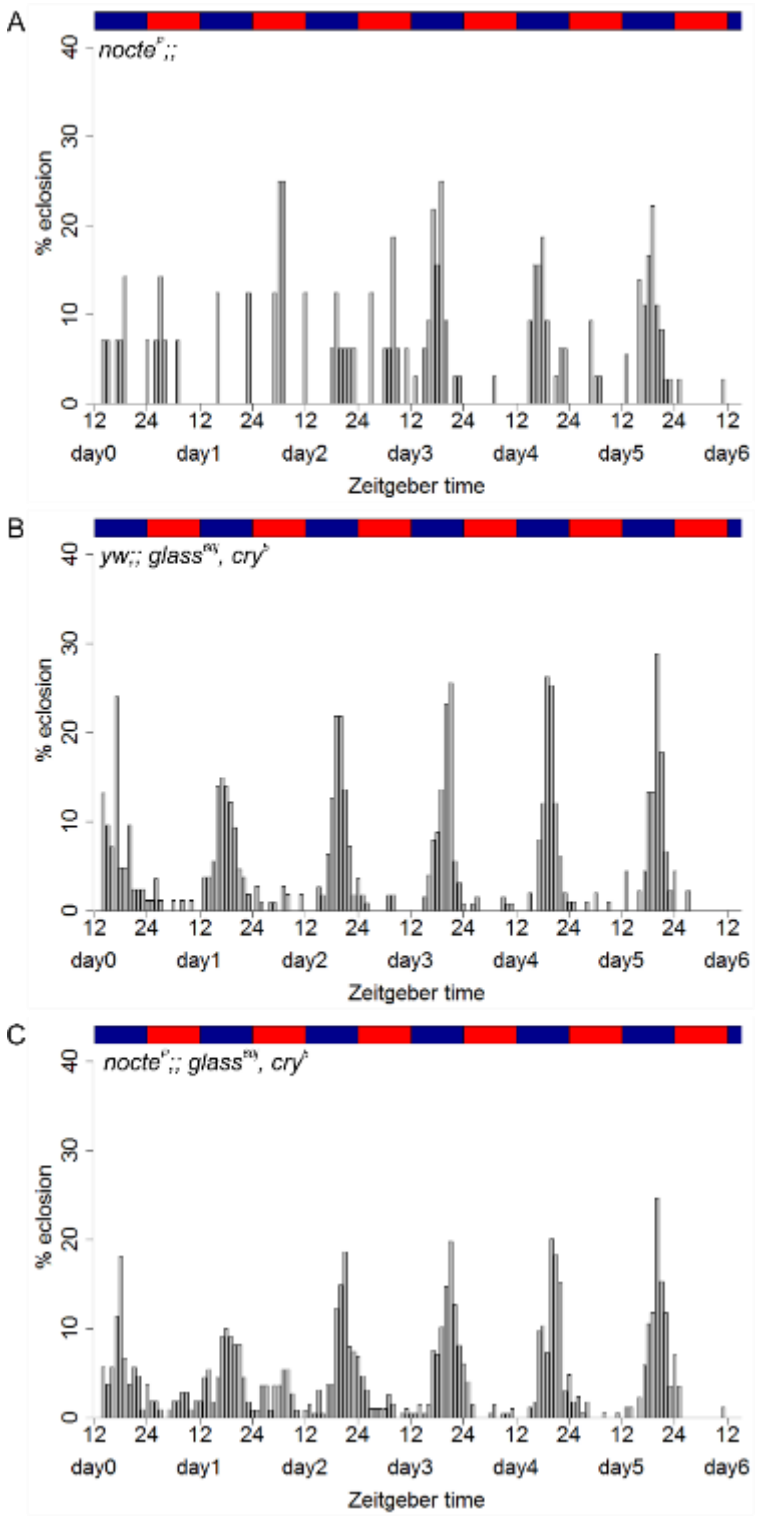

Figure S 17: Eclosion rhythms of temperature and light detections mutants under WC conditions

Eclosion profiles for populations of the temperature defective *nocte*^{P} mutant (A), the blind *yw;; glass*^{60j}*, cry*^{b} mutant (B) and the *nocte*^{P}*;; glass*^{60j}*, cry*^{b} double mutant (C) under WC (25°C:16°C) conditions. Each bar represents the percentage of eclosed flies per hour normalized to the number of eclosed flies per day. The blue and red rectangles represent the temperature regime. Experiments were performed under constant red light. (N=2, 4, 4; n=138, 577, 862)

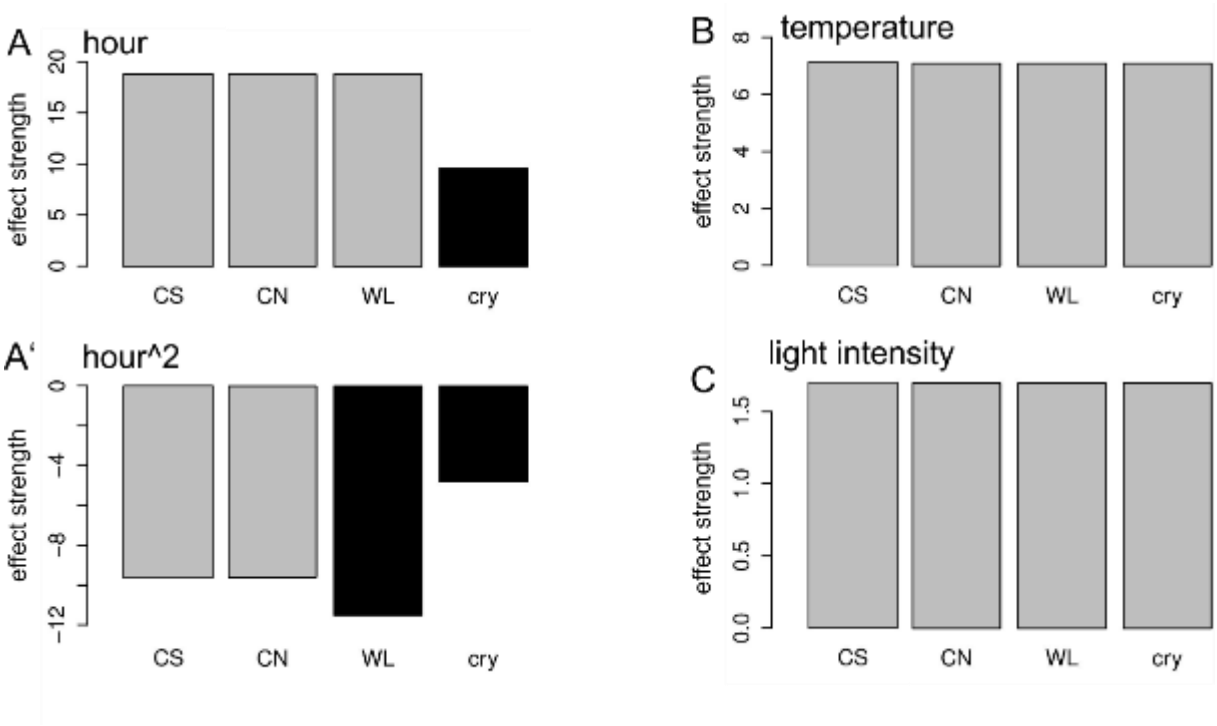

Figure S 18: Effect of the clock and abiotic factors on the daily eclosion pattern for data from 2015

Results of the statistical modelling of the effect strength of the clock (A, A') and of the abiotic parameters temperature (B) and light intensity (C) on the daily eclosion pattern. Effects in the wildtypes *Canton S* (CN) and *Lindelbach* (WL) as well as in the blind *yw;; glass*^{60j}*, cry*^{b} mutant (cry) from 2015 were analyzed and compared to the wildtype *Canton S* (CS) from 2014. Black bars in the mutant stand for a significant difference, gray bars for no significant difference.

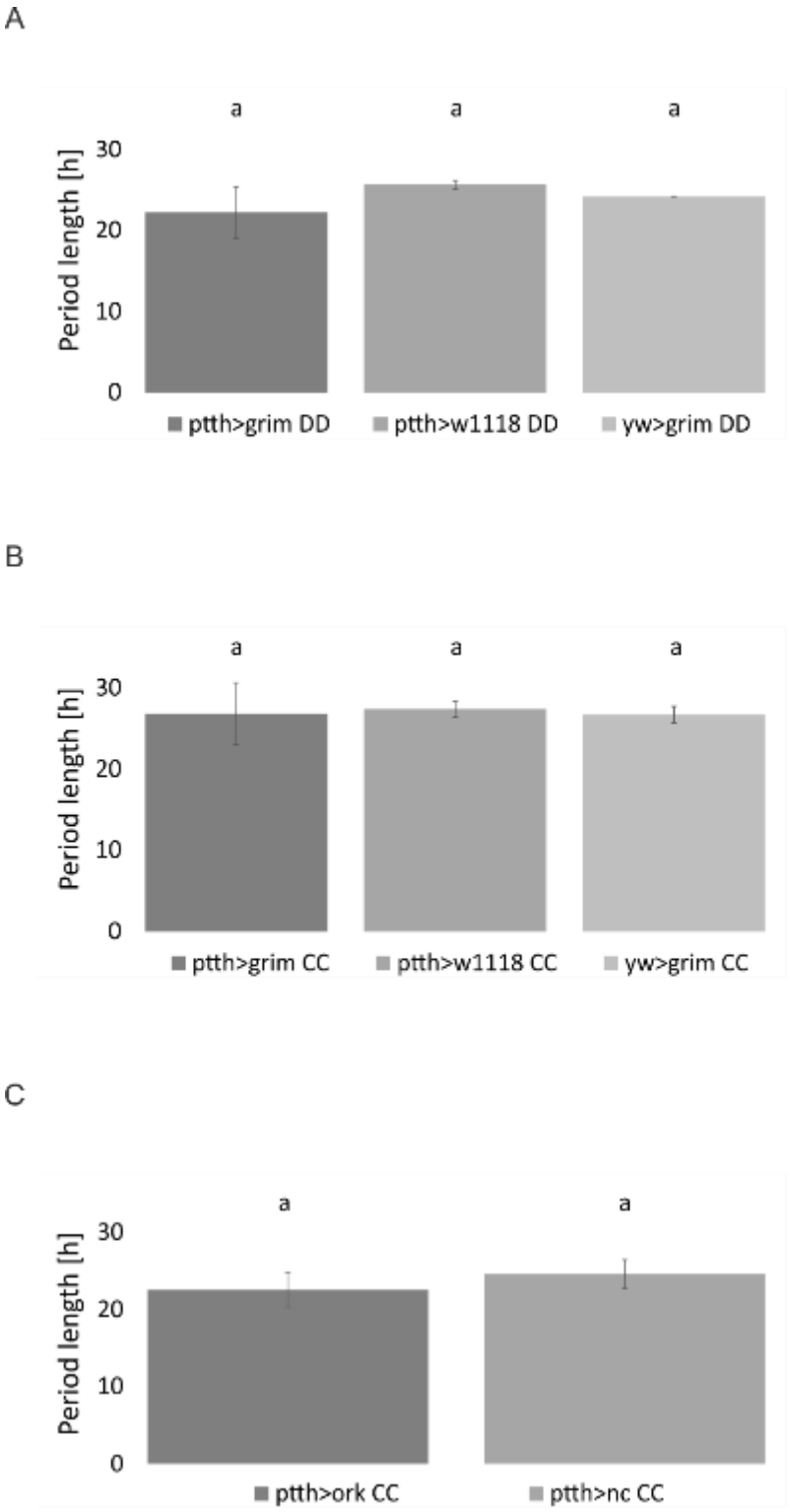

Figure S 19: Period lengths under constant conditions after ablation and silencing of the PTTH neurons

Means of the period lengths (±SD) after ablation (A, B) and silencing (C) of the PTTH neurons and the respective controls under DD (A, C) and CC (B) conditions. Different letters above columns indicate significant difference ($p<0.05$). (N=3, 3, 2; 7, 7, 6)

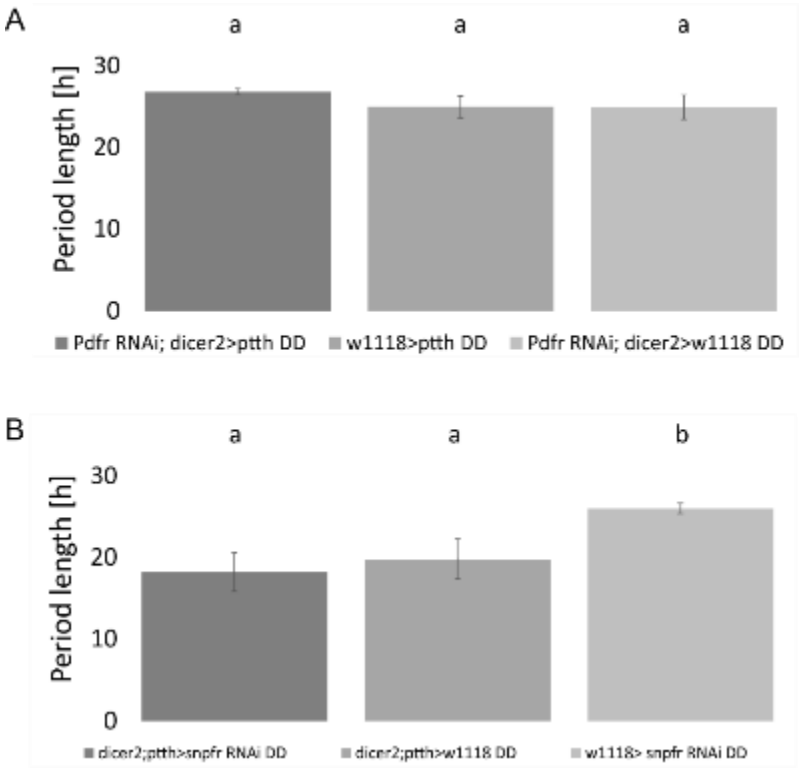

Figure S 20: Period lengths under DD conditions after knockdown of *Pdfr* and s*npfr* in PTTH neurons
Means of the period lengths (±SD) after knockdown of *Pdfr* (A) and *snpfr* (B) in the PTTH neurons and the respective controls under DD conditions. Different letters above columns indicate significant difference ($p<0.05$). (N=4, 4, 4; 6, 4, 4; 5, 2, 1)

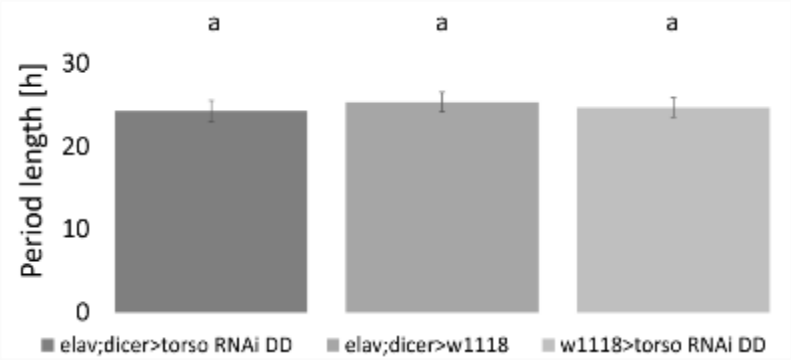

Figure S 21: Period lengths under DD conditions after knockdown of *torso i*n the brain
Means of the period lengths (±SD) after pan neuronal knockdown of *torso* and the respective controls under DD conditions. Different letters above columns indicate significant difference ($p<0.05$). (N=4, 3, 3)

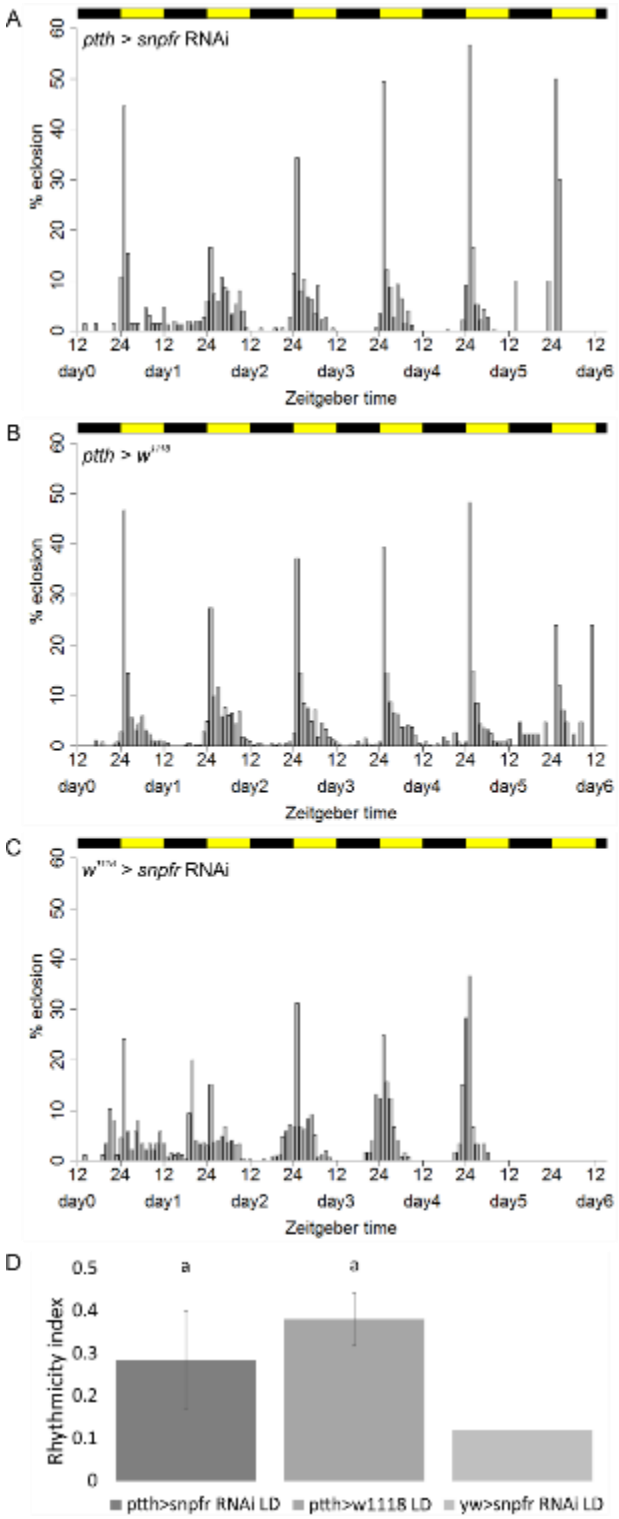

Figure S 22: Eclosion rhythms under LD conditions after knockdown of *snpfr* in PTTH neurons without dicer

Eclosion profiles for populations expressing UAS-*snpfr* RNAi driven by *ptth*-GAL4 (A) and the respective controls (B: GAL4 control, C: UAS control) under LD conditions. Each bar represents the percentage of eclosed flies per hour normalized to the number of eclosed flies per day. The black and yellow rectangles represent the light regime. (D) shows the means of the rhythmicity indices (±SD). Different letters above columns indicate significant difference ($p<0.05$). (N=3, 3, 1; n=760, 1863, 727)

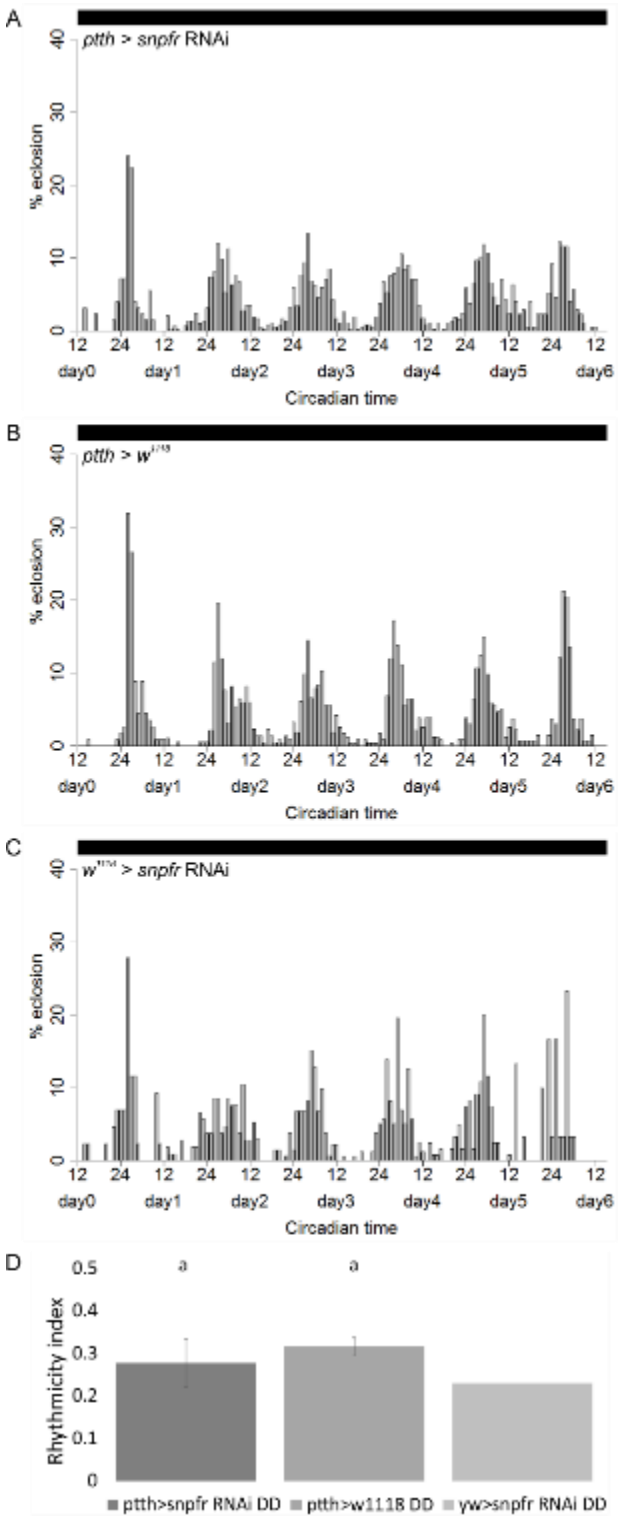

Figure S 23: Eclosion rhythms under DD conditions after knockdown of *snpfr* in PTTH neurons without dicer

Eclosion profiles for populations expressing UAS-*snpfr* RNAi driven by *ptth*-GAL4 (A) and the respective controls (B: GAL4 control, C: UAS control) under DD conditions. Each bar represents the percentage of eclosed flies per hour normalized to the number of eclosed flies per day. The black rectangles represent the light regime. (D) shows the means of the rhythmicity indices (±SD). Different letters above columns indicate significant difference ($p<0.05$). (N=5, 2, 1; n=1693, 1019, 465)

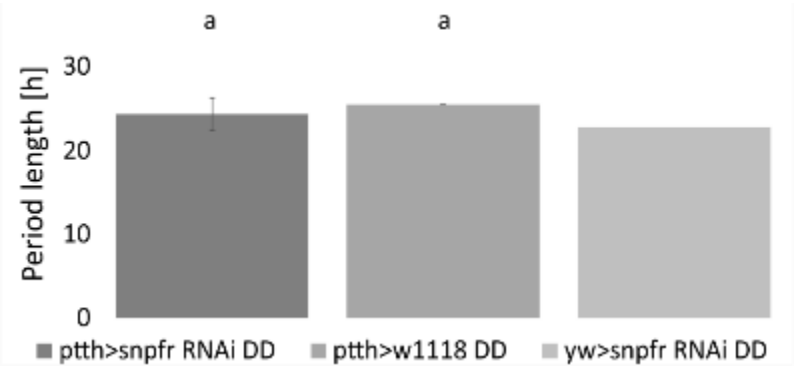

Figure S 24: Period lengths under DD conditions after knockdown of *snpfr* in PTTH neurons without dicer
Means of the period lengths (±SD) after knockdown of *snpfr* in PTTH neurons without dicer and the respective controls under DD conditions. Different letters above columns indicate significant difference ($p<0.05$). (N=4, 2, 1)

A

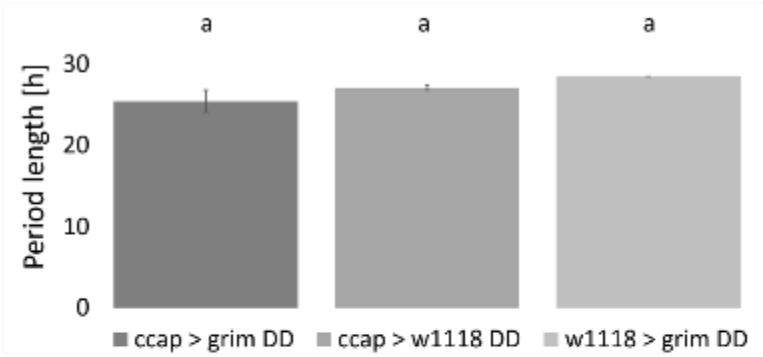

B

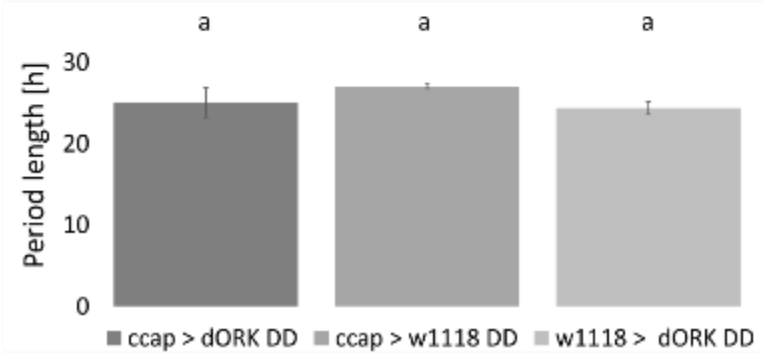

Figure S 25: Period lengths under DD conditions after ablation and silencing of CCAP neurons
Means of the period lengths (±SD) after ablation (A) and silencing (B) of CCAP neurons and the respective controls under DD conditions. Different letters above columns indicate significant difference ($p<0.05$). (N=3, 2, 1; 6, 2, 3)

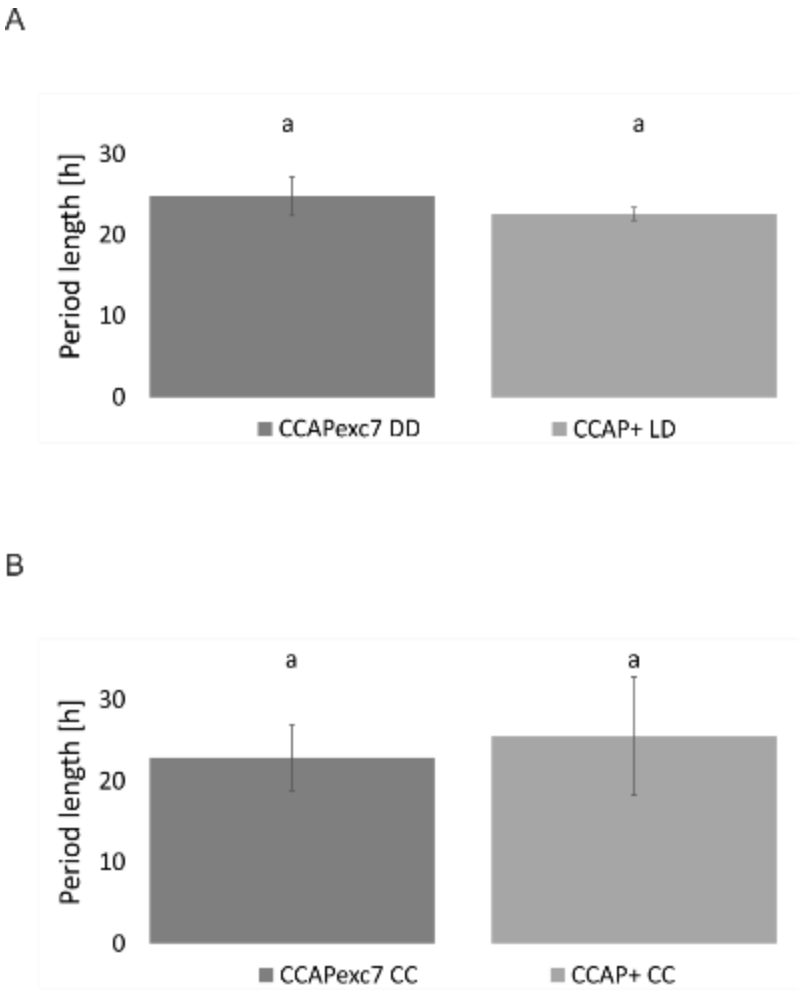

Figure S 26: Period lengths of the *CCAP^{exc7}* mutant under constant conditions
Means of the period lengths (±SD) of the *CCAP^{exc7}* mutant and the control under DD (A) and CC (B) conditions. Different letters above columns indicate significant difference ($p<0.05$). (N=3, 4; 2, 2)

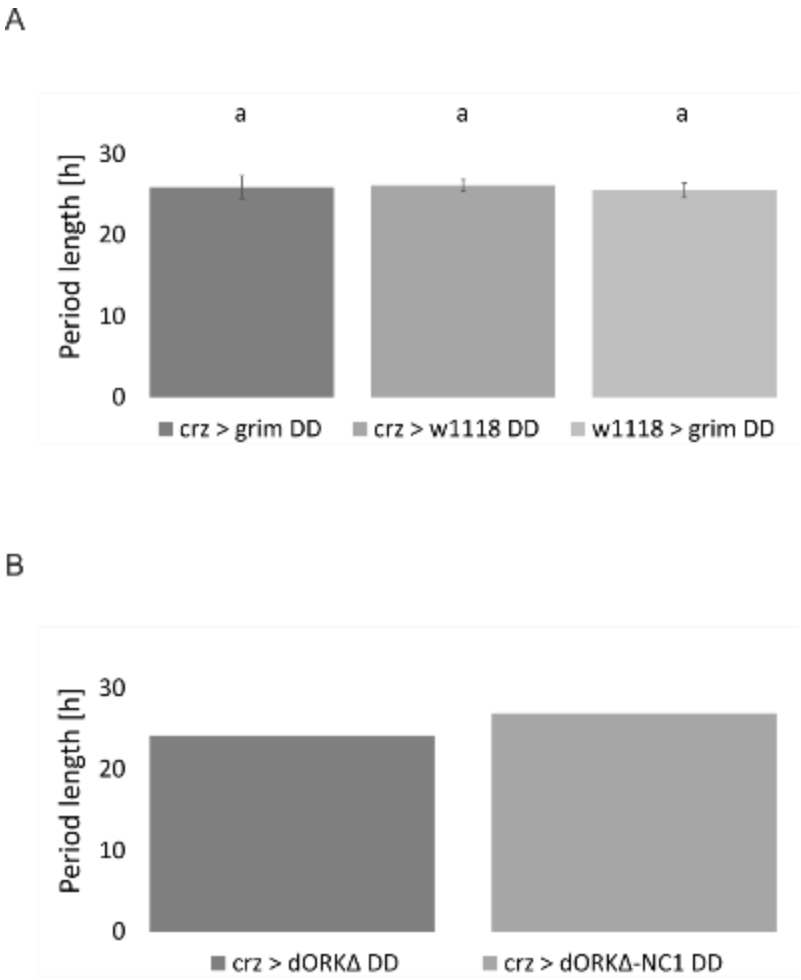

Figure S 27: Period lengths after the ablation and silencing of Crz neurons under DD conditions
Means of the period lengths (±SD) after ablation (A) and silencing (B) of the Crz neurons and the respective controls under DD conditions. Different letters above columns indicate significant difference ($p<0.05$). (N=2, 3, 2; 1, 1)

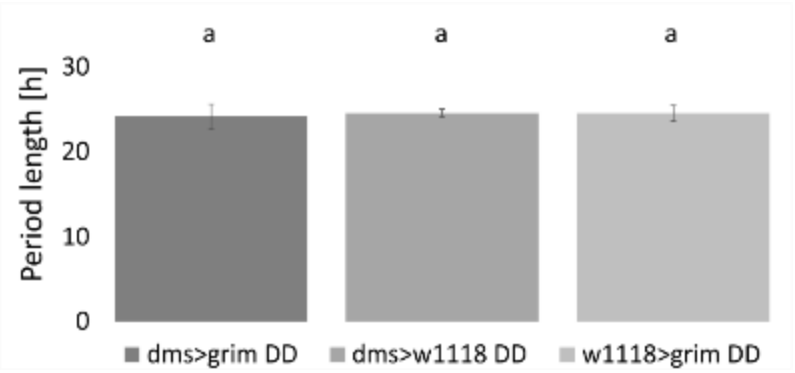

Figure S 28: Period lengths after the ablation of DMS neurons under DD conditions
Means of the period lengths (±SD) after silencing of the DMS neurons and the respective controls under DD conditions. Different letters above columns indicate significant difference ($p<0.05$). (N=2, 2, 2)

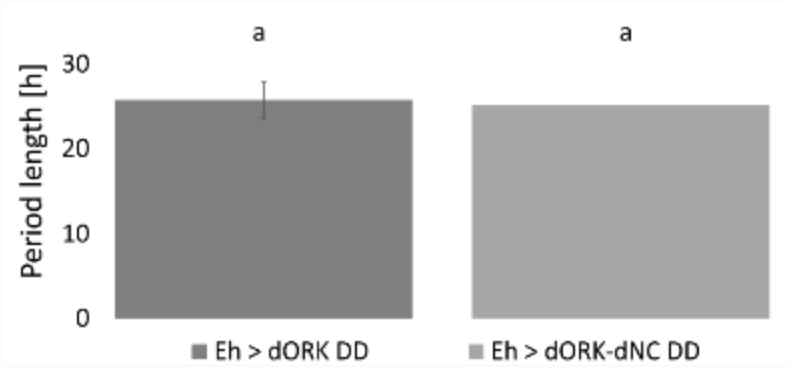

Figure S 29: Period lengths after silencing of EH neurons under DD conditions
Means of the period lengths (±SD) after silencing of EH neurons and the respective control under DD conditions. Different letters above columns indicate significant difference ($p<0.05$). (N=2, 1)

References

Allada, R., White, N. E., So, W. V., Hall, J. C. and Rosbash, M. (1998) A mutant *Drosophila* homolog of mammalian Clock disrupts circadian rhythms and transcription of period and timeless. Cell, 93, 791-804.

Allemand, R. (1976a) Influence of light condition modification on the circadian rhythm of vitellogenesis and ovulation in *Drosophila melanogaster*. Journal of Insect Physiology, 22, 1075-1080.

Allemand, R. (1976b) Rhythm of vitellogenesis and ovulation in photoperiod LD 12:12 of *Drosophila melanogaster*. Journal of Insect Physiology, 22, 1031-1035.

Ampleford, E. J. and Steel, C. G. (1985) Circadian control of a daily rhythm in hemolymph ecdysteroid titer in the insect *Rhodnius prolixus* (Hemiptera). General and Comparative Endocrinology, 59, 453-459.

Bader, R., Colomb, J., Pankratz, B., Schrock, A., Stocker, R. F. and Pankratz, M. J. (2007) Genetic dissection of neural circuit anatomy underlying feeding behavior in *Drosophila*: distinct classes of hugin-expressing neurons. Journal of Comparative Neurology, 502, 848-856.

Bainbridge, P. S. and Bownes, M. (1988) Ecdysteroid titers during *Drosophila* metamorphosis. Insect Biochemistry.

Beaver, L. M., Gvakharia, B. O., Vollintine, T. S., Hege, D. M., Stanewsky, R. and Giebultowicz, J. M. (2002) Loss of circadian clock function decreases reproductive fitness in males of *Drosophila melanogaster*. Proceedings of the National Academy of Sciences of the United States of America, 99, 2134-2139.

Becnel, J., Johnson, O., Luo, J., Nässel, D. R. and Nichols, C. D. (2011) The serotonin 5-HT7Dro receptor is expressed in the brain of *Drosophila*, and is essential for normal courtship and mating. PLoS One, 6, e20800.

Beltramí, M., Medina-Muñoz, M. C., Arce, D. and Godoy-Herrera, R. (2009) *Drosophila* pupation behavior in the wild. Evolutionary Ecology, 24, 347-358.

Benito, J., Houl, J. H., Roman, G. W. and Hardin, P. E. (2008) The blue-light photoreceptor CRYPTOCHROME is expressed in a subset of circadian oscillator neurons in the *Drosophila* CNS. Journal of Biological Rhytms, 23, 296-307.

Berry, J. A., Cervantes-Sandoval, I., Nicholas, E. P. and Davis, R. L. (2012) Dopamine is required for learning and forgetting in *Drosophila*. Neuron, 74, 530-542.

Blanchardon, E., Grima, B., Klarsfeld, A., Chelot, E., Hardin, P. E., Preat, T. and Rouyer, F. (2001) Defining the role of *Drosophila* lateral neurons in the control of circadian rhythms in motor activity and eclosion by targeted genetic ablation and PERIOD protein overexpression. The European Journal of Neuroscience, 13, 871-888.

Blau, J. and Young, M. W. (1999) Cycling vrille Expression Is Required for a Functional *Drosophila* Clock. Cell, 99, 661-671.

Bollenbacher, W. E., Agui, N., Granger, N. A. and L.I., G. (1979) In vitro activation of insect prothoracic glands by the prothoracicotropic hormone. roceedings of the National Academy of Sciences of the United States of America, 76, 5148 - 5152.

Brand, A. H. and Perrimon, N. (1993) Targeted gene expression as a means of altering cell fates and generating dominant phenotypes. Development, 118, 401-415.

Bremer, H. (1926) Über die tageszeitliche Konstanz im Schlupftermin der Imagines einiger Insekten und ihre experimentelle Beeinflussbarkeit. Zeitschrift für Wissenschaftliche Insektenbiologie, 21, 209-216.

Brown, M. R., Crim, J. W., Arata, R. C., Cai, H. N., Chun, C. and Shen, P. (1999) Identification of a *Drosophila* brain-gut peptide related to the neuropeptide Y family. Peptides, 20, 1035-1042.

Bünning, E. (1935) Zur Kenntnis der endogenen Tagesrhythmik bei Insekten und Pflanzen. Berichte der Deutschen Botanischen Gesellschaft, 53, 594-623.

Busza, A., Emery-Le, M., Rosbash, M. and Emery, P. (2004) Roles of the Two *Drosophila* CRYPTOCHROME Structural Domains in Circadian Photoreception. Science, 304, 1503-1506.

Busza, A., Murad, A. and Emery, P. (2007) Interactions between circadian neurons control temperature synchronization of *Drosophila* behavior. The Journal of Neuroscience: The officicial Journal of the Society for Neuroscience, 27, 10722-10733.

Bywalez, W., Menegazzi, P., Rieger, D., Schmid, B., Helfrich-Forster, C. and Yoshii, T. (2012) The dual-oscillator system of *Drosophila melanogaster* under natural-like temperature cycles. Chronobiology International, 29, 395-407.

Cabrero, P., Radford, J. C., Broderick, K. E., Costes, L., Veenstra, J. A., Spana, E. P., Davies, S. A. and Dow, J. A. (2002) The Dh gene of *Drosophila melanogaster* encodes a diuretic peptide that acts through cyclic AMP. The Journal of Experimental Biology, 205, 3799-3807.

Casali, A. and Casanova, J. (2001) The spatial control of Torso RTK activation: a C-terminal fragment of the Trunk protein acts as a signal for Torso receptor in the *Drosophila* embryo. Development, 128, 1709-1715.

Casanova, J. and Struhl, G. (1989) Localized surface activity of torso, a receptor tyrosine kinase, specifies terminal body pattern in *Drosophila*. Genes & Development, 3, 2025-2038.

Castle, W. E., Carpenter, F. W., Clark, A. H., Mast, S. O. and Barrows, W. M. (1906) The Effects of Inbreeding, Cross-Breeding, and Selection upon the Fertility and Variability of *Drosophila*. Proceedings of the American Academy of Arts and Sciences, 41, 731-786.

Cavanaugh, D. J., Geratowski, J. D., Wooltorton, J. R., Spaethling, J. M., Hector, C. E., Zheng, X., Johnson, E. C., Eberwine, J. H. and Sehgal, A. (2014) Identification of a circadian output circuit for rest:activity rhythms in *Drosophila*. Cell, 157, 689-701.

Ceriani, M. F., Darlington, T. K., Staknis, D., Más, P., Petti, A. A., Weitz, C. J. and Kay, S. A. (1999) Light-Dependent Sequestration of TIMELESS by CRYPTOCHROME. Science, 285, 553-556.

Chandler, J. A., Lang, J. M., Bhatnagar, S., Eisen, J. A. and Kopp, A. (2011) Bacterial communities of diverse *Drosophila* species: ecological context of a host-microbe model system. PLoS Genetics, 7, e1002272.

Chang, J. C., Yang, R. B., Adams, M. E. and Lu, K. H. (2009) Receptor guanylyl cyclases in Inka cells targeted by eclosion hormone. Proceedings of the National Academy of Sciences of the United States of America, 106, 13371-13376.

Chatterjee, A., Tanoue, S., Houl, J. H. and Hardin, P. E. (2010) Regulation of gustatory physiology and appetitive behavior by the *Drosophila* circadian clock. Current Biology, 20, 300-309.

Chen, J. (2012) Assaying the contribution of the prothoracic gland in timing eclosion behavior in *Drosophila melanogaster*. In Neurobiology and Genetics, Vol. Diploma University Würzburg, Würzburg.

Chen, W., Liu, Z., Li, T., Zhang, R., Xue, Y., Zhong, Y., Bai, W., Zhou, D. and Zhao, Z. (2014) Regulation of *Drosophila* circadian rhythms by miRNA let-7 is mediated by a regulatory cycle. Nature Communications, 5, 5549.

Cho, K. H., Daubnerová, I., Park, Y., Zitnan, D. and Adams, M. E. (2013) Secretory competence in a gateway endocrine cell conferred by the nuclear receptor βFTZ-F1 enables stage-specific ecdysone responses throughout development in *Drosophila*. Developmental Biology.

Choi, Y. J., Lee, G., Hall, J. C. and Park, J. H. (2005) Comparative analysis of Corazonin-encoding genes (Crz's) in *Drosophila* species and functional insights into Crz-expressing neurons. The Journal of Comparative Neurology, 482, 372-385.

Chown, S. L. and Gaston, K. J. (2010) Body size variation in insects: a macroecological perspective. Biological Reviews of the Cambridge Philosophical Society, 85, 139-169.

Clark, A. C., del Campo, M. L. and Ewer, J. (2004) Neuroendocrine control of larval ecdysis behavior in *Drosophila*: complex regulation by partially redundant neuropeptides. The Journal of Neuroscience : the official Journal of the Society for Neuroscience, 24, 4283-4292.

Coast, G. M., Webster, S. G., Schegg, K. M., Tobe, S. S. and Schooley, D. A. (2001) The *Drosophila melanogaster* homologue of an insect calcitonin-like diuretic peptide stimulates V-ATPase activity in fruit fly Malpighian tubules. The Journal of Experimental Biology, 204, 1795-1804.

Cohen, B., McGuffin, M. E., Pfeifle, C., Segal, D. and Cohen, S. M. (1992) apterous, a gene required for imaginal disc development in *Drosophila* encodes a member of the LIM family of developmental regulatory proteins. Genes & Development, 6, 715-729.

Cole, S. H., Carney, G. E., McClung, C. A., Willard, S. S., Taylor, B. J. and Hirsh, J. (2005) Two functional but noncomplementing *Drosophila* tyrosine decarboxylase genes: distinct roles for neural tyramine and octopamine in female fertility. The Journal of Biological Chemistry, 280, 14948-14955.

Collins, B. and Blau, J. (2007) Even a stopped clock tells the right time twice a day: circadian timekeeping in *Drosophila*. Pflugers Archiv : European Journal of Physiology, 454, 857-867.

Collins, B. H., Rosato, E. and Kyriacou, C. P. (2004) Seasonal behavior in *Drosophila melanogaster* requires the photoreceptors, the circadian clock, and phospholipase C. Proceedings of the National Academy of Sciences of the United States of America, 101, 1945-1950.

Costa, R., Peixoto, A. A., Barbujani, G. and Kyriacou, C. P. (1992) A latitudinal cline in a *Drosophila* clock gene. Proceedings of the Royal Society, 250, 43-49.

Crawley, M. J. (2007) Statistical modelling. In The R book John Wiley & Sons, pp. 323-386.

Curtin, K. D., Huang, Z. J. and Rosbash, M. (1995) Temporally regulated nuclear entry of the *Drosophila* period protein contributes to the circadian clock. Neuron, 14, 365-372.

Cyran, S. A., Buchsbaum, A. M., Reddy, K. L., Lin, M.-C., Glossop, N. R. J., Hardin, P. E., Young, M. W., Storti, R. V. and Blau, J. (2003) vrille, Pdp1, and dClock Form a Second Feedback Loop in the *Drosophila* Circadian Clock. Cell, 112, 329-341.

Daan, S., Spoelstra, K., Albrecht, U., Schmutz, I., Daan, M., Daan, B., Rienks, F., Poletaeva, I., Dell'Omo, G., Vyssotski, A. and Lipp, H. P. (2011) Lab mice in the field: unorthodox daily activity and effects of a dysfunctional circadian clock allele. Journal of Biological Rhythms, 26, 118-129.

Dacks, A. M., Green, D. S., Root, C. M., Nighorn, A. J. and Wang, J. W. (2009) Serotonin modulates olfactory processing in the antennal lobe of *Drosophila*. Journal of Neurogenetics, 23, 366-377.

Dai, J. D. and Gilbert, L. I. (1991) Metamorphosis of the corpus allatum and degeneration of the prothoracic glands during the larval-pupal-adult transformation of *Drosophila melanogaster*: a cytophysiological analysis of the ring gland. Developmental Biology, 144, 309-326.

Darlington, T. K., Wager-Smith, K., Ceriani, M. F., Staknis, D., Gekakis, N., Steeves, T. D., Weitz, C. J., Takahashi, J. S. and Kay, S. A. (1998) Closing the circadian loop: CLOCK-induced transcription of its own inhibitors *per* and *tim*. Science, 280, 1599-1603.

David, J. R. and Capy, P. (1988) Genetic variation of *Drosophila melanogaster* natural populations. Trends in Genetics : TIG, 4, 106-111.

Davies, S. A., Cabrero, P., Povsic, M., Johnston, N. R., Terhzaz, S. and Dow, J. A. (2013) Signaling by *Drosophila* capa neuropeptides. General and Comparative Endocrinology, 188, 60-66.

Davis, M. M., O'Keefe, S. L., Primrose, D. A. and Hodgetts, R. B. (2007) A neuropeptide hormone cascade controls the precise onset of post-eclosion cuticular tanning in *Drosophila melanogaster*. Development, 134, 4395-4404.

Dawydow, A., Gueta, R., Ljaschenko, D., Ullrich, S., Hermann, M., Ehmann, N., Gao, S., Fiala, A., Langenhan, T., Nagel, G. and Kittel, R. J. (2014) Channelrhodopsin-2-XXL, a powerful optogenetic tool for low-light applications. Proceedings of the National Academy of Sciences of the United States of America, 111, 13972-13977.

De, J., Varma, V. and Sharma, V. K. (2012) Adult Emergence Rhythm of Fruit Flies *Drosophila melanogaster* under Seminatural Conditions. Journal of Biological Rhythms, 27, 280-286.

Dewey, E. M., McNabb, S. L., Ewer, J., Kuo, G. R., Takanishi, C. L., Truman, J. W. and Honegger, H.-W. (2004) Identification of the Gene Encoding Bursicon, an Insect Neuropeptide Responsible for Cuticle Sclerotization and Wing Spreading. Current Biology, 14, 1208-1213.

Di Cara, F. and King-Jones, K. (2013) How clocks and hormones act in concert to control the timing of insect development. Current Topics in Developmental Biology, 105, 1-36.

Dickerson, M., McCormick, J., Mispelon, M., Paisley, K. and Nichols, R. (2012) Structure-activity and immunochemical data provide evidence of developmental- and tissue-specific myosuppressin signaling. Peptides, 36, 272-279.

Dierick, H. A. and Greenspan, R. J. (2007) Serotonin and neuropeptide F have opposite modulatory effects on fly aggression. Nature Genetics, 39, 678-682.

Dillmann, E. (2014) Selected peptidergic neurons in *Drosophila*: anatomical overlap with clock neurons and role during eclosion timing. In Neurobiology and Genetics, Vol. Zulassungsarbeit Julius-Maximilians-Universität Würzburg, Würzburg.

Dolezelova, E., Dolezel, D. and Hall, J. C. (2007a) Rhythm defects caused by newly engineered null mutations in *Drosophila'*s cryptochrome gene. Genetics, 177, 329-345.

Dolezelova, E., Dolezel, D. and Hall, J. C. (2007b) Rhythm Defects Caused by Newly Engineered Null Mutations in *Drosophila's* cryptochrome Gene. Genetics, 177, 329-345.

Dowse, H. B., Hall, J. C. and Ringo, J. M. (1987) Circadian and ultradian rhythms in period mutants of *Drosophila melanogaster*. Behavior Genetics, 17, 19-35.

Draizen, T. A., Ewer, J. and Robinow, S. (1999) Genetic and hormonal regulation of the death of peptidergic neurons in the *Drosophila* central nervous system. Journal of Neurobiology, 38, 455-465.

Dulcis, D., Levine, R. B. and Ewer, J. (2005) Role of the neuropeptide CCAP in *Drosophila* cardiac function. Journal of Neurobiology, 64, 259-274.

Dus, M., Lai, J. S., Gunapala, K. M., Min, S., Tayler, T. D., Hergarden, A. C., Geraud, E., Joseph, C. M. and Suh, G. S. (2015) Nutrient Sensor in the Brain Directs the Action of the Brain-Gut Axis in *Drosophila*. Neuron, 87, 139-151.

El-Kholy, S., Stephano, F., Li, Y., Bhandari, A., Fink, C. and Roeder, T. (2015) Expression analysis of octopamine and tyramine receptors in *Drosophila*. Cell and Tissue Research, 361, 669-684.

Emery, I. F., Noveral, J. M., Jamison, C. F. and Siwicki, K. K. (1997) Rhythms of *Drosophila* period gene expression in culture. Proceedings of the National Academy of Sciences of the United States of America, 94, 4092-4096.

Emery, P., So, W. V., Kaneko, M., Hall, J. C. and Rosbash, M. (1998) CRY, a *Drosophila* Clock and Light-Regulated Cryptochrome, Is a Major Contributor to Circadian Rhythm Resetting and Photosensitivity. Cell, 95, 669-679.

Emery, P., Stanewsky, R., Hall, J. C. and Rosbash, M. (2000a) A unique circadian-rhythm photoreceptor. Nature, 404, 456-457.

Emery, P., Stanewsky, R., Helfrich-Förster, C., Emery-Le, M., Hall, J. C. and Rosbash, M. (2000b) *Drosophila* CRY Is a Deep Brain Circadian Photoreceptor. Neuron, 26, 493-504.

Endres, K. (2013) Selected peptidergic neurons in *Drosophila:* anatomical overlap with clock neurons and role during eclosion timing. In Neurobiology and Genetics, Vol. Zulassungsarbeit Julius-Maximilians-Universität Würzburg, Würzburg.

Engelmann, W. (2003) Fliegende Uhren: Die Uhren der Taufliege. Universitätsbibliothek Tübingen, Tübingen.

Engelmann, W. and Mack, J. (1978) Different oscillators control the circadian rhythm of eclosion and activity in Drosophila. Journal of Comparative Physiology, 127, 229-237.

Ewer, J. (2005) Behavioral actions of neuropeptides in invertebrates: insights from *Drosophila*. Hormones and Behavior, 48, 418-429.

Ewer, J. (2007) The Neuroendocrinology of eclosion. In Invertebrate Neurobiology (Eds, Greenspan, R. J. and North, G.) Cold Spring Harbor Press, pp. 555-579.

Ewer, J., Frisch, B., Hamblen-Coyle, M. J., Rosbash, M. and Hall, J. C. (1992) Expression of the period clock gene within different cell types in the brain of *Drosophila* adults and mosaic analysis of these cells' influence on circadian behavioral rhythms. The Journal of Neuroscience: the official Journal of the Society for Neuroscience, 12, 3321-3349.

Ewer, J., Gammie, S. C. and Truman, J. W. (1997) Control of insect ecdysis by a positive-feedback endocrine system: roles of eclosion hormone and ecdysis triggering hormone. The Journal of Experimental Biology, 200, 869-881.

Ewer, J. and Truman, J. W. (1996) Increases in cyclic 3',5'-guanosine monophosphate (cGMP) occur at ecdysis in an evolutionarily conserved crustacean cardioactive peptide-immunoreactive insect neuronal network. The Journal of Comparative Neurology, 370, 330-341.

Fraenkel, G. and Hsiao, C. (1962) Hormonal and nervous control of tanning in the fly. Science, 138, 27-29.

Frank, K. D. and Zimmerman, W. F. (1969) Action spectra for phase shifts of a circadian rhythm in *Drosophila*. Science, 163, 688-689.

Friggi-Grelin, F., Coulom, H., Meller, M., Gomez, D., Hirsh, J. and Birman, S. (2003) Targeted gene expression in *Drosophila* dopaminergic cells using regulatory sequences from tyrosine hydroxylase. Journal of Neurobiology, 54, 618-627.

Fujii, S., Krishnan, P., Hardin, P. and Amrein, H. (2007) Nocturnal Male Sex Drive in *Drosophila*. Current Biology : CB, 17, 244-251.

Galliker, A. (2015) Simulation von naturähnlichen Bedingungen im Labor und die Auswirkungen auf die Schlüpfrhythmik bei *Drosophila Melanogaster*. In Neurobiology and Genetics, Vol. Bachelor Protocol University of Würzburg, Würzburg.

Gammie, S. C. and Truman, J. W. (1997) Neuropeptide hierarchies and the activation of sequential motor behaviors in the hawkmoth, *Manduca sexta*. The Journal of Neuroscience:the official Journal of the Society for Neuroscience, 17, 4389-4397.

Garen, A., Kauvar, L. and Lepesant, J. A. (1977) Roles of ecdysone in *Drosophila* development. Proceedings of the National Academy of Sciences of the United States of America, 74, 5099-5103.

Gattermann, R., Johnston, R. E., Yigit, N., Fritzsche, P., Larimer, S., Özkurt, S., Neumann, K., Song, Z., Colak, E., Johnston, J. and McPhee, M. E. (2008) Golden hamsters are nocturnal in captivity but diurnal in nature. Biology Letters, 4, 253-255.

Gekakis, N., Saez, L., Delahaye-Brown, A. M., Myers, M. P., Sehgal, A., Young, M. W. and Weitz, C. J. (1995) Isolation of timeless by PER protein interaction: defective interaction between timeless protein and long-period mutant PERL. Science, 270, 811-815.

Giebultowicz, J. M. and Hege, D. M. (1997) Circadian clock in Malpighian tubules. Nature, 386, 664.

Glaser, F. T. and Stanewsky, R. (2005) Temperature synchronization of the *Drosophila* circadian clock. Current Biology : CB, 15, 1352-1363.

Glossop, N. R. J., Houl, J. H., Zheng, H., Ng, F. S., Dudek, S. M. and Hardin, P. E. (2003) VRILLE Feeds Back to Control Circadian Transcription of Clock in the *Drosophila* Circadian Oscillator. Neuron, 37, 249-261.

Goodman, L. J. (1970) The Structure and Function of the Insect Dorsal Ocellus. In Advances in Insect Physiology, Vol. Volume 7 (Eds, J.W.L. Beament, J. E. T. and Wigglesworth, V. B.) Academic Press, pp. 97-195.

Govorunova, E. G., Spudich, E. N., Lane, C. E., Sineshchekov, O. A. and Spudich, J. L. (2011) New channelrhodopsin with a red-shifted spectrum and rapid kinetics from *Mesostigma viride*. MBio, 2, e00115-00111.

Green, E. W., O'Callaghan, E. K., Hansen, C. N., Bastianello, S., Bhutani, S., Vanin, S., Armstrong, J. D., Costa, R. and Kyriacou, C. P. (2015) Drosophila circadian rhythms in seminatural environments: Summer afternoon component is not an artifact and requires TrpA1 channels. Proceedings of the National Academy of Sciences of the United States of America, 112, 8702-8707.

Hall, J. C. (1995) Trippings along the trail to the molecular mechanisms of biological clocks. Trends in Neurosciences, 18, 230-240.

Hamasaka, Y. and Nässel, D. R. (2006) Mapping of serotonin, dopamine, and histamine in relation to different clock neurons in the brain of *Drosophila*. The Journal of Comparative Neurology, 494, 314-330.

Han, K. A., Millar, N. S. and Davis, R. L. (1998) A novel octopamine receptor with preferential expression in *Drosophila* mushroom bodies. The Journal of Neuroscience: the officialJournal of the Society for Neuroscience, 18, 3650-3658.

Handler, A. M. (1982) Ecdysteroid Titers during Pupal and Adult Development in *Drosophila melanogaster*. Developmental Biology, 93, 73-82.

Hardeland, R. (1972) Species differences in the diurnal rhythmicity of courtship behaviour within the melanogaster group of the genus *Drosophila*. Animal Behaviour, 20, 170-174.

Hardie, R. C. (2001) Phototransduction in *Drosophila melanogaster*. Journal of Experimental Biology, 204, 3403-3409.

Hardin, P. E. (1994) Analysis of period mRNA cycling in *Drosophila* head and body tissues indicates that body oscillators behave differently from head oscillators. Molecular and Cellular Biology, 14, 7211-7218.

Hardin, P. E., Hall, J. C. and Rosbash, M. (1990) Feedback of the *Drosophila period* gene product on circadian cycling of its messenger RNA levels. Nature, 343, 536-540.

Harris, R. M., Pfeiffer, B. D., Rubin, G. M. and Truman, J. W. (2015) Neuron hemilineages provide the functional ground plan for the *Drosophila* ventral nervous system. Elife, 4.

Helfrich-Förster, C. (1995) The *period* clock gene is expressed in central nervous system neurons which also produce a neuropeptide that reveals the projections of circadian pacemaker cells within the brain of *Drosophila melanogaster*. Proceedings of the National Academy of Sciences of the United States of America, 92, 612-616.

Helfrich-Förster, C. (1997) Development of pigment-dispersing hormone-immunoreactive neurons in the nervous system of *Drosophila melanogaster*. The Journal of Comparative Neurology, 380, 335-354.

Helfrich-Förster, C. (2001) The locomotor activity rhythm of *Drosophila melanogaster* is controlled by a dual oscillator system. Journal of Insect Physiology, 47, 877-887.

Helfrich-Förster, C., Edwards, T., Yasuyama, K., Wisotzki, B., Schneuwly, S., Stanewsky, R., Meinertzhagen, I. A. and Hofbauer, A. (2002) The extraretinal eyelet of *Drosophila*: development, ultrastructure, and putative circadian function. The Journal of Neuroscience: the official Journal of the Society for Neuroscience, 22, 9255-9266.

Helfrich-Förster, C., Shafer, O. T., Wulbeck, C., Grieshaber, E., Rieger, D., Taghert, P. (2007) Development and morphology of the clock-gene-expressing lateral neurons of *Drosophila melanogaster*. The Journal of Comparative Neurology, 500, 47-70.

Helfrich-Förster, C., Tauber, M., Park, J. H., Muhlig-Versen, M., Schneuwly, S. and Hofbauer, A. (2000) Ectopic expression of the neuropeptide pigment-dispersing factor alters behavioral rhythms in *Drosophila melanogaster*. The Journal of Neuroscience: the official Journal of the Society for Neuroscience, 20, 3339-3353.

Helfrich-Förster, C., Winter, C., Hofbauer, A., Hall, J. C. and Stanewsky, R. (2001) The circadian clock of fruit flies is blind after elimination of all known photoreceptors. Neuron, 30, 249-261.

Helfrich-Förster, C. a. E., W. (2002) Photoreceptors for the Circadian Clock of the Fruitfly. In Biological Rhythms (Ed, Kumar, V.) Narosa Publishing House, New Delhi, India, pp. 94 - 106.

Helfrich, C. and Engelmann, W. (1987) Evidences for circadian rhythmicity in the *per0* mutant of *Drosophila melanogaster*. Zeitschrift fur Naturforschung. C, Journal of Biosciences, 42, 1335-1338.

Hentze, J. L., Carlsson, M. A., Kondo, S., Nässel, D. R. and Rewitz, K. F. (2015) The Neuropeptide Allatostatin A Regulates Metabolism and Feeding Decisions in *Drosophila*. Scientific Reports, 5, 11680.

Hentze, J. L., Moeller, M. E., Jorgensen, A. F., Bengtsson, M. S., Bordoy, A. M., Warren, J. T., Gilbert, L. I., Andersen, O. and Rewitz, K. F. (2013) Accessory gland as a site for prothoracicotropic hormone controlled ecdysone synthesis in adult male insects. PLoS One, 8, e55131.

Hergarden, A. C., Tayler, T. D. and Anderson, D. J. (2012) Allatostatin-A neurons inhibit feeding behavior in adult *Drosophila*. Proceedings of the National Academy of Sciences of the United States of America, 109, 3967-3972.

Hermann, C., Saccon, R., Senthilan, P. R., Domnik, L., Dircksen, H., Yoshii, T. and Helfrich-Forster, C. (2013) The circadian clock network in the brain of different *Drosophila* species. The Journal of Comparative Neurology, 521, 367-388.

Hewes, R. S. and Taghert, P. H. (2001) Neuropeptides and neuropeptide receptors in the *Drosophila melanogaster* genome. Genome Research, 11, 1126-1142.

Hofbauer, A. and Buchner, E. (1989) Does *Drosophila* have seven eyes? Die Naturwissenschaften, 76, 335-336.

Hogenesch, J. B., Gu, Y.-Z., Jain, S. and Bradfield, C. A. (1998) The basic-helix–loop–helix-PAS orphan MOP3 forms transcriptionally active complexes with circadian and hypoxia factors.

Proceedings of the National Academy of Sciences of the United States of America, 95, 5474-5479.

Horodyski, F. M., Ewer, J., Riddiford, L. M. and Truman, J. W. (1993) Isolation, characterization and expression of the eclosion hormone gene of *Drosophila melanogaster*. European Journal of Biochemistry / FEBS, 215, 221-228.

Hoyer, S. C., Eckart, A., Herrel, A., Zars, T., Fischer, S. A., Hardie, S. L. and Heisenberg, M. (2008) Octopamine in male aggression of *Drosophila*. Current Biology : CB, 18, 159-167.

Hu, K. G., Reichert, H. and Stark, W. S. (1978) Electrophysiological characterization of *Drosophila* ocelli. Journal of Comparative Physiology, 126, 15-24.

Hyun, S., Lee, Y., Hong, S. T., Bang, S., Paik, D., Kang, J., Shin, J., Lee, J., Jeon, K., Hwang, S., Bae, E. and Kim, J. (2005) *Drosophila* GPCR Han is a receptor for the circadian clock neuropeptide PDF. Neuron, 48, 267-278.

Im, S. H., Li, W. and Taghert, P. H. (2011) PDFR and CRY signaling converge in a subset of clock neurons to modulate the amplitude and phase of circadian behavior in *Drosophila*. PloS One, 6, e18974.

Im, S. H. and Taghert, P. H. (2010) PDF receptor expression reveals direct interactions between circadian oscillators in *Drosophila*. The Journal of Comparative Neurology, 518, 1925-1945.

Ito, C. and Tomioka, K. (2016) Heterogeneity of the Peripheral Circadian Systems in *Drosophila melanogaster*: A Review. Frontiers in Physiology, 7, 8.

Jackson, F. R. (1993) Circadian rhythm mutants of *Drosophila*. Molecular Genetics of Biological Rhythms, Cellular Clocks Series, 91-121.

James, A. C., Azevedo, R. B. R. and Partridge, L. (1997) Genetic and Environmental Responses to Temperature of *Drosophila melanogaster* from a Latitudinal Cline. Genetics, 146, 881-890.

Jaumouille, E., Machado Almeida, P., Stahli, P., Koch, R. and Nagoshi, E. (2015) Transcriptional regulation via nuclear receptor crosstalk required for the *Drosophila* circadian clock. Current Biology : CB, 25, 1502-1508.

Johard, H. A., Yoishii, T., Dircksen, H., Cusumano, P., Rouyer, F., Helfrich-Forster, C. and Nassel, D. R. (2009) Peptidergic clock neurons in *Drosophila:* ion transport peptide and short neuropeptide F in subsets of dorsal and ventral lateral neurons. The Journal of Comparative Neurology, 516, 59-73.

Kadener, S., Stoleru, D., McDonald, M., Nawathean, P. and Rosbash, M. (2007) Clockwork Orange is a transcriptional repressor and a new *Drosophila* circadian pacemaker component. Genes & Development, 21, 1675-1686.

Kalmus, H. (1935) Periodizität und Autochronie (Ideochronie) als zeitregelnde Eigenschaften der Organismen. Biologia Generales, 11, 93-114.

Kalmus, H. (1938) Die Lage des Aufnahmeorgans für die Schlupfperiodik von *Drosophila*. Zeitschrift für Vergleichende Physiologie, 26, 362-365.

Kalmus, H. (1940) Diurnal rhythms in the Axolotl larvae and in *Drosophila*. Nature, 145, 72-73.

Kaneko, H., Head, L. M., Ling, J., Tang, X., Liu, Y., Hardin, P. E., Emery, P. and Hamada, F. N. (2012) Circadian rhythm of temperature preference and its neural control in *Drosophila*. Current Biology : CB, 22, 1851-1857.

Kataoka, H., Nagasawa, H., Isogai, A., Ishizaki, H. and Suzuki, A. (1991) Prothoracicotropic hormone of the silkworm, *Bombyx mori*: amino acid sequence and dimeric structure. Agricultural and Biological Chemistry, 55, 73-86.

Kawakami, A., Kataoka, H., Oka, T., Mizoguchi, A., Kimura-Kawakami, M., Adachi, T., Iwami, M., Nagasawa, H., Suzuki, A. and Ishizaki, H. (1990) Molecular cloning of the *Bombyx mori* prothoracicotropic hormone. Science, 247, 1333-1335.

Kim, D. H., Han, M. R., Lee, G., Lee, S. S., Kim, Y. J. and Adams, M. E. (2015) Rescheduling Behavioral Subunits of a Fixed Action Pattern by Genetic Manipulation of Peptidergic Signaling. PLoS Genetics, 11, e1005513.

Kim, Y. J., Spalovska-Valachova, I., Cho, K. H., Zitnanova, I., Park, Y., Adams, M. E. and Zitnan, D. (2004) Corazonin receptor signaling in ecdysis initiation. Proceedings of the National Academy of Sciences of the United States of America, 101, 6704-6709.

Kim, Y. J., Zitnan, D., Cho, K. H., Schooley, D. A., Mizoguchi, A. and Adams, M. E. (2006a) Central peptidergic ensembles associated with organization of an innate behavior. Proceedings of the National Academy of Sciences of the United States of America, 103, 14211-14216.

Kim, Y. J., Zitnan, D., Galizia, C. G., Cho, K. H. and Adams, M. E. (2006b) A command chemical triggers an innate behavior by sequential activation of multiple peptidergic ensembles. Current Biology : CB, 16, 1395-1407.

Kingan, T. G. and Adams, M. E. (2000) Ecdysteroids regulate secretory competence in Inka cells. Journal of Experimental Biology: Home, 203, 3011-3018.

Kingan, T. G., Gray, W., Zitnan, D. and Adams, M. E. (1997) Regulation of ecdysis-triggering hormone release by eclosion hormone. Journal of Experimental Biology: Home, 200, 3245-3256.

Kiss, B., Szlanka, T., Zvara, A., Zurovec, M., Sery, M., Kakaš, S., Ramasz, B., Heged?s, Z., Lukacsovich, T., Puskás, L., Fónagy, A. and Kiss, I. (2013) Selective elimination/RNAi silencing of FMRF-related peptides and their receptors decreases the locomotor activity in *Drosophila melanogaster*. General and Comparative Endocrinology, 191, 137-145.

Kloss, B., Price, J. L., Saez, L., Blau, J., Rothenfluh, A., Wesley, C. S. and Young, M. W. (1998) The *Drosophila* clock gene *double-time* encodes a protein closely related to human casein kinase Iepsilon. Cell, 94, 97-107.

Kloss, B., Rothenfluh, A., Young, M. W. and Saez, L. (2001) Phosphorylation of PERIOD Is Influenced by Cycling Physical Associations of DOUBLE-TIME, PERIOD, and TIMELESS in the *Drosophila* Clock. Neuron, 30, 699-706.

Konopka, R. J. and Benzer, S. (1971) Clock mutants of *Drosophila melanogaster*. Proceedings of the National Academy of Sciences of the United States of America, 68, 2112-2116.

Konopka, R. J., Pittendrigh, C. and Orr, D. (1989) Reciprocal behaviour associated with altered homeostasis and photosensitivity of *Drosophila* clock mutants. Journal of Neurogenetics, 6, 1-10.

Kopec, S. (1922) Studies on the necessity of the brain for the inception of insect metamorphosis. The Biological Bulletin, 42, 323-342.

Krishnan, B., Dryer, S. E. and Hardin, P. E. (1999) Circadian rhythms in olfactory responses of *Drosophila melanogaster*. Nature, 400, 375-378.

Krishnan, B., Levine, J. D., Lynch, M. K., Dowse, H. B., Funes, P., Hall, J. C., Hardin, P. E. and Dryer, S. E. (2001) A new role for cryptochrome in a *Drosophila* circadian oscillator. Nature, 411, 313-317.

Krüger, E., Mena, W., Lahr, E. C., Johnson, E. C. and Ewer, J. (2015) Genetic analysis of Eclosion hormone action during *Drosophila* larval ecdysis. Development, 142, 4279-4287.

Kumar, S., Chen, D., Jang, C., Nall, A., Zheng, X. and Sehgal, A. (2014) An ecdysone-responsive nuclear receptor regulates circadian rhythms in *Drosophila*. Nature Communications, 5, 5697.

Kume, K., Kume, S., Park, S. K., Hirsh, J. and Jackson, F. R. (2005) Dopamine is a regulator of arousal in the fruit fly. The Journal of Neuroscience: the official Journal of the Society for Neuroscience, 25, 7377-7384.

Kunst, M., Hughes, M. E., Raccuglia, D., Felix, M., Li, M., Barnett, G., Duah, J. and Nitabach, M. N. (2014) Calcitonin gene-related peptide neurons mediate sleep-specific circadian output in *Drosophila*. Current Biology : CB, 24, 2652-2664.

Kyriacou, C. P., Peixoto, A. A., Sandrelli, F., Costa, R. and Tauber, E. (2008) Clines in clock genes: fine-tuning circadian rhythms to the environment. Trends in Genetics : TIG, 24, 124-132.

Lachaise, D., Cariou, M.-L., David, J. R., Lemeunier, F., Tsacas, L. and Ashburner, M. (1988) Historical Biogeography of the *Drosophila melanogaster* Species Subgroup. In Evolutionary Biology (Eds, Hecht, M. K., Wallace, B. and Prance, G. T.) Springer US, Boston, MA, pp. 159-225.

Lahr, E. C., Dean, D. and Ewer, J. (2012) Genetic analysis of ecdysis behavior in *Drosophila* reveals partially overlapping functions of two unrelated neuropeptides. The Journal of Neuroscience: the official Journal of the Society for Neuroscience, 32, 6819-6829.

Lai, S. L. and Lee, T. (2006) Genetic mosaic with dual binary transcriptional systems in *Drosophila*. Nature Neuroscience, 9, 703-709.

Lange, A., Tawfik, B., Hermann, F., de Thurah, L., Nielsen, M. B., Larsen, S. L. and Larsen, S. (2010) PTTH-induced metamorphosis in *Drosophila melanogaster* is affected by TOR, retinoic acid and

Juvenile Hormone Signalling. In Department of Science, Systems and Models, Vol. Bachelor Report Roskilde University.

Lankinen, P. (1986) Genetic correlation between circadian eclosion rhythm and photoperiodic diapause in *Drosophila littoralis*. Journal of Biological Rhythms, 1, 101-118.

Lear, B. C., Merrill, C. E., Lin, J. M., Schroeder, A., Zhang, L. and Allada, R. (2005) A G protein-coupled receptor, groom-of-PDF, is required for PDF neuron action in circadian behavior. Neuron, 48, 221-227.

Lee, G., Bahn, J. H. and Park, J. H. (2006) Sex- and clock-controlled expression of the neuropeptide F gene in *Drosophila*. Proceedings of the National Academy of Sciences, 103, 12580-12585.

Lee, G. and Park, J. H. (2004) Hemolymph sugar homeostasis and starvation-induced hyperactivity affected by genetic manipulations of the adipokinetic hormone-encoding gene in *Drosophila melanogaster*. Genetics, 167, 311-323.

Lee, G., Sehgal, R., Wang, Z., Nair, S., Kikuno, K., Chen, C. H., Hay, B. and Park, J. H. (2013) Essential role of grim-led programmed cell death for the establishment of corazonin-producing peptidergic nervous system during embryogenesis and metamorphosis in *Drosophila melanogaster*. Biology Open, 2, 283-294.

Lee, K. M., Daubnerova, I., Isaac, R. E., Zhang, C., Choi, S., Chung, J. and Kim, Y. J. (2015) A neuronal pathway that controls sperm ejection and storage in female *Drosophila*. Current Biology : CB, 25, 790-797.

Lee, K. S., You, K. H., Choo, J. K., Han, Y. M. and Yu, K. (2004) *Drosophila* short neuropeptide F regulates food intake and body size. The Journal of Biological Chemistry, 279, 50781-50789.

Lenz, C., Williamson, M. and Grimmelikhuijzen, C. J. (2000) Molecular cloning and genomic organization of an allatostatin preprohormone from *Drosophila melanogaster*. Biochemical and Biophysical Research Communications, 273, 1126-1131.

Levine, J. D., Funes, P., Dowse, H. B. and Hall, J. C. (2002) Advanced analysis of a cryptochrome mutation's effects on the robustness and phase of molecular cycles in isolated peripheral tissues of *Drosophila*. BMC Neuroscience, 3, 5.

Lim, C., Chung, B. Y., Pitman, J. L., McGill, J. J., Pradhan, S., Lee, J., Keegan, K. P., Choe, J. and Allada, R. (2007) Clockwork orange encodes a transcriptional repressor important for circadian-clock amplitude in *Drosophila*. Current Biology : CB, 17, 1082-1089.

Lin, J. Y., Knutsen, P. M., Muller, A., Kleinfeld, D. and Tsien, R. Y. (2013) ReaChR: a red-shifted variant of channelrhodopsin enables deep transcranial optogenetic excitation. Nature Neuroscience, 16, 1499-1508.

Low, K. H., Lim, C., Ko, H. W. and Edery, I. (2008) Natural Variation in the Splice Site Strength of a Clock Gene and Species-Specific Thermal Adaptation. Neuron, 60, 1054-1067.

Luo, C. W., Dewey, E. M., Sudo, S., Ewer, J., Hsu, S. Y., Honegger, H. W. and Hsueh, A. J. (2005) Bursicon, the insect cuticle-hardening hormone, is a heterodimeric cystine knot protein that activates G protein-coupled receptor LGR2. Proceedings of the National Academy of Sciences of the United States of America, 102, 2820-2825.

Lyons, L. C. and Roman, G. (2009) Circadian modulation of short-term memory in *Drosophila*. Learning & Memory, 16, 19-27.

Majercak, J., Chen, W. F. and Edery, I. (2004) Splicing of the period Gene 3'-Terminal Intron Is Regulated by Light, Circadian Clock Factors, and Phospholipase C. Molecular and Cellular Biology, 24, 3359-3372.

Majercak, J., Sidote, D., Hardin, P. E. and Edery, I. (1999) How a circadian clock adapts to seasonal decreases in temperature and day length. Neuron, 24, 219-230.

Markow, T. and O'Grady, P. (2005b) *Drosophila*: a Guide to Species Identification and Use., Academic Press, London.

Markow, T. A. (2015) The secret lives of *Drosophila* flies. Elife, 4.

Martinek, S., Inonog, S., Manoukian, A. S. and Young, M. W. (2001) A role for the segment polarity gene *shaggy/GSK-3* in the *Drosophila* circadian clock. Cell, 105, 769-779.

Matsumoto, A., Ukai-Tadenuma, M., Yamada, R. G., Houl, J., Uno, K. D., Kasukawa, T., Dauwalder, B., Itoh, T. Q., Takahashi, K., Ueda, R., Hardin, P. E., Tanimura, T. and Ueda, H. R. (2007) A

functional genomics strategy reveals clockwork orange as a transcriptional regulator in the *Drosophila* circadian clock. Genes & Development, 21, 1687-1700.

Mayer, R. J. and Candy, D. J. (1969) Control of haemolymph lipid concentration during locust flight: An adipokinetic hormone from the corpora cardiaca. Journal of Insect Physiology, 15, 611-620.

McBrayer, Z., Ono, H., Shimell, M., Parvy, J. P., Beckstead, R. B., Warren, J. T., Thummel, C. S., Dauphin-Villemant, C., Gilbert, L. I. and O'Connor, M. B. (2007) Prothoracicotropic hormone regulates developmental timing and body size in *Drosophila*. Developmental Cell, 13, 857-871.

McCromick, J. and Nichols, R. (1993) Spatial and Temporal Expression Identify Dromyosuppressin as a Brain-Gut Peptide in *Drosophila melanogaster*. The Journal of Comparative Neurology, 338, 279-288.

McDonald, M. J. and Rosbash, M. (2001) Microarray analysis and organization of circadian gene expression in *Drosophila*. Cell, 107, 567-578.

McNabb, S., L., Baker, J. D., Agapite, J., Steller, H., Riddiford, L. M. and Truman, J. W. (1997a) Disruption of a Behavioral Sequence by Targeted Death of Peptidergic Neurons in *Drosophila*. Neuron, 19, 813-823.

McNabb, S. L., Baker, J. D., Agapite, J., Steller, H., Riddiford, L. M. and Truman, J. W. (1997b) Disruption of a behavioral sequence by targeted death of peptidergic neurons in Drosophila. Neuron, 19, 813-823.

McNabb, S. L. and Truman, J. W. (2008) Light and peptidergic eclosion hormone neurons stimulate a rapid eclosion response that masks circadian emergence in *Drosophila*. The Journal of Experimental Biology, 211, 2263-2274.

McNeil, G. P., Zhang, X., Genova, G. and Jackson, F. R. (1998) A molecular rhythm mediating circadian clock output in *Drosophila*. Neuron, 20, 297-303.

Mealey-Ferrara, M. L., Montalvo, A. G. and Hall, J. C. (2003) Effects of combining a cryptochrome mutation with other visual-system variants on entrainment of locomotor and adult-emergence rhythms in *Drosophila*. Journal of Neurogenetics, 17, 171-221.

Melcher, C. and Pankratz, M. J. (2005) Candidate gustatory interneurons modulating feeding behavior in the *Drosophila* brain. PLoS Biology, 3, e305.

Menegazzi, P., Vanin, S., Yoshii, T., Rieger, D., Hermann, C., Dusik, V., Kyriacou, C. P., Helfrich-Forster, C. and Costa, R. (2013) *Drosophila* clock neurons under natural conditions. Journal of Biological Rhythms, 28, 3-14.

Menegazzi, P., Yoshii, T. and Helfrich-Forster, C. (2012) Laboratory versus nature: the two sides of the *Drosophila* circadian clock. Journal of Biological Rhythms, 27, 433-442.

Meng, X., Wahlstrom, G., Immonen, T., Kolmer, M., Tirronen, M., Predel, R., Kalkkinen, N., Heino, T. I., Sariola, H. and Roos, C. (2002) The *Drosophila* hugin gene codes for myostimulatory and ecdysis-modifying neuropeptides. Mechanisms of Development, 117, 5-13.

Mertens, I., Vandingenen, A., Johnson, E. C., Shafer, O. T., Li, W., Trigg, J. S., De Loof, A., Schoofs, L. and Taghert, P. H. (2005) PDF receptor signaling in *Drosophila* contributes to both circadian and geotactic behaviors. Neuron, 48, 213-219.

Mirth, C., Truman, J. W. and Riddiford, L. M. (2005) The role of the prothoracic gland in determining critical weight for metamorphosis in *Drosophila melanogaster*. Current Biology : CB, 15, 1796-1807.

Mirth, C. K. and Shingleton, A. W. (2012) Integrating body and organ size in *Drosophila*: recent advances and outstanding problems. Frontiers in Endocrinology, 3, 49.

Miyasako, Y., Umezaki, Y. and Tomioka, K. (2007) Separate sets of cerebral clock neurons are responsible for light and temperature entrainment of *Drosophila* circadian locomotor rhythms. Journal of Biological Rhythms, 22, 115-126.

Montell, C. (2012) *Drosophila* visual transduction. Trends in Neurosciences, 35, 356-363.

Montelli, S., Mazzotta, G., Vanin, S., Caccin, L., Corra, S., De Pitta, C., Boothroyd, C., Green, E. W., Kyriacou, C. P. and Costa, R. (2015) *period* and *timeless* mRNA Splicing Profiles under Natural Conditions in *Drosophila melanogaster*. Journal of Biological Rhythms, 30, 217-227.

Morgan, T. H. (1910) Sex limited inheritance in *Drosophila.* Science, 32, 120-122.

Morgan, T. H. (1911) The origin of five mutations in eye color in *Drosophila* and their modes of inheritance. Science, 33, 534-537.

Morioka, E., Matsumoto, A. and Ikeda, M. (2012) Neuronal influence on peripheral circadian oscillators in pupal *Drosophila* prothoracic glands. Nature Communications, 3, 909.

Myers, E. M., Yu, J. and Sehgal, A. (2003) Circadian Control of Eclosion Interaction between a Central and Peripheral Clock in *Drosophila melanogaster*. Current Biology, 13, 526-533.

Nagel, G., Szellas, T., Huhn, W., Kateriya, S., Adeishvili, N., Berthold, P., Ollig, D., Hegemann, P. and Bamberg, E. (2003) Channelrhodopsin-2, a directly light-gated cation-selective membrane channel. Proceedings of the National Academy of Sciences of the United States of America, 100, 13940-13945.

Nagel, G. O., D.; Fuhrmann, M.; Kateriya, S.; Musti, A.; Bamberg, E.; Hegemann, P. (2002) Channelrhodopsin-1: A Light-Gated Proton Channel in Green Algae. Science, 296, 2395-2398.

Naidoo, N., Song, W., Hunter-Ensor, M. and Sehgal, A. (1999) A Role for the Proteasome in the Light Response of the Timeless Clock Protein. Science, 285, 1737-1741.

Nässel, D. R., Enell, L. E., Santos, J. G., Wegener, C. and Johard, H. A. (2008) A large population of diverse neurons in the *Drosophila* central nervous system expresses short neuropeptide F, suggesting multiple distributed peptide functions. BMC Neuroscience, 9, 90.

Nässel, D. R. and Wegener, C. (2011) A comparative review of short and long neuropeptide F signaling in invertebrates: Any similarities to vertebrate neuropeptide Y signaling? Peptides, 32, 1335-1355.

Nässel, D. R. and Winther, A. M. (2010) *Drosophila* neuropeptides in regulation of physiology and behavior. Progress in Neurobiology, 92, 42-104.

Neckameyer, W. S. and White, K. (1993) *Drosophila* tyrosine hydroxylase is encoded by the pale locus. Journal of Neurogenetics, 8, 189-199.

Nitabach, M. N., Blau, J. and Holmes, T. C. (2002) Electrical silencing of *Drosophila* pacemaker neurons stops the free-running circadian clock. Cell 109, 485-495.

Noyes, B. E., Katz, F. N. and Schaffer, M. H. (1995) Identification and expression of the *Drosophila* adipokinetic hormone gene. Molecular and Cellular Endocrinology, 109, 133-141.

Ohhara, Y., Shimada-Niwa, Y., Niwa, R., Kayashima, Y., Hayashi, Y., Akagi, K., Ueda, H., Yamakawa-Kobayashi, K. and Kobayashi, S. (2015) Autocrine regulation of ecdysone synthesis by beta3-octopamine receptor in the prothoracic gland is essential for *Drosophila* metamorphosis. Proceedings of the National Academy of Sciences of the United States of America, 112, 1452-1457.

Park, D., Han, M., Kim, Y. C., Han, K. A. and Taghert, P. H. (2004) Ap-let neurons-a peptidergic circuit potentially controlling ecdysial behavior in *Drosophila*. Developmental Biology, 269, 95-108.

Park, J. H. and Hall, J. C. (1998) Isolation and chronobiological analysis of a neuropeptide pigment-dispersing factor gene in *Drosophila melanogaster*. Journal of Biological Rhythms, 13, 219-228.

Park, J. H., Schroeder, A. J., Helfrich-Förster, C., Jackson, F. R. and Ewer, J. (2003) Targeted ablation of CCAP neuropeptide-containing neurons of *Drosophila* causes specific defects in execution and circadian timing of ecdysis behavior. Development, 130, 2645-2656.

Park, Y., Filippov, V., Gill, S. S. and Adams, M. E. (2002) Deletion of ETH gene leads to lethal ecdysis deficiency. Development (Cambridge, England), 129, 493-503.

Park, Y., Zitnan, D., Gill, S. S. and Adams, M. E. (1999) Molecular cloning and biological activity of ecdysis-triggering hormones in *Drosophila melanogaster*. FEBS Letters, 463, 133-138.

Pauls, D., Chen, J., Reiher, W., Vanselow, J. T., Schlosser, A., Kahnt, J. and Wegener, C. (2014) Peptidomics and processing of regulatory peptides in the fruit fly Drosophila. EuPA Open Proteomics, 3, 114-127.

Peabody, N. C., Diao, F., Luan, H., Wang, H., Dewey, E. M., Honegger, H. W. and White, B. H. (2008) Bursicon functions within the *Drosophila* CNS to modulate wing expansion behavior, hormone secretion, and cell death. The Journal of Neuroscience: the official Journal of the Society for Neuroscience, 28, 14379-14391.

Peschel, N. and Helfrich-Förster, C. (2011) Setting the clock-by nature: circadian rhythm in the fruitfly *Drosophila melanogaster*. FEBS Lett, 585, 1435-1442.

Picot, M., Klarsfeld, A., Chelot, E., Malpel, S. and Rouyer, F. (2009) A role for blind DN2 clock neurons in temperature entrainment of the *Drosophila* larval brain. The Journal of Neuroscience: the official journal of the Society for Neuroscience, 29, 8312-8320.

Pittendrigh, C. and Bruce, V. (1959a) Daily rhythms as coupled oscillator systems and their relation to thermoperiodism and photoperiodism. (Ed, Withrow, e.) American Association for the Advancement of Science, Washington, DC, pp. 475–505.

Pittendrigh, C., Bruce, S. (1957) An oscillator model for biological clocks. Rhythmic and Synthetic Processes in Growth, 75-109.

Pittendrigh, C. S. (1954) On Temperature Independence in the Clock System Controlling Emergence Time in *Drosophila*. Proceedings of the National Academy of Sciences of the United States of America, 40, 1018-1029.

Pittendrigh, C. S. and Minis, D. H. (1972) Circadian systems: longevity as a function of circadian resonance in *Drosophila melanogaster*. Proceedings of the National Academy of Sciences of the United States of America, 69, 1537-1539.

Pittendrigh, C. S. and Skopik, S. D. (1970) Circadian Systems V. The driving oscillation and the temporal sequence of development.

Plautz, J. D., Kaneko, M., Hall, J. C. and Kay, S. A. (1997) Independent photoreceptive circadian clocks throughout *Drosophila*. Science, 278, 1632-1635.

Pollock, J. A. and Benzer, S. (1988) Transcript localization of four opsin genes in the three visual organs of *Drosophila*; RH2 is ocellus specific. Nature, 333, 779-782.

Ponton, F., Chapuis, M. P., Pernice, M., Sword, G. A. and Simpson, S. J. (2011) Evaluation of potential reference genes for reverse transcription-qPCR studies of physiological responses in *Drosophila melanogaster*. Journal of Insect Physiology, 57, 840-850.

Pooryasin, A. and Fiala, A. (2015) Identified Serotonin-Releasing Neurons Induce Behavioral Quiescence and Suppress Mating in *Drosophila*. The Journal of Neuroscience: the official Journal of the Society for Neuroscience, 35, 12792-12812.

Price, J. L., Blau, J., Rothenfluh, A., Abodeely, M., Kloss, B. and Young, M. W. (1998) *double-time* Is a Novel *Drosophila* Clock Gene that Regulates PERIOD Protein Accumulation. Cell, 94, 83-95.

Reaume, C. J. and Sokolowski, M. B. (2006) The nature of *Drosophila melanogaster*. Current Biology : CB, 16, R623-628.

Renn, S. C. P., Park, J. H., Rosbash, M., Hall, J. C. and Taghert, P. H. (1999) A pdf neuropeptide gene mutation and ablation of PDF neurons each cause severe abnormalities of behavioral circadian rhythms in *Drosophila*. Cell, 99, 791-802.

Rewitz, K. F., Rybczynski, R., Warren, J. T. and Gilbert, L. I. (2006a) The Halloween genes code for cytochrome P450 enzymes mediating synthesis of the insect moulting hormone. Biochemical Society Transactions, 34, 1256-1260.

Rewitz, K. F., Rybczynski, R., Warren, J. T. and Gilbert, L. I. (2006b) Identification, characterization and developmental expression of Halloween genes encoding P450 enzymes mediating ecdysone biosynthesis in the tobacco hornworm, *Manduca sexta*. Insect Biochemistry and Molecular Biology, 36, 188-199.

Rewitz, K. F., Yamanaka, N., Gilbert, L. I. and O'Connor, M. B. (2009) The insect neuropeptide PTTH activates receptor tyrosine kinase torso to initiate metamorphosis. Science, 326, 1403-1405.

Richter, K. (2001) Daily changes in neuroendocrine control of moulting hormone secretion in the prothoracic gland of the cockroach *Periplaneta americana* (L.). Journal of Insect Physiology, 47, 333-338.

Rieger, D., Stanewsky, R. and Helfrich-Förster, C. (2003) Cryptochrome, Compound Eyes, Hofbauer-Buchner Eyelets, and Ocelli Play Different Roles in the Entrainment and Masking Pathway of the Locomotor Activity Rhythm in the Fruit Fly *Drosophila melanogaster*. Journal of Biological Rhythms, 18, 377-391.

Riemensperger, T., Isabel, G., Coulom, H., Neuser, K., Seugnet, L., Kume, K., Iché-Torres, M., Cassar, M., Strauss, R., Preat, T., Hirsh, J. and Birman, S. (2011) Behavioral consequences of dopamine deficiency in the *Drosophila* central nervous system. Proceedings of the National Academy of Sciences of the United States of America, 108, 834-839.

Rivas, G. B., Bauzer, L. G. and Meireles-Filho, A. C. (2015) "The Environment is Everything That Isn't Me": Molecular Mechanisms and Evolutionary Dynamics of Insect Clocks in Variable Surroundings. Frontiers in Physiology, 6, 400.

Roberts, S. K. D. F. (1956) "Clock" Controlled Activity Rhythms in the Fruit Fly. Science, 124, 172-172.

Rosato, E., Trevisan, A., Sandrelli, F., Zordan, M., Kyriacou, C. P. and Costa, R. (1997) Conceptual translation of timeless reveals alternative initiating methionines in *Drosophila*. Nucleic Acids Research, 25, 455-458.

Rutila, J. E., Suri, V., Le, M., So, W. V., Rosbash, M. and Hall, J. C. (1998) CYCLE is a second bHLH-PAS clock protein essential for circadian rhythmicity and transcription of *Drosophila period* and *timeless*. Cell, 93, 805-814.

Saez, L. and Young, M. W. (1996) Regulation of nuclear entry of the *Drosophila* clock proteins *period* and *timeless*. Neuron, 17, 911-920.

Salcedo, E., Huber, A., Henrich, S., Chadwell, L. V., Chou, W.-H., Paulsen, R. and Britt, S. G. (1999) Blue- and Green-Absorbing Visual Pigments of *Drosophila*: Ectopic Expression and Physiological Characterization of the R8 Photoreceptor Cell-Specific Rh5 and Rh6 Rhodopsins. The Journal of Neuroscience, 19, 10716-10726.

Sandrelli, F., Tauber, E., Pegoraro, M., Mazzotta, G., Cisotto, P., Landskron, J., Stanewsky, R., Piccin, A., Rosato, E., Zordan, M., Costa, R. and Kyriacou, C. P. (2007) A molecular basis for natural selection at the timeless locus in *Drosophila melanogaster*. Science, 316, 1898-1900.

Satake, S., Kaya, M. and Sakurai, S. (1998) Hemolymph ecdysteroid titer and ecdysteroid-dependent developmental events in the last-larval stadium of the silkworm, *Bombyx mori:* role of low ecdysteroid titer in larval-pupal metamorphosis and a reappraisal of the head critical period. Journal of Insect Physiology, 44, 867-881.

Saunders, D. S. (1990) The circadian basis of ovarian diapause regulation in *Drosophila melanogaster:* is the *period* gene causally involved in photoperiodic time measurement? Journal of Biological Rhythms, 5, 315-331.

Saunders, D. S. (2002) Insect clocks, Elsevier, Amsterdam [u.a.].

Saunders, D. S., Henrich, V. C. and Gilbert, L. I. (1989) Induction of diapause in *Drosophila melanogaster:* photoperiodic regulation and the impact of arrhythmic clock mutations on time measurement. Proceedings of the National Academy of Sciences of the United States of America, 86, 3748-3752.

Sawyer, L. A., Hennessy, J. M., Peixoto, A. A., Rosato, E., Parkinson, H., Costa, R. and Kyriacou, C. P. (1997) Natural variation in a *Drosophila* clock gene and temperature compensation. Science, 278, 2117-2120.

Schaffer, M. H., Noyes, B. E., Slaughter, C. A., Thorne, G. C. and Gaskell, S. J. (1990) The fruitfly *Drosophila melanogaster* contains a novel charged adipokinetic-hormone-family peptide. Biochemical Journal, 269, 315-320.

Schlichting, M., Menegazzi, P. and Helfrich-Forster, C. (2015) Normal vision can compensate for the loss of the circadian clock. Proceedings of the Royal Society, 282.

Schmidt, P. S., Paaby, A. B. and Heschel, M. S. (2005) Genetic variance for diapause expression and associated life histories in *Drosophila melanogaster*. Evolution: International Journal of Organic Evolution, 59, 2616-2625.

Schmitz, J. (2014) Der Einfluss von Corazonin auf das Schlopfverhalten und dessen circadiane Rhythmik bei *Drosophila melanogaster*. In Neurobiology and Genetics, Vol. Zulassungsarbeit Julius-Maximilians-Universität Würzburg, Würzburg.

Schoofs, L., Holman, G. M., Hayes, T. K., Nachman, R. J. and De Loof, A. (1991) Isolation, identification and synthesis of locustamyoinhibiting peptide (LOM-MIP), a novel biologically active neuropeptide from *Locusta migratoria*. Regulatory Peptides, 36, 111-119.

Schroeder, A. J., Genova, G. K., Roberts, M. A., Kleyner, Y., Suh, J. and Jackson, F. R. (2003) Cell-specific expression of the lark RNA-binding protein in *Drosophila* results in morphological and circadian behavioral phenotypes. Journal of Neurogenetics, 17, 139-169.

Sehadova, H., Glaser, F. T., Gentile, C., Simoni, A., Giesecke, A., Albert, J. T. and Stanewsky, R. (2009) Temperature entrainment of *Drosophila's* circadian clock involves the gene *nocte* and signaling from peripheral sensory tissues to the brain. Neuron, 64, 251-266.

Sehgal, A., Rothenfluh-Hilfiker, A., Hunter-Ensor, M., Chen, Y., Myers, M. P. and Young, M. W. (1995) Rhythmic expression of timeless: a basis for promoting circadian cycles in *period* gene autoregulation. Science, 270, 808-810.

Selcho, M., Millàn, C., Palacios, A., Ruf, F., Ubillo, L., Chen, J., Ito, C., Silva, V., Wegener, C. and Ewer, J. (unpublished-a) The PTTH neuropeptide couples central and peripheral clocks in *Drosophila*.

Selcho, M., Pauls, D., El Jundi, B., Stocker, R. F. and Thum, A. S. (2012) The role of octopamine and tyramine in *Drosophila* larval locomotion. The Journal of Comparative Neurology, 520, 3764-3785.

Selcho, M., Pauls, D., Han, K. A., Stocker, R. F. and Thum, A. S. (2009) The role of dopamine in *Drosophila* larval classical olfactory conditioning. PLoS One, 4, e5897.

Selcho, M., Shiga, S., Wegener, C. and Yasuyama, K. (unpublished-b) Neuroanatomy, fine structure and relationship of transitory PDF-Tri neurons and peptidergic neurons associated with ecdysis behavior of *Drosophila*.

Sellami, A., Wegener, C. and Veenstra, J. A. (2012) Functional significance of the copper transporter ATP7 in peptidergic neurons and endocrine cells in *Drosophila melanogaster*. FEBS Letters, 586, 3633-3638.

Shafer, O. T. and Yao, Z. (2014) Pigment-dispersing factor signaling and circadian rhythms in insect locomotor activity. Current Opinion in Insect Science, 1, 73-80.

Sheeba, V., Chandrashekaran, M. K., Joshi, A. and Sharma, V. K. (2001) A case for multiple oscillators controlling different circadian rhythms in *Drosophila melanogaster*. Journal of Insect Physiology, 47, 1217-1225.

Shimada-Niwa, Y. and Niwa, R. (2014) Serotonergic neurons respond to nutrients and regulate the timing of steroid hormone biosynthesis in *Drosophila*. Nature Communications, 5, 5778.

Siegmund, T. and Korge, G. (2001) Innervation of the ring gland of *Drosophila melanogaster*. The Journal of Comparative Neurology, 431, 481-491.

Sineshchekov, O. A., Jung, K. H. and Spudich, J. L. (2002) Two rhodopsins mediate phototaxis to low- and high-intensity light in *Chlamydomonas reinhardtii*. Proceedings of the National Academy of Sciences of the United States of America, 99, 8689-8694.

Sitaraman, D., LaFerriere, H., Birman, S. and Zars, T. (2012) Serotonin is critical for rewarded olfactory short-term memory in *Drosophila*. Journal of Neurogenetics, 26, 238-244.

Sitaraman, D., Zars, M., Laferriere, H., Chen, Y. C., Sable-Smith, A., Kitamoto, T., Rottinghaus, G. E. and Zars, T. (2008) Serotonin is necessary for place memory in *Drosophila*. Proceedings of the National Academy of Sciences of the United States of America, 105, 5579-5584.

Skopik, S. D. and Pittendrigh, C. S. (1967) Circadian Systems II. The oscillation in the individual *Drosophila* pupa; its independence of developmental stage.

Stanewsky, R., Frisch, B., Brandes, C., Hamblen-Coyle, M. J., Rosbash, M. and Hall, J. C. (1997) Temporal and spatial expression patterns of transgenes containing increasing amounts of the *Drosophila* clock gene *period* and a lacZ reporter: mapping elements of the PER protein involved in circadian cycling. The Journal of Neuroscience: the official Journal of the Society for Neuroscience, 17, 676-696.

Stanewsky, R., Kaneko, M., Emery, P., Beretta, B., Wager-Smith, K., Kay, S. A., Rosbash, M. and Hall, J. C. (1998) The cryb mutation identifies cryptochrome as a circadian photoreceptor in *Drosophila*. Cell, 95, 681-692.

Stangier, J., Hilbich, C., Beyreuther, K. and Keller, R. (1987) Unusual cardioactive peptide (CCAP) from pericardial organs of the shore crab *Carcinus maenas*. Proceedings of the National Academy of Sciences of the United States of America, 84, 575-579.

Steel, C. G. and Vafopoulou, X. (2006) Circadian orchestration of developmental hormones in the insect, *Rhodnius prolixus*. Comparative biochemistry and physiology. Part A, Molecular & Integrative Physiology, 144, 351-364.

Stern, C. and Schaeffer, E. W. (1943) On Primary Attributes of Alleles in *Drosophila Melanogaster*. Proceedings of the National Academy of Sciences of the United States of America, 29, 351-361.

Stoleru, D., Nawathean, P., Fernandez, M. P., Menet, J. S., Ceriani, M. F. and Rosbash, M. (2007) The *Drosophila* circadian network is a seasonal timer. Cell, 129, 207-219.

Sundram, V., Ng, F. S., Roberts, M. A., Millan, C., Ewer, J. and Jackson, F. R. (2012) Cellular requirements for LARK in the *Drosophila* circadian system. Journal of Biological Rhythms, 27, 183-195.

Suster, M. L., Seugnet, L., Bate, M. and Sokolowski, M. B. (2004) Refining GAL4-driven transgene expression in *Drosophila* with a GAL80 enhancer-trap. Genesis, 39, 240-245.

Tanaka, K. and Watari, Y. (2009) Is early morning adult eclosion in insects an adaptation to the increased moisture at dawn? Biological Rhythm Research, 40, 293-298.

Tauber, E., Zordan, M., Sandrelli, F., Pegoraro, M., Osterwalder, N., Breda, C., Daga, A., Selmin, A., Monger, K., Benna, C., Rosato, E., Kyriacou, C. P. and Costa, R. (2007) Natural selection favors a newly derived *timeless* allele in *Drosophila melanogaster*. Science, 316, 1895-1898.

Tawfik, A. I., Tanaka, S., De Loof, A., Schoofs, L., Baggerman, G., Waelkens, E., Derua, R., Milner, Y., Yerushalmi, Y. and Pener, M. P. (1999) Identification of the gregarization-associated dark-pigmentotropin in locusts through an albino mutant. Proceedings of the National Academy of Sciences of the United States of America, 96, 7083-7087.

Thibault, S. T., Singer, M. A., Miyazaki, W. Y., Milash, B., Dompe, N. A., Singh, C. M., Buchholz, R., Demsky, M., Fawcett, R., Francis-Lang, H. L., Ryner, L., Cheung, L. M., Chong, A., Erickson, C., Fisher, W. W., Greer, K., Hartouni, S. R., Howie, E., Jakkula, L., Joo, D., Killpack, K., Laufer, A., Mazzotta, J., Smith, R. D., Stevens, L. M., Stuber, C., Tan, L. R., Ventura, R., Woo, A., Zakrajsek, I., Zhao, L., Chen, F., Swimmer, C., Kopczynski, C., Duyk, G., Winberg, M. L. and Margolis, J. (2004) A complementary transposon tool kit for *Drosophila melanogaster* using P and piggyBac. Nature Genetics, 36, 283-287.

Tomioka, K., Uwozumi, K. and Matsumoto, N. (1997) Light Cycles Given During Development Affect Freerunning Period of Circadian Locomotor Rhythm of *period* Mutants in *Drosophila melanogaster*. Journal of Insect Physiology, 43, 297-305.

Trapp, R. (2014) Beeinflussen die Neuropeptide Corazonin und Capa das zeitliche Schlupfverhalten von *Drosophila melanogaster*? In Department of Neurobiology and Genetics, Vol. Bachelor Julius-Maximilians-Universität Würzburg.

Truman, J. W. (1972) Physiology of insect rhythms. Journal of Comparative Physiology, 81, 99-114.

Truman, J. W. and Riddiford, L. M. (1970) Neuroendocrine control of ecdysis in silkmoths. Science, 167, 1624-1626.

Truman, J. W. and Riddiford, L. M. (1974) Physiology of insect rhythms. 3. The temporal organization of the endocrine events underlying pupation of the tobacco hornworm. Journal of Experimental Biology, 60, 371-382.

Truman, J. W., Rountree, D. B., Reiss, S. E. and Schwartz, L. M. (1983) Ecdysteroids regulate the release and action of eclosion hormone in the tobacco hornworm, Manduca sexta (L.). Journal of Insect Physiology, 29, 895-900.

Ueda, H. R., Matsumoto, A., Kawamura, M., Iino, M., Tanimura, T. and Hashimoto, S. (2002) Genome-wide transcriptional orchestration of circadian rhythms in *Drosophila*. The Journal of Biological Chemistry, 277, 14048-14052.

Van Vickle-Chavez, S. J. and Van Gelder, R. N. (2007) Action spectrum of *Drosophila* cryptochrome. The Journal of Biological Chemistry, 282, 10561-10566.

Vanderveken, M. and O'Donnell, M. J. (2014) Effects of diuretic hormone 31, drosokinin, and allatostatin A on transepithelial K(+) transport and contraction frequency in the midgut and hindgut of larval *Drosophila melanogaster*. Archives of Insect Biochemistry and Physiology, 85, 76-93.

Vanin, S., Bhutani, S., Montelli, S., Menegazzi, P., Green, E. W., Pegoraro, M., Sandrelli, F., Costa, R. and Kyriacou, C. P. (2012) Unexpected features of *Drosophila* circadian behavioural rhythms under natural conditions. Nature, 484, 371-375.

Vedeckis, W. V., Bollenbacher, W. E. and Gilbert, L. I. (1976) Insect prothoracic glands: a role for cyclic AMP in the stimulation of alpha-ecdysone secretion. Molecular and Cellular Endocrinology, 5, 81-88.

Veenstra, J. A. (1989) Isolation and structure of corazonin, a cardioactive peptide from the American cockroach. FEBS Letters, 250, 231-234.

Veenstra, J. A. (2009) Does corazonin signal nutritional stress in insects? Insect Biochemistry and Molecular Biology, 39, 755-762.

Vömel, M. and Wegener, C. (2007) Neurotransmitter-induced changes in the intracellular calcium concentration suggest a differential central modulation of CCAP neuron subsets in *Drosophila*. Developmental Neurobiology, 67, 792-808.

Vömel, M. and Wegener, C. (2008) Neuroarchitecture of aminergic systems in the larval ventral ganglion of *Drosophila melanogaster*. PLoS One, 3, e1848.

Warren, J. T., Petryk, A., Marques, G., Parvy, J. P., Shinoda, T., Itoyama, K., Kobayashi, J., Jarcho, M., Li, Y., O'Connor, M. B., Dauphin-Villemant, C. and Gilbert, L. I. (2004) Phantom encodes the 25-hydroxylase of *Drosophila melanogaster* and *Bombyx mori:* a P450 enzyme critical in ecdysone biosynthesis. Insect Biochemistry and Molecular Biology, 34, 991-1010.

Wegener, C., Reinl, T., Jansch, L. and Predel, R. (2006) Direct mass spectrometric peptide profiling and fragmentation of larval peptide hormone release sites in *Drosophila melanogaster* reveals tagma-specific peptide expression and differential processing. Journal of Neurochemistry, 96, 1362-1374.

Wheeler, D. A., Hamblen-Coyle, M. J., Dushay, M. S. and Hall, J. C. (1993) Behavior in Light-Dark Cycles of *Drosophila* Mutants That Are Arrhythmic, Blind, or Both. Journal of Biological Rhythms, 8, 67-94.

Williamson, M., Lenz, C., Winther, A. M., Nässel, D. R. and Grimmelikhuijzen, C. J. (2001) Molecular cloning, genomic organization, and expression of a B-type (cricket-type) allatostatin preprohormone from *Drosophila melanogaster*. Biochemical and Biophysical Research Communications, 281, 544-550.

Wing, J. P., Zhou, L., Schwartz, L. M. and Nambu, J. R. (1998) Distinct cell killing properties of the *Drosophila reaper*, *head involution defective*, and *grim* genes. Cell Death and Differentiation, 5, 930-939.

Wülbeck, C., Szabo, G., Shafer, O. T., Helfrich-Förster, C. and Stanewsky, R. (2005) The novel *Drosophila* tim(blind) mutation affects behavioral rhythms but not periodic eclosion. Genetics, 169, 751-766.

Xu, K., Zheng, X. and Sehgal, A. (2008) Regulation of feeding and metabolism by neuronal and peripheral clocks in *Drosophila*. Cell Metabolism, 8, 289-300.

Yamanaka, N., Hua, Y. J., Mizoguchi, A., Watanabe, K., Niwa, R., Tanaka, Y. and Kataoka, H. (2005) Identification of a novel prothoracicostatic hormone and its receptor in the silkworm *Bombyx mori*. The Journal of Biological Chemistry, 280, 14684-14690.

Yamanaka, N., Hua, Y. J., Roller, L., Spalovska-Valachova, I., Mizoguchi, A., Kataoka, H. and Tanaka, Y. (2010) *Bombyx* prothoracicostatic peptides activate the sex peptide receptor to regulate ecdysteroid biosynthesis. Proceedings of the National Academy of Sciences of the United States of America, 107, 2060-2065.

Yamanaka, N., Romero, N. M., Martin, F. A., Rewitz, K. F., Sun, M., O'Connor, M. B. and Leopold, P. (2013) Neuroendocrine control of *Drosophila* larval light preference. Science, 341, 1113-1116.

Yanfei Feng, A. U. a. C.-F. W. (2004) A modifies minimal hemolymphlike solution, HL3.1, for physiological recordings at the neuromuscular junctions of normal and mutant *Drosophila* larvae. Journal of Neurogenetics, 18, 377-402.

Yang, Z., Yu, Y., Zhang, V., Tian, Y., Qi, W. and Wang, L. (2015) Octopamine mediates starvation-induced hyperactivity in adult *Drosophila*. Proceedings of the National Academy of Sciences of the United States of America, 112, 5219-5224.

Yew, J. Y., Wang, Y., Barteneva, N., Dikler, S., Kutz-Naber, K. K., Li, L. and Kravitz, E. A. (2009) Analysis of neuropeptide expression and localization in adult *Drosophila melanogaster* central nervous

system by affinity cell-capture mass spectrometry. Journal of Proteome Research, 8, 1271-1284.

Yoon, J. G. and Stay, B. (1995) Immunocytochemical localization of Diploptera punctata allatostatin-like peptide in *Drosophila melanogaster*. The Journal of Comparative Neurology, 363, 475-488.

Yoshii, T., Heshiki, Y., Ibuki-Ishibashi, T., Matsumoto, A., Tanimura, T. and Tomioka, K. (2005) Temperature cycles drive *Drosophila* circadian oscillation in constant light that otherwise induces behavioural arrhythmicity. European Journal of Neuroscience, 22, 1176-1184.

Yoshii, T., Sakamoto, M. and Tomioka, K. (2002) A temperature-dependent timing mechanism is involved in the circadian system that drives locomotor rhythms in the fruit fly *Drosophila melanogaster*. Zoological Science, 19, 841-850.

Yoshii, T., Todo, T., Wülbeck, C., Stanewsky, R. and Helfrich-Förster, C. (2008) Cryptochrome is present in the compound eyes and a subset of *Drosophila's* clock neurons. The Journal of Comparative Neurology, 508, 952-966.

Yoshii, T., Vanin, S., Costa, R. and Helfrich-Forster, C. (2009) Synergic entrainment of *Drosophila's* circadian clock by light and temperature. Journal of Biological Rhythms, 24, 452-464.

Yu, Q., Colot, H. V., Kyriacou, C. P., Hall, J. C. and Rosbash, M. (1987a) Behaviour modification by in vitro mutagenesis of a variable region within the *period* gene of *Drosophila*. Nature, 326, 765-769.

Yu, Q., Jacquier, A. C., Citri, Y., Hamblen, M., Hall, J. C. and Rosbash, M. (1987b) Molecular mapping of point mutations in the *period* gene that stop or speed up biological clocks in *Drosophila melanogaster*. Proceedings of the National Academy of Sciences of the United States of America, 84, 784-788.

Yuan, Q., Joiner, W. J. and Sehgal, A. (2006) A sleep-promoting role for the *Drosophila* serotonin receptor 1A. Current Biology : CB, 16, 1051-1062.

Yuan, Q., Lin, F., Zheng, X. and Sehgal, A. (2005) Serotonin modulates circadian entrainment in *Drosophila*. Neuron, 47, 115-127.

Zeng, H., Qian, Z., Myers, M. P. and Rosbash, M. (1996) A light-entrainment mechanism for the *Drosophila* circadian clock. Nature, 380, 129-135.

Zhang, F., Prigge, M., Beyriere, F., Tsunoda, S. P., Mattis, J., Yizhar, O., Hegemann, P. and Deisseroth, K. (2008) Red-shifted optogenetic excitation: a tool for fast neural control derived from *Volvox carteri*. Nature Neuroscience, 11, 631-633.

Zhang, W., Ge, W. and Wang, Z. (2007) A toolbox for light control of *Drosophila* behaviors through Channelrhodopsin 2-mediated photoactivation of targeted neurons. European Journal of Neuroscience, 26, 2405-2416.

Zhao, Y., Bretz, C. A., Hawksworth, S. A., Hirsh, J. and Johnson, E. C. (2010) Corazonin neurons function in sexually dimorphic circuitry that shape behavioral responses to stress in *Drosophila*. PloS One, 5, e9141.

Zimmerman, W. F., Pittendrigh, C. S. and Pavlidis, T. (1968a) Temperature compensation of the circadian oscillation in *Drosophila pseudoobscura* and its entrainment by temperature cycles. Journal of insect physiology, 14, 669-684.

Zitnan, D., Kingan, T. G., Hermesman, J. L. and Adams, M. E. (1996) Identification of ecdysis-triggering hormone from an epitracheal endocrine system. Science (New York, N.Y.), 271, 88-91.

Zitnan, D., Ross, L. S., Zitnanova, I., Hermesman, J. L., Gill, S. S. and Adams, M. E. (1999) Steroid induction of a peptide hormone gene leads to orchestration of a defined behavioral sequence. Neuron, 23, 523-535.

Zordan, M., Costa, R., Macino, G., Fukuhara, C. and Tosini, G. (2009) Circadian Clocks: What Makes Them Tick? Chronobiology International, 17, 433-451.

Publications

Ruf, F., Fraunholz, M., Öchsner, K., Kaderschabek, J., Wegener, C. (2016) WEclMon - a new eclosion monitoring system. *In preparation*

Selcho, M., Millán, C., Palacios, A., Ruf. F., Ubillo, L., Chen, J., Ito, C., Silva, V., Wegener, C., Ewer, J. (2016) The PTTH neuropeptide couples central and peripheral clocks in *Drosophila*. *In preparation*

Acknowledgments

This work would not have been possible without the help of many people. Therefore I want to give my thanks:

first and foremost, to Prof. Dr. Christian Wegener for giving me the opportunity to conduct my doctoral thesis under his supervision, for his ideas, advice and patience

to Prof. Dr. Wolfgang Rössler for being second supervisor of this doctoral thesis and to Prof. Dr. Sakiko Shiga for being my external supervisor

to the whole department of Neurobiology and Genetics, especially to the AG Wegener, for always helping me with my questions and problems and for the great working atmosphere

to Gertrud Gramlich, for always helping me with the molecular work and never losing patience with me and my projects

to Susanne Klühspies, for all the preparations, stainings, the fly work and especially for all the nice breaks

to Konrad Öchsner and Hans Kaderschabek, who made the WEclMon project possible, for always helping me with technical problems

to Dr. Oliver Mitesser and Prof. Dr. Thomas Hovestadt, for the cooperation and the development of the statistical model, and especially to Oliver for fulfilling all my R wishes

to Dr. Martin Fraunholz, who created the Eclosion Toolbar, for taking time to help me with ImageJ

to the Würzburg Stammtisch and all friends, for all the fun hours after work and for always being there for me

to my family, who made it all possible and who supported me all along

to Frank, for everything; for supporting me in every way and for our wonderful life together

Affidavit

I hereby confirm that my thesis entitled “The circadian regulation of eclosion in *Drosophila melanogaster*” is the result of my own work. I did not receive any help or support from commercial consultants. All sources and / or materials applied are listed and specified in the thesis.
Furthermore, I confirm that this thesis has not yet been submitted as part of another examination process neither in identical nor in similar form.

Würzburg, 24.06.2016

Place, Date Signature

Eidesstattliche Erklärung

Hiermit erkläre ich an Eides statt, die Dissertation “Die zeitliche Steuerung des Adultschlupfes in *Drosophila melanogaster*” eigenständig, d.h. insbesondere selbständig und ohne Hilfe eines kommerziellen Promotionsberaters, angefertigt und keine anderen als die von mir angegebenen Quellen und Hilfsmittel verwendet zu haben.
Ich erkläre außerdem, dass die Dissertation weder in gleicher noch in ähnlicher Form bereits in einem anderen Prüfungsverfahren vorgelegen hat.

Würzburg, 24.06.2016

Ort, Datum Unterschrift